Genetic and Epigenetic Profiling of Human Prostate Cancer Cell-Subsets

Alberto John Taurozzi

PhD

University of York

Biology

September 2016

Abstract

Perturbation of androgen signalling drives progression of human prostate cancer (CaP) to castration-resistant prostate cancer (CRPC). Additionally, CaP is initiated and maintained by cancer stem cells (CSC)s which are analogous to normal prostate stem cells (SC)s. This study presents a qPCR assay to detect androgen receptor gene amplification (GAAR), which is the most common mechanism of castration resistance (>30%). Also, the epigenetic regulation and function of two SC-silenced genes with tumour-suppressive activity (Latexin (LXN) and Retinoic Acid Receptor Responder 1 (RARRES1)) were interrogated using micro-ChIP, transcriptional profiling and mass spectrometry.

Traditionally, GAAR is detected using FISH which is labour-intensive and semi-quantitative, limiting clinical applicability. The mechanism of action of LXN or RARRES1 in CaP is unknown, and epigenetic regulation by DNA methylation has been ruled-out in primary CaP.

The qPCR assay can detect GAAR in minor cell populations (~1%) within a heterogeneous sample and also quantifies X chromosome aneuploidy (XCA) - a predictor of poor-prognosis in CaP. GAAR and XCA were detected in near-patient xenografts derived from CRPC-tissue indicating that these abnormalities are present in cells capable of in vivo tumour-reconstitution.

Micro-ChIP analysis of fractionated primary CaP cultures identified bivalent chromatin at LXN and RARRES1 promoters. Transcriptomic profiling failed to reveal significant changes in gene expression after transduction with LXN or RARRES1. However, an interactome for LXN and RARRES1 was successfully generated in PC3 cells. Additionally, confocal microscopy of mVenus-tagged LXN revealed a pan-cellular distribution which is reflected in the interactome.

Screening for GAAR and XCA, using a high-throughput qPCR assay, could facilitate a targeted-medicine strategy in the treatment of CaP and CRPC. Further investigation of the LXN and RARRES1 interactomes may identify their mechanism(s) of action and the micro-ChIP assay could be used to identify epigenetic-inducers of LXN and RARRES1 which could provide a CSC-targeted strategy for CaP treatment.

List of Contents

List of Figures

List of Tables

Acknowledgements

Author's declaration

I declare this thesis to be the product of my own unaided work, except where acknowledged otherwise in the text. All sources are acknowledged as references. This work has not been submitted previously in consideration for a degree at this, or at any other university.

1. General Introduction

1.1. The Prostate

The prostate is a male-specific organ located at the base of the bladder. This walnut sized and shaped glandular organ plays an important role in reproduction by producing prostatic fluid; a major constituent of semen (Huggins et al., 1942). Prostate fluid is alkaline and contains bio-available zinc as well as various proteins. Increased pH protects sperm from the acidic environment encountered in the vagina, while protein constituents of prostate fluid, which include: prostate specific antigen (PSA) and prostatic acid phosphatase (PAP), are essential for sperm function along with zinc (Carpino et al., 1994). Additionally, the prostate also has a contractile function acting as a 'tap' for bladder flow.
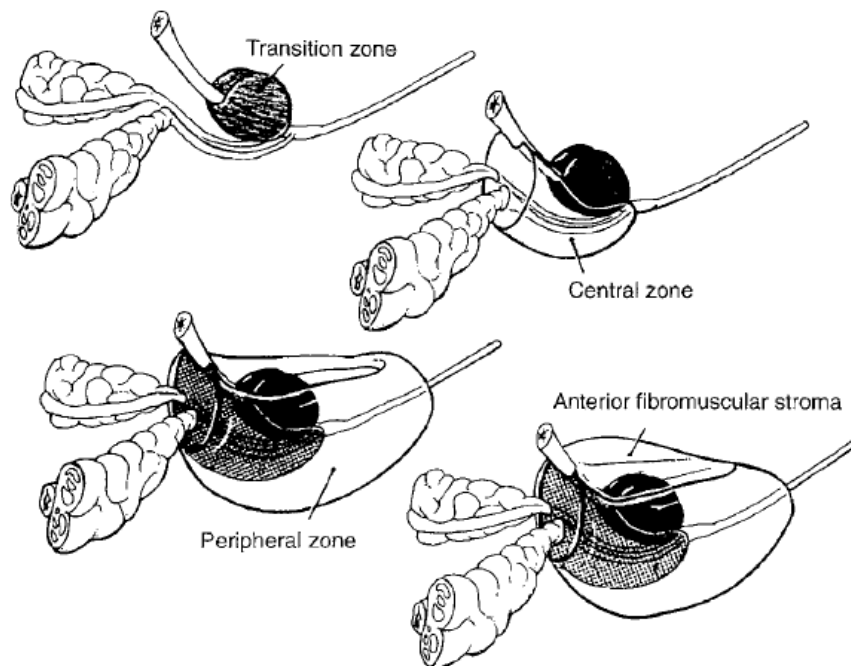
Fig. 1. Zonal Anatomy of the Normal Prostate.

The zonal anatomy of the prostate showing the relative locations of the Transitional zone, Central zone, Anterior fibromuscular stroma and Peripheral zone.

From: (Hammerich, 2009)

1.1.1. Topographical Anatomy of the Human Prostate

In contrast to the murine prostate, which is composed of distinct anatomic lobes, the human gland can be divided into four anatomical zones, which were identified by McNeal in a comprehensive study of 500 prostates. McNeal used the relationship of each region to the urethra to provide a central reference point (McNeal, 1981). An anatomical diagram of the prostate is shown in (Fig. 1.) (Hammerich, 2009).

These four zones are listed below:

- Anterior fibromuscular stroma
- Central zone
- Peripheral zone
- Transition zone

A simplified two zone scheme is more often used, which comprises:

- Inner section (transition zone)
- Outer section (peripheral and central zones)

Anterior fibromuscular stroma comprises one third of the prostate. This zone contains very few or no acini and is composed primarily of smooth muscle and dense fibrous tissue. A major function of this zone is in voluntary and involuntary sphincter functions.

Approximately 20% of the glandular tissue is contained within the cone-shaped central zone. At the apex of the central zone is the verumontanum whilst at its base is the bladder neck. It has been calculated that 5% of adenocarcinomas occur within the central zone.

The peripheral zone is the largest, containing approximately 75% of the glandular tissue. It is distal to the central zone and has a horseshoe-shaped structure. Chronic prostatitis and post-inflammatory atrophy primarily afflict this zone, which is also the primary site for malignant transformations; ~70% of adenocarcinomas originate at this site (McNeal et al., 1988).

The transitional zone is composed of two equal sections which surround the urethra. Whilst only representing 5% of the prostatic volume it has significant clinical importance,

as the location in which age-related benign prostatic hyperplasia (BPH) occurs (McNeal, 1978).

1.1.2. Histological Anatomy of the Human Prostate

Glandular prostate tissue consists of epithelial and stromal cells, physically separated by a basement membrane (BM). Laminins and collagen are the primary constituents of the BM (Yurchenco and O'Rear, 1994, Navdaev and Eble, 2011) which is also composed of glycoproteins and proteoglycans which play an important role in fundamental cellular processes including proliferation and differentiation (Gonçalves et al., 2015). In the case of proteoglycans these functions are attributed to the glycosaminoglycan side chains such as chondroitin sulphate which has shown to be enriched in areas of active proliferation (Gonçalves et al., 2015). The stroma is located beneath the BM and helps serve the metabolic needs of the epithelium (in which blood vessels are normally absent) in a paracrine manner (Hayward et al., 1997, Giri et al., 1999).

Phenotypically the stromal compartment is composed of both smooth muscle cells and fibroblasts, which can be distinguished from each other immunohistochemically: The short and broad smooth muscle cells express high levels of alpha-smooth muscle actin and have very low expression of prolyl 4-hydroxylase (Goodpaster et al., 2008, Kooistra et al., 1995). In contrast, the fibroblasts show the reciprocal expression pattern for these two markers (Kooistra et al., 1995).

Functionally the stroma plays a role in the survival, proliferation and differentiation of epithelial cells by secreting growth factors, which include fibroblast growth factor (FGF) and epidermal growth factor (EGF) (Berry et al., 2008, Giri et al., 1999). Of important note is that a proportion of the stromal cells express the androgen receptor (AR) and thus serve as an androgen signalling link to basal cells within the epithelium, in which AR expression is low or absent (Berry et al., 2008).

The epithelial compartment is arranged in glands composed of ducts, which branch out from the urethra and terminate into acini. Several distinct types of epithelial cells exist within in the prostate: (a) secretory luminal cells, (b) basal cells, and (c) rare neuroendocrine cells (Liu and True, 2002). Architecturally, the epithelium is arranged in a bilayer, consisting of a basal layer which is in direct contact with the BM and an upper

luminal layer which is physically separated from the BM by the basal layer (Collins and Maitland, 2006) (Fig. 2.).
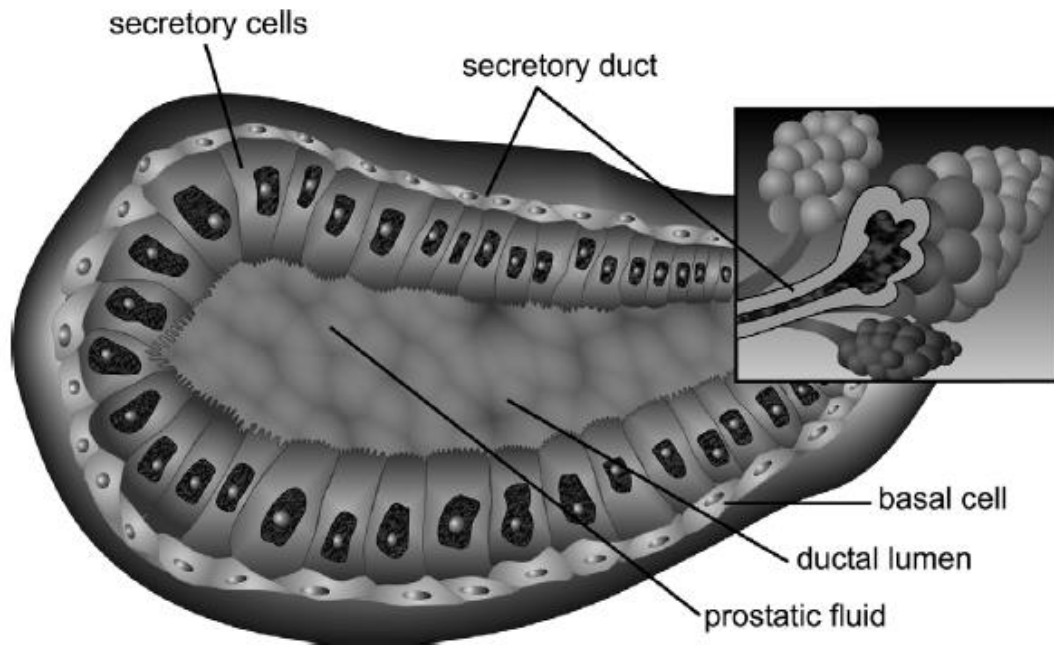
Fig. 2. Organisation of the Prostate Gland.

Cross-section of the ductal region of the prostate, with labels indicating cell types present in prostatic ducts, including luminal secretory cells and basal cells.

From: (Collins and Maitland, 2006)

The luminal cell fraction is terminally differentiated, performing the highly specialised role of manufacturing and secreting proteins, such as PSA and PAP (Collins and Maitland, 2006, Lang et al., 2009) into the glandular lumina. They can be distinguished from the basal cells by their columnar morphology and expression of PSA, PAP, cytokeratin 8 (CK8), CK18 and high expression AR (Yu et al., 2012, Wang et al., 2012). These cells are also dependent on androgens for their survival.

In contrast, basal cells have a very low secretory activity (Collins and Maitland, 2006, Lang et al., 2009) and are relatively undifferentiated. Morphologically, they are small and flattened or cuboidal. In contrast to luminal cells, they are independent of androgens for their survival and they express CD44, $\alpha 2\beta 1$ integrin (which facilitates there attachment to the BM via collagen type IV (Liu et al., 2009, Collins et al., 2005)) tumour protein p63 (p63), CK5 and CK14 (Wang et al., 2012, Collins et al., 2005). A summary of prostate epithelial markers is shown in (Table. 1.).

The basal cells also represent the proliferative compartment within the prostate epithelium as shown by the expression of markers of proliferation, such as tyrosine-protein kinase Met (c-met), antigen KI-67 (Ki67) and proliferating cell nuclear antigen (PCNA) (Bonkhoff et al., 1994). For example, it has been shown that 70% of the Ki67 positive cells are located within the basal layer (Bonkhoff et al., 1994).

A third group of prostatic epithelial cells are the terminally differentiated, post-mitotic neuroendocrine cells. These cells represent a small proportion of cells within the prostate epithelium and stroma (Lang et al., 2009). They secrete neuropeptides such as bombesin, neurotensin, serotonin, chromogranin A, neuron-specific enolase, and calcitonin (Rumpold et al., 2002), and are devoid of both luminal and basal markers.

Cell Type	Markers
Luminal Cell	AR, CK8, CK18, Nkx3.1, PSA, PAP
Basal Cell	CK5, CK14, CD44, p63, $\alpha 2\beta 1$ integrin, BCL-2
Neuroendocrine Cell	bombesin, neurotensin, chromogranin A, neuron-specific enolase

Table. 1. Common Antigenic Markers Used to Distinguish Prostate Epithelial Cells.

1.1.3. Development and Maturation of the Prostate

By understanding the development and maturation of the prostate during embryogenesis and puberty respectively, one can elucidate important pathways, which may be pertinent to diseases of the prostate, including cancer. Due to ethical constraints the vast majority of evidence on prostate development comes from laboratory rodents. One major caveat in the translation of these findings is that the murine and human prostates have significant morphological differences. For example, murine acini have a discontinuous epithelial bi-layer in which a proportion of luminal cells are in direct contact with the BM (Marker et al., 2003).

The murine embryonic development of the prostate is dependent on androgens, namely 5α-dihydrotestosterone which is synthesized from foetal testosterone by the action of 5α-reductase (Hammerich, 2009). Androgens exert their effect directly upon the AR-expressing urogenital sinus mesenchyme (USM). Prostate development occurs late in embryogenesis whereby the prostate gland develops from epithelial invaginations within the posterior USM (Bhavsar and Verma, 2014), resulting in a multi-layered epithelium encapsulated by stroma. As development continues the basal epithelium invades the surrounding stroma producing immature secretory structures. Apart from the well-defined androgen axis there are several other signalling pathways that play an essential role in organogenesis of the prostate; including the wingless-related integration site protein (Wnt), retinoid, fibroblast growth factor (FGF), and Hedgehog pathways (Yu et al., 2012, Maitland, 2013) (Fig. 3.). This figure also depicts both mesenchymal and epithelial stem cells (SC)s of the prostate, which persist in the adult organ. Importantly the diagram depicts the prostate epithelial stem cell as being located basally in close contact with the stromal compartment to facilitate 'cross-talk' between the two cell types.

While AR mediated transcriptional activity is a requirement for prostate formation (patients with complete androgen insensitivity syndrome (CAIS) don't develop a prostate (Quigley et al., 1995)), it is only essential within the USM (Cunha and Donjacour, 1987, Cunha et al., 1987). This was shown by grafting of AR-deficient murine urogenital sinus epithelium (UGE) in combination with wild type murine USM, which resulted in androgen-dependent ductal morphogenesis (Fig. 4.). The complementary experiment i.e. AR- USM and wild type UGE resulted in vaginal-like differentiation (Cunha et al., 1987, Cunha and Donjacour, 1987).

Other key transcription factors involved in cell fate decisions during prostate embryogenesis include; p63 (deletion of which causes a complete absence of epithelial cells (Senoo et al., 2007), forkhead box protein A1 (Foxa1), and homeobox protein Nkx-3.1 (Nkx3.1) (Bhatia-Gaur et al., 1999, Gao et al., 2005) (Fig. 4.). Knockout of *Foxa1* in murine models results in a population of cells that individually express markers representative of both luminal and basal cell types namely co-expression of Ck8 (luminal marker), Ck5 and Ck14 (basal markers) (Gao et al., 2005). *Nkx3.1*-deletion results in prostate epithelial cell hyperplasia and incomplete differentiation and curtailed secretory activity (Gao et al., 2005).

Expansion of the prostate is induced by the testosterone surge that occurs during puberty, and consequent increase in 5α-dihydrotestosterone (DHT). A significant morphological feature of maturation is the differentiation of the multi-layered epithelium, to produce the mature epithelial bi-layer (Wang et al., 2012, Yu et al., 2012, Collins and Maitland, 2006, Liu et al., 2009, Lang et al., 2009, Collins et al., 2005). The prostate continuously enlarges, reaching the adult weight of approximately (mean 11g) by 25–30 years of age (Berry et al., 1984).
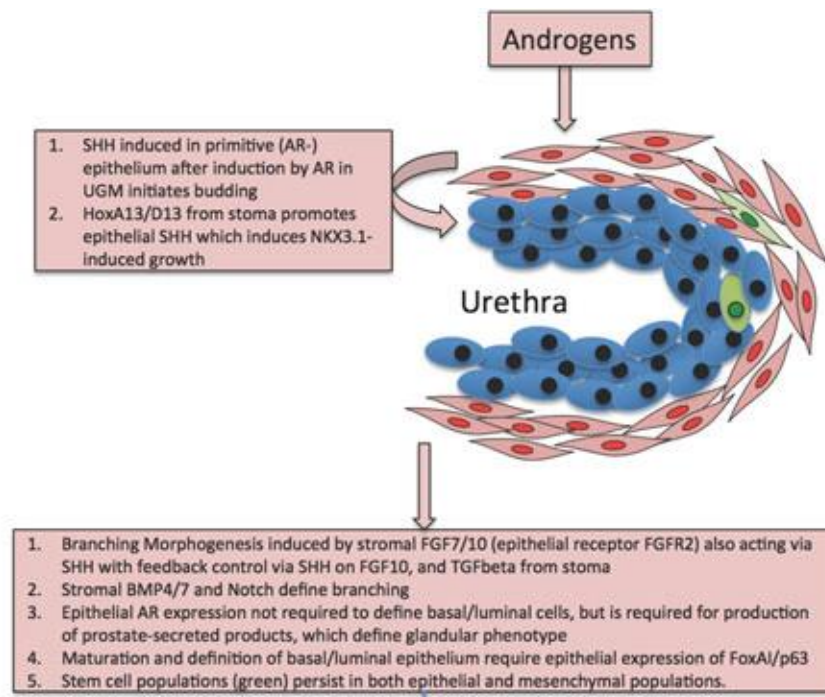
Fig. 3. Development of the Normal Prostate.

Stem cells in the epithelial and stromal compartments are shown in *green,* basal cells in *blue,* and luminal cells in *pink,* with cells positive for AR-expression depicted by *red* nuclei. Hormone-responsive stromal cells are also shown in *pink.*

From: (Maitland, 2013)

Undifferentiated Stromal Cell
Urogenital sinus epithelium

Embryonic UGS

Smooth Muscle
Basal-like Epithelial Cell
Intermediate Epithelial Cell

Foxa1-null

Smooth Muscle
Hyperplastic Epithelial Cell

Nkx3.1-null

Smooth Muscle
Mature Basal Epithelial Cell
Immature Luminal Epithelial Cell

Epithelial AR-null

Smooth Muscle
Mature Basal Epithelial Cell
Mature Luminal Epithelial Cell

Normal Adult Prostate

Fig. 4. Elucidating the Roles of Key Transcription Factors (Foxa1, Nkx3.1 and AR) in Prostate Embryogenesis by Utilising Murine Knockout Models.

Normal development of the adult murine prostate results in differentiation of the embryonic urogenital sinus (UGS) into fully differentiated basal and luminal compartments the latter exhibiting secretory activity of proteins such as PSA and PAP.

The early growth and differentiation of the UGS is driven by androgen signalling, elevated Foxa1 and Nkx3.1 transcription factors.

In the epithelium, knockout of Foxa1 results in a block of luminal cell differentiation with the luminal cell compartment exhibiting an cytokeratin expression profile consistent with a luminal-basal intermediate phenotype namely co expression of Ck5, Ck8 and Ck14. Another morphological abnormality of the Foxa-1 null mice is an unusually thick layer of smooth muscle cells which is a perturbation of normal differentiation of the mesenchyme. On a molecular level Foxa1 knockout results elevation of Bmp, Shh and Notch signalling and a reduction of Nkx3.1 signalling. Functionally the resulting prostate has an impaired secretory activity.

The early prostate development in Nkx3.1 knockout mice is characterised by the accumulation of epithelial cells that show limited differentiation and secretory activity. As development continues, the Nkx3.1-null prostate exhibits prostatic intraepithelial neoplasia (PIN).

Knockout of AR only in the prostate epithelium (stromal compartment retains AR expression) results in normal structural development and epithelial-compartmentalisation. However, the luminal cell compartment fails to fully differentiate and secretory proteins are not expressed.

From: (Gao et al., 2005)

1.2. Non-Malignant Disorders of the Prostate

There are several disorders which affect the prostate including, prostatitis, benign prostatic hyperplasia (BPH), prostate intraepithelial neoplasia (PIN) and prostate cancer (CaP).

1.2.1. Prostatitis

Prostatitis is the most frequent disorder of the prostate with an incidence rate of 2-10% of males (Krieger et al., 2008). It is caused by inflammation and typically occurs in the central zone. Prostatitis is strongly implicated as a major contributory factor to the development of BPH (Nickel, 2008).

This inflammatory response can be elicited by many factors including:

- pathogenic infection
- stress
- autoimmunity
- physical injury

1.2.2. Benign Prostatic Hyperplasia

Benign Prostatic Hyperplasia (BPH) is a non-malignant proliferative disease which affects the stromal and epithelial compartments of the transition zone. It is well established that BPH is an age-related disease (Berry et al., 1984). BPH leads to an enlargement of the prostate and subsequently obstruction of the urethra leading to increased resistance of urine flow and frequency of urination (Muruganandham et al., 2007). Palliative treatment of BPH typically involves trans-urethral resection of the prostate (TURP) to reduce the pressure on the bladder and obstruction of the urethra (Bozdar et al., 2010).

1.2.3. Prostate Intraepithelial Neoplasia

Prostate Intraepithelial Neoplasia (PIN) is a pre-invasive abnormal proliferation within pre-existing ducts and acini, most commonly affecting the peripheral zone (Bostwick et al., 2004). Cytological and histological abnormalities, such as nuclear and nucleolar enlargement as well as loss of stratification of the epithelial bilayer are also apparent. These abnormalities are also associated with CaP and therefore it is unsurprising that high-grade PIN (HGPIN) is considered to be a predictive precursor of malignant disease. A

molecular example of this is *ERG* rearrangement present in at least some HGPIN specimens (Morais et al., 2016).

1.3. Prostate Cancer

1.3.1. Epidemiology of Prostate Cancer

The lifetime risk of developing prostate cancer is 1 in 8 for men in the UK. In 2013, there were 47,300 new cases of prostate cancer in the UK (Cancer Research UK, 2016) (Fig. 5.). The latest analysis of prostate cancer incidence shows that there is no statistically significant geographical variation in prostate cancer incidence within the UK (Cancer Research UK, 2016). In contrast, there is a significant correlation between prostate cancer incidence and age. For example, 54% of new cases of prostate cancer were diagnosed in men aged 70 years and over, whilst only 1% were diagnosed in the under-50s (Cancer Research UK, 2016). However, in men aged 75 and over (in the UK) incidence has decreased from 46% to 36% in the last 30 years (Cancer Research UK, 2016). This can be explained by the more efficient detection of early stage disease in relatively younger patients by PSA testing.

Prostate cancer incidence rates have increased overall in the UK since the late-1970s and this finding is mirrored around the globe (Cancer Research UK, 2016). Much of the increase in incidence both in the UK and in many other countries worldwide can be attributed to incidental detection of prostate cancers following transurethral resection of the prostate (TURP) and PSA screening. In addition to more efficient detection of CaP, it is also likely that increased CaP incidence is rising alongside the average age of the population.

The genetic background of the individual is also a major contributing factor to the development of CaP. This is evident when looking at the age-standardised rates of CaP for different racial profiles. These data show that white males have an incident rate of 96.0 to 99.9 per 100,000 which is significantly greater than the rates for Asian males (28.7 to 60.6 per 100,000) and significantly lower than the most at risk population – black males (120.8 to 247.9 per 100,000) (Cancer Research UK, 2016).

In general CaP has a low mortality rate when compared to other cancers, such as pancreatic cancer (Carter and Nguyen, 2012). A demonstrative statistic of this is: in 2012

more than 181,000 men with prostate cancer were still alive ten years after diagnosis (Cancer Research UK, 2016).

A

B
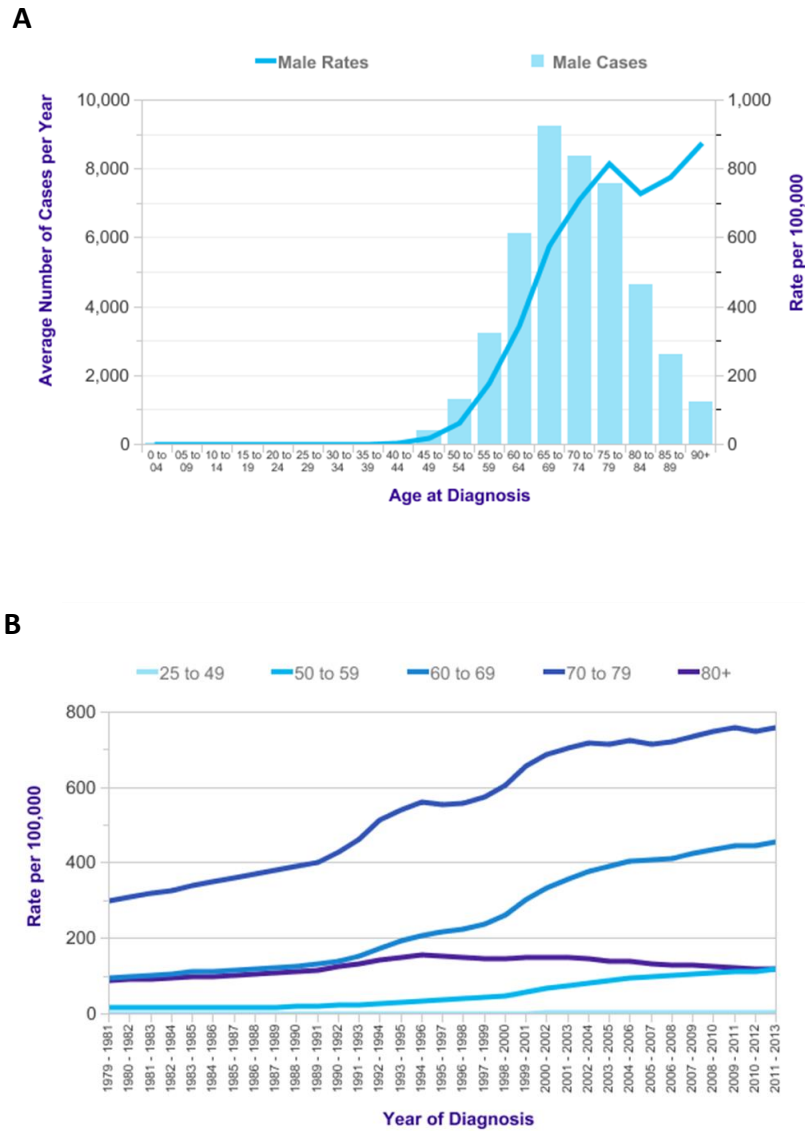
Fig. 5. Prostate Cancer Statistics.

A. The mean number of new CaP cases diagnosed (grouped by age) and age-specific incidence rates per 100,000 people of CaP diagnosed in the UK between 2011-2013. Modified from (Cancer Research UK).

B. European age-standardised incidence rates per 100,000 plotted against year of diagnosis for several age groups.

From: (Cancer Research UK, 2016)

1.3.2. Low Grade-Organ Confined CaP

CaP is characterised by aberrant differentiation resulting in the accumulation of abnormally differentiated and replicating AR expressing luminal cells, (to >99% of all epithelial cells) (Nagle et al., 1987). Alongside this dramatic increase in luminal cells there is a concomitant decrease in the percentage of basal cells (Grisanzio and Signoretti, 2008) and a progressive loss of glandular structure as the disease progresses. These observations were originally made by Gleason, who classified them in the grading system for CaP that bears his name (Fig. 6.) (Gleason, 1966, Humphrey, 2004). Another gross histological change associated with invasive CaP is the destruction of the BM.
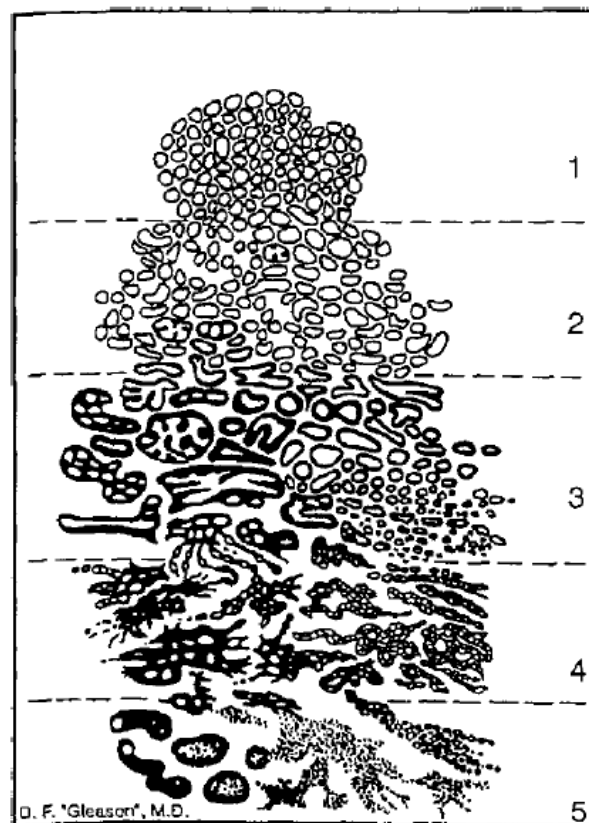
Fig. 6. Schematic of the Gleason Grading Criterion.

Histology patterns of CaP corresponding to Gleason grade. All black depicts cancer, most cytological detail is omitted except in the right side of pattern 4, where tiny structures are intended to describe a hypernephroid pattern.

From: (Humphrey, 2004)

1.3.3. Cancer-Cell Invasion and Metastasis

Escape of CaP from the prostate capsule is associated with a significant increase in mortality, i.e. the five-year survival rate for organ-confined CaP is 100%, whereas for metastatic disease, it is 30.6% (Schroder, 2012). Prostatectomy and radiotherapy are only effective in treating locally invasive lesions and as such they do not represent curative therapy once the tumour has disseminated (Lang et al., 2009, Schroder, 2012). Skeletal metastasis is the most significant cause of morbidity and mortality in CaP and is present in 90% of patients who die as a result of CaP. According to the 'seed and soil hypothesis' (proposed by Stephen Paget in 1889 as a means to explain the non-random distribution of breast cancer metastasis) disseminating tumour cells (seeds) will preferentially grow at sites with a compatible microenvironment (soil) (Langley and Fidler, 2011). This frequency indicates that the microenvironment of the bone is well suited to promote survival and expansion of CaP cells. Alternatively (or concomitantly) CaP may have the propensity to develop a homing ability specific to this site. Other common sites for metastatic spread of CaP are the lymphatic system, liver and lung (Schroder, 2012).

Distant metastases are established through a complex cascade of events termed the invasion-metastasis cascade: The first step is local-invasion through the BM and stroma typically through epithelial-to-mesenchymal transition (EMT). Cancer cells may invade via mesenchymal or amoeboid invasion programs depending on the microenvironmental conditions (Valastyan and Weinberg, 2011). The best characterised change during EMT is loss of E-cadherin expression. After escape from the local-environment the disseminating cells enter lymphatic system or blood vessels by intravasation. Circulating tumour cells (CTC) can be isolated from liquid biopsies taken from patients with a range metastatic cancers including but not limited to breast, colon, and prostate cancer (Giuliano et al., 2014, Danila et al., 2011, Nagrath et al., 2007). After transport the metastatic cells must then arrest at a compatible site. Individual primary tumours preferentially metastasise to specific secondary organs. In the case of CaP, the primary site of metastasis is the bone (90%) (Bubendorf et al., 2000). In order to enter the secondary tissue the metastatic carcinoma cells must escape the circulatory system. One mechanism by which extravasation can be achieved in a non-specific manner is by inducing capillary vessel failure by pressure exerted by colony expansion within the vessel, allowing the cancer cells to be in direct contact with the new tissue (Al-Mehdi et al., 2000, Stoletov et al., 2010). Finally the metastatic cells must be able to survive and proliferate at the secondary

site in order to produce a secondary tumour. The microenvironment of the metastatic site usually differs vastly from the primary site, but may have enough similarity or compensate with alternative growth/survival factors to allow outgrowth. Alternatively the new site may be co-opted to produce the necessary factors to allow survival and proliferation (Psaila and Lyden, 2009). After overcoming the challenges of a new microenvironment, a small fraction of disseminated cancer cells may form a clinically significant metastasis. Not every cell in a tumour possesses the ability to metastasise to distant organs, and the evidence suggests that metastases directly arise from cancer stem cells (CSC)s (Hermann et al., 2007).

1.3.4. Diagnostics in Prostate Cancer

As with all cancers, prognosis is drastically improved if the disease is discovered at an early stage. As such serum biomarker measurements have been developed to augment detection, via traditional digital rectal examination and symptomatic presentation. Serological biomarkers used in the screening of CaP include, but are not limited to, prostate cancer gene 3 (PCA3) and PSA (Schroder, 2012). However, the most prognostic diagnostic procedure is histological analysis of biopsied tissue according to the Gleason score (Gleason, 1966).

1.3.4.1. PSA Testing

Currently, diagnosis of CaP relies on the quantification of serum PSA levels (Placer and Morote, 2011). Increased PSA in the serum is linked to CaP progression. PSA testing (using >4 ng/ml as a cut-off) has a false positive rate of 34.5% and a false negative rate of 28.8% (Brawer, 1999). The false positive rate can be cut by approximately one third by increasing the cut-off to 10 ng/ml however this also comes with concomitant doubling in the false negative rate (Brawer, 1999). PSA occurs in blood as stable complexes with protease inhibitors (complexed PSA (cPSA)) or as free PSA (fPSA). Calculating the percentage of fPSA increases the diagnostic accuracy compared to total PSA levels, especially when cPSA is in the 'grey area' (4-10 ng/ml) (Catalona et al., 1998). Perhaps the biggest problem of using PSA as a diagnostic marker for CaP, is that PSA is detectable in other tissues, including: ovary, breast and lung (Smith et al., 1995). Moreover, high PSA levels are associated with other conditions including: inflammation or infection and PIN. Perhaps most importantly, it has been shown that many CaP patients have serum PSA levels within the 'normal range' i.e. less than 4 ng/ml (Thompson et al., 2004). Consequently, the use

of PSA levels as a diagnostic test should be combined with further tests, to give an accurate diagnosis.

1.3.4.2. Gleason Grading

Once elevated serum PSA is detected, multiple biopsies are taken and the histological – morphology of the tissue is graded according to the Gleason system (Fig. 7.) (Gleason, 1992). Two areas of the tissue with the most prevalent disease are graded with a value of 1-5. The grade of the two areas is then combined to give Gleason score between 2 and 10. Towards the end of the last decade, the Gleason grading system was revisited with the major aim of reducing subjectivity (Epstein, 2010). Key updates included designating all cribiform cancers and poorly formed glands as Gleason grade 4 (Epstein, 2010).

1.3.5. Current Treatments for Prostate Cancer

1.3.5.1. Active Surveillance

Some cases of low-grade CaP will not progress to a clinically relevant disease state, so active surveillance represents the most appropriate strategy. The aim of active surveillance is to omit treatment (which will negatively impact on quality of life) until the cancer is showing signs of progression. Upon which curative treatment strategies will be employed. Active surveillance involves monitoring PSA serum levels every 3 months and repeat-biopsies for histological analysis every 6-12 months

1.3.5.2. Radical Prostatectomy

Radical prostatectomy is the surgical removal of the prostate, and can be laparoscopic or via traditional open surgery (Walsh, 2005, Bill-Axelson et al., 2005). This form of intervention is the most common and most successful in treating organ confined CaP, but is obsolete when the cancer has disseminated (Bill-Axelson et al., 2005). Side-effects of this therapy include impotence (Catalona et al., 1999, Bill-Axelson et al., 2005).

1.3.5.3. Radiotherapy

Radiotherapy represents an alternative to prostatectomy (Duchesne, 2011). It involves the use of ionising radiation to destroy the malignant tissue based on the fact that cancer cells often have defects in DNA repair mechanisms which make them more susceptible to DNA damage. There are two main forms of radiotherapy namely, external beam radiation

therapy and brachytherapy (Duchesne, 2011). External beam radiotherapy, utilises an external source of radiation focused at the tumour mass. Brachytherapy involves the surgical implantation of small radioactive pellets as close as possible to the tumour mass. As such, brachytherapy is more invasive than the external beam method but has the advantage of fewer side-effects as normal surrounding tissue is exposed to much lower doses of radiation.

1.3.5.4. Androgen Deprivation Therapy

The treatment of choice for locally metastatic CaP and disseminated cancer is androgen deprivation therapy (ADT) which utilises the androgen dependent survival of luminal cells to cause dramatic reduction in tumour burden. This form of treatment was pioneered by Huggins in the 1940's, using orchiectomy to dramatically reduce androgen production (Maitland et al., 2006, Huggins et al., 1941). Orchiectomy has since been largely replaced as a therapy by chemical blockade of AR-ligand binding. Today there are several therapeutic agents that act to disrupt the androgen axis at various points, this ranges from disruption of androgen biosynthesis via inhibition of the cytochrome P450 17A1 (CYP17) enzyme (Abiraterone) to suppression of testosterone production through the gonadotropin-releasing hormone (GnRH) agonist – Zoladex (de Bono et al., 2011, Peeling, 1989).

After the initial success of ADT there is an almost inevitable re-emergence of the disease, which returns with increased aggressiveness. As such ADT has been described as palliative rather than curative (Azzouni and Mohler, 2012, Lorente et al., 2015).

1.3.6. Castration-Resistant Prostate Cancer

CaP which has relapsed following ADT is termed castrate resistant CaP (CRPC). CRPC is incurable by current treatment strategies and is associated with dramatically increased mortality due to its highly aggressive nature. CRPC has an average survival rate of 2-3 years. Even with the initiation of chemotherapy regimens, such as docetaxel (alone or as part of a combination therapy) median survival is only extended by a few months (Dubrovska et al., 2012).

The prevailing model proposes that CRPC arises through neo-Darwinian evolution of CaP in response to ADT (Stanevsky et al., 2013, Gingrich et al., 1996, Saraon et al., 2011). In

this model, rare cells with an inherent survival advantage to low androgen levels are selected by ADT.

Counter intuitively, CRPC remains dependent on AR function for maintenance and expansion (Shen and Abate-Shen, 2010). This can be explained by examining the common mechanisms by which castrate resistance has been shown to evolve. Genomic amplification of the *AR* gene (GAAR) (located on the X chromosome at Xq11-12) is the most frequent genetic alteration in CaP which results in increased AR expression (Waltering et al., 2012). It has been shown that amplification of the *AR* gene leads to increased AR expression at both the mRNA and protein levels (Waltering et al., 2012). Increasing AR expression sensitises CaP cells to very low levels of circulating androgens that persist during ADT (Waltering et al., 2012). GAAR has been detected in up to 80% of CRPCs, of which 30% have a high level amplification (≥3.8 copies per cell) (Visakorpi et al., 1995, Waltering et al., 2012). In contrast, *AR* amplification represents a very rare event in hormone-naïve CaP.

Gain of function mutations can result in a mutated-AR with increased affinity for androgens compared to wild type or relaxed ligand specificity (Nadiminty and Gao, 2012). In addition, constitutively active splice variants of AR also contribute to the development of a CRPC phenotype (Marcias et al., 2010, Hu et al., 2011, Hörnberg et al., 2011, Hu et al., 2012). Alternatively, mutation can result in a constitutively active AR which is independent of ligand binding for its function (Dubrovska et al., 2012, Céraline et al., 2004, Lapouge et al., 2007).

1.4. Cancer Stem Cells

The initiation and development of prostate cancer can be described by two models, 'the stochastic model' and the 'hierarchy model'.

The stochastic model views the tumour as a homogeneous cellular mass, with every cell possessing the ability to initiate tumour formation (Iyer and Saksena, 1970).

Currently the most widely accepted model of cancer initiation and progression is the hierarchy model which is also referred to as the CSC model. The hierarchy model views the cancer as a heterogeneous population displaying a hierarchical organisation. Cancer

is proposed to be the outcome of aberrant organogenesis (Chandler and Lagasse, 2010). Within this hierarchy only a subset of cells are capable of founding and maintain a cancer, these cells are termed cancer CSCs (Chandler and Lagasse, 2010).

The first discovery of CSCs was in acute myeloid leukaemia in the mid-1990s (Lapidot et al., 1994). These leukemic stem cells represented only a small fraction of leukaemia cells (0.2%) and shared key cell surface expression characteristics with normal hematopoietic stem cells (CD34+ CD38-) (Bonnet and Dick, 1997). Only those cells were able to recapitulate the original tumour when serially transplanted in non-obese diabetic severe combined immunodeficiency (NOD-SCID) mice (Bonnet and Dick, 1997). There is now a plethora of evidence for CSCs in many diverse solid cancers (Al-Hajj et al., 2003, Singh et al., 2004, Ricci-Vitiani et al., 2007, Eramo et al., 2008, He et al., 2009) including CaP (Collins et al., 2005). This explosion in CSC identification was facilitated by the identification of normal tissue stem cells and the markers used to isolate them. A matter of debate within the CSC field is the origin of the CSC, which is proposed to be the normal stem cell or short lived progenitor cells that have acquired the ability to self-renew (Fig. 7.) (Al-Hajj et al., 2004) (Chandler and Lagasse, 2010).
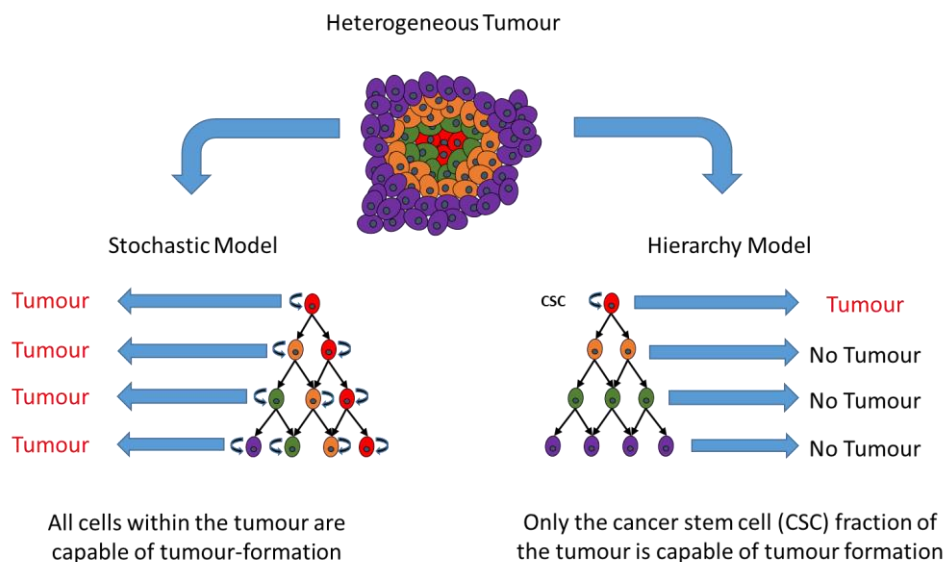
Fig. 7. Comparison of the Stochastic and Hierarchy Models of Cancer.

Comparison of the two major models of cellular heterogeneity in cancer namely the stochastic model and the hierarchy model. In the stochastic model every cell has the potential for toumorigenisis. In the hierarchy model only the CSC compartment is tumuorigenic.

⊊ = self-renewal

There are two core properties of CSCs, which are shared with normal SCs, 'property 1' the ability to self-renew i.e. a proportion of the CSC-progeny are themselves CSCs and 'property 2' is the ability to give rise to the various cells found in the original malignancy (Vermeulen et al., 2008). Experimentally, both properties are interrogated by serial-xenotransplantation into immune-compromised mice. This experiment allows histological analysis of the resulting tumour allowing comparison to the original tumour. Additionally if the resulting tumour can be serially transplanted, this demonstrates the self-renewal capacity of the CSC population (Vermeulen et al., 2008).

1.4.1. Therapeutic Implications of CSCs

Conventional cancer therapy regimens specifically target rapidly dividing cells which is a hallmark of the majority of cells within a tumour. Such therapies can be very efficient at inducing clinical remission associated with a reduction in tumour-mass and disease biomarkers (Smith and Pienta, 1999, Tabarestani and Ghafouri-Fard, 2012). A major caveat of this form of intervention is that CSCs are inherently resistant to traditional chemotherapy and radiotherapy (Kim et al., 2009). They are therefore preferentially spared by these treatments, leading to a net enrichment (Gupta et al., 2009, Rich, 2007, Costello et al., 2000). After initial treatment success, relapse often occurs with the returning disease having a more invasive and resistant phenotype (Crawford et al., 1989, Scher et al., 2008). The development of resistance in the returning bulk tumour is due to the CSC population (accelerated by their genetic and epigenetic plasticity) resulting in the ability to produce resistant progeny (Vinogradova et al., 2015, Tabarestani and Ghafouri-Fard, 2012, Yang et al., 2014).

Mechanisms of CSC resistance include: low mitotic activity, resistance to DNA damage, efflux of cytotoxic compounds and an elevated apoptotic threshold. One of the reasons why normal SCs divide infrequently and cellular amplification is undertaken by intermediate cells on the path to differentiation is to minimise the potential for replication errors and hence mutation within the SC population. This lack of proliferation confers resistance to drugs that induce cell-death by causing mitotic arrest e.g. taxanes (Murray et al., 2012).

For normal homeostatic turnover and function of a tissue to be maintained throughout the lifetime of an organism, the SC compartment must be maintained. When non-stem

cells incur DNA damage that is beyond a threshold of repair they undergo senescence or apoptosis, preventing the propagation of mutations. The same is true for SCs however, the threshold is much greater due to increased expression of DNA repair pathways. CSCs also have augmented DNA repair systems which grants them increased resistance to genotoxic stress induced by radiotherapy (Bao et al., 2006, Rich, 2007, Ishii et al., 2008).

Chemical agents must achieve a certain concentration to exert their effect on a particular system. A further mechanism by which normal SCs limit the potential for DNA damage is to actively pump cytotoxic compounds out of the cell (Dean, 2009). This is achieved by high expression of ATP-binding cassette (ABC) transporters (Dean, 2009, Elliott et al., 2010). These pumps offer multi-drug resistance, as a single transporter (within this gene family) has the ability to efflux several diverse molecules. It has been shown that CSCs also share this feature (Dean, 2009, Gatti et al., 2009).

As well as indirect mechanisms to reduce apoptotic events, CSCs also have perturbed apoptosis pathways, such as increased expression of anti-apoptotic proteins such as B-cell lymphoma 2 (bcl-2) and survivin (Hambardzumyan et al., 2008, Altieri, 2013, An et al., 2007).

1.4.2. Prostate Stem cells and Cancer Stem Cells

Early and compelling evidence of a SC population within the normal adult prostate came from observations of androgen cycling experiments (castration followed by androgen restoration in male rats) (Kyprianou and Isaacs, 1988, English et al., 1989, Evans and Chandler, 1987). Upon castration it was observed that the prostate undergoes rapid involution and, with the restoration of androgens, the gland regenerates both morphologically and functionally (English et al., 1989). The key findings of these experiments were: Firstly, the cycle of involution and regeneration can be performed many times and restoration of physiological levels of androgens even after long term castration (>3 years) resulted in full prostate regeneration (Isaacs et al., 1987). This implies the existence of a long lived prostate SC within the prostatic epithelium (Isaacs et al., 1987). Secondly, 90% of prostate epithelial are cells lost through apoptosis upon castration. This, alongside the loss of secretory activity of the prostate, indicates that the secretory luminal compartment is preferentially destroyed by castration (Bonkhoff and Remberger, 1996, Wang et al., 2015). Thus the prostate SCs are independent of

androgens for survival, but are capable of producing differentiated luminal progeny upon restoration of androgens (Bonkhoff and Remberger, 1996, Wang et al., 2015).

The phenotype of the murine SC, i.e. basal or luminal is a topic of much debate and experimental endeavour. 5-bromo-2'-deoxyuridine (BRDU) incorporation assays showed that quiescent label retaining cells were present in both basal and luminal populations (Tsujimura et al., 2002). Fractionation experiments utilising the stem cells antigen-1 (Sca-1) cell surface antigen led to the identification of rare (lineage markers (Lin)-, Sca-1+, cluster of differentiation (CD)133+, CD44+, CD117+) cells which have the capacity to recapitulate a complete prostate acinus *in vivo* (Leong et al., 2008). In support of a luminal phenotype, castration-resistant Nkx3.1-expressing cells (CARN cells), which express CK18, AR and are p63 negative, are capable of regenerating both luminal and basal cells after androgen cycling (Wang et al., 2009). CARN cells were also capable of reconstituting vestigial prostate structures *in vivo*, upon engraftment of a single cell (Wang et al., 2009). Both basal and luminal progenitor fractions are capable of tumourigenesis when manipulated in a physiologically relevant way i.e. after phosphatase and tensin homolog (*PTEN*) deletion (Lawson et al., 2010, Choi et al., 2012, Korsten et al., 2009). The likelihood is that several murine prostate-progenitor compartments could be the cell type of origin of CaP, but which one is dominant in nature is hard to establish as mice, unlike dogs and humans, do not spontaneously develop CaP without genetic manipulation. Furthermore due to the morphological and histological differences between the rodent and human prostate, both pre- and post- castration (Fig. 8.), it is debatable whether translation of paradigms from mouse to man is valid (Maitland, 2013).

In contrast to rodent models, there is a large body of evidence that the normal human prostate epithelial SC resides in the basal compartment. For example, it was found that only p63 positive cells were present after the xenografting of benign human prostate glands into immunocompromised mice and subjecting the host to prolonged periods of castration (Huss et al., 2004). Additionally, tumour-associated calcium signal transducer 2 (Trop2)+, CD44+, CD49f-high, basal cells had sphere-forming ability *in vitro* and could regenerate prostate structures *in vivo* (Goldstein et al., 2010, Garraway et al., 2010).

Perhaps the most compelling evidence of a common SC for all human prostate epithelial cells came from *in situ* lineage tracking, which utilises the unique accumulation of

mitochondrial mutations in SCs which leads to traceable respiratory chain defects e.g. cytochrome c oxidase activity (Blackwood et al., 2011). This natural 'barcoding' is retained in their progeny (Blackwood et al., 2011). These experiments performed in human tissue showed an entire acinus including basal, luminal, and even neuroendocrine cells were formed from the progeny of a single cell (Blackwood et al., 2011).

Collins et al., (2001) utilised the combined knowledge of prostate SCs residing within the basal cell compartment and the composition of the BM (collagen type I and IV) to develop a method for enriching for cells with stem-like properties. This group used CD44 expression to fractionate the basal cells followed by selection of cells which adhered rapidly (within 5 minutes) to collagen type I (high expression of α2β1 integrin). It was found that the enriched basal population had enhanced colony forming efficiency *in vitro* and when transplanted into immune compromised mice, formed prostatic-like acini which stained positively for basal and luminal cytokeratins, AR, PAP and PSA (Collins et al., 2001). There are similarities with other SC systems, such as the skin, where adhesion to the BM is important for spatial regulation of SCs within a niche (Jones and Watt, 1993). Work from the same laboratory showed that the $\alpha2\beta1^{hi}$ population could be further enriched for colony forming efficiency and development of prostatic acini *in vivo* by including the SC marker CD133 in the selection protocol (Richardson et al., 2004).

As with other cancers (Adhikari et al., 2011) it was found that CSCs resident within CaP tumours could be isolated based on the presence of the same cell surface markers as their non-malignant counterparts, namely: CD44, α2β1 and CD133 (Collins et al., 2005). These cells have extensive proliferation potential, increased invasiveness in Matrigel™ assays and the ability to differentiate into cells with a luminal phenotype (AR+, PAP+, CK18 (Collins et al., 2005, Lang et al., 2009)). Even more compelling evidence for the existence of a basal CSC in CaP comes from xenotransplantation studies in which fewer than 100 cells expressing glycosylated CD133 were required to initiate tumour growth in immunodeficient mice harbouring homozygous deletion of recombination activating gene 2 (*Rag2*) and Interleukin (IL)-2 receptor γ-chain gene (*γC*) (leading to a complete block of both B and T cell development) bred on a BALB/c background (BALB/c/RAG2-/-/γC-/-). This was in contrast to cells displaying a luminal phenotype (CD24) from the same tumours (Maitland et al., 2011).

Further evidence in support of human CaP CSCs having a basal phenotype was provided by (Rajasekhar et al., 2011), who isolated *in vivo* tumour-initiating cells (TICs) that did not express luminal markers such as AR or PSA, but were positive for basal markers (CD44 and elevated integrin expression). These cells were capable of *in vitro* sphere-formation and *in vivo* tumour-initiation in which they recapitulated the heterogeneity of the original parent tumour (Rajasekhar et al., 2011). Conversely fractionated tumour prostate-specific membrane antigen (PSMA) positive cells were not tumourigenic *in vivo* (Rajasekhar et al., 2011). Using a modified Hoechst 33342 dye efflux assay, Brown *et al* identified a stem cell enriched side population (SP) with high efflux capacity consistent with other SC and CSC systems (Brown et al., 2007). These cells could be induced to form spheroids with acinus like morphology *in vitro* by 3D culture in the presence of androgens (Brown et al., 2007). The SP population was immuno-phenotyped and was found to be enriched for cells expressing basal markers such as CK5 and CK14 (Brown et al., 2007).

In conclusion, the available evidence suggests that the human prostate SC is resident within the basal compartment and has a cell surface expression and cytokeratin profile consistent with basal cells. Currently there is little evidence to suggest a luminal stem cell compartment as seen in rodents.
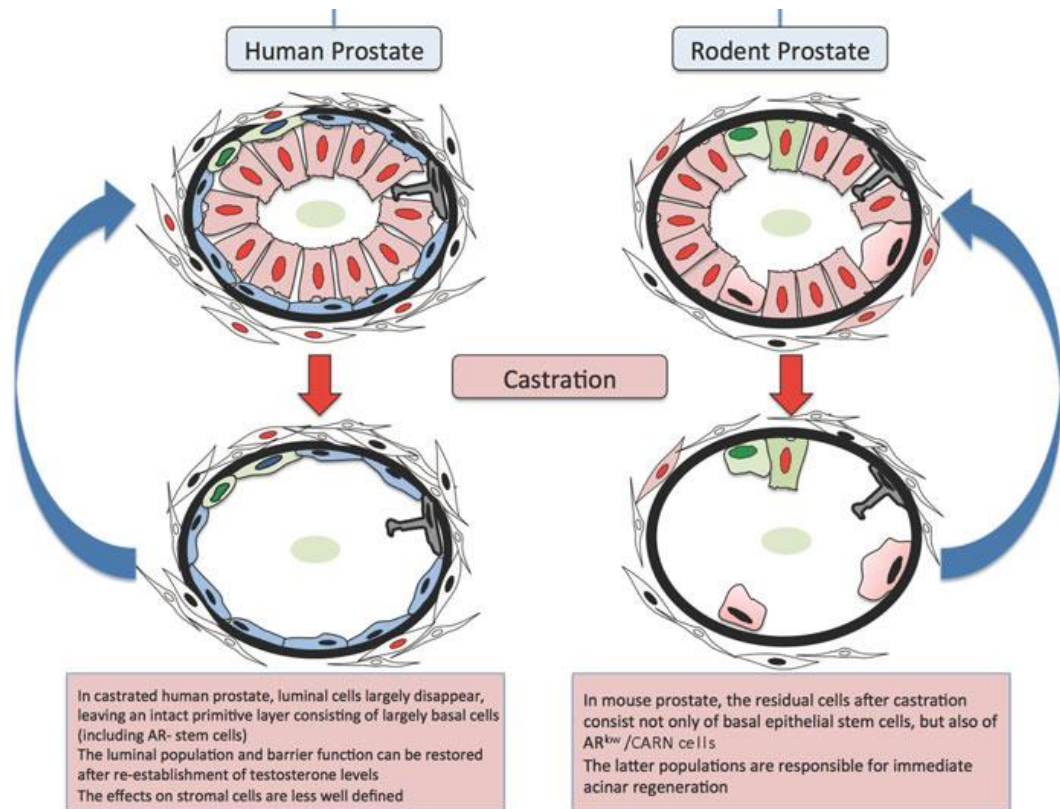
Fig. 8. Castration-Induced Prostate Gland Involution.

Stem cells in the epithelial and stromal compartments are shown in *green,* basal cells in *blue,* and luminal cells in *pink,* with cells positive for AR-expression are depicted by *red* nuclei*.* Hormone-responsive stromal cells are also shown in *pink*. The effects of androgen withdrawal upon castration are distinct in human and rodent, prostates, reflecting the distinctive anatomies of the prostate tissue from these sources.

From: (Maitland, 2013)

1.5. Introduction to Models

1.5.1. Cell Lines

There are several established cell lines representing normal, BPH, CaP and CRPC phenotypes (Berthon et al., 1995, Hayward et al., 1995, Maitland et al., 2001, Miki et al., 2007, Attard et al., 2009, Marques et al., 2006, Horoszewicz et al., 1980, Korenchuk et al., 2001, Stone et al., 1978, Kaighn et al., 1979). They represent the traditional modes for studying CaP, and are as such well-studied experimentally. Cell lines have several advantages as model systems, they can be maintained for extended passages, are easily manipulated, can be adapted to culture under different conditions and are readily transfectable.

Alongside these advantages there are also significant disadvantages in the predictive value of cell lines. Long-term culture of cells in serum-containing media can induce karyotype defects (Lee et al., 2006). Also there are gross changes in gene expression profiles due to genome-wide DNA hypermethylation (Meissner et al., 2008). Perhaps most importantly, due to their clonal nature, they do not represent the cellular heterogeneity observed in human disease.

In summary, cell lines are an excellent model for optimising protocols, testing hypothesis and generating preliminary data. However, due to the limitations discussed above they are often not clinically predictive. As such a number of well characterised cell lines are used in this project representing benign, malignant and metastatic models of CaP, isolated from various tissues (Table. 2).

Cell Line	Origin	Method of immortalisation	Reference	Increasing Malignancy
PNT1a PNT2-C2	Normal prostate cells originating from young male organ donors	Transfection with SV40 large T antigen	(Berthon et al., 1995)	
BPH-1	TURP of a BPH tissue	Transfection with SV40 large T antigen	(Hayward et al., 1995)	
P4E6	Well-differentiated early Gleason 4 cancer tissue	Transfection with human papillomavirus-16 *E6* gene	(Maitland et al., 2001).	
RC165	Primary benign tissues of African-American prostate cancer patients	Telomerase	(Miki et al., 2007).	
Bob	TURP of CRPC tissue	Spontaneous	(Attard et al., 2009)	
Serbob	TURP of CRPC tissue	Spontaneous	(Attard et al., 2009)	
PC346C	Advanced, but not metastatic, prostate adenocarcinoma removed via TURP and subcutaneously implanted into athymic mice	Transfection with retrovirus	(Marques et al., 2006)	
LNCaP	Left supraclavicular lymph node metastasis		(Horoszewicz et al., 1980)	
VCaP	Bone metastasis		(Korenchuk et al., 2001)	
DU145	Isolated from the brain of a patient with CaP metastasis		(Stone et al., 1978)	
PC3	Bone metastasis from grade 4 prostate adenocarcinoma		(Kaighn et al., 1979)	

Table. 2. Prostate Cell Lines.

From: (Oldridge, 2012)

1.5.2. Primary Cultures

Primary prostate cells from normal, benign or malignant patient tissues can be cultured *in vitro* following enzymatic cellular-dissociation or explant outgrowth (Niranjan et al., 2013, Frame et al., 2016, Peehl, 2005). Epithelial cultures were derived from samples taken, with consent and ethical approval, from patients undergoing radical prostatectomy, TURP or cystectomy. Primary cultures offer several advantages over cell line models. Most importantly, primary cultures have not been immortalised by strong oncogenes such as simian vacuolating virus 40 (SV40) large T antigen. They also retain cellular heterogeneity in early passage cultures which is lost in cell lines after repeated passages. Additionally, there is less culture-related karyotype and methylome changes although these abnormalities increase with serial passaging (Liang and Zhang, 2013).

There are also several disadvantages of primary *in vitro* prostate cultures as an experimental tool. Importantly, primary cultures have a limited life-span and are difficult to manipulate by traditional transfection. Also, primary cultures select for more proliferative cells with a predominantly basal phenotype. Prostate cancer is characterised by an accumulation of luminal cells which do not survive or proliferate *in vitro* (Peehl et al., 1994, Peehl, 2005, Frame et al., 2016). Another major disadvantage of primary cultures, is that there are currently no cell-surface markers that can distinguish normal from malignant cells. Consequently, normal cells overgrow malignant cells after extended passage (Chen et al., 2012, Peehl, 2005).

Primary cultures represent the best *in vitro* strategy to investigate CaP having been shown to be a better predictive model than cell lines (Peehl, 2005, Niranjan et al., 2013, Miki et al., 2007). However, it must be noted that several (typically three or more) patient samples must be investigated due to the inter-patient heterogeneity of disease. This can be in both a gross (Gleason grade) and subtle way e.g. presence of transmembrane protease, serine 2 (*TMPRSS2*) to ETS-related gene (*ERG*) gene fusion (*TMPRSS2-ERG*) and/or PTEN status.

1.5.3. Mouse Models

Transgenic mouse models, have traditionally utilised a potent oncogene, typically SV40 large T antigen under the control of a prostate specific promoter such as the probasin promoter (e.g. Transgenic Adenocarcinoma Mouse Prostate (TRAMP) mice)) (Greenberg et al., 1995, Asamoto et al., 2001). SV40 large T antigen is a viral oncogene, known to

inactivate the critical cellular tumour-suppressor protein - tumour protein p53 (p53) and retinoblastoma protein (Rb) (Ahuja et al., 2005). The TRAMP model is characterized by spontaneous and rapid progression to prostatic neoplasia at 28 weeks, with 100% penetrance of lymph node metastasis (Greenberg et al., 1995).

One major criticism of these early transgenic mouse models is that the frequency of p53 mutations seems to be lower in CaP than in other cancers (Schlomm et al., 2008, Kubota et al., 1995), which is consistent with the observation that Li-Fraumeni patients carrying germline p53 mutation have a low incidence of CaP compared to other malignancies (Malkin, 2011).

More recent transgenic mouse models have sought to more closely mimic the human disease by utilising deletion of PTEN to induce oncogenic transformation (Wang et al., 2003, Parisotto and Metzger, 2013, Grabowska et al., 2014). PTEN deletion is the most common genetic abnormality in CaP, deletions occur in approximately 23% of HGPIN, 69% of localised CaP, and 86% of metastatic CRPC (Yoshimoto et al., 2006, Holcomb et al., 2009, Grabowska et al., 2014).

Due to neoplasia arising in multiple organs of the PTEN+/- mice and the embryonic lethality of PTEN knock-out mice, subsequent models have used targeted PTEN deletion in an organ-specific manner using CRE-LOX recombination (Kwak et al., 2013). Unfortunately these models fail to recapitulate key features of the human disease. In animals aged 11-17 weeks with established CaP, castration did extend the survival time compared to control animals. Additionally, castrated animals maintained prostates 5-10 fold larger than wild-type (WT) controls even after 11 weeks of castration (Grabowska et al., 2014, Wang et al., 2003). In these castrated animals, AR levels measured by immunohistochemistry were diminished, which is not the case in human CRPC (Wang et al., 2003, Grabowska et al., 2014, Holzbeierlein et al., 2004). Perhaps most importantly, castration or genetic ablation of the AR at any age in the PTEN flox/flox model does not prevent tumour formation, suggesting that these tumours are inherently androgen independent (Mulholland et al., 2011, Grabowska et al., 2014).

In summary, transgenic models have major advantages in terms of amenability to genetic manipulation and lineage tracking experiments which are impossible to perform in man (for ethical reasons). However, they represent at best an approximation of the human

disease which is inherently deficient due to the morphological and histological differences between the human and mouse prostate.

An alternative to transgenic systems is near-patient xenotransplantation, in which donor prostate biopsies are engrafted into immunocompromised mice such as NOD-SCID or BALB/c/RAG2-/-/γC-/- (Rea et al., 2016, Valkenburg and Williams, 2011, Nemeth et al., 1999, Lawrence et al., 2013). The grafting can be either subcutaneous, to the renal capsule (advantage of increased blood supply) or orthotopic (have the advantage of growth within the prostate microenvironment).

Subcutaneous grafts demonstrated the lowest 'take rates' and differentiation (Tentler et al., 2012). Renal subcapsular engraftment is most efficient (>90%), additionally this form of engraftment also demonstrated differentiation and expression of AR and PSA (Tentler et al., 2012). However, the orthotopic models exhibit the highest degree of differentiation e.g. AR and PSA expression (Wang et al., 2005, Tentler et al., 2012).

Xenotransplantation has many advantages over transgenic models, as no transgenes are necessary for transformation, cells retain the same unique array of genetic abnormalities present in the original disease and cells can be manipulated *ex-vivo*. As with primary cultures, inter-patient disease-heterogeneity is a confounding factor that must be accounted for by experimentation on several grafts. The presence of both benign and malignant epithelial cells in grafts accurately reflects the original tumour, but it makes analyses more difficult. A further complication is incurred by the tendency of host (murine) fibroblasts to invade the graft (Hayward et al., 1992). In conclusion, near-patient xenograft models are the 'gold standard' in which human TICs can be studied *in vivo* (Siolas and Hannon, 2013, DeRose et al., 2011). In comparison, transgenic mouse models give rise to murine tumours which may have different properties to the corresponding human disease, and *in vitro* cultures of primary human cells fail to fully replicate epithelial-stroma interactions, angiogenesis and metastasis.

1.6. Regulation of Gene Expression in the Prostate Epithelium

For the prostate epithelium to function properly it is essential that tissue homeostasis is maintained i.e. there is an equilibrium between proliferation, differentiation and self-renewal of a long-term progenitor pool. Ultimately it is the differing expression of genes at the protein level that bestows the unique properties upon each distinct cell type within the prostate epithelium. Gene expression can be modulated by controlling the

transcription of a gene and/or by controlling the translation of mRNA to protein. Transcriptional control involves regulation by specific transcription factors and co-factors within the cell which bind to their target sequences within the promoter and/or enhancer regions of the target gene. The transcriptional activity of a particular region of DNA can be silenced by reversible DNA methylation (Jones and Laird, 1999). Additionally, the accessibility of the gene to transcription factors, cofactors and the transcription machinery can be modulated at the epigenetic level by modification of histone proteins which dictate how condensed the DNA is at a particular region (Ducasse and Brown, 2006). Post-transcriptional control of gene expression has many forms which influence the rate of translation by modulating the half-life of the target mRNA species. mRNA half-life can be modulated by polyadenylation of the 3' end, capping of the 5' end, and by targeted translation silencing and/or degradation by microRNAs (miRNAs) (Ghosh and Jacobson, 2010, Huntzinger and Izaurralde, 2011).

It is accepted that androgens and therefore AR is a critical regulator of prostate epithelial cell differentiation during development (Kellokumpu-Lehtinen et al., 1981) (discussed in the next section). In addition AR signalling is essential for the survival of the exocrine luminal cells, in the adult prostate (English et al., 1987).

Inactivation of PTEN facilitates activation of phosphoinositide 3-kinase (PI3K) (Majumder and Sellers, 2005). PI3K generates phosphatidylinositol (3, 4, 5)-trisphosphate (PIP3) from phosphatidylinositol 4,5-bisphosphate (PIP2) via phosphorylation at the inner leaflet of the plasma membrane. Important downstream targets of PI3K via PIP3 include serine/threonine Kinase 1 (Akt) (Majumder and Sellers, 2005). PIP3, once generated in the plasma membrane, recruits Akt and phosphoinositide-dependent kinase-1 (PDK1) to the plasma membrane through an interaction between the phosphoinositide and Akt or PDK1 pleckstrin homology domains. Once recruited to the plasma membrane, Akt is phosphorylated and activated by PDK1. Thus, PTEN-null cells also harbour constitutively high-levels of Akt signalling, resulting in enhanced survival and proliferation (Majumder and Sellers, 2005).

Several other pathways are important in the development and differentiation of the prostate epithelium. The regulation of prostate morphogenesis is mediated, in part, by androgens, but also involves numerous signalling pathways, including Sonic hedgehog (SHH) (Sanchez et al., 2004), Fibroblast Growth Factor 10 (FGF10) (Prins and Putz, 2008) and Bone Morphogenetic Protein 4 and 7 (BMP4 and BMP7) (Pu et al., 2004). SHH and

FGF10 have been shown to promote prostate growth, while BMP4 and 7 suppress prostate branching (Prins and Putz, 2008, Pu et al., 2004, Grishina et al., 2005). A less studied signalling molecule is all-trans-retinoic acid (atRA). atRA has been shown to be a potent inducer of budding in the mouse prostate (Lohnes et al., 1995, Seo et al., 1997, Vezina et al., 2008), which involves SHH and BMP4 (increased SHH expression, and downregulation of BMP4) (Vezina et al., 2008, Lohnes et al., 1995, Seo et al., 1997).

It is important to note that signalling pathways do not operate in isolation, there is considerable cross-talk and compensatory pathways with overlapping functions to fine tune cellular behaviour (Fig. 9.) (Sarker et al., 2009).
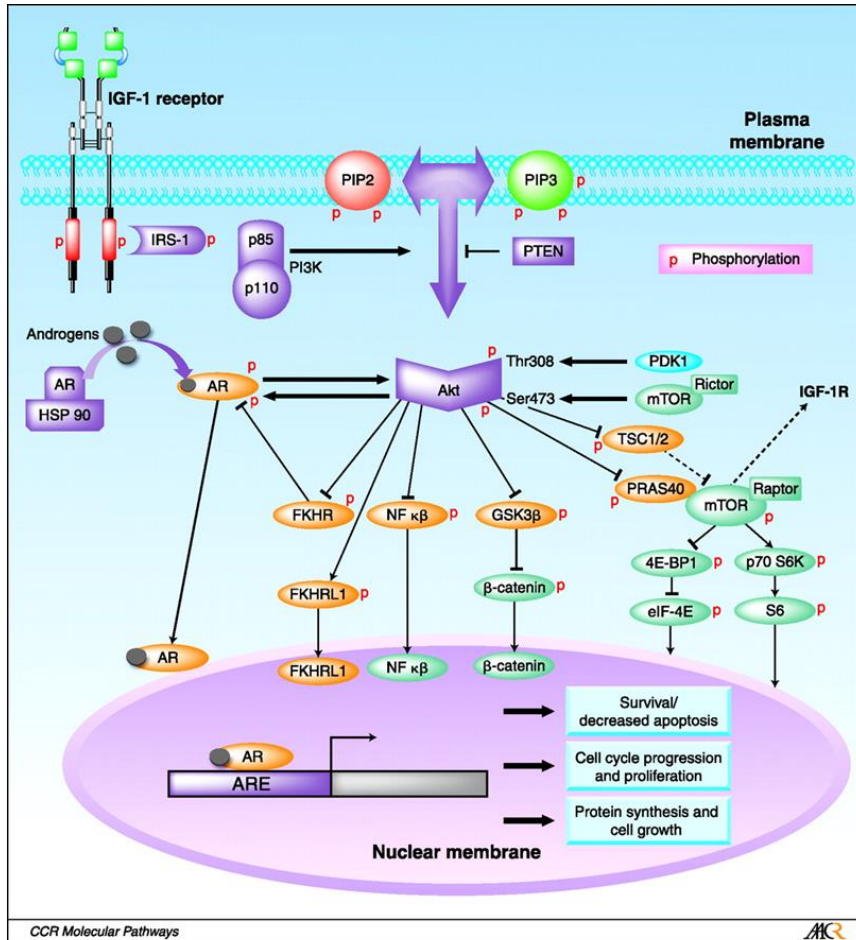
Fig. 9. Pathway Cross-talk.

The figure depicts the interaction of the PI3K/AKT pathway with AR signalling as an example of 'pathway cross-talk. In the cytoplasm, AR is bound to heat-shock protein 90 (HSP-90), this interact stabilises AR and prevents nuclear localisation. Upon androgen binding, AR undergoes a conformational change leading to dissociation from HSP-90 and subsequent phosphorylation of AR. The AR-androgen complex then able to enter the nucleus and bind androgen response elements (AREs) present within the promoters of AR-responsive genes. Binding of AR to ARE sequences induces gene expression. Activation of the PI3K pathway induces AKT phosphorylation and downstream signalling. Several downstream signalling events are likely to interact with AR transcriptional activity. These include interaction of the AR with FKHR and FKHRL1 transcription factors, cross-talk of AR and AKT with NF κβ; regulation of AR via coactivator Wnt/β- catenin, and activation of AR via the mTOR pathway.

From: (Sarker et al., 2009)

1.6.1. Androgen Signalling

The human *AR* gene is located on the X chromosome at Xq11-12 and encodes a 110 kDa nuclear transcription factor. The AR is composed of an amino (N)-terminal transactivation domain, a central DNA-binding domain, a short hinge region, and a carboxy (C)-terminal region containing a ligand-binding domain and a nuclear localization sequence (Nadiminty and Gao, 2012). The AR serves a fundamental role in prostate development, maturation and homeostasis as it mediates the stimulus produced by androgens, causing genome-wide alterations in gene expression of prostate cells, promoting proliferation, survival and differentiation (Nadiminty and Gao, 2012). DHT is the primary ligand of AR however, testosterone can bind AR directly, albeit with significantly lower affinity (Klokk et al., 2007).

In the absence of ligand, AR exists in a functionally inactive state, residing in the cytoplasm as a monomeric protein complexed with chaperones, which include heat-shock proteins (HSPs) (Saraon et al., 2011). Ligand binding induces a conformational change in AR resulting in dissociation of chaperone proteins, dimerisation and transport to the nucleus (Saraon et al., 2011). In the nucleus, AR binds to specific DNA sequences termed androgen response elements (AREs), via the DNA-binding domain, promoting further association of transcription machinery, culminating in transcription. A schematic diagram of androgen signalling is shown in (Fig. 10.) (Saraon et al., 2011, Li and Al-Azzawi, 2009).
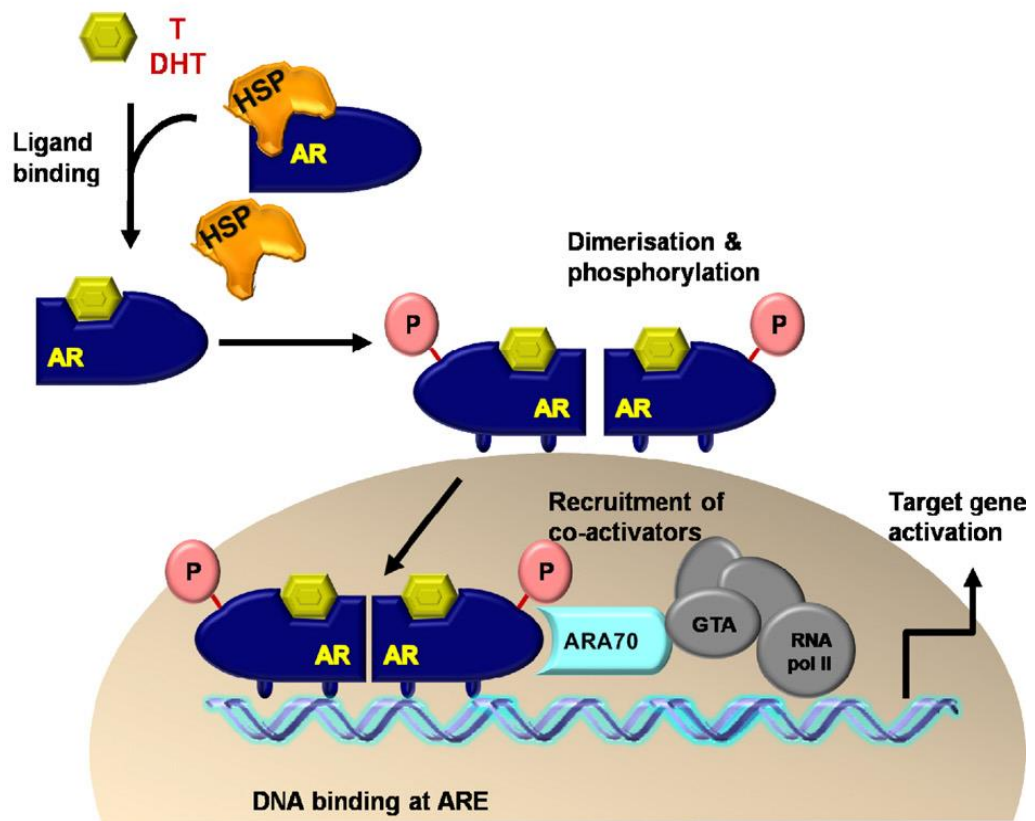
Fig. 10. Androgen Signalling.

AR binding of testosterone (T) or the more potent dihydrotestosterone (DHT) leads to dissociation of molecular heat shock protein (HSP) chaperones. This allows dimerization of AR and subsequent translocation to the nucleus where AR binds to AREs, causing recruitment of DNA transcriptional machinery and subsequent gene transcription.

From: (Li and Al-Azzawi, 2009)

1.6.2. Retinoic Acid

Retinoic acid (RA) is known to play a crucial role in the development and homeostasis of a wide range of tissues including prostate, neuronal and liver, by its regulation of numerous genes involved in differentiation, proliferation and homeostasis (Seo et al., 1997, Ito et al., 2011, Huang et al., 2009, Rhinn and Dollé, 2012).

RAs are the ligands of a family of six nuclear ligand-activated receptors, termed retinoic acid receptors (RARα, β, and γ) and retinoid X receptors (RXRα, β, and γ) (Leid et al., 1992, Kastner et al., 1997). These heterodimeric transcription factors (RAR/RXR) bind retinoic acid response elements (RAREs) in target genes in the absence of RA where they act to inhibit expression (Bastien and Rochette-Egly, 2004, Rhinn and Dollé, 2012). Upon ligand binding, a conformational change is induced which leads to transcription via displacement of a co-repressor complex and subsequent recruitment of transcriptional co-activators, thereby stimulating transcription of target genes (Fig. 11.) (Leid et al., 1992, Rhinn and Dollé, 2012).

RA has been shown to induce apoptosis through upregulation of caspase 7 and 9 in breast cancer (Donato and Noy, 2005). RA signalling promotes differentiation and also inhibits proliferation of SCs from many tissues including, mouse embryonic SC, human haematopoietic stem cells (HSCs), stem-like glioma cells and breast CSCs (Luo et al., 2007, Simandi et al., 2010, Campos et al., 2010, Ginestier et al., 2009). In agreement with these observations, inhibition of retinoid signalling induces the expansion of HSCs (Chute et al., 2006).
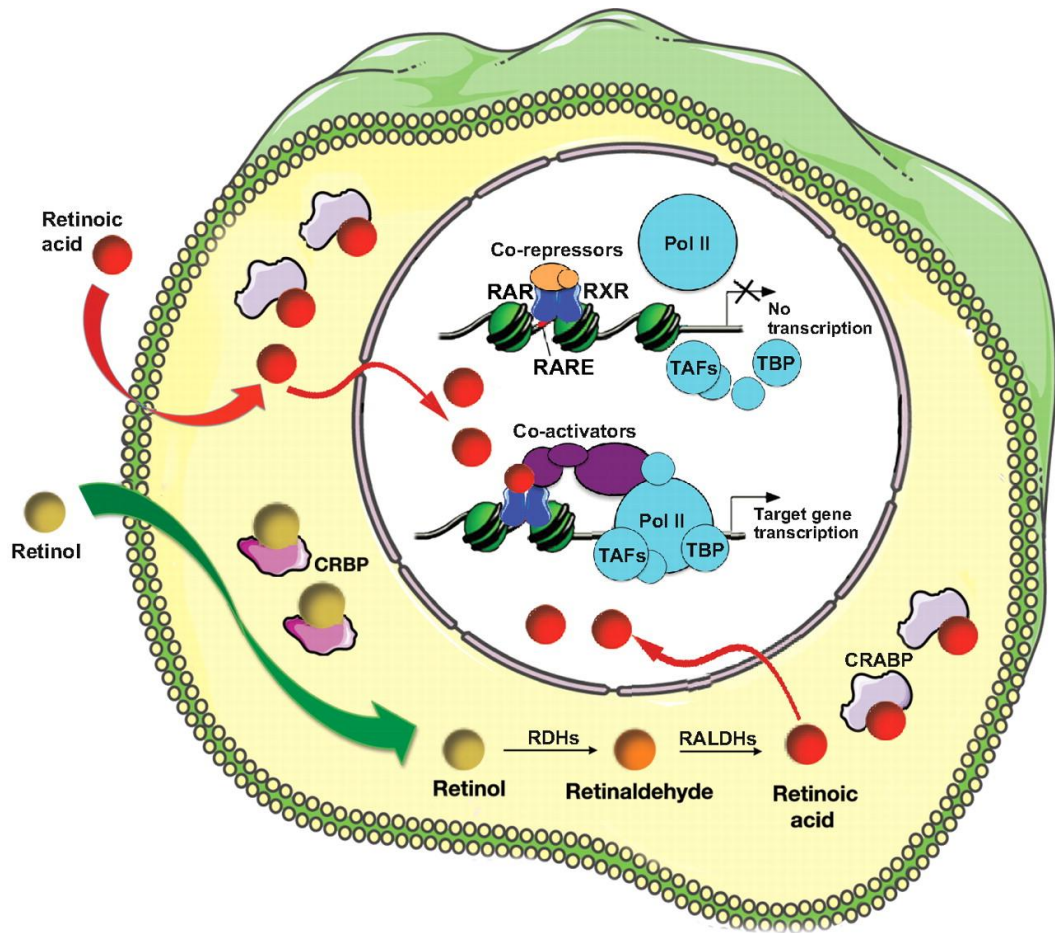
Fig. 11. Retinoic Acid Signalling.

RA is generated from circulating retinol or by diffusion from an adjacent cell (curved red arrow). RA enters the nucleus where it binds RA receptors (RARs) and retinoid X receptors (RXRs) dimers (RAR/RXR). RAR/RXR are able to bind to RA-response elements (RAREs) in target genes promoters in the absence of ligand, where the act to inhibit transcription. RA binding induces a conformational change in RAR/RXR, thereby inducing the release of co-repressors and subsequent recruitment of co-activator complexes which facilitate transcription by recruitment of RNA polymerase II (Pol II), TATA-binding protein (TBP) and TBP-associated factors (TAFs).

From: (Rhinn and Dollé, 2012)

1.7. Epigenetic Regulation

Epigenetics is the study of heritable changes in gene activity or function, in contrast to genetics, these changes are not associated with modification of the DNA sequence itself.

1.7.1. Histone Modifications and Chromatin Remodelling

The histone code (posttranslational modification(s) of histone tails) influences higher-order chromatin structure by affecting contacts between different histones and between histones and DNA (Bowman and Poirier, 2015). DNA exists in the cell as compacted chromatin, this packaging is achieved through the formation of nucleosomes in which DNA is wound round an octamer of two subunits of each of the core histones: H2A, H2B, H3, H4 and linker H1 (Mariño-Ramírez et al., 2005). By controlling chromatin architecture, the histone code is fundamental to several key cellular processes such as transcription, replication and DNA repair (Bártová et al., 2008). Chromatin exists in two major states:

- Highly condensed heterochromatin that is transcriptionally silent.
- Relaxed euchromatin that is transcriptionally active.

The core histone domain is flanked by protruding N- and C-terminal tails which are targets for several covalent modifications that determine histone-DNA interaction, including: methylation, acetylation, phosphorylation, poly-adenosine diphosphate (ADP) ribosylation, ubiquitination and glycosylation (Fig. 12.) (Bannister and Kouzarides, 2011, Kim, 2014).
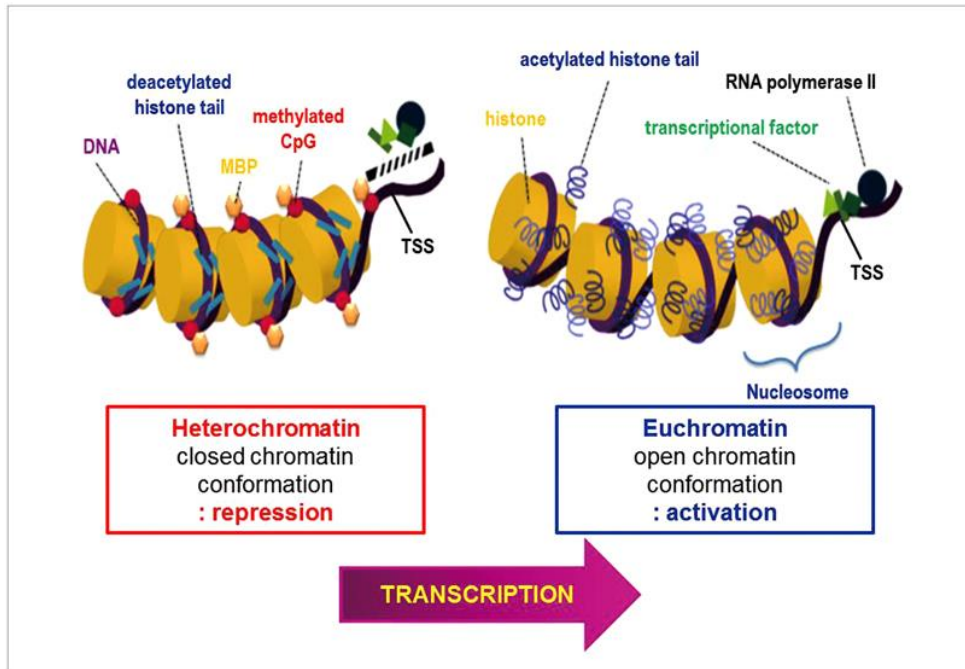
Fig. 12. Chromatin Conformations.

Schematic diagram illustrating euchromatin and heterochromatin. Heterochromatin on the left is characterized by DNA methylation and deacetylated histones, is condensed and inaccessible to transcription factors (closed chromatin conformation), which is repressive regulation of transcription. On the contrary, euchromatin on the right is in a loose form and transcriptionally active; DNA is unmethylated and histone tails acetylated (open chromatin conformation), which is active regulation of transcription

From: (Kim, 2014)

The most well studied histone-phosphorylation event is the formation of gamma H2A histone family, member X (γH2AX) which is the product of phosphorylation of serine 139 of the H2AX variant histone (Rossetto et al., 2012). This modification is one of the earliest events in response to DNA damage, and functions to direct diverse DNA repair mechanisms to the site of DNA damage. It is now recognised that histone phosphorylation also plays an important role in transcriptional regulation as well as chromatin organisation (Rossetto et al., 2012).

Acetylation and methylation are two of the best-studied histone modifications, both can play a positive and negative role in gene activation (Bannister and Kouzarides, 2011). The outcome is dependent on the nature and position of the alteration, e.g. mono-, di- or tri-methylation of lysine 27 on histone 3 (H3K4), lysine 36 on histone 3 (H3K36) and lysine 79 on histone 3 (H3K79) results in enhanced transcription but, methylation of lysine 9 on histone 3 (H3K9), lysine 27 on histone 3 (H3K27) and lysine 20 on histone 4 (H4K20) usually results in gene silencing (Vakoc et al., 2006).

Histone acetyltransferases (HATs) catalyse the acetylation of lysine residues, removing the positive charge on the histone tail, resulting in reduced affinity between histones and DNA. As a result the DNA is more accessible to the transcription machinery (Gallinari et al., 2007, Bannister and Kouzarides, 2011).

Histone deacetylases (HDACs) act in the opposite way to HATs. They deacetylate lysine residues resulting in condensed chromatin and repression of transcription in the majority of cases (Fig. 13.) (Bannister and Kouzarides, 2011, Kim, 2014). Acetylation of histones can be experimentally modified by treating cells with HDAC inhibitors (HDACI), which include trichostatin A, sodium butyrate and valproic acid (Biermann et al., 2011).
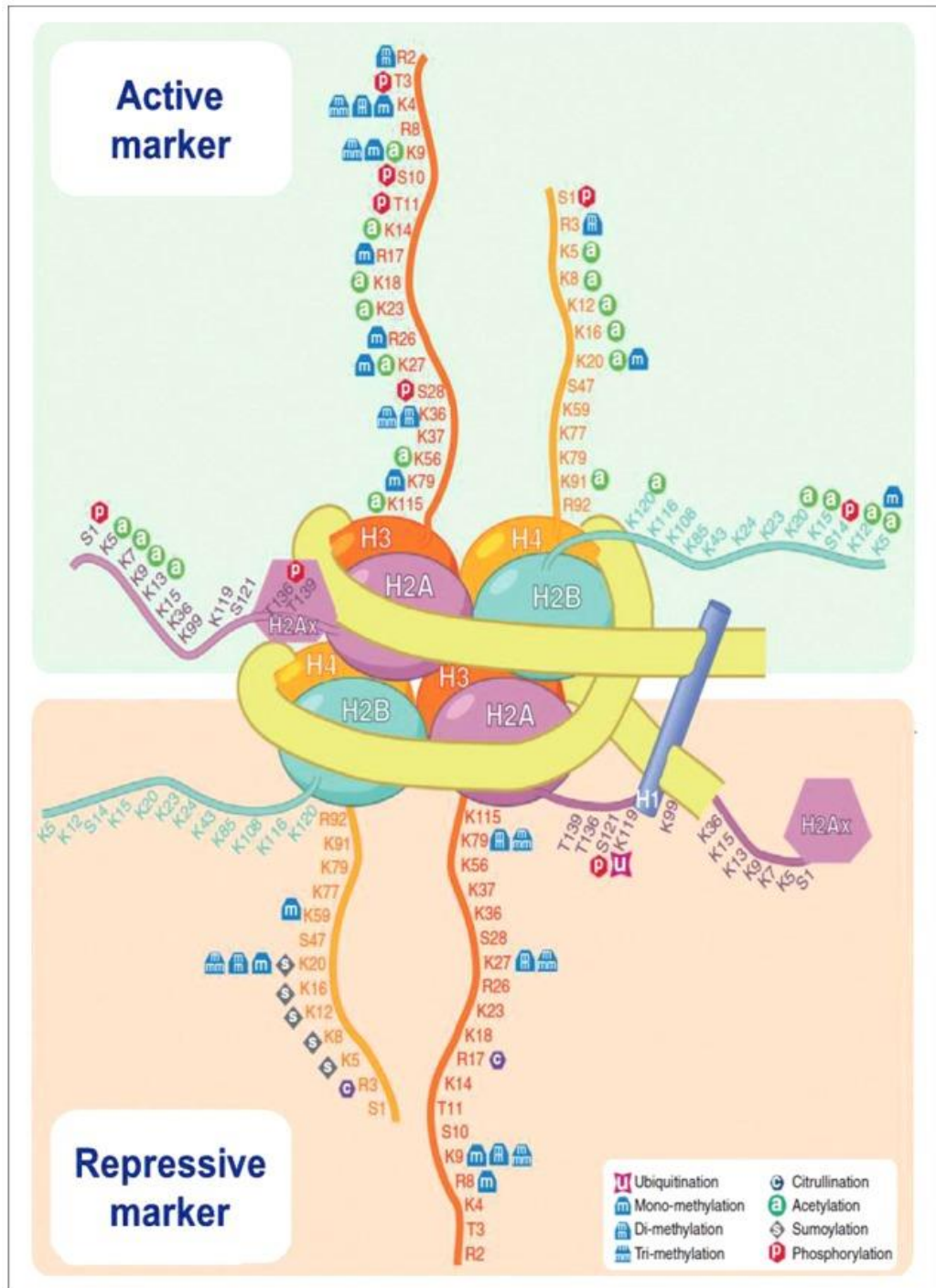
Fig. 13. Histone Tail Modifications.

Illustration of histone code according to active and repressive markers. DNA is wrapped around histone octamer of the four core histones H2A, H2B, H3, and H4. Histone H1, the linker protein, is bound to DNA between nucleosomes. Different amino acids constituting histone tails are represented along with the different covalent modification specific of each residue. Active marks are represented in the upper part of the figure and repressive marks are represented in the lower part of the figure. Lysine (K), arginine (R), serine (S), and threonine (T)

From: (Kim, 2014)

1.7.2. MicroRNAs

miRNA are small non-coding RNAs (18-25 nucleotides long), which are first synthesised as primary (Pri)-miRNA species before being subsequently processed into precursor (Pre)-miRNA (Macfarlane and Murphy, 2010). Pre-miRNAs are then exported from nucleus and cleaved in the cytoplasm to produce the mature miRNA. The mature miRNAs function by binding to complementary mRNA molecules. Modulation of mRNA expression is achieved through a RNA-induced silencing complex (RISC) which degrades target mRNAs (Macfarlane and Murphy, 2010). Cancer often displays an altered miRNA expression profile compared to normal cells, typically overexpressing oncogenic miRNAs and downregulating miRNAs that function as tumour suppressors (Sassen et al., 2008).

1.7.3. Long Non-Coding RNAs

The advent of next generation sequencing technology has facilitated the discovery of novel transcripts, a significant portion of which are not from known protein coding genes. Long non-coding RNAs (lncRNA) are >200 nucleotides in Length. lncRNAs can be antisense transcripts, pseudogenes, transcribed intronic regions, divergent transcripts (from either the sense or antisense strand of protein coding genes) or stand-alone i.e. the genomic location of these lncRNA does not overlap with protein coding genes (Kung et al., 2013).

lncRNAs are involved in several aspects of biology including imprinting and developmental regulation. One well studied role is in the inactivation of one copy of the X chromosome in females providing dosage compensation. X chromosome inactivation mainly controlled by cluster of lncRNAs collectively called the X-inactivation centre (Kung et al., 2013). In CaP, the lncRNA – PCA3 is used as a diagnostic marker as its expression is restricted to prostate tissue and is overexpressed in CaP (Schroder, 2012).

1.7.4. DNA Methylation

The only known epigenetic modification of DNA itself is DNA methylation. Typically this is through methylation of cytosine, at position C5 in CpG dinucleotides (Jin et al., 2011). DNA methylation represses transcription directly, by inhibiting the binding of specific transcription factors, and indirectly, by recruiting methyl-CpG-binding proteins and their associated repressive chromatin remodelling activities (Curradi et al., 2002). DNA methylation patterns are critical regulators of development and are also required for correct functioning of differentiated tissues. They must therefore be established and maintained with high fidelity (Robertson, 2005). DNA methylation has been shown to

regulate transcription, embryonic development, genomic imprinting, genome stability and chromatin structure (Robertson, 2005, Jin et al., 2011).

In normal cells, DNA methylation is most commonly associated with satellite DNA and parasitic elements e.g. endogenous retroviruses (Barros and Offenbacher, 2009). DNA methylation is controlled by DNA methyltransferases, methyl-CpG binding proteins and other chromatin-remodelling factors (Bogdanović and Veenstra, 2009).

The link between cancer and DNA methylation can be demonstrated by comparing the genome-wide methylation status of cancer relative to normal cells. This analysis revealed that the genomes of cancer cells are hypomethylated (Robertson, 2005). The major cause of genome-wide hypomethylation in tumour cells is due to the loss of methylation from repetitive regions, while this may seem innocuous, it results in genomic instability (Yoder et al., 1997).

1.8. Research Aims

There is currently an 'unmet need' in the molecular profiling of CaP, as well as theranostic evaluation of CaP evolution due to ADT. This is of importance as healthcare organisations prioritise the use of 'next-generation' of ADT compounds in patients that are likely to respond i.e. GAAR. Traditionally, GAAR is detected by the labour intensive and semi-quantitative fluorescent *in situ* hybridization (FISH) technique which is not compatible with high-throughput screening.

A major hypothesis of the project is that a quantitative polymerase chain reaction (qPCR) assay could be established that is capable of detecting GAAR in a heterogeneous sample, and that this assay could be used to interrogate the GAAR status of primary prostate epithelial cultures, patient-derived tissue biopsies and near-patient xenograft models of CaP.

The specific objectives to achieve the above hypothesis were as follows:
- Develop and validate a qPCR based method for the identification and quantification of GAAR.
- Determine the GAAR status of several near-patient xenograft models of CaP to investigate if the GAAR could be found in the progeny of *in vivo* TIC.

The investigation of Latexin (LXN) and Retinoic Acid Receptor Responder 1 (RARRES1) in CaP, was initiated by (Oldridge et al., 2013, Oldridge, 2012) through the analysis of the expression, regulation and function of these genes/proteins in the prostate epithelium. These studies determined that both LXN and RARRES1 are induced by atRA and that both genes have tumour-suppressive functions *in vitro* which were independent of carboxypeptidase A (CPA)-4. Additionally, it was shown that DNA methylation was the primary form of epigenetic regulation in prostate cell lines but not in primary cultures, patient tissue samples or near-patient xenograft models.

The other major aim of this project was to further the study of the regulation of LXN and RARRES1 by testing the hypothesis that LXN and RARRES1 are epigenetically regulated by post-translational modification of histones. Additionally, a combined transcriptomic and proteomic analysis were used to elucidate the mechanism of action of LXN and RARRES1.

Specific objectives were as follows:
- Investigate the potential for epigenetic regulation of LXN and RARRES1 by post-translational modification of histones in the putative promoter sequences of these genes.
- Examine changes in gene expression upon LXN and RARRES1 overexpression using microarray technology.
- Explore potential interacting partners of LXN and RARRES1 using mass spectrometry

2. Materials and Methods

2.1. Mammalian Cell Culture

2.1.1. Maintenance of Mammalian Cells

Cell lines were maintained and passaged in T25, T75 or T175 flasks in a humidified 37°C incubator with 5% CO_2. Medium constituents were supplied by Invitrogen, unless otherwise stated. As cultures reached 80-100% confluence they were sub-cultured using commercial grade 0.05% trypsin- ethylenediaminetetraacetic acid (EDTA) in phosphate-buffered saline (PBS). The cells were passaged at a cell line dependent ratio, typically 1:3 to 1:12. Specific culture conditions are shown in (Table. 3.).

Cell Line	Origin	Culture media
PNT2-C2	Clone derived in the YCR CRU lab at York	RPMI, 10% (v/v) FCS, 2 mM L-Glutamine (**R10**)
PNT1a	Obtained with kind permission from Dr. P Berthon	R10
BPH-1	Obtained with kind permission from Dr. Simon Hayward	RPMI, 5% (v/v) FCS, 2 mM L-Glutamine (**R5**)
RC-165N/ hTERT	Obtained with kind permission from Dr. Jun Miki	KSFM , 50µg/ml bovine pituitary extract, 5ng/ml human EGF, 2mM L-Glutamine
P4E6	Derived in the YCR CRU lab at York	Keratinocyte Serum-Free Medium (KSFM, Invitrogen), 2% (v/v) FCS, 2mM L-Glutamine, 5ng/ml human EGF (Invitrogen), 50µg/ml bovine pituitary extract (Invitrogen) (**K2**)
Bob	Obtained with kind permission from Dr. David Hudson	KSFM, 5 ng/ml human EGF, 50 µg/ml bovine pituitary extract, 2 ng/ml leukaemia inhibitory factor, 100 ng/ml cholera toxin, 1 ng/ml granulocyte macrophage colony stimulating factor, 2 ng/ml stem cell factor, 2mM L-Glutamine (**SCM**)
SerBob	Obtained with kind permission from Dr. David Hudson	SCM, 10% (v/v) FCS
PC3	ECACC	Ham's F-12 medium (Lonza Laboratories), 7% (v/v) FCS, 2 mM L-Glutamine (**H7**)
DU145	ATCC	R10
VCaP	ATCC	R10
LNCaP	ECACC	R10
PC346C	Obtained with kind permission from Prof. Chris Bangma	1:1 mix of Dulbecco's Modified Eagle's Medium (DMEM) and Ham's F-12 medium, 100 µg/ml streptomycin, 100 U/ml penicillin G, 2% FCS, 0.01% (w/v) BSA (Sigma), 10 ng/ml EGF (Sigma), 1% (v/v) ITS-G (GIBCO), 0.1 nM R1881 (DuPont-New England Nuclear), 1.4 µM hydrocortisone (Sigma), 1 nM triiodothyronine (Sigma), 0.1 mM phosphoethanolamine (Sigma), 50 ng/ml cholera toxin (Sigma), 0.1 µg/ml fibronectin (Sigma), 20 µg/ml fetuin (Sigma)
MDA-MB-231	ATCC	DMEM, 10% (v/v) FCS, 2 mM L-Glutamine (**D10)**
STO	ATCC	D10

Table. 3. Culture Conditions of Prostate Cell Lines.

RPMI = Roswell Park Memorial Institute 1640 cell culture medium, FCS = foetal calf serum, KSFM = keratinocyte serum-free medium, BSA = Bovine serum albumin, SCM = stem cell medium, EGF = Epidermal growth factor, DMEM = Dulbecco's modified Eagle's medium, ATCC = American Type Culture Collection, ECACC = European Collection of Authenticated Cell Cultures

From: (Oldridge, 2012)

2.1.2. Isolation and Maintenance of Primary Cultures

Primary prostate tissue was obtained from patients undergoing radical prostatectomy or TURP procedures. Samples were taken with informed patient consent and approval from the York Research Ethics Committee. Diagnosis (BPH or CaP) was confirmed by histological examination. Sample details are provided in (Appendix 1.).

A disposable scalpel was first used to remove a section of the tissue to be retained for histology. Then, the patient sample was chopped into small pieces. The pieces were enzymatically digested using 200 U/mg collagenase (Lorne Laboratories) which was dissolved in a 1:2 mixture of Keratinocyte Serum-Free Medium (KSFM) and Roswell Park Memorial Institute-1640 medium (RPMI) to a total volume of 7.5 ml per gram of tissue. The KFSM medium was supplemented with human epidermal growth factor (EGF) (5 ng/ml) and bovine pituitary extract (50 µg/ml). The RPMI was supplemented with 100 U/ml antibiotic solution and 2 mM L-Glutamine. The digestion was allowed to proceed overnight at 37 °C with shaking at 80 revolutions per minute (RPM). The digested tissue was then mechanically disrupted using trituration first by passing the digestion through a 5 ml pipette and subsequently a blunt needle. After centrifugation at 500 x g for 10 min to sediment cells the collagenase was diluted out with PBS: the supernatant was aspirated, 10 ml PBS was added, the cell pellet was re-centrifuged at 500 x g for 10 min and the procedure repeated. The resulting cell pellet was further disrupted by incubation with 5 ml 0.05% trypsin-EDTA for 30 min at 37°C with shaking at 80 RPM. Trypsin-EDTA was inactivated with R10 medium, and epithelial cells centrifuged at 300 x g for 3 min. Primary cells were co-cultured on type I Collagen-coated 100 mm plates (BD Biosciences) with STO fibroblast feeder cells (mouse origin) in stem cell media (SCM). SCM is composed of keratinocyte serum-free medium, 1 ng/ml granulocyte macrophage colony stimulating factor (Miltenyi Biotec), 5 ng/ml human EGF, 50µg/ml bovine pituitary extract, 2 ng/ml leukaemia inhibitory factor (Chemicon), 100 ng/ml cholera toxin (Sigma), 2 ng/ml stem cell factor (First Link UK Ltd) and 2 mM L-Glutamine. Sub-culturing of primary cultures was performed using 0.05% trypsin-EDTA. Typically, primary cultures were passaged 1:2-1:6 and maintained until passage 6.

2.1.3. Irradiation of Fibroblasts

For inducing cell cycle arrest through irradiation of mouse STO fibroblast cells, cells were first grown to 80-90% confluency before being harvested by trypsinisation and centrifugation at 300 x g for 3 min. STO cells were then resuspended in 10 ml SCM per 100 cm^2 of culture surface and exposed to 60 Gy of radiation. Cells were routinely stored at 4°C for up to 3 days before use. This was routinely performed by all members of the lab as a rota system (although Paul Berry, Fiona Frame or John Packer performed the irradiation).

2.1.4. Generation and Maintenance of Xenografts

Xenograft models were generated by subcutaneously engrafting patient-derived tissue into the left flank of BALB/c/RAG2-/-/γC-/- mice. A 5α-DHT pellet (Innovative Research of America) was placed under the right flank (subcutaneously) to ensure the availability of androgens. Once the tumour volume had exceeded a width of 15 mm, it was removed and a small piece was passaged into a different mouse in the same manner as the primary engraftment. The remainder of the tissue was either fixed in formalin for histology or used experimentally. This was performed by Dr. Anne Collins or Paul Berry.

2.1.5. Cryopreservation of Mammalian Cells

For long term storage, mammalian cells were kept frozen in liquid nitrogen in the liquid phase. Cells to be frozen were then trypsinised and sedimented by centrifugation at 300 x g for 3 min. The resulting cell pellet was then resuspended in freezing medium at a concentration of 1-2 x 10^6 cells per ml. The cell suspension was then divided into 1 ml aliquots which were frozen in cryovials. Upon thawing, cells were diluted into 15 ml of R10 culture medium, sedimented by centrifugation and plated in either T25 flasks (cell lines) or 100 mm collagen-I coated plates (primary cultures).

2.1.6. Determination of Live Cell Number Using a Haemocytometer

Total cell number live cell number was determined using Trypan Blue exclusion as a surrogate for viability. Live cells (non-stained cells) were then counted using a haemocytometer (Neubauer). To determine live cell counts 10 μl 0.4% Trypan Blue Stain (Sigma-Aldrich) was diluted 1:1 with 10 μl cell suspension.

2.2. Primary Culture Enrichment

Primary prostate epithelial cultures were enriched into three major subpopulations representing different states of cellular differentiation. The enrichment exploits the differential expression of two cell surface markers namely: α2β1-integrin and CD133 as described previously (Collins et al., 2001; Richardson et al., 2004):

- SCs have high cell surface levels of α2β1-integrin and CD133 (α2β1-integrin^{high}CD133+).

- Transit amplifying (TA) cells high levels of α2β1-integrin but negative for CD133 (α2β1-integrin^{high}CD133-).

- Committed basal cells (CB) low levels of α2β1-integrin and negative for CD133 (α2β1-integrin^{low}CD133-).

2.2.1 Enrichment of α2β1-Integrin Expressing Cells

At least 2-3 ~80% confluent 10 cm culture dishes of primary prostate cultures were used in the enrichment process. STO cells were removed by 5 min incubation with 0.05% trypsin-EDTA at room temperature. The trypsin was then removed and fresh 0.05% trypsin-EDTA was added to harvest the epithelial cells. Type I collagen-coated 100 mm plates were blocked with 0.3% (w/v) heat-denatured Bovine serum albumin (BSA) dissolved in PBS for 1 h at 37°C. 3 ml of cell suspension was plated out onto the blocked-plates and incubated at 37°C for 20 min. Media was aspirated and the plates were washed 5 times with 5 ml PBS which was also collected. The stored media and washes were spun at 300 x g for 5 min to pellet the cells expressing low levels of α2β1-integrin (α2β1-integrin^{low}; CB). The α2β1-integrinhigh adherent cells were then harvested by incubation with 0.05% trypsin-EDTA and used for CD133 cell isolation.

2.2.2. Enrichment of CD133 Expressing Cells

The Direct-CD133 Cell Isolation Kit (Miltenyi Biotec) was used to isolate CD133-expressing cells from primary prostate epithelial cultures. α2β1-integrin^{high} cells were enriched (as described in Section 2.2.1). Up to 10^8 cells were resuspended in 300 µl magnetic-activated cell sorting (MACS) buffer (2 mM EDTA, 0.5% (v/v) foetal calf serum (FCS) in PBS), 100 µl FcR blocking reagent (Miltenyi Biotec) and 100 µl CD133 beads (Miltenyi Biotec) the

reaction was incubated at 4°C for 30 min. Cells were washed with 3 ml MACS buffer, centrifuged at 300 x g for 5 min and the cell pellet was suspended in 500 µl MACS buffer. Magnetic cell labelling and cell separation on MACS-MS columns were performed as directed by the manufacturer. Briefly, the MACS-MS column was first equilibrated with 500 µl MACS buffer then cells bound to magnetic beads were allowed to pass through the column by gravity. Three wash steps each with 500 µl MACS buffer were utilised to collect the CD133- population. Finally, 1 ml MACS buffer was added to the column and the CD133+ cells were eluted from the beads with the 'plunger' provided. To increase the purity of the CD133+ fraction from 70-75% to 95%, the cells were passed through a second MACS-MS column. The CD133- and CD133+ cells were sedimented by centrifugation at 300 x g for 3 min, the supernatant was then carefully removed and the resulting cell pellets were frozen at -80°C to use in downstream applications.

2.3. Transfection of Cell Lines with Plasmid DNA

ViaFect transfection reagent (Promega) was used to transfect cell lines plasmid DNA. Typically, 0.1-2 x 10^5 cells per ml were plated 24 h before transfection to ensure that cells were at least 50% confluent at the time of transfection. The optimal ViaFect plasmid ratio was determined empirically for each cell line. Typically 1-3 µl of ViaFect per µg of plasmid was used. ViaFect reagent was first equilibrated to room temperature (RT) and was mixed by gentle vortexing before each use. Each transfection reaction consisted of 100-2500 ng plasmid DNA diluted in OptiMEM serum-free medium which was mixed by pipetting. ViaFect reagent was then added to the tube, and the solution was again gently mixed by pipetting. The DNA-ViaFect mixture was incubated at RT for 20 min to allow complex-formation. The complexes were then introduced to cells in a drop-wise fashion. Cells were incubated in the presence of complexes overnight at 37°C. After incubation the DNA-ViaFect complexes were aspirated and replaced with fresh culture medium. Cells were then incubated for a further 18-90 h before evaluation.

2.4. Lentivirus Production

Lentiviral donor, destination plasmids and packaging plasmids were a very kind gift from Prof Stephan Geley, Innsbruck Medical University. Details of the plasmids can be found in (Appendix 4.).

2.4.1. Bacterial Transformation

Aliquots of chemically-competent bacteria, typically DH5α *E. coli* cells (Fisher Scientific Limited) were placed on ice for 30 min to gently thaw. Next, 1-5 ng of plasmid DNA was added to each aliquot and the resulting mixture was incubated for a further 30 min on ice. The bacteria were then heat-shocked for 30 s at 42°C, and immediately returned to ice for 2 min. 250 µl super optimal broth (SOC) medium was then added to the bacteria and incubated at 37°C for 1 h at 220 RPM in a shaking incubator. The bacteria were then plated onto lysogeny broth (LB) agar plates containing a selection antibiotic and incubated for 24 h at 37°C. After incubation colony screening was performed.

2.4.2. Bacterial Cultures and Plasmid Purification

A starter culture was initiated from a single colony from a freshly streaked selective plate. This was used to inoculate 5 ml of LB medium (tryptone (10 g/L), yeast (5 g/L) extract and NaCl (10 g/L)) containing an antibiotic for selection, before incubation for 8 h at 37°C at 220 RPM in a shaking incubator. The starter culture was then used to inoculate 250 ml selective LB media. The 250 ml cultures were allowed to grow by incubation at 37°C overnight with shaking (220 RPM). Bacteria were harvested by centrifugation at 1800 x g for 10 min using a Heraeus Megafuge 1.0R centrifuge (Thermo Fisher Scientific). The EndoFree Maxi kit (Qiagen) was used to generate endotoxin-free plasmid DNA according to manufacturer's instruction. Bacterial cell pellets were resuspended in 10 ml Buffer p1 (50 mM Tris-HCl pH 8.0, 10 mM EDTA, 100 µg/ml ribonuclease (RNase) A). 10 ml Buffer p2 (200 nM NaOH, 1% SDS (w/v)) was then added to the mixture which mixed thoroughly. Ice-cold Buffer P3 (3 M potassium acetate, pH 5.5) was added and the solution was immediately mixed. The lysate was then transferred to a QIAfilter cartridge and incubated at RT for 10 min. The lysate was then filtered by forcing it through the column using a plunger. After the lysate had been filtered, 2.5 ml Buffer ER was added to the lysate. The tube was then inverted several times to mix and was incubated on ice for 30 min. Meanwhile a Qiagen tip 500 was equilibrated with 10 ml Buffer QBT (750 mM NaCl, 5 mM 3-(N-morpholino)propanesulfonic acid (MOPS), pH 7.0, 15% isopropanol (v/v), 0.15% Triton X-100 (v/v)), the lysate was applied to the Qiagen tip and was allowed to pass through the Qiagen tip by gravity. The Qiagen tip was then washed twice using 30 ml of Buffer QC (1.0 M NaCl, 50 mM MOPS pH 7.0, 15% isopropanol (v/v), 0.15% Triton X-100 (v/v)). The plasmid was eluted by the addition of 15 ml QN buffer (1.6 M NaCl, 50 mM

MOPS pH 7.0, 15% isopropanol (v/v)). The plasmid DNA was then precipitated by adding 0.7 volumes (10.5 ml) of isopropanol and was centrifuged at 15000 x g for 30 min at 4°C using a Heraeus Multifuge X1R centrifuge (Thermo Fisher Scientific). The resulting plasmid DNA pellet was washed with 70% ethanol (v/v) at RT, re-sedimented, and air-dried for 10 min. Finally, the plasmid DNA was then resuspended in PCR grade water (Sigma).

2.4.3. Gateway™ Cloning

The sequence specific recombination sites attB1.1 and attB2.1 were used to flank the gene of interest. These were added by 2 separate PCR reactions. The first PCR reaction used gene specific primers with overhangs to add the inner half of the attB sequences. This product was the run on a 1% agarose gel at 100 V for 1.5 h before the band was excised and the DNA purified from the agarose gel using Qiagen gel extraction kit (as described in 2.6.6.). This product was used as the template for the 2nd PCR reaction to add the outer half of the attB sites. The product was then separated by electrophoresis on a 1% agarose gel at 100 V for 1.5 h before the band was excised and the DNA purified from the agarose gel using Qiagen gel extraction kit as described earlier.

The attB flanked PCR product was then cloned into pDONR-221 which contains attP sites using the BP clonase. 25 fmol of attB flanked PCR product was combined with 75 NG of pDONR-221 and 1 μl of BP clonase. This was then made up to a volume of 5μl with PCR grade water. The reaction was allowed to proceed for 24 h at 25°C. 0.5 μl of proteinase K was added to the reaction which was then incubated at 37°C for 10 min. The entire content of the reaction was then used to transform bacteria as described in section 2.4.1. Four single colonies were isolated and cultured for plasmid purification as described in section 2.4.2. The four clones where then sent for sequencing to ensure that the sequence had not been mutated.

A pDONR-221 clone containing the un-mutated gene of interest was used as the substrate for generating destination plasmids (pDEST) capable of producing lentiviral vectors in the presence of packaging plasmids. Briefly, 25 ng of pDONR-221 containing the gene of interest in a volume of 1 μl was mixed with 50 ng of the required pDEST (containing attR) sites in a volume of 1 μl. This reaction was made up to a total volume of 4 μl with PCR grade water (Sigma). 1 μl of 5X LR clonase II was added to the reaction the reaction was mixed by centrifugation. The reaction was left to proceed for 24 hours at 25°C. 0.5 μl of

Proteinase K solution was added and the reaction was incubated for 10 min at 37°C. The entire reaction was used to transform bacteria as described in section 2.4.1. Four single colonies were isolated and cultured for plasmid purification as described in section 2.4.2. These clones were then tested for presence of the gene of interest by PCR before further verification of expression of the gene of interest by western blot.

2.4.4. Virus Packaging

HEK293FT cells (Thermo Fisher Scientific) were used as the packaging cell line. The 293FT cell line is a fast-growing, highly transfectable clonal isolate derived from human embryonal kidney cells transformed with the SV40 large T antigen to enhance lentiviral production.

HEK293FT cells were transfected with the pDEST of interest and the viral packaging plasmids psPAX2 and pVSV-G. In order to ensure consistent viral production at any scale and any size of transgene insert the number of molecules of each plasmid per cell used to transfect the HEK293FT cells was standardised. This was 1.62×10^5 molecules of psPAX2, 9.25×10^4 molecules of pVSV-G and 3.30×10^5 molecules of pDEST per cell. The molecular ratio of the plasmids was 1.75 molecules of psPAX2: 1.00 molecules of pVSV-G: 3.57 molecules of pDEST.

ViaFect transfection reagent (Promega) was used to transfect HEK293FT cells with the plasmid cocktail at a ratio of 2 µl of ViaFect per µg of plasmid. This was performed in the same way as described in section 2.3.1 but with some minor differences. Firstly the HEK293FT cells were grown to 90% confluency before transfection. Secondly, the HEK293FT cells were plated on to tissue culture plastic coated with Poly-L-lysine (Sigma Aldrich) this was to prevent the confluent HEK293FT cells from sloughing off during harvesting of the virus-containing supernatant. Finally the scale of virus production needed for large scale experimentation necessitated the transfection to be carried out on 10 cm dishes.

HEK293FT cells were transfected as described above. 12 h post transfection the culture media was replaced with fresh culture medium to remove transfection reagents which may be cytotoxic. 24 h after the medium change the culture medium containing viral particles was harvested, filtered through a 0.44 µm syringe filter, aliquoted and stored at

-80⁰C. Culture medium was replaced and the virus producing HEK293FT cells cultured for a further 24 h before a second harvesting of viral particles which was performed in the same way.

2.4.5. Determining Lentiviral Titres

All titrations of virus containing solutions were performed on solutions that had previously been frozen. This was to accurately assess the viral titre of frozen aliquots over virus containing solutions. Most viruses used contained a visible marker (enhanced green fluorescent protein (eGFP)). Where a visible selectable marker was not present a virus was produced using the same backbone as experimental viruses but with eGFP as an insert. This was used to estimate the titre of experimental viruses.

Serial dilutions of the virus containing solution were made, typically: neat, 1:5, 1:50, 1:500 and 1:5000. 250 µl of each solution was mixed with 250 µl of 1.2×10^5 HEK293FT cells/ml suspension. The resulting cell virus mixture was plated on to a 48 well plate at a total volume of 500 µl per condition with each condition containing 3×10^4 HEK293FT cells. Final virus dilutions would therefore be 1:2, 1:10, 1:100, 1:1000 and 1:10000.

48 h after plating the cells were harvested by trypsinisation and were interrogated using flow cytometry to determine the percentage of eGFP positive cells per condition. SYTOX (Thermo Fisher Scientific) was used to exclude dead cells from analysis. The lowest serial dilution that was >1 % but <10% eGFP positive cells was used to calculate the viral titre using the following calculation:

$$Titre = (number\ of\ HEK\ cells\ plated\ \times viral\ dilution\ factor \\ \times \%\ positive\ cells) \div volume\ of\ virus\ solutio$$

2.5. Transduction of Mammalian Cells

Mammalian cells were transduced with the lentivirus of choice depending on experimental demands. Typically cells were transduced with 1-10 virus particles per cell with 3 virus particles per cell being the most commonly used in this project. Cells were trypsinised and counted as described previously. They were then mixed with the pre-titrated supernatant from the viral packaging cells. Cells were then plated on to a suitable

multi-well plate, flask or petri dish. After 16 h the cell culture medium was removed and replaced with fresh media. After 48 h from the initial transduction the percentage transduction was calculated and a small sample was taken to determine the number of viral integrations per cell (described below) and protein expression of the transgene by western blot.

2.5.1. Determination of Viral Integration

In order to avoid a situation where affects could be due to insertional mutagenesis it is important to determine the number of viral integrations per cell. By using a specific qPCR assay, primers were designed to be specific to the woodchuck hepatitis virus posttranscriptional regulatory element (WPRE). This element is found on all destination vectors used in the project and is integrated along with the transgene. The assay also incorporated primers designed to be specific for the single copy RNase P gene.

Briefly, genomic DNA (gDNA) was extracted as described in section 2.6.1, 10 ng of sample was interrogated with both the WPRE and RNase P primers along with a 5 point standard curve for each set of primers (normal human gDNA for RNase P and pDEST for WPRE). This allowed the copy number of each gene within the sample to be determined. With this information the average number of integrations per cell is calculated as follows:

$$Integrations\ per\ cell = WPRE\ copy\ number\ \div (RNase\ P\ copy\ number\ \div 2)$$

2.5.2. Generation of Stable Lines

Stably expressing cell lines were generated by transducing cells with lentivirus made using the pDEST-236 plasmid. These viruses also contain the selectable puromycin-resistance gene (PURO-R) which confers resistance to the antibiotic puromycin. The sensitivity of non-transduced cells to puromycin was determined empirically, typically this was 10 ng/ml. After 48 h post transduction the cell culture medium was supplemented with a concentration of puromycin to which the non-transduced cells were sensitive. Cells were cultured in the culture medium containing puromycin, which was refreshed every 2 days, for a minimum of 2 weeks.

2.6. Isolation and Analysis of Mammalian Cell DNA

2.6.1. DNA Extraction (Qiagen)

gDNA was extracted from tissues and cultures using the DNeasy Blood and Tissue Kit (Qiagen) according to the manufactures' instruction. Briefly, up to 5 x 10^6 cells were washed once in PBS and dissociated by trypsinisation (0.05% trypsin-EDTA at 37°C). R10 was added to inactivate the trypsin, before the cell suspension was centrifuged at 300 x g for 3 min and the supernatant removed and discarded. The cell pellet was then resuspended in 200 µl PBS supplemented with 20 µl proteinase K and 4 µl RNase A (100 mg/ml). Next, 200µl Buffer AL was added to the cell suspension, which were then thoroughly mixed by vortexing before incubation at 56°C for 10 min to lyse the cells. 200 µl ethanol was added to the tube which was again vortexed to ensure thorough mixing. The cell lysate was introduced to a DNeasy mini spin column and was then centrifuged at 6000 x g for 1 min. The flow-through and collection tube were discarded and the column was placed into a fresh collection tube, 500 µl Buffer AW1 was then added to the column which was then centrifuged at 6000 x g for 1 min. The flow-through and collection tube were discarded and the column placed into a new collection tube, 500 µl Buffer AW2 was added to the column before centrifugation at 15000 x g for 3 min. The flow through was discarded and the column was centrifuged at 15000 x g for 3 min without the addition of any buffer. This was to remove any remaining ethanol from the column prior to elution. Elution of gDNA was performed by the addition of 50 µl of PCR-grade water to the column, which was then a centrifuged at 6000 x g for 1 min.

2.6.2. DNA Extraction (Phenol Chloroform)

Modified from (Collas, 2011).

Cell pellet, tissue (both fresh and frozen in optimal cutting temperature (OCT) compound or previously isolated DNA to be 'cleaned up' was treated the same way.

The sample was re-suspended in 500 µl of complete elution buffer which consisted of: 20 mM Tris–HCl (pH 7.5), 5 mM EDTA, 50 mM NaCl, 1% (wt/vol) sodium dodecyl sulphate (SDS) and 50 mg/ml proteinase K. The sample was then incubated at 68°C at 1300 rpm in a heated shaking cabinet (Hybade) for 2 hours. The resulting solution was briefly

centrifuged before 500 µl of phenol–chloroform–isoamylalcohol pH 8 (25:24:1) (Sigma) was added directly to the sample. The sample was then vortexed and centrifuged at 15000 x g for 5 mins at 25°C to separate the aqueous and phenol phases. 480 µl of the aqueous phase was transferred to a new 1.5ml centrifuge tube. 480 µl of chloroform–isoamylalcohol (24:1) was added to the aqueous phase. The sample was then vortexed before centrifugation at 15000 x g for 5 mins at 25°C to separate the aqueous and chloroform phases. 450 µl of the aqueous phase was transferred to a clean 2 ml tube.

The DNA in the aqueous phase was precipitated by the addition of 44 µl of 3 M NaAc (pH 5.2), 5 µl of linear acrylamide carrier (Ambion) and 1 ml of 96% ethanol at -20°C. The solution was mixed by inverting 10 times before being incubated overnight at -80°C.

The sample was then thawed on ice before being centrifuged at 20000 x g for 15 min at 4°C. At this point a clearly visible pellet consisting of DNA and carrier could be seen. The supernatant was removed 1 ml of 70% ethanol at -20°C was added. The sample was then centrifuged at 20000 x g for 15 min at 4°C. The supernatant was removed and the pellet was dried using an Eppendorf Concentrator 5301 at 30°C. The pellet was then re-suspended in an appropriate volume of PCR grade water (Sigma), typically 30-100 µl. DNA concentration and quality checks were performed using a Nanodrop spectrophotometer and DNA samples were routinely stored at -20°C.

2.6.3. DNA Extraction from Formalin Fixed Paraffin Embedded Tissue

This method used the ReliaPrep™ FFPE gDNA Miniprep System (Promega) with minor modification.

The Formalin Fixed Paraffin Embedded (FFPE) tissue was transferred to a 1.5 ml centrifuge tube. Deparaffinisation was performed using mineral oil. For sections ≤ 50 microns, 300 µl of mineral oil was added and for sections ≥ 50 microns, 500 µl of mineral oil. The sample was then incubated at 80°C for 1 min and was then vortexed. 200 µl of Lysis Buffer (supplied as part of the kit) was added to the sample which was then centrifuged at 10000 x g for 15 seconds at 25°C. At this point an aqueous and a mineral oil phase became apparent. 20 µl of Proteinase K was then added directly to the lower phase which was then mixed by pipetting. The sample was then incubated for 1 h at 56°C and then for 1 h at 80°C. The sample was then allowed to cool to room temperature before a brief

centrifugation. 10 μl of RNase A was directly added to the lysed sample in the lower phase which was then mixed by pipetting. The sample was then incubated at 25°C for 5 mins. 220 μl of BL Buffer (supplied as part of the kit) was added to the lysed sample along with 240 μl of ethanol (95–100%) the sample was then vortexed. The sample was the centrifuged at 10000 x g 15 seconds at 25°C. At this point the aqueous and mineral oil phases were separated. The entire lower (aqueous) phase of the sample, including any precipitate that may have formed was transferred to the column. The remaining mineral oil was discarded. The assembly was centrifuged at 10000 x g for 30 secs at 25°C the flow through was discarded. 500 μl of 1X Wash Solution (supplied as part of the kit) was added to the column before centrifugation at 10000 G for 30 seconds at 25°C the flow through was discarded. The column was the then dried by centrifugation at 16000 g for 6 minutes at 25°C. The Binding Column was transferred to a clean 1.5 ml microcentrifuge tube. 30–50 μl of PCR grade water was added to the column (to elute the DNA) which was then centrifuged at 16000 x g for 1 min at 25°C. DNA concentration and quality checks were performed using a Nanodrop spectrophotometer and DNA samples were routinely stored at -20°C. Often the DNA was cleaned up by a further phenol chloroform extraction as described in section 2.6.2.

2.6.4. Agarose Gel Electrophoresis

Agarose gel electrophoresis was used to assess the quality and purity as well as the specificity of the amplification reaction. Typically, each sample or PCR product was analysed on 1-2% (w/v) Tris-acetate-EDTA (TAE) agarose gel using GelRed nucleic acid stain (1:10,000 (v/v); Biotium) to visualise DNA. 20 μl PCR product, PCR grade water (Sigma) and 4 μl DNA loading dye (4 mg Ficoll 400, 0.1 M EDTA, 0.1% (w/v) SDS, 0.05% (w/v) bromophenol blue and 0.05% (w/v) xylene cyanol) were added, homogenised and loaded onto a gel which was submerged in TAE buffer. 100 bp or 12 kb plus molecular weight (MW) DNA ladders were run alongside samples to allow sizing. Gels were visualised using GeneSnap ID software (Syngene).

2.6.5. PCR Amplification

 A full list of primer sequences and corresponding PCR conditions can be found in (Appendix 2). PCR reactions were performed using Platinum™ Taq polymerase and associated reaction components (Thermo Fisher Scientific) or using Phusion polymerase

kit (Thermo Fisher Scientific). Typically reactions were between 20-50 µl and involved a 3 step amplification protocol consisting of denaturation at 98°C, primer annealing (typically 52-65°C) and extension at 72°C using a thermocycler.

2.6.6. Gel Extraction

Gel extraction of a PCR product was performed using the QIAquick® Gel Extraction Kit (Qiagen) according to the manufacturers' protocol. Briefly, the gel was made using Syber-safe DNA stain (Thermo Fisher Scientific) to allow visualisation of the band under blue light which is less energetic compared with ultraviolet (UV) light and should therefore minimise DNA modifications and hence mutation of the extracted product. The DNA band was excised from the gel using a clean, sharp scalpel. The gel piece was then weighed and 3 volumes of Buffer QG (supplied as part of the kit) to 1 volume of gel (100 mg gel ~ 100 µl). This was then incubated at 50°C for 10 min (or until the gel slice dissolved completely). The tube was vortexed every 2–3 min to help dissolve gel. One gel volume of isopropanol was added to the sample which was then mixed. The solution was then transferred to a QIAquick® spin column and centrifuged for 1 min and the flow-through was discarded. 500 µl Buffer QG was added to the column which was then centrifuged for 1 min and the flow-through was discarded. 750 µl Buffer PE (supplied as part of the kit) was added to the column which was centrifuged for 1 min and the flow-through discarded. The column was transferred to a clean 1.5 ml microcentrifuge tube and DNA was eluted with 50 µl of PCR grade water.

2.6.7. Quantitative PCR of Genomic DNA

qPCR reactions were composed of 7.5 µl of SsoFast™ EvaGreen® Supermix 2 X master mix (Bio-Rad), 2 µl of DNA, 0.6µl Of 10 mM forward primer, 0.6 µl Of 10 mM reverse primer and PCR grade water (Sigma) up to a total volume of 15 µl. All reactions were performed on FrameStar white-tubed (4titude) 96 well plates in triplicate. Reactions were run on a CFX96 Real-Time PCR Detection System, and analysed using the Bio-Rad CFX Manager 2.0 (Bio-Rad. Standard thermal-cycling conditions included or 2 min at 98°C followed by 40 cycles of 98°C for 5 s and 60°C for 5 s (Bio-Rad CFX96). To ensure specificity of the reactions a melt curve step was added at the end of each cycle: 95°C for 15 s, 52-60°C for 20 s and 95 °C for 15 s.

Melt curve analysis utilises the ability of an intercalating dye (used to detect the abundance of an amplicon) to fluoresce when bound to double-stranded DNA (dsDNA) (no fluorescence is detected in the presence of single-stranded DNA (ssDNA)). By gradually heating the DNA present at the end of a qPCR reaction and analysing the fluorescence it is possible to determine the point at which dsDNA denatures becoming single-stranded. As the denaturation is dependent on the length of the amplicon and its GC:AT nucleotide ratio it is possible to determine if a single product (one denaturation event) or multiple products (multiple denaturation events) are present.

2.6.8. Analysis of AR Genomic Copy Number Alterations

Samples were interrogated using specific primers for *AR*, dystrophin (*DMD*) and glyceraldehyde 3-phosphate dehydrogenase (*GAPDH*) by qPCR as described in section 2.6.7. A standard curve using normal female DNA was generated to allow absolute quantification of these genomic regions. The copy number of *AR* and *DMD* was expressed relative to the copy number of *GAPDH*. Also included was a reference sample of normal male DNA to which the copy number of samples could be normalised. Additionally a sample of VCaP DNA was included which is well documented to have a specific amplification of the *AR* gene and therefore serves as a positive control.

2.7. Isolation and Analysis of Mammalian Cell RNA

2.7.1. RNA Extraction

RNA was extracted using the RNeasy Mini Kit (Qiagen). Typically, 5 x 10^6 cells were first washed using PBS before being tripsinised (0.05% trypsin-EDTA at 37°C). R10 was then added to inactivate the trypsin, before centrifugation at 300 x g for 3 min and the supernatant removed. The resulting cell pellet(s) were resuspended in 350 μl Buffer RLT buffer (supplied as part of the kit) supplemented with 2-mercaptoethanol and vortexed to mix. The cell lysate was then introduced into a QIAshredder homogeniser column (Qiagen) and centrifuged at 15000 x g for 2 min. 350 μl 70% ethanol diluted in diethyl pyrocarbonate (DEPC)-treated water was added to the homogenised lysate which was then thoroughly mixed by pipetting. The homogenised sample was then transferred to an RNeasy spin column to allow RNA binding and centrifuged at 15000 x g for 15 s. The column was then washed with 700 μl Buffer RW1 (supplied as part of the kit), spun at

15000 x g for 15 s, followed by further washing with 500 µl Buffer RPE (supplied as part of the kit). At each wash step the 'flow-through' was discarded. Elution of RNA was performed with 30 µl RNase-free water by centrifugation at 15000 x g for 1 min. Determination of RNA quality and concentration was performed using a NanoDrop ND-1000 spectrophotometer (Thermo Fisher Scientific) or using Bioanalyser (Agilent). RNA samples were routinely stored at -80°C.

2.7.2. Complementary DNA Synthesis

Total RNA was reversed transcribed in 14.25 µl, mixed with 0.75 µl PCR grade water (Sigma) and 0.75 µl Random primers and heated to 70°C for 10 min. The 14.25 µl reaction mix included 6 µl of 5x First strand buffer, 3 µl 0.1 M dithiothreitol (DTT), 0.75 µl PCR grade water (Sigma), 3 ML 10 mM Deoxynucleotide (dNTP)s. 1.5 µl Superscript III enzyme was added and the mixture was incubated at 45°C for 2 h. Ethanol-precipitation was used to purify the cDNA this was performed with the addition of 15 µl 3 M NaCl and 120 µl 100% ethanol and samples placed at -80°C for 30 min. The complementary DNA (cDNA) was pelleted by centrifugation at 15000 x g for 10 min and the supernatant was aspirated. The pelleted cDNA was then washed by the addition 100 µl of 70% and centrifugation at 15000 x g for 5 min. The supernatant was then aspirated and the cDNA pellet was dried using an Eppendorf Concentrator 5301 (Eppendorf), before resuspension in PCR grade water (Sigma).

2.7.3. Reverse Transcription PCR

Reverse transcription polymerase chain reaction (RT-PCR) was performed in 10 µl reactions which consisted of 5 µl TaqMan Gene Expression Master Mix (Applied Biosystems) or SsoFast Probes Supermix (Bio-Rad), 0.5 µl TaqMan gene expression assays (Applied Biosystems) and 4.5 µl cDNA (30 ng) diluted in PCR grade water (Sigma). Reactions were performed on FrameStar white-tubed (4titude) 96 well plates in triplicate. Reactions were run on a CFX96 Real-Time PCR Detection System, and the resulting data was analysed using the Bio-Rad CFX Manager 2.0 software (Bio-Rad). Standard thermal cycling conditions were 2 min at 95°C (initial denaturation), 40 cycles of 95°C for 5 s and 60°C for 5 s (Bio-Rad CFX96). The delta-delta Ct method (Schmittgen and Livak, 2008) was used to analyse the results of RT-PCR. Where relative quantification was appropriate, the target gene expression was normalised to the expression of a control gene(s). Typical

control genes include *GAPDH*, 60S acidic ribosomal protein P0 (*RPLPO*) or 18S ribosomal RNA (*18S*).

2.8. Chromatin Immunoprecipitation

2.8.1. Chromatin Preparation

$10^7 - 10^8$ cells were harvested by trypsinisation (0.05% trypsin-EDTA at 37°C). R10 was added to inactivate the trypsin, before the cell suspension was centrifuged at 300 x g for 3 min and the supernatant removed and discarded. The resulting cell pellet was then resuspended in 5 ml of the same culture medium in which the cell were grown. Cell-fixation was performed by the addition of formaldehyde to achieve a concentration of 1% (w/v). The formaldehyde-fixation was allowed to proceed for 10 min at RT. The fixation was then stopped by the addition of 0.125 M glycine and subsequent incubation at RT for 5 min. The cells were then pelleted by centrifuged at 300 x g for 5 min at 4°C. The cell pellet was then washed twice using 20 ml of ice-cold PBS and centrifugation at 300 x g for 5 min at 4°C. Cell pellets were then resuspended in ice-cold swelling buffer (5 mM Piperazine-N,N'-bis(2-ethanesulfonic acid) (PIPES) pH 8, 85 mM KCl), supplemented with Tergitol-type NP-40 (NP-40) (0.2% (v/v)) and complete EDTA-free protease inhibitors (Roche). The reaction was allowed to proceed for 20 min on ice with gentle rocking before centrifugation at 300 x g for 10 min at 4°C. The resulting pellet was then resuspended in TSE 150 (0.1% (w/v) SDS, 1% (v/v) Triton X-100, 2 mM EDTA, 20 mM Tris-HCl pH 8, 150 mM NaCl) supplemented with complete EDTA-free protease inhibitors. The sample was sonicated using a Biorupter sonicator (Diagenode), for 20 cycles of 30 s on / 30 s off at maximum power. Chromatin was centrifuged at 15000 x g for 30 min at 4°C and the supernatant was aliquoted and stored at -80°C.

2.8.2. Sonication Control DNA Extraction

DNA form a sample (20 µl) of the sonicated chromatin was isolated using phenol chloroform extraction (described in section 2.6.2.). The extracted sonicated chromatin was analysed on a 0.75% (w/v) TAE agarose gel using GelRed nucleic acid stain (1:10000 dilution) to visualise. 5 µl sonicated chromatin, 7.5 µl PCR grade water (Sigma) and 2.5 µl DNA loading dye were mixed and loaded onto the gel run in TAE buffer for a minimum of

1 h at 80 V. 100 bp and 1 Kb+ MW DNA ladders were run in alongside the sonicated DNA. Gels were visualised using the GeneSnap ID software.

2.8.3. Immunoprecipitation

Protein A or Protein G-sepharose beads (Sigma) were first blocked by incubation in buffer TSE 150 (20 mM Tris-HCl (pH8),150 mM NaCl, 2 mM EDTA, 0.1% SDS,1% Triton X-100) supplemented with 1 µg/ml yeast transfer ribonucleic acid (tRNA) (Sigma) pre-denatured at 95°C for 5 min) and 250 µg/ml BSA (Sigma). The blocking reaction was performed with rotation at 4°C for 4 h. The blocked beads were then washed three times using buffer TSE 150 and centrifugation at 800 x g for 1 min, before storage at 4°C.

Chromatin pre-cleared by incubating the sample (20 µg per immunoprecipitation (IP)) with 50 µl of 50% pre-blocked protein A or protein G-sepharose beads in 1 ml IP buffer TSE 150, supplemented with complete EDTA-free protease inhibitors for 1.5 h at 4°C while rotating. The beads were removed by centrifugation at 800 x g for 1 min. The supernatant (pre-cleared chromatin) was transferred into a new tube. 20 µl pre-cleared chromatin was used as input control. The remaining pre-cleared chromatin was used for the IP reactions by incubation with the relevant primary antibody (Appendix 3.) at 4°C overnight with end over end mixing.

Antibody-protein-DNA complexes were recovered by incubation with 50 µl of 50% pre-blocked protein A or protein G sepharose beads for 1.5 h at 4°C with end over end mixing. Beads were pelleted by centrifugation at 800 x g for 1 min at RT and were swashed once with 1 ml of IP buffer TSE 150. The beads were then pelleted by centrifugation at 800 x g for 1 min at RT and washed with 1 ml of IP buffer TSE 500 (0.1% SDS, 1% Triton, 2 mM EDTA, 20 mM Tris-HCl pH 8 and 500 mM NaCl). A third was performed using 1 ml of washing buffer (10 mM Tris-HCl pH 8, 0.25 M LiCl, 0.5% (v/v) NP-40). The final two wash steps were performed using 1 ml Tris-EDTA (TE) buffer (1 mM EDTA, 10 mM Tris-HCl pH 8). After the washes, DNA was eluted from the beads by the addition of 100 µl of elution buffer (1% (w/v) SDS, 10 mM EDTA, 50 mM Tris-HCl pH 8), the bead-elution buffer mixture was first mixed by vortexing before incubation at 65°C for 15 min with shaking. The beads were then pelleted by centrifugation at 15000 x g for 1 min. The supernatant containing the eluted DNA was transferred to a new tube. A second elution was performed by

resuspending the beads in 150 µl TE/1% SDS buffer, mixing using a vortex and centrifugation at 15000 x g. The supernatant from the second elution was then combined with that of the first elution. Immuno-precipitated was extracted using the phenol chloroform extraction method described in section 2.6.2.

2.8.4. Quantitative PCR Analysis

Quantitative PCR (qPCR) was performed using 7.5 µl of SsoFast™ EvaGreen® Supermix 2 X master mix (Bio-Rad), 2 µl of DNA, 0.6 µL of 10 mM forward primer, 0.6 µL of 10 mM reverse primer and PCR grade water (Sigma) up to a total volume of 15 µl. All reactions were run in at least triplicate wells on FrameStar white-tubed (4titude) 96 well plates. Reactions were run on a CFX96 Real-Time PCR Detection System. The data was analysed using Bio-Rad CFX Manager 2.0 (Bio-Rad) software. Typical cycling conditions were 2 min at 98°C (initial denaturation) followed by 40 cycles of 95°C for 5 s and 60°C for 5 s. Reaction specificity was determined using melt curve analysis. The level of enrichment was interrogated using 5 specific primers spanning each of the *RARRES1* and *LXN* promoter sequences. The enrichment of the sequences by IP was calculated relative to INPUT (chromatin with no IP) by the following equation.

$$\% \ input = ((2^{-CT \ of \ IP}) \times Dilution \ factor \ 1 \ \times Dilution \ factor \ 3 \div (2^{-CT \ of \ INPUT}) \\ \times Dilution \ factor \ 2 \ \times Dilution \ factor \ 3) \ \times 100$$

- Dilution factor 1 – the number of IPs that the chromatin is split between i.e. if the chromatin is split between 3 IPs the value of dilution factor 1 would be 3.
- Dilution factor 2 – the relative size of the input sample taken from the chromatin i.e. if a 20 µl sample is taken for the input from 1 ml of chromatin then dilution factor 2 would be 50.
- Dilution factor 3 – the dilution of the extracted DNA that enters the qPCR reaction i.e. if eluted DNA is resuspended in 50 µl of PCR grade water and 2 µl is used per reaction then dilution factor 3 would be 25.

2.8.5. Micro-Chromatin Immunoprecipitation

$10^3 - 10^5$ cells were trypsinised, sedimented and resuspended in 500 µl PBS. Cell-fixation was performed by the addition of 1% formaldehyde to a concentration of 1% (w/v). The fixation was allowed to proceed for 10 min at RT. The fixation was then stopped by the addition glycine to a final concentration of 0.125 M and incubation for 5 min at RT. The fixed cells were then pelleted by centrifugation at 470 x g for 10 min at 4°C. The cells were then washed twice with 500 µl ice-cold PBS and centrifuged at 470 x g for 10 min at 4°C. The supernatant was then aspirated so that only 20 µl remained before addition of 120 µl of lysis buffer (50 mM Tris-HCl, pH 8.0, 10 mM EDTA, 1% (wt/vol) SDS, and protease inhibitors) followed by vortexing, a 5 min incubation on ice and a further vortexing. The sample was sonicated using a Biorupter (Diagenode), for 20 cycles of 30 s on / 30 s off at maximum power. 400 µl of Radioimmunoprecipitation assay (RIPA) buffer (10 mM Tris-HCl, pH 7.5, 140 mM NaCl, 1 mM EDTA, 0.5 mM ethylene glycol-bis(β-aminoethyl ether)-N,N,N',N'-tetraacetic acid (EGTA), 1% (vol/vol) Triton X-100, 0.1% (wt/vol) SDS, 0.1% (wt/vol) Na-deoxycholate and protease inhibitors) was added and the sample was centrifuged at 12000 x g for 10 min at 4°C. The supernatant (chromatin) was removed, aliquoted and stored at -80°C.

Due to the very low levels of DNA isolated from small samples, the adequacy of sonication could not be determined by gel electrophoresis. However, by employing A qPCR method established by (Dahl and Collas, 2008) it is possible to estimate the level of fragmentation. Briefly, the DNA was amplified In a qPCR reaction using two sets of primers, one set amplifies a product of 100 bp while the second amplifies a product of 300 bp. The qPCR ratio of the 100 bp to a 300 bp products increases as a function of sonication cycles, indicating that the mean chromatin fragment size is reducing with the number of cycles. This is because 300 bp template is broken at a greater rate than the 100 bp template, due to its size.

IP was performed as described in section 2.8.3. however, magnetic protein A or protein G dynabeads were used instead of sepharose beads as it was found empirically that dynabeads have less non-specific binding of chromatin and hence provide a better signal to noise ratio.

qPCR analysis was performed as described in section 2.8.4.

2.9. Analysis of Protein Expression

2.9.1. Cell Lysis

Cells were first washed once in PBS before cell-lysis using either CytoBuster protein extraction reagent (Novagen) or RIPA. Complete EDTA-free protease inhibitor cocktail was routinely included and the resulting mixture was incubated with the cells, on ice for 5 min. The culture surface was then scraped and the lysate centrifuged at 4°C at 16000 x g for 5 min using a Hettich Mikro 220R Centrifuge (SLS). The lysates were routinely stored at -80°C.

2.9.2. Bicinchoninic Acid Assay

The protein concentration of samples was determined using the bicinchoninic acid (BCA) assay protein assay kit (Thermo Fisher Scientific). 25 µl of BSA standards or samples were added to (an individual well each) a 96 well plate. 200 µl working reagent was added to each well and the reaction was allowed to proceed at 37°C for 30 min. Absorbance of samples and standards were measured at 562 nm on a POLARstar OPTIMA microplate reader (BMG Labtech). The protein concentration of unknown samples was determined by interpolation from the standard curve.

2.9.3. Sodium Dodecyl Sulphate Polyacrylamide Gel Electrophoresis

Cell-lysate equivalent to 20 µg of protein was mixed in a 3:1 ratio with 4 x SDS loading buffer (10% (v/v) glycerol, 62.5 mM Tris-HCl pH 6.8, 1% (w/v) SDs, 65 mM DTT and bromophenol blue). Mixing was performed using a vortex for 10 s and was then incubated at 100°C for 15 min using a Grant QBD2 heating block (Grant). Samples were then vortexed to mix before loading onto a 8-12% Tris-SDS acrylamide gel, cast using the Bio-Rad Protean II system. The gel was then and run at 100 V in 1 x SDS running buffer (25 mM Tris-HCl, 0.19 M glycine and 3.5 mM SDS). Biotinylated (Cell Signalling Technology) and Kaleidoscope (Bio-Rad) molecular weight ladders were run alongside samples to allow sizing.

2.9.4. Western Blot

Methanol was used to activate Immobilon-P membrane which was then washed with distilled H_2O and equilibrated in transfer buffer (48 mM Tris-HCl, 39 mM glycine and 10% (v/v) methanol). Proteins were transferred from the gel to the membrane at 100 V for 2 h. After transfer, the membranes were blocked by incubation with 5% (w/v) non-fat skimmed milk (Marvel) solution for 1 h at RT. The blocking solution was then removed and primary antibody in a 1% Marvel solution was added. The binding of primary antibody was performed RT for 1 h. The primary antibody solution was then removed and the membrane was washed three times using TBST (150 mM NaCl, 50 mM Tris-HCl and 0.1% (v/v) Tween-20 at pH 7.4). Next, Peroxidase-labelled secondary antibodies at a dilution factor of 1:10,000 (Cell Signalling Technologies/Boehringer) in 5% marvel were added and allowed to bid by incubation at RT for 1 h. The secondary antibody solution was then removed before the membrane was washed four times using TBST. Peroxidase substrate (Roche) was then added to the membrane. Luminescence was detected using GeneGnome XRQ Chemiluminescence imager (Syngene).

2.9.5. Protein Immunoprecipitation

2×10^6 cells were lysed with RIPA and precleared with anti-keratin conjugated sepharose beads. All IPs were performed using pre-conjugated anti-HA conjugated sepharose beads (Sigma). The resulting precipitation was washed 5x with high salt RIPA (300 mM NaCl) to remove non-specific binding proteins. Interacting proteins were eluted with Laemmli buffer with the addition of 2-Mercaptoethanol. The resulting eluate was either analysed by western blot as previously described or by mass spectrometry which was performed by the technology facility at the University of York.

2.10. Protein Localisation Assays

2.10.1. Immunofluorescence

The culture surface for immunofluorescence was BD-Biocoat collagen-I-coated for primary cells. When cell lines were to be analysed BD-Falcon uncoated 8-well chamber slides (BD Bioscience) were used. 300 µl cell suspensions were plated into chamber slides

at 2-5 x 10^4 cells per well and incubated at 37°C. Culture medium was then removed before the cells were washed twice with PBS. Cells were then fixed with 200 μl 4% (w/v) paraformaldehyde pH 7.4 for 20 min. Three washes were performed after fixation, each with 500 μl of PBS for 5 min. The cells were then permeabilised with 300 μl 0.5% (v/v) Triton X-100 for 25 min. After permeablisation, cells were washed 3 times with PBS. Blocking was done using with 200 μl 10% (v/v) goat serum diluted 1% (w/v) BSA in PBS for 30 min. The sample was then incubated in the presence of primary antibody diluted in 1% BSA in PBS for 1 h. Before incubation with secondary antibody the cells were then washed three times with 500 μl PBS for 5 min. 200 μl of secondary antibody diluted in 1% BSA in PBS was then added and allowed to incubate for 45 min at RT. Next, the cells were washed three times using 500 μl PBS with 5 min incubation per wash. The chambers were then removed from the slide and Vectashield mounting medium with 4',6-diamidino-2-phenylindole (DAPI) (Vector laboratories) was added to the cells. A coverslip (SLS) was then placed on top of the sample, which was sealed with nail varnish. Analysis was performed using a Nikon Eclipse TE300 fluorescent microscope (Nikon) or a LSM 720 meta confocal microscope (Zeiss). Primary antibody dilutions used for immunofluorescence are listed in (Appendix 2.). Secondary Alexafluor 488 or 568 goat anti-rabbit or goat anti-mouse IgG antibodies (Invitrogen) were typically used at a dilution factor of 1:200.

2.10.2. Subcellular Fractionation

Nucleocytoplasmic fractionation of PC3, PC3M, 293 cell lines and primary cells was performed using NE-PER Nuclear and Cytoplasmic Extraction kit (Thermo Fisher Scientific) and according to the manufactures' protocol. Cells were harvested by trypsinisation, washed once with culture medium and then once with PBS 1X at 300 x g for 5 min at 4°C. The pellet was resuspended in 1 ml PBS and transferred to a 1.5 ml microcentrifuge tube and washed once more in PBS. The supernatant was then removed and the cells were re-suspended in ice-cold CER I buffer (supplied as part of the kit) with protease inhibitors. The sample was then vortexed vigorously on the highest setting for 15 s before being incubated on ice for 10 min. Ice-cold CER II buffer (supplied as part of the kit) was then added to the sample which was then vortexed for 5 s. The sample was then incubated on ice for 1 min and was then vortexed for 5 s before being centrifuged at 16000 x g for 5 min at 4°C. The top 90% of the supernatant (cytoplasmic extract) to a clean pre-chilled microcentrifuge tube this is the cytoplasmic fraction. The final 10% of the supernatant

was then removed and discarded and the pellet was re-suspended in 1 ml of ice-cold PBS and centrifuged at 16000 x g for 10 min at 4°C the supernatant was discarded and the pellet was suspended in ice-cold NER buffer (supplied as part of the kit) with protease inhibitors. The sample was then vortexed for 15 s and incubated on ice for 40 min with vortexing every 10 min. The sample was the centrifuged at 16000 x g for 10 min at 4°C. The top 90% of the supernatant (nuclear extract) was then transferred to a clean pre-chilled tube. Both nuclear and cytoplasmic fractions were stored at -8.

3. Development and Validation of a qPCR Test for Simultaneous Detection of AR Amplification and X Chromosome Aneuploidy

3.1. Introduction

As discussed in section 1.3.6. GAAR has been detected in up to 80% of CRPCs, of which 30% of these have a high level amplification (≥3.8 copies per cell) (Visakorpi et al., 1995, Waltering et al., 2012). In contrast, the prevailing consensus is that AR amplification represents a very rare event in ADT-naïve CaP e.g. in only 2 out of 205 cases in a study by (Bubendorf et al., 1999) were positive for GAAR. This view has recently been challenged by (Merson et al., 2014) who showed, through extensive FISH experiments, that very small foci of cells with X chromosome aneuploidy (XCA) and/or locus specific GAAR (≤ 600 nm, ≤1% of tumour volume) (Fig. 14B.) were present in patients (33 out of 261 cases examined (12.6%) of Gleason 6 cancers) with low grade disease, who had not undergone hormone deprivation therapy (Fig. 14.) (Merson et al., 2014). Therefore, GAAR could be the result of evolution of CaP in direct response to the selection pressure of ADT leading to the specific clonal expansion of very these rare clones (Saraon et al., 2011, Merson et al., 2014).

GAAR and/or XCA is associated with reduced survival, demonstrated by (Merson et al., 2014), this study showed that patients with small foci of tumour cells with four or more copies of the X chromosome (Cat 4) had a hazard ratio of 7.92 (95% confidence interval (CI)= 2.50–25.13) and patients with small focal tumours cells containing specific AR gene amplification (Cat 5) had a hazard ratio of 5.08 (95% CI=1.85–13.95) compared to patients with a single X chromosome and no amplification of the AR gene (Cat 1). This dramatic effect on survival can be seen in (Fig. 14C.). However, GAAR has been shown to predict the patients who will respond to 'second-line' combined androgen blockade i.e. combination of androgen antagonist and androgen synthesis inhibitors (Palmberg et al., 1997). The androgen signalling axis is presumed to be intact, but with a lower threshold of activation, in these patients.

A.
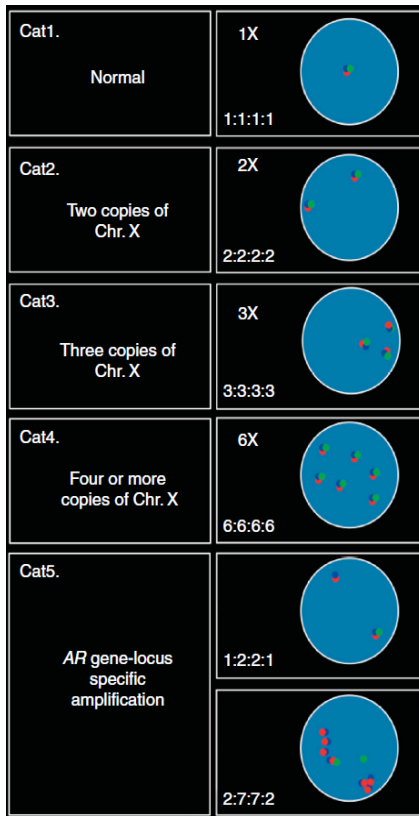
B.
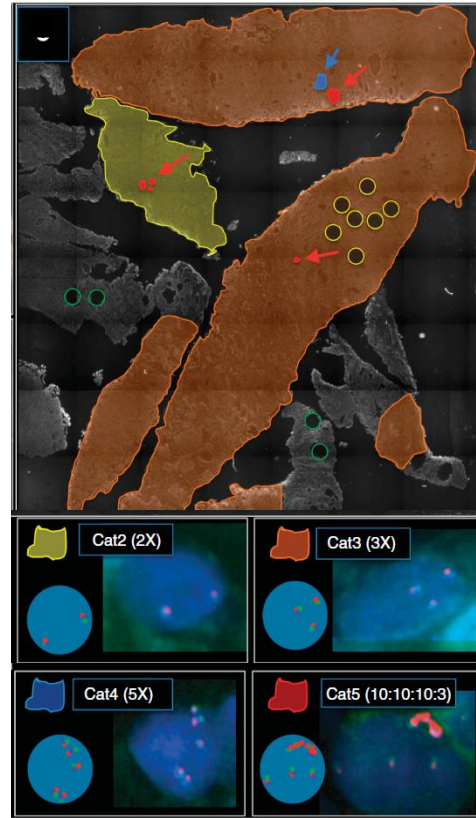
C.
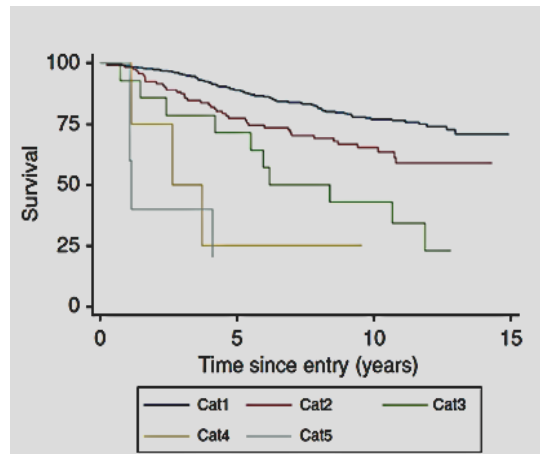
Fig. 14. AR Amplification and X Chromosome Aneuploidy can be Detected in Small Foci of Hormone Naïve CaP Tumours and is Associated with Poor Prognosis.

A. Definition of the five categories (Cat1–5) of AR and X chromosome copy number alterations. Cat1–4 represents of increasing level of X chromosome aneuploidy. Cat5 is defined by locus-specific amplification of AR with or without X chromosome aneuploidy. Tumours were scored by counting the Green (probe is specific to a region 1.15 Mb upstream of AR), Blue (probe specific to the AR gene), Red (probe specific to a region 0.1 Mb downstream of AR) and signals. Cat1 contain a single X chromosome and AR gene. This is visualised as single and overlapping Green, Blue and Red signals which correlated with an X chromosome centromere probe (not shown). This normal pattern was counted as 1:1:1:1. X chromosome aneuploidy was inferred when multiples of this pattern were seen (Cat2–4) e.g. 2:2:2:2 represents two copies of the X chromosome. A Cat5 amplification (locus-specific gain of AR) was defined as an unequal accumulation of the probes e.g. a 1:2:2:1 pattern represents a single X chromosome with a duplication of the AR gene. It was found that amplifications could involve all three probes or just multiples of adjacent probes. Exclusive amplification of the Blue probe was detected I this study.

B. Whole TURP-block sections analysed by FISH for AR and X chromosome accumulations. Yellow regions are positive for a Cat2 X chromosome amplification, Orange regions are positive for a Cat3 X chromosome amplification, Blue regions are positive for Cat4 X chromosome amplification and Red regions are positive for a Cat5 locus-specific amplification of the AR gene. Grey regions are not positive for CaP (determined by histological analysis) and were not scored. Yellow and green circles indicate positions of the 600 μm diameter cores taken from areas of tumour and normal, respectively, for TMA construction. Blue and red arrows highlight the small foci of Cat4 and Cat5 tumour, respectively. In all patients analysed, CaP foci that were designated as Cat5 were less than 1% of the whole-block tumour area.

The ability of clinicians to stratify patients, according to their likelihood of responding to 2nd line androgen blockade, is likely to have several clinical and economic benefits. One major benefit in terms of patient outcome would be in the timing of optimal therapy i.e. if a patient is unlikely to respond to 2nd line androgen blockade, then a chemotherapeutic regimen can be implemented immediately rather than waiting for 2nd line androgen blockade to fail.

Since the formation of the National Institute for Health and Care Excellence (NICE), to govern the use of therapeutics in the UK National Health Service (NHS) and the healthcare reforms due to occur in the USA, the economics of cancer therapy must now be considered, e.g. the incremental cost-effectiveness ratio (Cerri et al., 2013). An affordable assay that predicts patient response to 2nd line androgen blockade would enable clinicians to justify the use of high-cost therapies, such as Abiraterone and Enzulutamide in a particular group of patients that are likely to respond i.e. those with GAAR.

Detection of GAAR is most commonly performed using FISH. This technique has limitations however, as it is semi-quantitative and subjective. A report highlighted these inadequacies when determining genomic amplification (Albertson, 2012). In which it was shown that the differing results between groups were clearly the result of FISH-artefacts specifically the detection of Oestrogen receptor alpha (ESR1) transcripts, confirmed by RNase treatment eliminating these signals (Albertson, 2012).

An alternative method to identify GAAR is genomic sequencing. While this approach is likely to reveal a lot of additional information, which may aid patient care and guide treatment options, it is at present prohibitively expensive. Even though the cost of genomic sequencing is falling year on year, a 10 times coverage of the human genome, (which is required to accurately sequence both alleles in 90% of human genes, from 25 base pair reads, using shotgun sequencing) would cost in the region of $5,000 per patient (Cho et al., 2012). A lower-cost sequencing strategy would be to use targeted-sequencing of *AR* alleles. However this approach would not provide the additional information generated by whole-genome sequencing.

The most appropriate platform for accurate and cost-effective detection of genomic copy number variations is qPCR. As such several assays for the detection of *AR* copy number

variations are commercially available, such as TaqMan® Copy Number Assays (Life Technologies™) and qBiomarker Copy Number Assays (Qiagen). However, these 'off the shelf' assays are not without their limitations. For example, it is important to note that these assays do not include a non-CaP associated X-chromosome normalising gene as standard, and are thus unable to discriminate between specific GAAR and amplification due to XCA, which is common in prostate cancer (Brothman et al., 1994).

In this chapter a qPCR method has been developed for the detection of locus-specific GAAR as well as XCA, furthermore, it is capable of discriminating between these gross genetic changes. It is specific, sensitive, amenable to high-throughput screening and less time-consuming than FISH, whilst retaining the ability to resolve minor cell populations in a heterogeneous biopsy. It could provide an affordable and effective means for identifying patients with 'high-risk disease'. It also has the potential to aid triaging of CaP patients (through theranostic evaluation) as disease progresses from a hormone responsive and non-metastatic phenotype to castration-resistant, metastatic disease. Aiding the selection of the most appropriate treatment from the many options available (Fig. 15.), in a timely manner, to improve patient outcomes (Heidenreich et al., 2013).
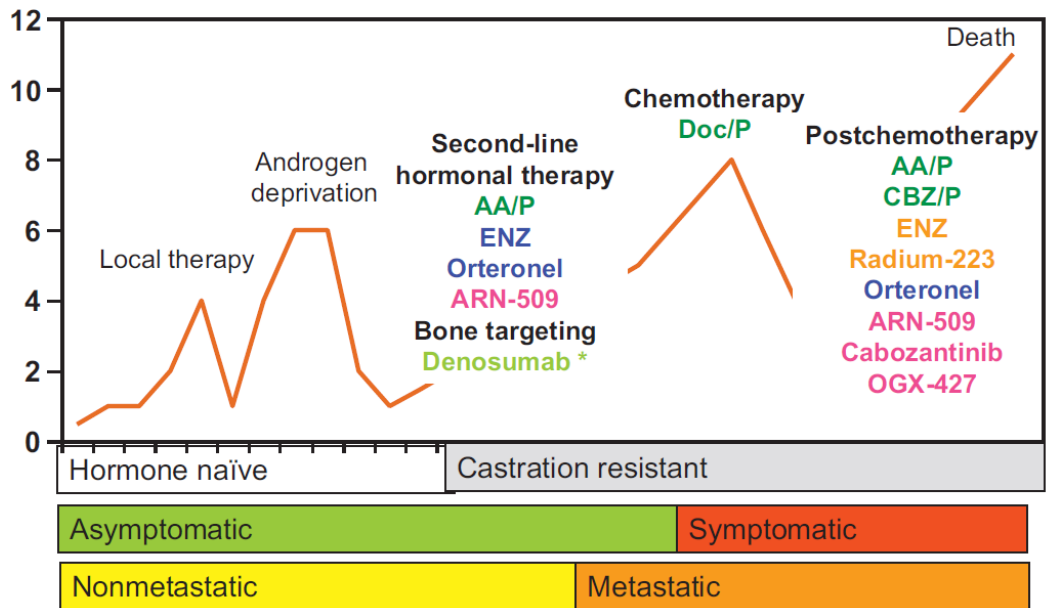
Fig. 15. Current, Ongoing, and Future Landscape in the Management of Castration-Resistant Prostate Cancer.

Depiction of the various treatment choices as CaP progresses from a hormone-naïve, non-metastatic, asymptomatic disease to a metastatic CRPC phenotype.

Drug colour key: green = US Food and Drug Administration/European Medicines Agency (FDA/EMA) approved; light green = positive trial results in high-risk patients but the compound is not approved; orange = completion of phase 3 clinical trial with positive results; blue = prospective, randomized, phase 3 clinical trial completed, results awaited; purple = promising agent.

From: (Heidenreich et al., 2013)

3.2. Premise of the Assay

The assay is composed of three qPCR reactions using primers specific to *AR*, *DMD* and *GAPDH* genes. The locations of these genes on their respective chromosome are shown in (Fig. 16.). The *GAPDH* gene is used as a somatic chromosome control to which *AR* and *DMD* copy numbers can be normalised to. Additionally the copy number of *AR* can be normalised to both *GAPDH* and *DMD* genes, this allows distinction between locus-specific GAAR and *AR* gain due to XCA.

The *DMD* gene was chosen as a good control gene to analyse XCA as after an exhaustive literature search (not shown) it was found to be not implicated in CaP initiation, susceptibility, maintenance, expansion or metastasis. Also it is located far from the *AR* gene so is highly unlikely to be included in a specific *AR* amplification. It could be argued that several genes on the X chromosome should be utilised as X chromosome control genes however, this would lead to an increase in assay preparation, sample usage and analysis time, without providing any more information.

When *AR* copy number is normalised to *GAPDH* copy number, female DNA shows twice the compliment *AR* relative to male DNA i.e. male DNA = 1 copy of *AR* divided by 2 copies of *GAPDH* = 0.5 relative ratio. Female DNA = 2 copies of *AR* divided by 2 copies of *GAPDH* = 1 relative ratio. When samples are normalised to both *GAPDH* and *DMD* copy numbers, both male and female DNA have equal relative ratios of *AR* i.e. male DNA = (1 copy *AR* divided by 2 copies of *GAPDH*) divided by (1 copy of *DMD* divided by 2 copies of *GAPDH*) = 0.5/0.5 = 1. Female DNA = (2 copies of *AR* divided by 2 copies of *GAPDH*) divided by (2 copies of *DMD* divided by 2 copies of *GAPDH*) = 1/1 =1. This has the effect of eliminating any *AR* copy number gains which are due to XCA.

All primers are located within either an intronic region or exon-intron junction within their respective genes (sequences in Appendix 2.). This precludes any unintended amplification of mRNA species. In the case of the *AR* primers they were designed to amplify the junction between intron two and exon two as well as the majority of the short exon two (Fig. 17.). This is of importance because exon two encodes part of the DNA-binding domain allowing detection of WT and mutant *AR* genes which are most commonly corrupted in the ligand binding domain.
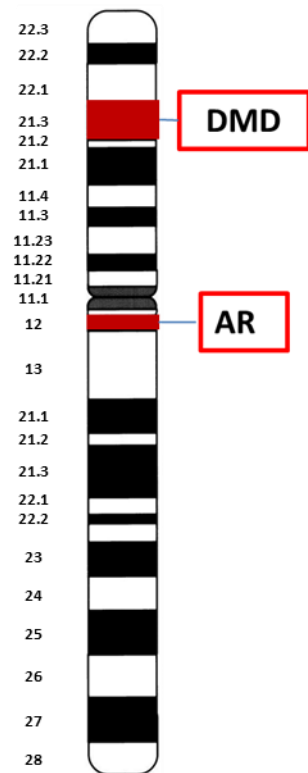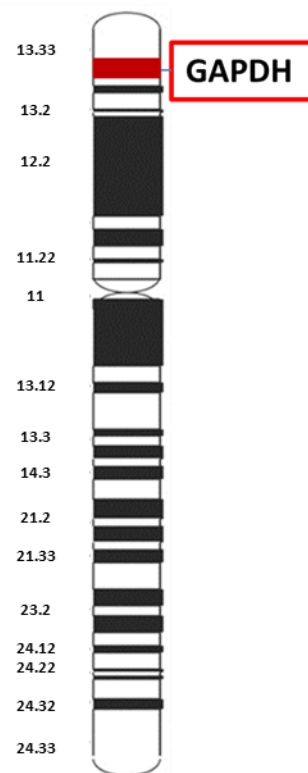
Fig. 16. Location of AR, DMD and GAPDH Genes.

X chromosome and chromosome12 gene-maps, with the approximate regions (highlighted in red) where the *AR*, *DMD* and *GAPDH* genes are located.

Chapter 3. Results
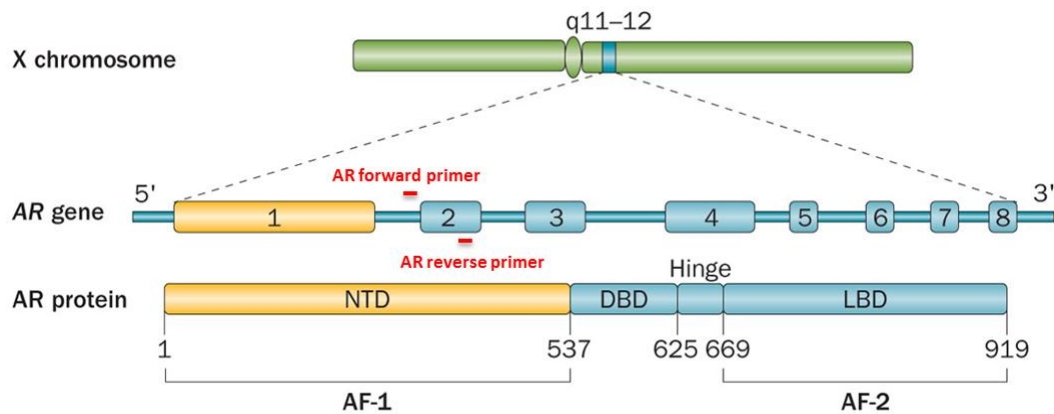
Fig. 17. Location of AR Primers.

Modular structure of the AR gene and protein. The approximate locations of the forward and reverse primers used in the assay are shown in red.

AF = activation function, AR = androgen receptor, DBD = DNA-binding domain, LBD = ligand-binding domain and NTD = amino-terminal domain.

Adapted from: (Lorente et al., 2015)

3.3. Assay Work-Flow

This section describes in brief how genetic material from a sample is prepared and analysed.

Any human gDNA is compatible with the assay. gDNA from cell lines, primary cultures and lymphocytes can be extracted using Qiagen kits or phenol-chloroform extraction. When analysing tissue samples either frozen in OCT or FFPE, it is necessary to ensure that a cancerous lesion is present in the tissue section from which DNA is extracted. This is achieved by serially sectioning the tissue and performing haematoxylin and eosin (H&E) staining on flanking tissue slices (Fig. 18.).

Once the DNA was extracted it was amplified using primers specific to *AR*, *DMD* and *GAPDH* genes according to the cycling protocols in (Table. 4.).

Certain control samples were analysed on every run of the assay to ensure the assay was performing consistently these were normal male DNA, normal female DNA and VCaP DNA. Comparison of male and female DNA ensured that the assay was sensitive enough to detect the extra copy of both the *AR* and *DMD* genes whilst the VCaP DNA was utilised as a positive control for GAAR. Wherever possible, patient lymphocytes were analysed alongside the primary tissue, culture or xenograft tissue. The assay also incorporated a standard curve of normal female DNA to enable absolute quantification.

Target Gene	Melting Temperature (°C)	Annealing and Extension Temperature (°C)	Number of Cycles
AR	98	58	38
DMD	98	58	38
GAPDH	98	58	38

Table. 4. qPCR Cycling Conditions for AR, DMD and GAPDH Primers
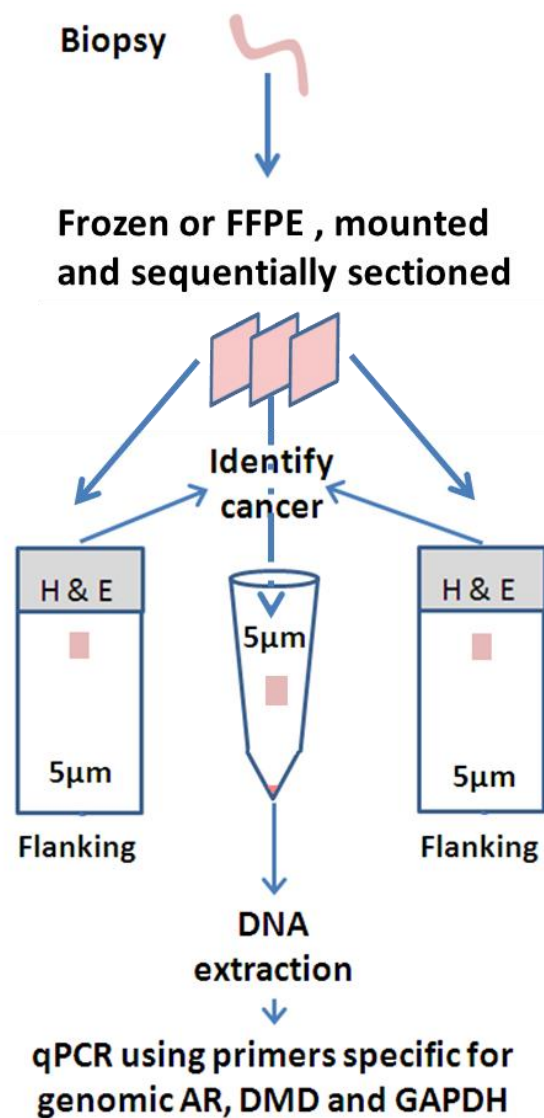
Fig. 18. Preparation of Genetic Material for Analysis of AR, DMD and GAPDH Copy Numbers from Tissue Samples.

A sample of the patient or xenograft tissue is taken either through biopsy or direct excision from whole tumour. The sample is then prepared for histological sectioning by either preservation by freezing in OCT or by formalin fixing and paraffin embedding. Once the sample has been mounted it can then be serially sectioned. Flanking tissue slices are used to identify a cancerous lesion by H&E staining. Once an area of cancer has been located it can then be further processed to extract the genomic DNA (gDNA) by either Qiagen kits or phenol-chloroform extraction. Once the gDNA has been extracted the copy number of AR, DMD and GAPDH genes is elucidated by qPCR using gene specific primers.

3.4. Results

3.4.1. Semi-Quantitative Analysis of AR Copy Number in Male and Female Genomic DNA by PCR

A pilot study was performed using standard PCR on male and female genomic DNA (10 ng) using primers specific for *AR* and *GAPDH* (Fig. 19.). Both 25 and 30 cycles were investigated to increase the chance of seeing an unsaturated reaction. 25 cycles did not yield any visible DNA bands (Fig. 19A. lanes 9-14). 30 cycles yielded no bands in the non-template control (-ve) lanes, faint bands of in the AR lanes (an expanded view is shown in (Fig. 19C.) for clarity) which correspond to the expected AR PCR product and relatively bright bands in the GAPDH lanes which correspond to the expected GAPDH PCR product (Fig. 19A.).

The gel image was analysed using ImageJ software results of this are tabulated in (Fig. 19D.). The area under the curve was used to compare the copy number of *AR* between male and female DNA once normalised to *GAPDH* (Fig. 19E.). This analysis gave a 1.44 fold difference in AR copy number in female DNA compared to male DNA. An expected value for this analysis is a fold difference of two, representing the two X chromosomes present in females versus the single X copy in males. A potential explanation for this discrepancy is that the increased products in the female DNA reaction may have inhibited said reaction causing a plateau (particularly in the GAPDH reactions). Additionally, measuring band intensity by densitometry has inherent inaccuracies i.e. drawing around the band and unequal brightness across the band, which also contribute to this method being semi-quantitative. However, this pilot study confirmed the feasibility of the project and allowed the progression to qPCR.

A

B

LANE	CONTENTS
1	100bp Ladder
2	-ve AR 30 cycles
3	♂ AR 30 cycles
4	♀ AR 30 cycles
5	-ve GAPDH 30 cycles
6	♂ GAPDH 30 cycles
7	♀ GAPDH 30 cycles
8	BLANK
9	-ve AR 25 cycles
10	♂ AR 25 cycles
11	♀ AR 25 cycles
12	-ve GAPDH 25 cycles
13	♂ GAPDH 25 cycles
14	♀ GAPDH 25 cycles
15	100bp Ladder

C

D

SAMPLE	AuC
♂ AR 30 cycles	682.113
♀ AR 30 cycles	1033.305
♂ GAPDH 30 cycles	3394.326
♀ GAPDH 30 cycles	3565.79

E AR band intensity normalised to GAPDH intensity

	♀	0.289783
	♂	0.200957
Fold difference	NA	1.44

Fig. 19. Semi-Quantitative Analysis of AR Copy Number in Male and Female Genomic DNA by PCR.

A. Agarose gel following gel electrophoresis loaded as described in the lane legend depicted in **B**. **C.** Expanded image of the area of the gel encircled in red. **D.** Tabulated data acquired using ImageJ software to analyse the size and intensity of the bands in lanes 3, 4, 6 and 7. **E.** Table of the AR bands normalised to the corresponding GAPDH bands along with the fold difference between the male and female DNA analysed.

3.4.2. Primer Efficiency and Species Specificity of AR, GAPDH and DMD Primers in qPCR

Primers were designed using the National Center for Biotechnology Information (NCBI) primer designing online tool. The following parameters of the qPCR assay for each primer pair were validated: efficiency, R^2 (a statistical measure of how close the data are to the fitted regression line), presence of non-specific amplifications and species specificity. Human female DNA was used to generate a standard curve using *AR* (Fig. 20A.), GAPDH (Fig. 20C.) and DMD (Fig. 20E.) primers. The starting quantities analysed were 10 ng, 3 ng, 1 ng, 0.3 ng, 0.1 ng, 0.03 ng and 0.0 1ng. Melt curves for all primers were also generated to ensure only a single specific product was amplified (Fig. 20B, D and F). Mouse DNA was also tested using the same primers to determine species specificity at a starting quantity of 10 ng. Each condition was measured in triplicate.

The *AR* primer pair had an efficiency of 97.1% an R^2 value of 0.997 and a species specificity of 5093-fold (Fig. 20G.). The *DMD* primer pair had an efficiency of 101.4% an R^2 value of 0.990 and a species specificity of 1343-fold. The *GAPDH* primer pair had an efficiency of 101.5% an R^2 value of 0.991 and a species specificity of 2042-fold. The efficiency and R^2 values and species specificity of all the primers tested were deemed acceptable such that it was possible to proceed to the validation of the assay.

A. AR Standard Curve

B. AR Melt Peak

C. DMD Standard Curve

D. DMD Melt Peak

E. GAPDH Standard Curve

F. GAPDH Melt Peak

G.

Primer Pair	Efficiency (%)	R^2 Value	Species Specificity (Fold)
AR	97.1	0.997	5093
DMD	101.4	0.990	1343
GAPDH	101.5	0.991	2042
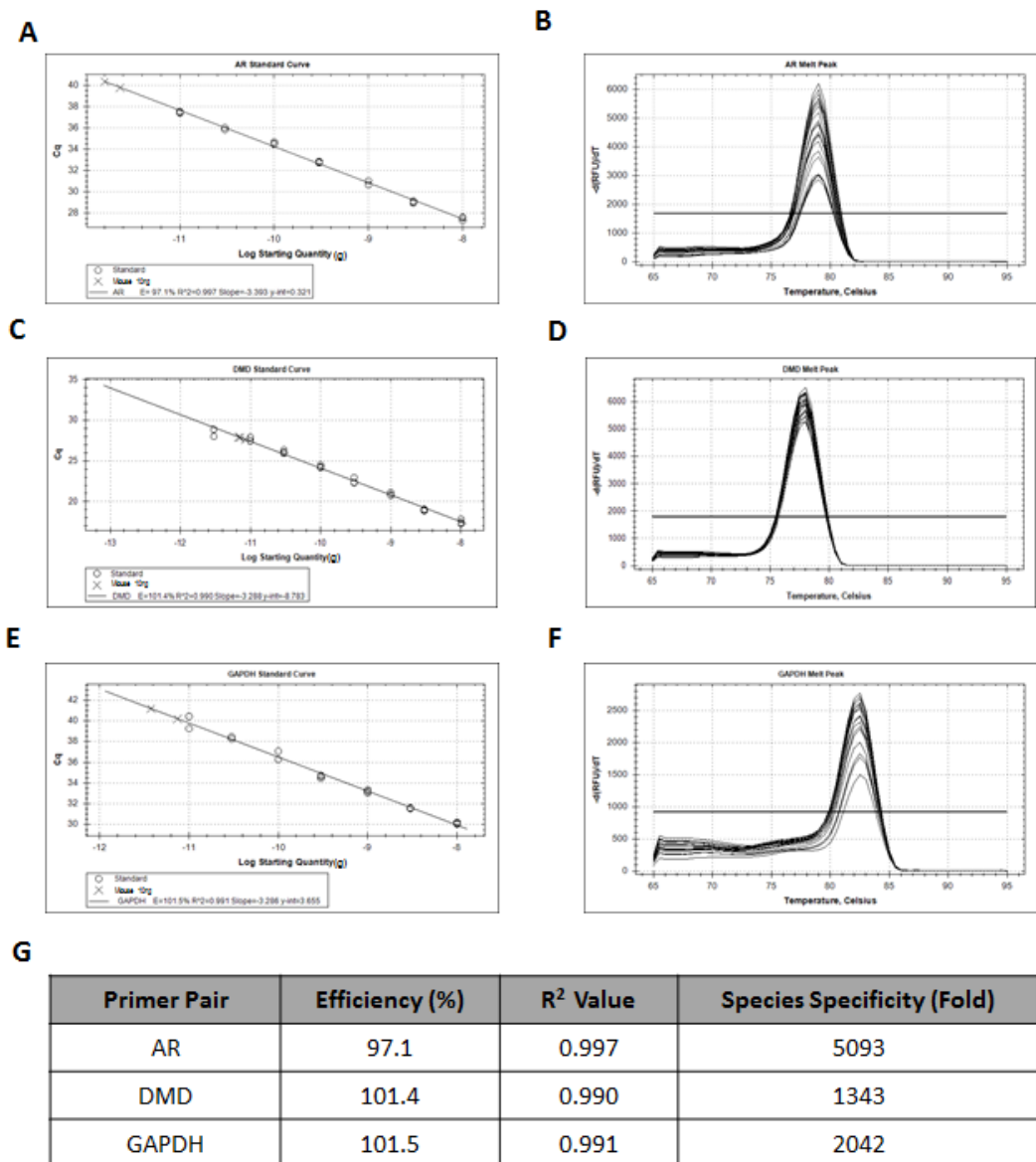
Fig. 20. Primer Evaluation - Standard Curve Analysis and Species Specificity.

The suitability of each primer pair for investigating genomic copy number variation was determined by generating a 7-point standard curve from female DNA covering 4 log units ranging from a starting DNA quantity of 10ng to 0.01ng of normal female DNA. **A.** AR, **C.** DMD and **E.** GAPDH. Specific amplification of the target sequence was assessed by generating a melt peak for each primer pair **B.** AR, **D.** DMD and **F.** GAPDH. The species specificity was also determined by comparing the 10 ng of Mouse Liver DNA to 10 ng of normal male DNA. **G.** Summary of the standard curve analysis and species specificity for AR, DMD and GAPDH primer pairs. All samples were measured in triplicate. Analysis was performed using Bio-Rad CFX software.

3.4.3. Genomic Copy Number of AR and DMD in Human Prostate Cancer Cell Lines

To validate the assay, genomic copy number of *AR*, *DMD* and *GAPDH* were elucidated in a number of prostate cancer cell lines. Human female DNA was used to generate standard curves, and acted as a control together with normal male DNA. *AR* copy number is expressed relative to *GAPDH* (Fig. 21A.) or normalised to *GAPDH* and *DMD* (Fig. 21B.).

As expected, female DNA had a copy number of 2, for *AR* and *DMD*, whilst normal male DNA had a copy number of 1 for both genes (Fig. 21A.). Both PNT1A and PNT2C2 (immortalised normal prostate cell lines) had a single copy of *AR* and *DMD*. The only cell line tested that showed specific amplification of the *AR* gene was the CaP cell line, VCaP, which showed dramatic amplification of approximately 28 fold. In contrast, DU145, PC3, PC346C (which is not derived from PC3) and RWPE1 had increased copy numbers of *AR* and *DMD*. However, when the *AR*:*DMD* ratio was examined it revealed that these cells had not specifically amplified the AR gene but had increased X chromosome copy number (Fig. 21B.). These results highlight the importance of controlling for XCA. A similar level of AR amplification in the VCaP cell line was reported by Li et al (2012) who also showed that LNCaP cells have a single copy of *AR* (Li et al., 2012).

One deficiency of this experiment was that any potential *GAPDH* amplification was not taken into account. The major goal of this experiment was to obtain a positive control of specific GAAR to interrogate the sensitivity and accuracy of the assay. This was found to be the VCaP cell line.
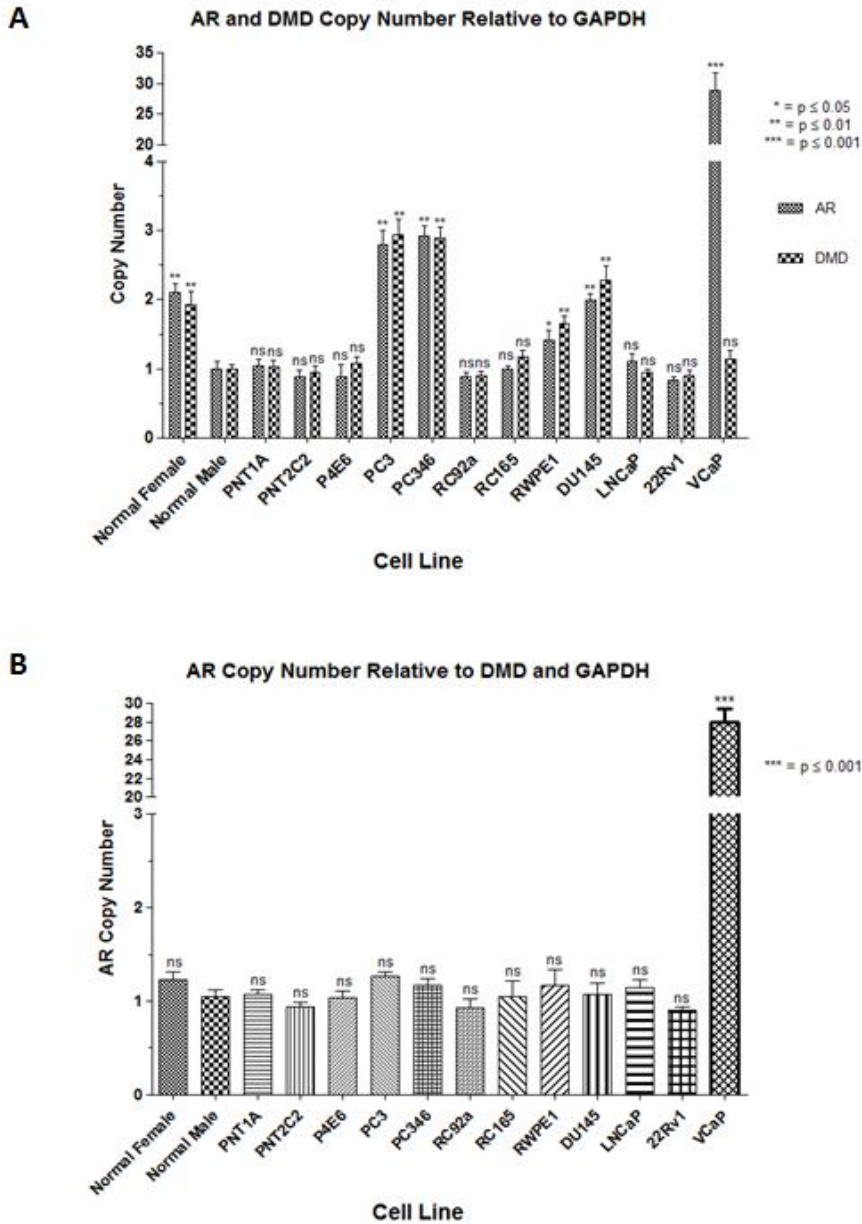
Fig. 21. AR Copy Number Variation in CaP Cell Lines.

The AR copy number of several CaP cell lines was analysed by normalising the AR starting-quantity (SQ) to the SQ of GAPDH **A**. or AR to GAPDH and DMD **B**. All samples are expressed relative to normal male DNA. A four-point standard curve (ranging from 10 ng to 0.3 ng) was generated from female DNA for AR, DMD and GAPDH. Analysis was performed using Bio-Rad CFX software. The total starting quantity for all conditions (excluding the standard curve) was 3 ng and all samples were measured in quadruplicate.

Error bars = one standard error of the mean.

Each sample represents at least 3 experimental replicates each comprising 3 technical replicates.

* = p≤ 0.05   ** = p≤ 0.01   *** = p≤ 0.001   ns = non-significant

3.4.4. Assay Validation – Sensitivity and Accuracy

Biopsy samples display cellular heterogeneity and contain areas of normal tissue. This could lead to false negative results, potentially masking GAAR in a sample. The sensitivity and accuracy of the assay was determined using differing amounts of VCaP and normal male DNA mixed together to simulate a heterogeneous population. The total starting quantity for all conditions (excluding the standard curve) was 3 ng and all samples were measured in quadruplicate. Human female DNA was used to generate standard curves for *AR*, *GAPDH* and *DMD* primer pairs as previously described. The conditions analysed were as follows: 10% VCaP - 90% normal male, 5% VCaP - 95% normal male, 2% VCaP - 98% normal male and 1% VCaP - 99% normal male. The expected AR copy number for VCaP – normal male DNA mixtures were calculated and used to investigate the sensitivity and accuracy of the assay.

The assay succeeded in detecting an *AR* amplification above normal male DNA in all of the conditions tested including 1% VCaP - 99% normal (Fig. 22A.). The achieved *AR* copy numbers of all the VCaP - normal male mixtures did not deviate significantly from predicted values (Fig. 22B.).

Similar to the cut-off threshold in PSA testing a threshold for GAAR detection was established using three standard deviations above the average normal AR value of 23 normal samples (data not shown). This was done to account for variability of the assay. Using this threshold it was possible to generate an equation to determine the minimum percentage of abnormal DNA required for detection of GAAR (Fig. 22C.). This equation was used to calculate the minimum percentage of abnormal DNA required to detect GAAR in a heterogeneous sample containing cells with a normal *AR* gene copy number (Fig. 22D.). The analysis revealed that an AR amplification of 2-fold can be detected in a heterogeneous sample if only 20% of cells are positive for the amplification.

A Assay Sensitivity

AR Copy Number

100% Normal Male
1% VCaP + 99% Normal Male *
2% VCaP + 98% Normal Male **
5% VCaP + 95% Normal Male **
10% VCaP + 90% Normal Male **

* = $p \leq 0.05$
** = $p \leq 0.01$

B Assay Accuracy

AR Copy Number vs VCaP DNA (%)

— Theoretical
✗ Experimental Values

ns
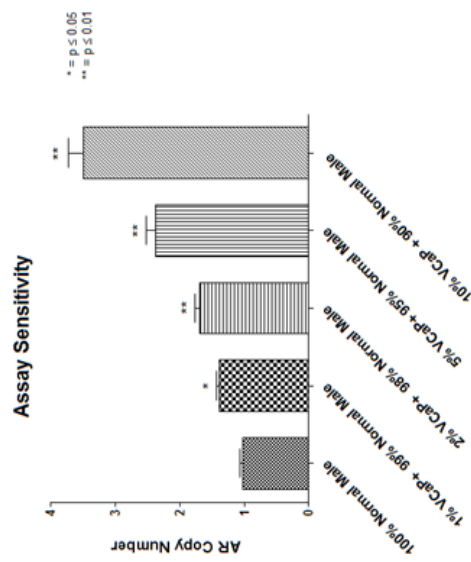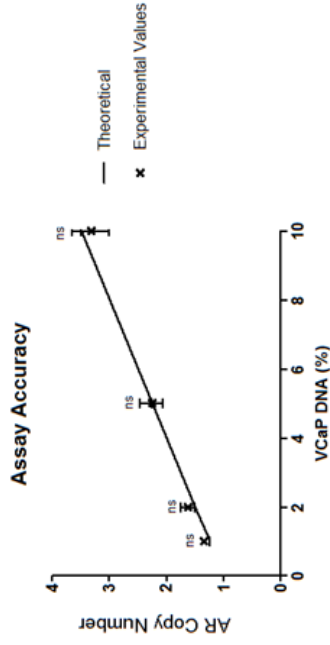
C

$$X = \frac{-20}{(1-A)}$$

X = Minimum amount of abnormal DNA required for detection of an increase in AR copy number

A = AR copy number of the abnormal cells present within a sample

D

AR Copy Number of Abnormal Cells	Minimum Amount of Abnormal DNA Required for Detection of an Increase in AR Copy Number (%)
20	1.05
15	1.43
10	2.22
9	2.5
8	2.86
7	3.33
6	4.00
5	5.00
4	6.67
3	10.00
2	20.00

Fig. 22. Assay Sensitivity, Accuracy and Heterogeneity Limitations.

A. Assay sensitivity: the overall AR copy number was measured in various mixtures of VCaP and normal male DNA, mimicking the dilution of CaP DNA which is likely to occur in a heterogeneous biopsy containing normal DNA from origins such as infiltrating leukocytes, stroma and non-malignant epithelial cells.

B. Assay Accuracy: using the known AR copy numbers of VCaP and normal male DNA (as determined experimentally) theoretical overall AR copy numbers for VCaP and normal male DNA mixtures were calculated and compared to experimental values.

C. Heterogeneity Limitations: Three standard deviations above the mean AR copy number (relative to GAPDH and DMD) of 23 normal samples was used to determine a threshold of significance GAAR detection. This value was used to generate a formula **C.** which would calculate the minimum amount of CaP DNA within a sample necessary to detect a genomic AR amplification, this is relative to the level of genomic AR amplification within CaP cells shown in Table **D**.

All conditions were measured in quadruplicate at a starting quantity of 3ng. Analysis was performed using Bio-Rad CFX software.

Error bars = one standard error of the mean.

Each sample represents 3 experimental replicates each comprising 4 technical replicates.

* = p≤ 0.05   ** = p≤ 0.01   ns = non-significant

3.4.5. Genomic Copy Number of AR and DMD in Several Primary Cultures of Human CaP and BPH

Human female DNA was used to generate standard curves as previously described, against which several human prostate cancer primary cultures, BPH derived primary cultures, patient lymphocytes and normal male gDNA were tested. Both normal male and normal female DNA are appropriate controls to which test samples can be normalised to. The total starting quantity for all conditions (excluding the standard curve) was 3 ng and all samples were measured in quadruplicate (data shown in Fig. 23A. and B.).

As expected, female DNA had a copy number of 2 for *AR* and *DMD* with normal male DNA having a copy number of 1 for these genes. The BPH derived cell cultures (H226/12 and H227/12) and lymphocyte DNA preparations displayed normal values for *AR* and *DMD* copy number. None of the primary human prostate cancer derived cultures tested positively for GAAR.

The importance of controlling for XCA was further highlighted in the samples: H229/12 L, H229/12 P, H217/12 Rb L, H217/12 Rb P, H110/11 Lb L, H110/11 Lb P, H135/11 L, H135/11 P, H224/12 L and H224/12 P. These samples all had a value above 1 for *AR* copy number when normalised to *GAPDH*. However when these values were further normalised by generating an *AR*:*DMD* ratio, it was revealed that these cells had not specifically amplified the AR gene but had instead have XCA.
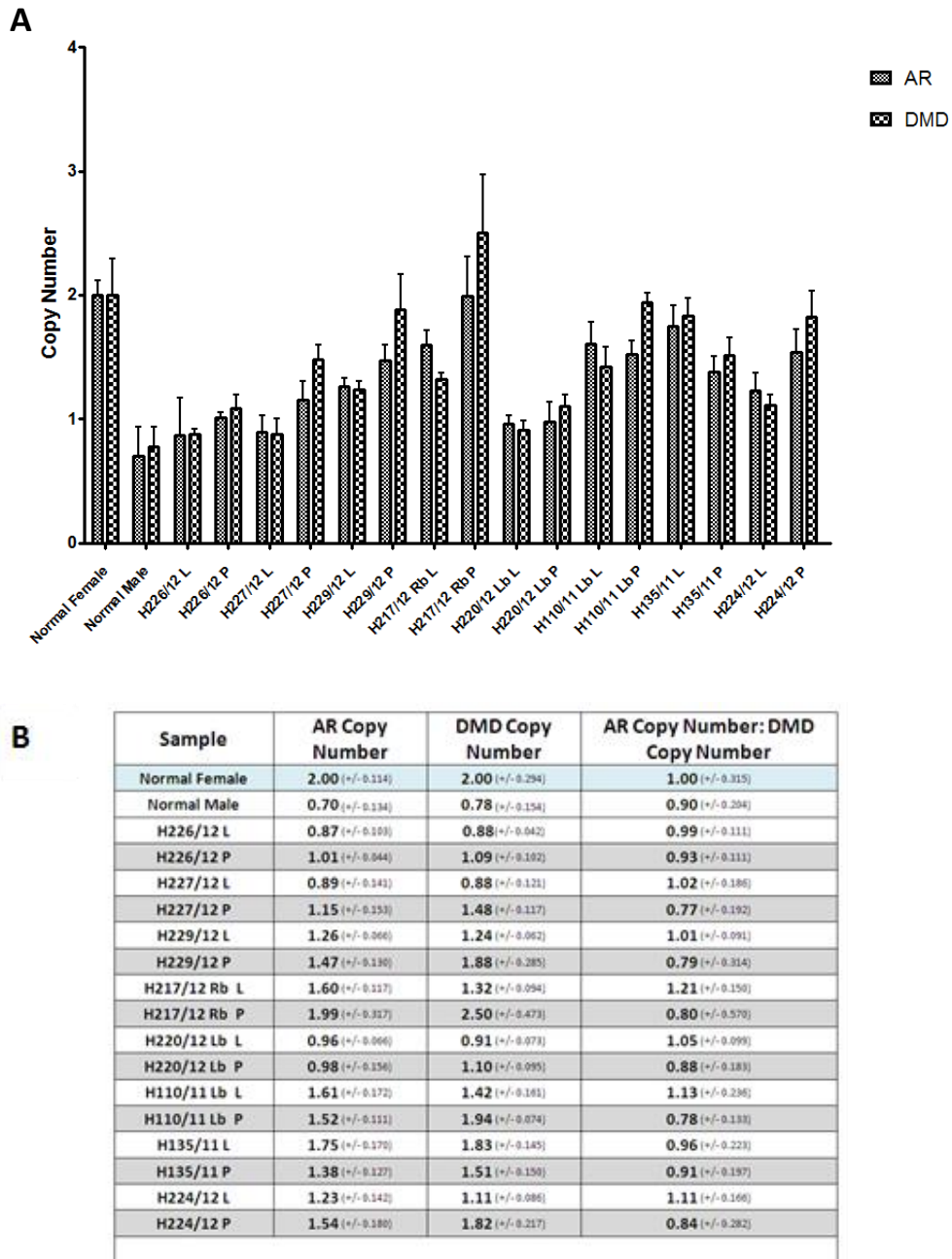
Fig. 23. Genomic Copy Number of AR and DMD in Several Primary Cultures of Human CaP and BPH.

A. Graphical representation (generated using Bio-Rad CFX software gene expression analysis feature) of the genomic copy number of *AR* and *DMD* in all conditions tested. Data shown has been normalised to the control gene GAPDH with values being expressed relative to female genomic DNA (Error bars = one standard error of the mean.)

B. Tabulated version of data shown in (Fig. 23A.) with a further column depicting the *AR:DMD* ratio. Values depicted are mean averages with +/-1 standard error of the mean in brackets.

3.4.6. Genomic Copy Number of AR and DMD in Several Tissue Samples of Human Prostate Cancer

Human female DNA was used to generate standard curves as previously described, against which several human prostate cancer tissues, patient lymphocytes and normal male genomic DNA were tested. The total starting quantity for all conditions (excluding the standard curve) was 3 ng and all samples were measured in quadruplicate (data shown in Fig. 24A. and B.).

As expected, female DNA had a copy number of two for *AR* and *DMD*. However the normal male DNA showed reduced copy number compared to the predicted value of 1 and previous results, as such the data for this experiment was expressed relative to female DNA. Also as expected none of the lymphocyte DNA preparations significantly deviated from the expected value of one for *AR* copy number.

The importance of controlling for XCA was even further demonstrated in the HO24/10 L, H027/10 T and HACaP T samples. These samples all had a value above one for *AR* copy number when normalised to *GAPDH* however when these values were further normalised by generating an *AR*:*DMD* ratio it was revealed that these cells had not specifically amplified the *AR* gene.

A. Graphical representation of the genomic copy number of AR and DMD.
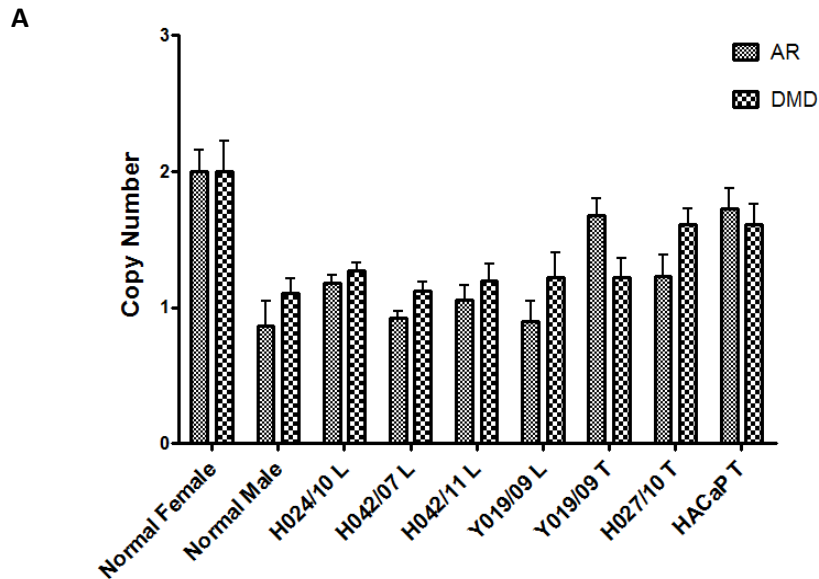
Sample	AR Copy Number	DMD Copy Number	AR Copy Number: DMD Copy Number
Normal Female	2.00 (+/-0.159)	2.00 (+/-0.221)	1.00 (+/-0.272)
Normal Male	0.87 (+/-0.127)	1.11 (+/-0.101)	0.78 (+/-0.162)
H024/10 L	1.18 (+/-0.058)	1.27 (+/-0.059)	0.93 (+/-0.083)
H042/07 L	0.92 (+/-0.055)	1.12 (+/-0.069)	0.82 (+/-0.088)
H042/11 L	1.06 (+/-0.106)	1.20 (+/-0.120)	0.88 (+/-0.160)
Y019/09 L	0.90 (+/-0.146)	1.22 (+/-0.188)	0.74 (+/-0.238)
Y019/09 T	1.68 (+/-0.122)	1.22 (+/-0.141)	1.38 (+/-0.186)
H027/10 T	1.23 (+/-0.162)	1.61 (+/-0.114)	0.77 (+/-0.198)
HACaP T	1.73 (+/-0.149)	1.61 (+/-0.154)	1.07 (+/-0.215)

Fig. 24. Genomic Copy Number of AR and DMD in Several Tissue Samples of Human CaP.

A. Graphical representation (generated using Bio-Rad CFX software gene expression analysis feature) of the genomic copy number of *AR* and *DMD* in all conditions tested. Data shown has been normalised to the control gene GAPDH with values being expressed relative to female genomic DNA (Error bars = one standard error of the mean.)

B. Tabulated version of data shown in **A.** with a further column depicting the *AR:DMD* ratio. Values depicted are means +/-1 standard error of the mean in brackets).

Each sample represents 3 experimental replicates each comprising 3 technical replicates.

3.4.7. Analysis of 10 Blinded Samples - Independently Assessed for AR Amplification Using FISH

To test the ability of the assay to detect samples known to be positive for GAAR, 10 samples, which had been independently screened for GAAR using FISH, were assessed.

The total starting quantity for all conditions (excluding the standard curve) was 3 ng and all samples were measured in quadruplicate. Human female DNA was used to generate standard curves for *AR*, *GAPDH* and *DMD* primer pairs as previously described. Copy number was expressed relative to *GAPDH*.

Specific *AR* amplification (indicated by an *AR:DMD* ratio greater than 1) was detected in all samples that tested positive using FISH: B, C, LuCaP 35, H, and I (Fig. 25A., 25B. and 25C.). LuCaP 41, D and E showed elevated *AR* copy number (Fig. 25A. and 25B.) however in these cases there was a concurrent and equal elevation in the *DMD* copy number. As previously described, this phenomenon indicates that XCA is the mechanism of increased *AR* gene in these samples.

(Linja et al., 2001) previously demonstrated XCA In the LuCaP 35 xenograft indicated by multiple green signals (label for X centromeres). This is consistent with the increase in DMD copy number detected by THE qPCR method. Personal communication with Professor Visakorpi confirmed that the level of *AR* amplification seen in these samples was consistent with their FISH analysis. However, it was also communicated that focal amplifications of *AR* that exceed 10 copies are difficult to enumerate by FISH as the fluorescent signals from the *AR* copies (in close proximity to one-another) merge.

A.

B			
Sample	**AR Copy Number**	**DMD Copy Number**	**AR Copy Number:DMD Copy Number**
Female	1.87 (+/-0.180)	2.01 (+/-0.191)	0.93 (+/-0.263)
Male	1.00 (+/-0.028)	1.00 (+/-0.99)	1.00 (+/-0.103)
LuCaP 41	2.36 (+/-0.208)	2.31 (+/-0.173)	1.02 (+/-0.270)
B	22.52 (+/-2.020)	3.03 (+/-0.214)	7.44 (+/-2.032)
C	5.13 (+/-0.693)	1.74 (+/-0.239)	2.95 (+/-0.733)
D	1.95 (+/-0.197)	1.87 (+/-0.120)	1.04 (+/-0.231)
E	1.43 (+/-0.111)	1.25 (+/-0.112)	1.14 (+/-0.158)
LuCaP 35	11.07 (+/-0.882)	2.58 (+/-0.187)	4.29 (+/-0.902)
LuCaP 73	1.14 (+/-0.126)	1.21 (+/-0.112)	0.94 (+/-0.169)
H	9.97 (+/-0.653)	3.93 (+/-0.224)	2.54 (+/-0.690)
I	4.27 (+/-0.714)	2.36 (+/-0.253)	1.81 (+/-0.758)
J	1.26 (+/-0.185)	1.13 (+/-0.154)	1.11 (+/-0.241)

C	
Sample	**AR Amplification (FISH)**
LuCaP 41	✗
B	✓
C	✓
D	✗
E	✗
LuCaP 35	✓
LuCaP 73	✗
H	✓
I	✓
J	✗

Fig. 25. Genomic Copy Number of AR and DMD in Clinical Samples and Cell Line Xenografts.

A. Graphical representation of the genomic copy number of *AR* and *DMD* in all samples tested. Data shown has been normalised to the control gene *GAPDH* with values expressed relative to male genomic DNA. Error bars = 1 standard error of the mean. Insert is dual-colour FISH analysis of prostate cancer xenograft LuCaP 35 showing two chromosome X centromeres (green signals) and *AR* clusters (red signals) Insert adapted from (Linja et al., 2001).

B. Tabulated version of data shown in figure 25A. Including *AR:DMD* ratio. Values depicted are means (+/-1 standard error of the mean in brackets).

C. Table showing the results of independent analysis of the amplification status of the samples tested, assessed using FISH.

* = p≤ 0.05   ** = p≤ 0.01   *** = p≤ 0.001   ns = non-significant

Each sample represents 3 experimental replicates each comprising 3 technical replicates.

3.4.8. Analysis of X Chromosome Aneuploidy and AR Amplification in Near-Patient Xenografts

Recently our lab has derived several near-patient xenograft (PDX) models derived from different stages of CaP including hormone naïve, hormone responsive and CRPC (Fig. 26B.) This sample set was investigated for the frequency and nature of GAAR and XCA in comparison with patient-specific lymphocyte DNA (Fig. 26A.).

The total starting quantity for all conditions (excluding the standard curve) was 3 ng and all samples were measured in quadruplicate. Human female DNA was used to generate standard curves for *AR*, *DMD* and *GAPDH* primer pairs as previously described. Copy number is expressed relative to *GAPDH*.

GAAR was detected in two samples namely; H427X and H455X. However, upon closer analysis it can be seen that the nature of these amplification events is different between the two samples (Fig. 27.). H427X has an equal amplification of *AR* and *DMD* sequences. In contrast, H455X has elevated *AR* over and above the increase in *DMD* which itself is significantly different compared to normal male DNA.

A

AR and DMD Copy Number Near-Patient Xenografts
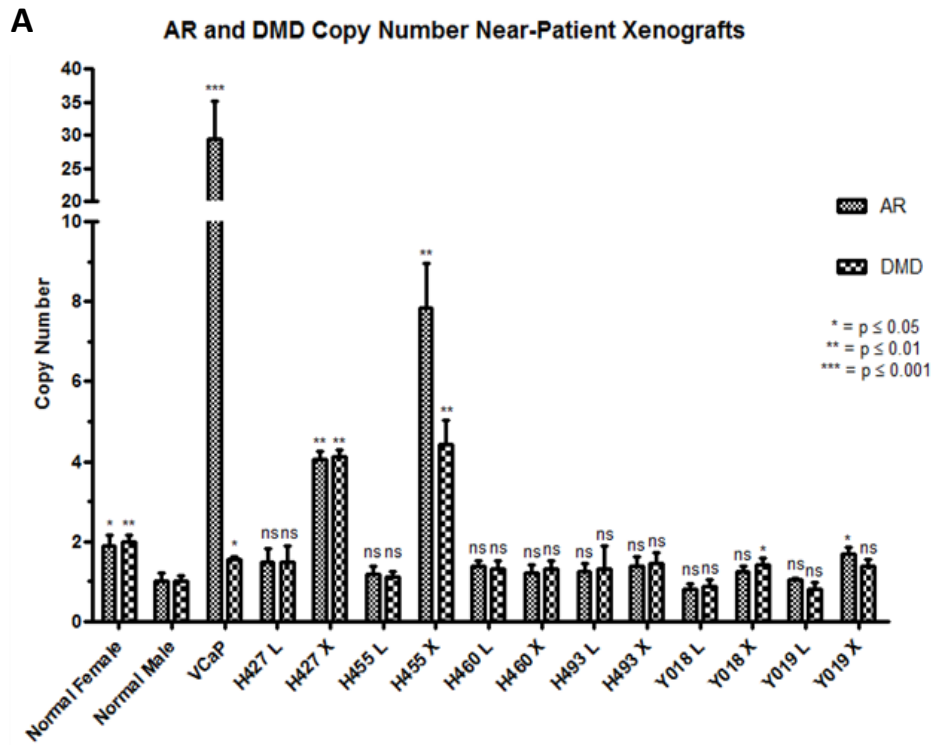
B

PDX ID	Pathology (at engraftment)	Pathology (TRUS)	Hormone Status (at engraftment)	Patient Outcome
H460x	Hormonal effects	T3, (2002)	HR	Rising PSA
H493x	Hormonal effects	G4+5,n1,b 1,T3b	HR	Stable disease
H427x	Hormonal effects	G4+5, b1	HR	Advanced, but stable
Y019x	Hormone effects	G4+5	CRPC	
Y018x	Hormone effects		CRPC	
H455x	Hormonal/CT effects	b1	CRPC	Progressive disease

Fig. 26. Genomic Copy Number of AR and DMD in Near-Patient Xenograft Models.

A. Genomic copy number of *AR* and *DMD* in patient-derived xenografts of prostate cancer. Data has been normalised to the control gene *GAPDH* with values being expressed relative to male genomic DNA. Error bars = 1 standard error of the mean.

B. Pathology data for the near-patient xenograft models at engraftment.

HR = hormone responsive, CRPC = castration resistant prostate cancer, G = Gleason score, N1 = metastasis to lymph nodes, T3 = locally-advanced prostate cancer, b1 = metastasis to bones

Each sample represents 3 experimental replicates each comprising 4 technical replicates.
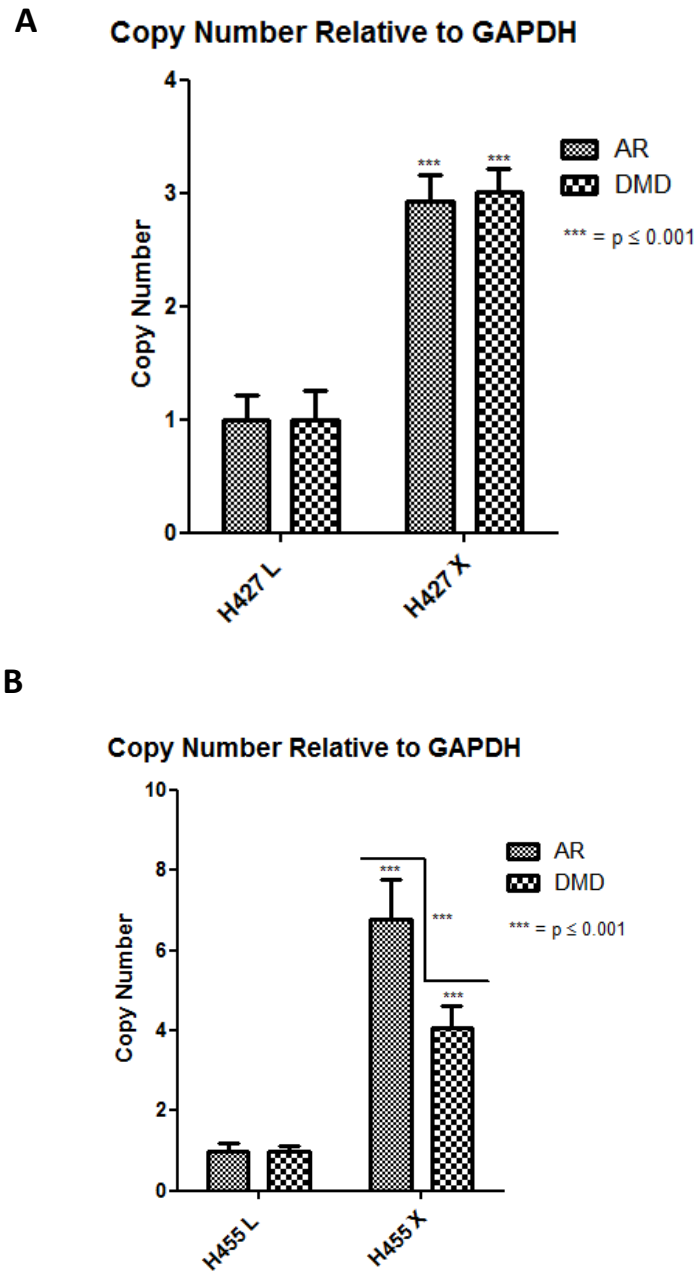
Fig. 27. Genomic Copy Number of AR and DMD in Near-Patient Xenograft Models Relative to Patient Lymphocyte DNA.

Genomic copy number of *AR* and *DMD* in xenografts H427 and H455 and corresponding lymphocytes. Data shown has been normalised to the control gene *GAPDH* with values expressed relative to patient lymphocyte DNA. Error bars = 1 standard error of the mean. **A.** = H427X **B.** = H455X.

Each sample represents 3 experimental replicates each comprising 4 technical replicates.

    *** = p≤ 0.001

3.4.9. Assay Compatibility with Formalin-Fixed Paraffin-Embedded Tissue

FFPE samples represent the most common form of patient tissue preparations within the clinic. Additionally, there are a tremendous number of FFPE samples in hospital archives. In order for this assay to have maximum applicability, it is necessary for the assay to function properly using DNA extracted from FFPE tissue as template. This represents a challenge as DNA extracted from FFPE tissue is often of poor quality compared with DNA extracted from fresh or fresh-frozen samples.

Initial validation was performed using the cell line VCaP, as the assay was established using this cell line and it has a large-magnitude GAAR. VCaP cells were clotted in cell-free human blood plasma and then either formalin-fixed and paraffin-embedded or frozen in OCT. DNA was subsequently extracted from FFPE VCaP, OCT VCaP and fresh VCaP cell-pellet. When DNA from all three preparations was interrogated, no statistical significant difference was observed with respect to *AR* and *DM*D genomic copy number (Fig. 28A.). The ability of the assay to function in FFPE tissue was also investigated in two near-patient xenograft models (H427X and H455X), and again no significant differences between DNA extracted from fresh cell pellet and FFPE tissue (with respect to *AR* and *DMD* copy number) was seen (Fig. 28B. and C.).

A

Copy Number Relative to GAPDH

B

Copy Number Relative to GAPDH, Normalised to Patient Lymphocytes

Chapter 3. Results

C Copy Number Relative to GAPDH, Normalised to Patient Lymphocytes
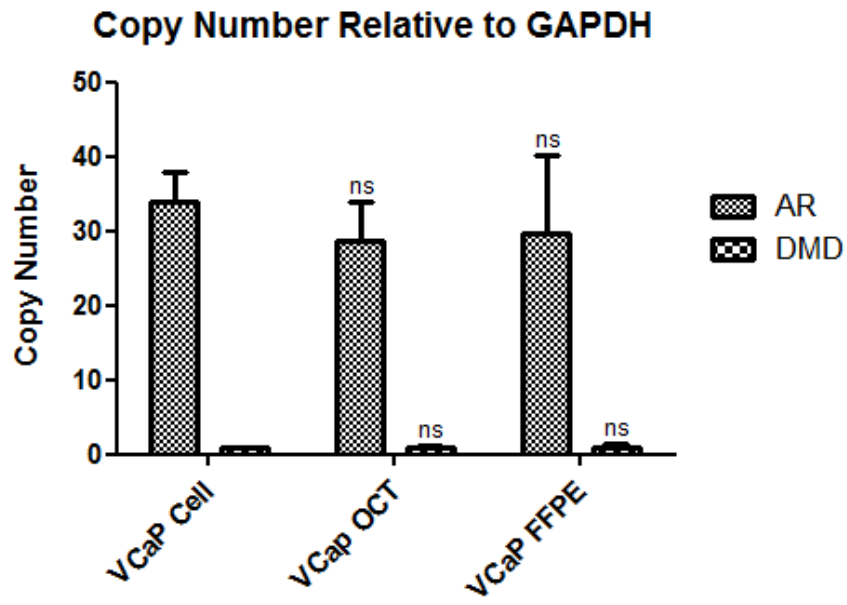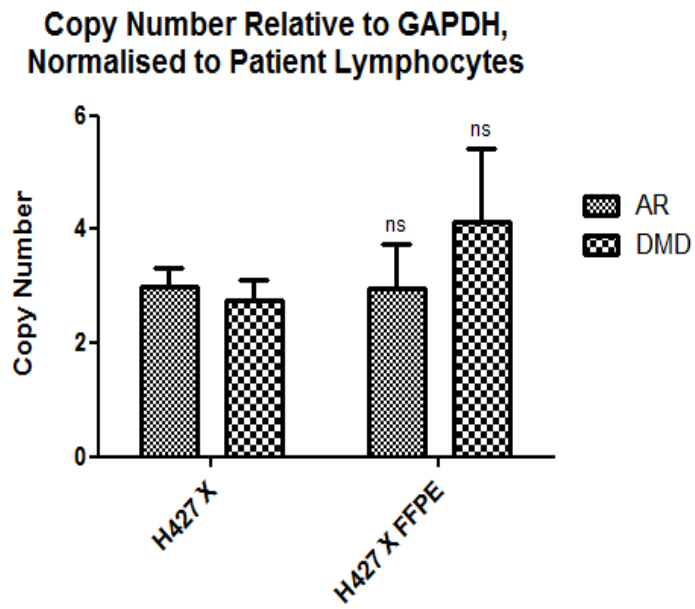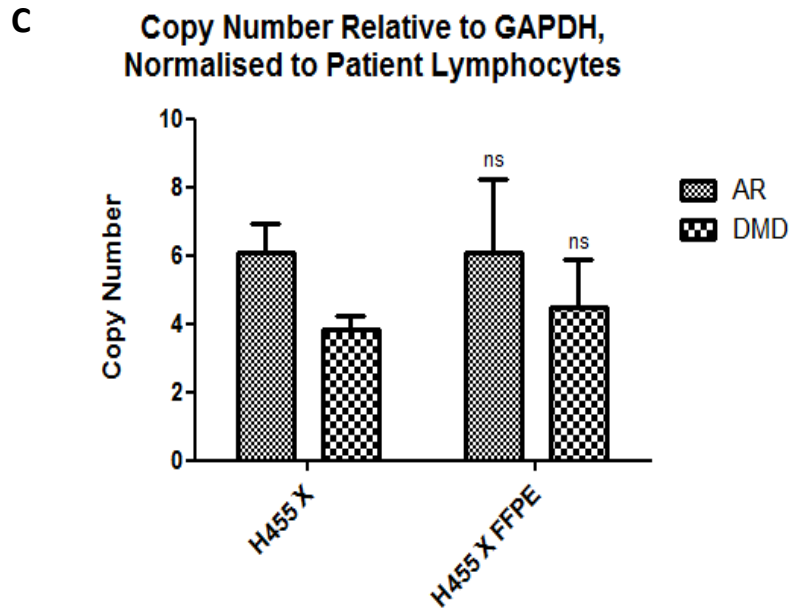
Fig. 28. Assay Compatibility with Formalin-Fixed Paraffin-Embedded Tissue Samples.

A. Genomic copy number of *AR* and *DMD* in the VCaP cell line in freshly isolated cells, those embedded in OCT, and FFPE

B. Genomic copy number of *AR* and *DMD* in PDX sample H427X.

C. Genomic copy number of *AR* and *DMD* in PDX sample H455X.

Data shown has been normalised to the control gene *GAPDH* with values being expressed relative to male genomic DNA (VCaP) or patient derived lymphocyte DNA (H427X and H455X). Error bars = 1 standard error of the mean.

Each sample represents 3 experimental replicates each comprising 4 technical replicates.

 ns = non-significant

3.5. Discussion

CaP is often a clinically irrelevant disease with many patients dying with CaP rather than as a result of CaP (Swanson and Basler, 2010). This has led to unacceptably high overtreatment in which patients undergo surgery (with all associated risks) and 'life altering' side-effects. In an effort to curb over-treatment of CaP by radical prostectomy, an approach often termed 'watchful waiting' is employed by urologists. This involves repeated PSA screening and biopsies to ensure that a patient is only operated on when the disease is likely to progress into a potential life-threatening form i.e. grade 4 cancer or escape from the capsule (Swanson and Basler, 2010).

The rationale for an GAAR test is that by providing a molecular interrogation of one of the most fundamental genes for CaP progression, urologists' (which mostly rely on morphological changes in the CaP to determine the likelihood of disease progression) could use this assay to identify patients at risk of disease progression and stratify them accordingly. Also the assay can be used to monitor disease evolution in response to therapy i.e. progression to incurable CRPC. This is of particular relevance as (Linja et al., 2001) demonstrated that GAAR correlated with AR expression.

Evolution of cancer to acquire a treatment-resistant phenotype through the mechanism of gene amplification is a well-established phenomenon. For instance methotrexate (MTX) is an important chemotherapeutic for the treatment of acute lymphoblastic leukaemia (ALL) (Göker et al., 1995). While complete remission is seen in the vast majority of patients (upwards of 90%) this is often followed by relapse, with the recurrent cells possessing a MTX resistance phenotype (Göker et al., 1995). This situation has several parallels with that of CRPC emergence following ADT treatment of CaP. Not least of these parallels is the most common mechanism by which resistance is acquired – gene amplification. In ALL the gene in question is dihydrofolate reductase (DHFR) (Göker et al., 1995, Srimatkandada et al., 1983). The protein encoded by this gene is the therapeutic target of MTX in ALL. The amount of MTX required to achieve inhibition of the DHFR enzyme is directly proportional to the level of DHFR expression in target cells. Several MTX-resistant cell lines have increased levels DHFR activity, due to gene amplification and it has also been shown that even low-level genomic amplification (2-4 copies/cell) is sufficient for cells to show MTX resistance in ALL (Göker et al., 1995, Srimatkandada et al., 1983). It should be noted that the MTX resistance by DHFR amplification is not exactly

equivalent to AR amplification in response to ADT as the former is based competitive inhibition of DHFR whilst the latter is based on a reduction of AR ligand(s).

3.5.1. A qPCR Assay Capable of Detecting AR Amplification in a Variety of Heterogeneous Biological Samples has been Successfully Established

The rationale behind using qPCR to identify genomic amplification of the *AR* gene has been verified. This was most rigorously demonstrated by the repeated ability to achieve the predicted AR genomic copy number difference, of two, between male and female DNA. Further demonstration of the technique's ability to detect genomic amplification of the AR gene comes from the ability to determine the high numbers of *AR* copies in the VCaP cell line 26.17 (+/- 1.797) ($p \leq 0.001$) which is known to be GAAR positive (Waltering et al., 2012). This is in contrast to the LNCaP cell line which has acquired castration resistance through a mutation in the AR gene to produce a constitutively active variant (Waltering et al., 2012).

The qPCR based assay is sensitive, accurate and comparable to FISH when using primary tumours and xenograft samples. Coupled with a reduced 'turnaround time', this amenability to high through-put screening and objectivity implies that this assay could prove useful in a clinical setting to ascertain GAAR and XCA status of a patient and thus help patient triaging in CRPC.

The inclusion of a further control gene in the form of *DMD* has proven essential in order to discriminate between GAAR and XCA. This was shown in the following samples: RWPE1, DU145, PC3, PC346c, H229/12 L, H229/12 P, H217/12 Rb L, H217/12 Rb P, H110/11 Lb L, H110/11 Lb P, H135/11 L, H135/11 P, H224/12 L, H224/12 P, HO24/10 L, H027/10 T, HACaP LuCaP 41, D, E, H427X and H455X.

None of the primary cell cultures derived from human CaP showed a specific amplification of the *AR* gene. This result may be attributed to the culture conditions used in the generation and maintenance of these cells, which are devoid of androgens. As such, current cell culture conditions may be selecting against the survival of cells positive for *AR* amplification. Additionally, many of the samples were from early CaP or from those that had not been on long-term ADT. It is possible that there are some rare cells in the cultures which have GAAR but are below the level of detection.

The data accrued from the primary tissue samples only yielded one sample that tested positive for a very modest increase in AR copy number namely YO19/09 T. This sample was from a tumour biopsy that was taken from a patient that had relapsed post ADT thus is CRPC. In order to ascertain the significance of this result, a total of 23 normal sample data sets, each of which being a mean of at least three replicates was used to determine a threshold for significance. A threshold of three standard deviations above the mean of these normal samples was determined (data not shown) this equalled 1.20. The corrected *AR* copy number for YO19/09 T was 1.38(+/-0.186). Subtracting the standard error of this sample from the mean value results in a value of 1.194, this is just below the threshold for the existence of GAAR. It is most noteworthy that the DNA preparation of this sample (and the other tissue samples tested) was performed without any targeted cancer cell enrichment. Within a CaP tumour there are still normal glands and non-malignant stromal cells, furthermore there are often infiltrating leukocytes present within a tumour. These normal cells may have diluted out the cancer cells and as a result could have masked the presence of GAAR within these samples.

In terms of sensitivity, the assay was also able to detect the presence of a GAAR from a mixture of normal and abnormal DNA e.g. 1% VCaP – 99% normal male DNA mixture (Fig. 22.). Using the threshold of detection a formula was generated to predict the maximum amount of normal DNA within a sample that would not mask a given *AR* copy number gain (Fig. 22C.). This revealed that an *AR* duplication could still be detected if 80% of the DNA within a sample was normal. This is particularly important when considering the heterogeneity of prostate cancer biopsies.

Due to the lack of samples that tested positive for GAAR, the accuracy of the assay in comparison to FISH was investigated by assaying ten samples which had been independently analysed for AR amplification by FISH and subsequently blinded. The assay successfully detected the presence of specific GAAR gene all samples that were scored positive by FISH (five samples) but not in samples that were scored as negative by FISH (five samples). It must be stated that a much larger sample size would be necessary to obtain a reliable estimation of false positive and negative rates.

The last batch of samples interrogated by the assay included samples of the latest round of PDXs generated in our laboratory (funded by Movember with an emphasis on generating xenografts from CRPC patients) as well as the xenograft generated from the Y019/09 T sample. This resulted in the identification of two samples that both had GAAR

and XCA, namely H427X and H455X. However, upon closer analysis it can be seen that the nature of these amplification events is different between the two samples. H427X has an equal accumulation of *AR* and *DMD* sequences which is indicative of XCA. H455X on the other hand, has elevated *AR* over and above the increase in *DMD* which itself is significant. This could represent an initial XCA event with subsequent locus-specific GAAR. It is of great importance to the biology of CaP initiation, in regards to the cell type of origin of the disease, that GAAR and XCA have been detected in passage zero PDXs, indicating that these genetic abnormalities are present in cells capable of tumour reconstitution *in vivo*.

An interesting future direction to increase the likelihood of detecting GAAR in xenograft models would be to assess xenograft samples under castration conditions. The xenograft samples analysed in this project were grown within a male mouse, as such androgen supply is not a limiting factor for tumour growth. In this scenario, cells that have GAAR would not have a selectable advantage over cells that are negative for *AR* gene amplification. It would be interesting to see if samples previously negative for GAAR could form GAAR-positive tumours which would indicate that rare GAAR-positive cells were present in the original patient-tumour biopsy.

The Y019X (xenograft) sample was negative for both GAAR and XCA. However, very recent data generated by our laboratory has thrown the provenance of this xenograft into disrepute as it tested positive for both Epstein–Barr virus (EBV) presence and immunoglobulin heavy locus (*IGH*) rearrangement (Appendix 5.) indicating that graft out-growth was the result of a contaminating transformed B cell and not CaP epithelia.

Further experiments were designed to investigate the compatibility of the assay with FFPE tissue, as this represents the most common form of sample preparation and archived tissue in the clinic. The results show that the assay produces copy number values for *AR* and *DMD* (from FFPE sources) that are not statistically significant from those derived from OCT. However, the standard error of copy number values was greater in FFPE samples, indicating that fresh or OCT preserved tissue is preferable.

3.5.2. The Assay also Gives Information Regarding X Chromosome Aneuploidy – a Relatively Common Event in CaP Associated with Poor Prognosis

As demonstrated by *DMD* copy number of the cell lines, xenografts and primary samples tested it appears that XCA is common in CaP. Being present in DU145, PC3, PC346c and VCaP, LuCaP 41, LuCaP 35, LuCaP 73, H427X, H455X, B, C, D, E, H samples.

A relationship between XCA chromosome and poor prognosis is not unique to CaP. Loss of X chromosome inactivation is a marker of aggressiveness in breast and ovarian cancers (Kang et al., 2015). It was also found that all male breast cancer cases harboured a XCA (100%) (Di Oto et al., 2015). This shows that XCA plays a role in the neoplastic transformation of male breast epithelial cells. In chronic neutrophilic leukaemia (CNL) which is an uncommon myeloproliferative disorder characterised by neutrophilia and myeloid hyperplasia in the absence of BCR/ABL gene fusion events (Elliott et al., 2001). A study has found that whilst most patients with CNL have normal karyotypes, those with 46,XY,+X (15 cases studied) had disease progression to myeloid crises accompanied by poor prognoses (Yamamoto et al., 2002). The authors concluded that XCA may play a role in the transition of CNL from a chronic to crisis phase of the disease (Yamamoto et al., 2002).

In CaP it is now established that there is a significant frequency of XCA, even in 'treatment naïve' patients. In a FISH study by (Merson et al., 2014) 152 out of 596 (25.5%) demonstrating gain of at least one copy of the X chromosome. A correlation between XCA and reduced survival is shown in (Fig. 14.) (Merson et al., 2014). This data corroborates a much earlier study by (Röpke et al., 2004) in which 9 out of 80 prostate cancers (11.25%) tested positive for XCA by FISH. The same group also found that XCA correlates with pathological classification and tumour volume (Röpke et al., 2004).

The exact mechanism by which XCA contributes to poor prognosis in CaP is currently unresolved. However, there are two hypotheses which need not be mutually exclusive. One explanation shared by both (Röpke et al., 2004, Merson et al., 2014) is that XCA results in CRPC by driving AR expression (Fig. 29.). An alternative view which can also explain the poor prognosis of non-endocrine cancers (when additional copies of X chromosome are present) is that XCA is the product and therefore a marker and driver of genomic instability, a hallmark of cancer (Fig. 30.) (Giam and Rancati, 2015).

Whichever mechanism is correct, the fact that this assay can simultaneously detect two genetic aberrations associated with poor prognosis and therapeutic resistance in CaP greatly enhances its applicability in a clinical setting. Also as XCA is not unique to CaP the assay described here may also be useful as a tool to stratify patients according to risk in several oncology fields.
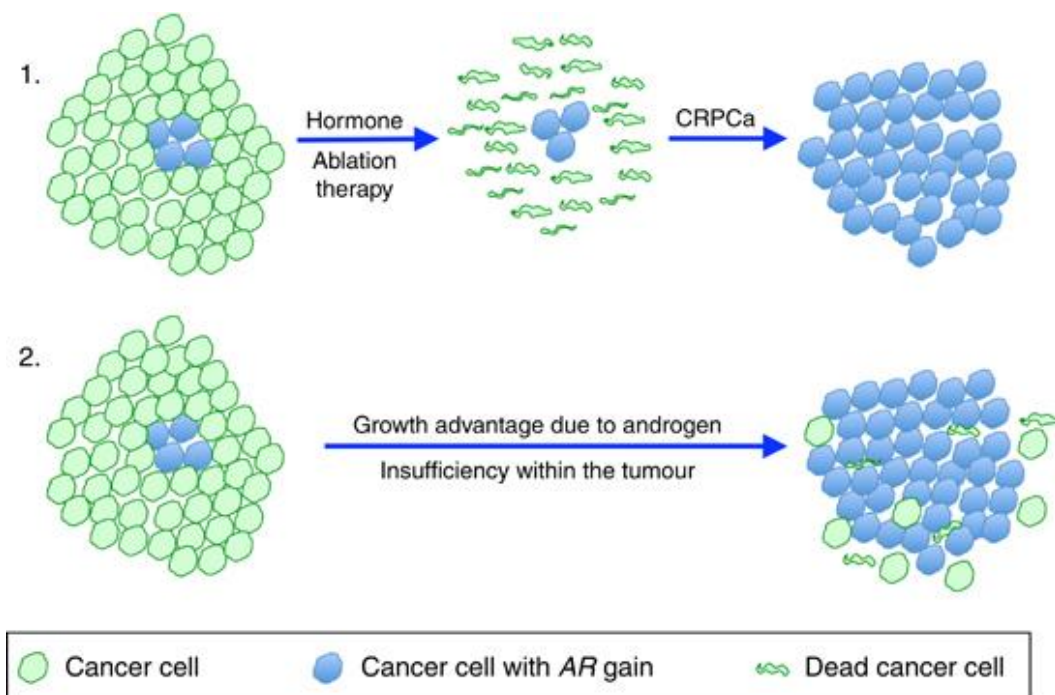
Fig. 29. Selection of Cells with AR Gain by ADT.

Small foci of CaP cells that are positive for genomic amplification of the AR gene could expand to form a CRPC tumour by positive selection by (1) androgen deprivation therapy or (2) natural androgen insufficiency within the tumour.

From: (Merson et al., 2014)
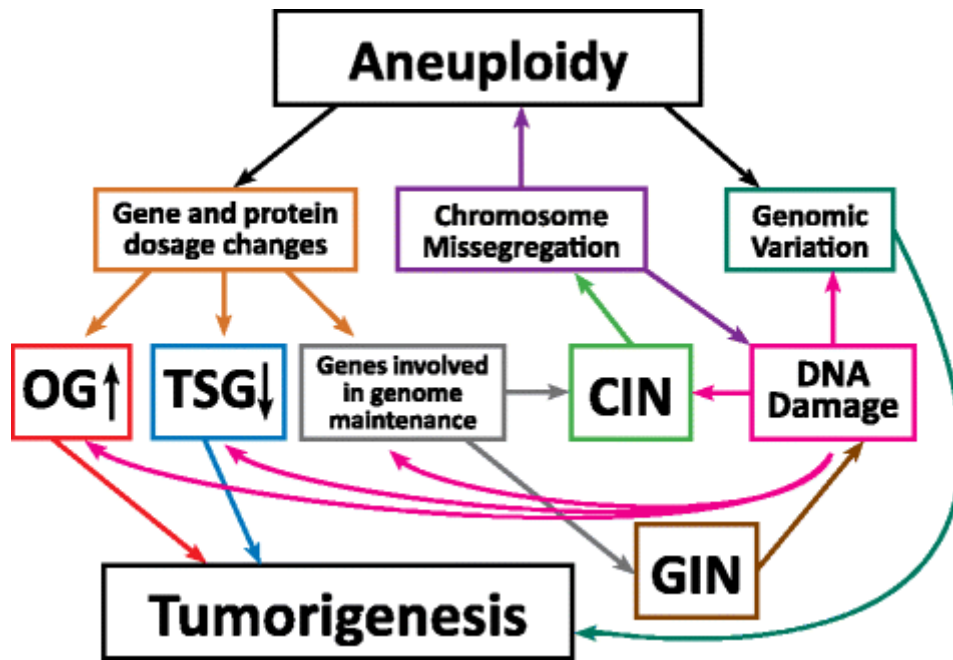
Fig. 30. XCA Contributes to Genomic Instability.

The combination of aneuploidy, chromosomal instability (CIN) and genomic instability (GIN) can have additive or even synergistic effects on tumourigenesis. Aneuploidy leads to increased gene expression of the genes located on the aneuploid chromosome, potentially leading to deregulation oncogenes (OG) and tumour suppressor genes (TSG) – directly effecting oncogenic transformation. CIN can result in aneuploidy by increasing chromosome missegregation events. Additionally, aneuploidy could result in CIN through changing the stoichiometry of protein-complexes responsible for genome maintenance. Chromosomal-missegregation could also lead to DNA damage and GIN. CIN and GIN are thought to promote tumourigenesis by increasing the chance of accumulating oncogenic mutations. The 'by-products' of CIN and GIN namely: aneuploidy and DNA damage result in increased intra-tumour diversity potentially increasing the potential of the bulk tumour to adapt to changes in the microenviroment due to metastasis or therapeutic intervention.

From: (Giam and Rancati, 2015)

4. Epigenetic Regulation and Investigation of the Mechanism of Action of LXN and RARRES1 in Prostate Epithelial Cells

4.1. RARRES1

RARRES1 was originally isolated from the skin epithelial cells, as the gene with greatest increase of expression in response to the synthetic retinoid – tazarotene (Nagpal et al., 1996), which is effective in the treatment of psoriasis (characterised by aberrant proliferation) (Weinstein et al., 2003). RARRES1 is a type III membrane protein (Sahab et al., 2011), and is located adjacent to the LXN gene on the long arm of chromosome 3. Two isoforms of RARRES1 are produced through alternative splicing: RARRES1 TS1 is a 294 amino acid protein and RARRES1 TS2 is 228 amino acids in length. The two encoded proteins have very high amino acid sequence homology. The major distinction is a putative CPA binding site (present in RARRES TS1 and is highly conserved with LXN) which is absent in RARRES1 TS2 (Aagaard et al., 2005). The CPA binding site was found to be an inhibitory loop that protrudes into the CPA4 active site, including five critical amino acids (QEIIP) (Oldridge, 2012, Pallarès et al., 2005).

RARRES1 expression is tightly linked to the differentiation status of cells and is most abundantly expressed in terminally differentiated cells from normal tissues (Wu et al., 2006). This expression pattern is retained in malignant conditions where it was found that RARRES1 was generally down-regulated in metastatic lymph nodes compared to those in the primary tumours in breast cancer (Peng et al., 2012). Among 122 colorectal adenocarcinomas, the poorly differentiated adenocarcinomas and Dukes' stage D tumours showed a significant decrease in RARRES1 expression i.e. expression of RARRES1 is closely associated with the differentiation of colorectal adenocarcinoma (Wu et al., 2006, Peng et al., 2012).

In the prostate, reduction of RARRES1 expression is specifically associated with cancer progression. In one study, RARRES1 mRNA was detected in ten normal human prostate tissues and 51 BPH tissues, but was only present in fewer than 8% of the CaP tissues analysed (Jing et al., 2002)**.** The silencing of RARRES1 expression seems to be an early event in CaP: 73% of very low grade CaP (Gleason scores of 2–3) do not express of RARRES1 (Jing et al., 2002). However, it is debateable whether such low Gleason scores are truly CaP.

There is substantial evidence that RARRES1 acts as a tumour suppressor in multiple cancers. Re-introduction of RARRES1 expression in the highly aggressive CaP cell line: PC-

3M, resulted in a dramatic reduction of the *in vitro* invasiveness and a 2.4-fold reduction in tumour burden in the PC-3M xenograft model (Jing et al., 2002, Youssef et al., 2004). In the leukaemic cell line K562, restoration of RARRES1 expression promoted apoptosis after treatment with all-trans retinoic acid (Wang et al., 2008). Also, RARRES1 was shown to retard cell proliferation and invasive features of nasopharyngeal carcinoma cells mediated by Epstein-Barr virus transformation (Kwok et al., 2009). In breast cancer, re-expression of RARRES1 reduced cell invasion and augmented cell death induced by cytotoxic agents (Wang et al., 2008). Additionally, both RARRES1 isoforms inhibited the growth of SW620 colon cancer cells (Wu et al., 2011a).

In concordance with the above studies, our laboratory has shown that RARRES1 negatively regulates colony forming efficiency and invasion in malignant and benign prostate tissue (Oldridge, 2012, Oldridge et al., 2013). It has also been demonstrated that there is reduced (barely detectable) expression of RARRES1 in prostate SCs compared to their more differentiated progeny, implicating a role of RARRES1 in regulating differentiation within the prostatic epithelium (Oldridge, 2012, Oldridge et al., 2013). In cells derived from CaP, RARRES1 is barely detectable in CSCs and transit amplifying populations and is expressed at very low levels in committed basal cells. This is in stark contrast to normal tissues (Oldridge, 2012, Oldridge et al., 2013).

There have been several reported mechanisms of RARRES1 mediated inhibition of proliferation and survival. Both RARRES1 isoforms inhibited prostaglandin E2 (PGE2)-stimulated colon cancer cell proliferation (Wu et al., 2011a, Tsai et al., 2011). This was shown to be the result of suppressing subsequent β-catenin nuclear localization, β-catenin/T cell factor (TCF) transactivation, and cyclic adenosine monophosphate (cAMP)/cAMP response element-binding protein (CREB) signalling in response to PGE2 (Tsai et al., 2011). It was further reported that these actions were at least in part mediated through the up regulation of G-protein-coupled receptor kinase 5 (GRK5) expression (Wu et al., 2011a). GRK5 is a serine/threonine kinase, which suppresses the activation of ligand-activated G-protein-coupled receptors (GPCRs) by inducing internalisation (Harris et al., 2008, Wang et al., 2008). The importance of GRK5-mediated phosphorylation is further highlighted by its ability to increases histone deacetylase activity and promote p53 degradation (Chen et al., 2010, Liu et al., 2010a).

RARRES1 knock-down has been shown to down-regulate the serine/threonine-protein phosphatase 2A (PP2A) and its catalytic subunit - β isoform encoded by *PPP2CB* (Sahab

et al., 2010). PP2A has broad substrate specificity, targeting proteins of oncogenic signalling cascades including proto-oncogene serine/threonine-protein kinase (Raf), mitogen-activated kinase (Mek), and Akt (29) (Ory et al., 2003). PP2A is also a negative regulator of the growth factor stimulated signalling pathways. Furthermore, mutation of this enzyme has been identified in lung and breast cancer (Wang et al., 1999, Esplin et al., 2006).

RARRES1 has also been implicated in the regulation of cell cycle dynamics through mediation of End-binding protein-1 (EB1) (Sahab et al., 2010). The major function attributed to EB1 is the regulation of spindle dynamics and chromosome alignment during mitosis. As such downregulation of RARRES1 may have a role in enhancing genomic plasticity by increasing abnormal division events leading to aneuploidy (Green et al., 2005).

4.2. LXN

LXN is a 29kDa protein composed of 222 amino acids. The gene encoding LXN is located on the long arm of chromosome 3. LXN is the sole carboxypeptidase inhibitor (CPI) in mammals. Experimentally it has been shown to act as a potent competitive inhibitor of CPA4 in humans (Liang and Van Zant, 2008). CPAs are first synthesised as inactive zymogens which are activated by proteolytic cleavage. They function as exopeptidases i.e. mediate cleavage of C-terminal amino acids. The LXN primary sequence does not share significant homology with other known CPIs (Reverter et al., 2000). However, it does share 30% sequence homology with a cysteine protease inhibitor, cystatin C (Liang and Van Zant, 2008). It also shares structural homology with RARRES1 (Liu et al., 2012) which is encoded by an adjacent gene. The location of RARRES1 and its homology to LXN suggests that the two genes are the product of duplication and subsequent divergence (Fig. 31.) (Aagaard et al., 2005). Indeed evolutionary analysis of both genes shows that RARRES1 and LXN are paralogues, with RARRES1 implicated as the ancestral gene (Sahab et al., 2011).
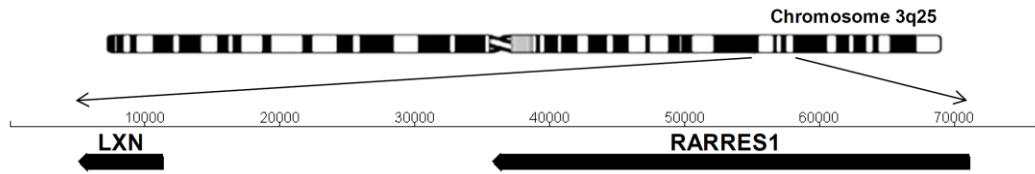
Fig. 31. Adjacent Location of the RARRES1 and LXN Genes.

The genes are located adjacent to one another on the long arm of chromosome 3 at the region 3q25.32-q25.33.

From: (Oldridge, 2012)

CPA4 expression has been detected in hormone-regulated tissues including the prostate, where it has been shown to be involved in CaP and is specifically implicated in CaP aggressiveness (Huang et al., 1999, Kayashima et al., 2003). CPA4 serum activity has also been suggested as a potential biomarker for pancreatic cancer. These two examples have implicated LXN as a tumour suppressor by proxy (Matsugi et al., 2007). However, evidence that LXN does not function through inhibition of CPA4 comes from a study on rat peritoneal mast cells where it was found that the two proteins are not localized in the same granular compartment in the cytoplasm (Uratani et al., 2000). Further evidence comes from work conducted in our laboratory which showed that CPA4 was secreted and LXN was localised to the nucleus in CaP cells (Oldridge, 2012). In conclusion, LXN is highly unlikely to perform its tumour suppressive and SC regulatory functions through an interaction with CPA4.

Forward genetics has implicated LXN as a regulator of normal HSC number in mice, through decreasing self-renewal and increasing apoptosis (Bolger et al., 2012). This work was further extrapolated into leukaemia with the working hypothesis that LXN was down-regulated in malignant disease (Liu et al., 2012). In this study several leukaemia and lymphoma cell lines were analysed, along with primary cells, showing that LXN expression at both the mRNA and protein level was decreased compared to normal controls (Liu et al., 2012). Moreover, re-initiation of LXN expression in two lymphoma cell lines reduced their growth *in vitro* and *in vivo* (Liu et al., 2012). Mechanistically it was found that LXN-mediated suppression was achieved by down-regulation of anti-apoptotic genes, including bcl-2, leading to an increase in apoptosis (Liu et al., 2012). These actions could not be replicated by the treatment of cells with a CPI derived from potato, which is further evidence for an alternative function of LXN (Liu et al., 2012).

Further evidence of a role for LXN in cancer comes from the study of gastric carcinoma. Initial evidence for an involvement in the disease came from the comparison between the 'normal' immortalised gastric epithelial cell line GES-1, and its malignant derivative the MC cell line. Comparison between the two showed that high levels of LXN were found in GES-1 compared to the MC cells (Ke Y, 1996). Further evidence was gained through the analysis of primary samples and *in vivo* models where it was shown that LXN was significantly down-regulated in areas of disease compared to paired samples of adjacent normal tissue, and that over expression of LXN in MGC803 cells inhibited colony formation and tumour growth in nude mice (Li et al., 2011). Microarray analysis of changes in expression following knock-in of LXN, revealed several genes implicated in cancer progression that were differentially expressed in response to LXN namely, Maspin, WAP Four-Disulfide Core Domain 1 (WFDC1), secretory leukocyte protease inhibitor (SLPI), S100 calcium-binding protein P (S100P), and platelet derived growth factor receptor beta PDGFRB (Li et al., 2011).

4.3. Low Expression of RARRES1 or LXN has a Negative Impact on Recurrence-Free Survival in CaP

As discussed in sections 4.1 and 4.2, both RARRES1 and LXN have tumour suppressive functions in a variety of cancers. Furthermore, both genes have been shown to be downregulated in primary malignant samples compared to adjacent normal control tissues.

(Taylor et al., 2010) assessed DNA copy number, exon expression and miRNA expression in 218 prostate cancers. This data is open access and through the betastasis initiative, it is possible to construct Kaplan-Meier plots for LXN and RARRES1 (Fig. 32.). From this data it can be seen that low expression of LXN or RARRES1 within CaP tumours correlates with a statistically significant reduction in recurrence-free survival (LXN p=0.000122 and RARRES1 p=0.00576) (Taylor et al., 2010). This data is consistent with the proposed tumour suppressive functions of these genes. However, the data presented in (Taylor et al., 2010) is the product of all the cells within the prostate tumour biopsy, and as such the data may be skewed by the presence of stroma and immune-cell infiltrates.

LXN
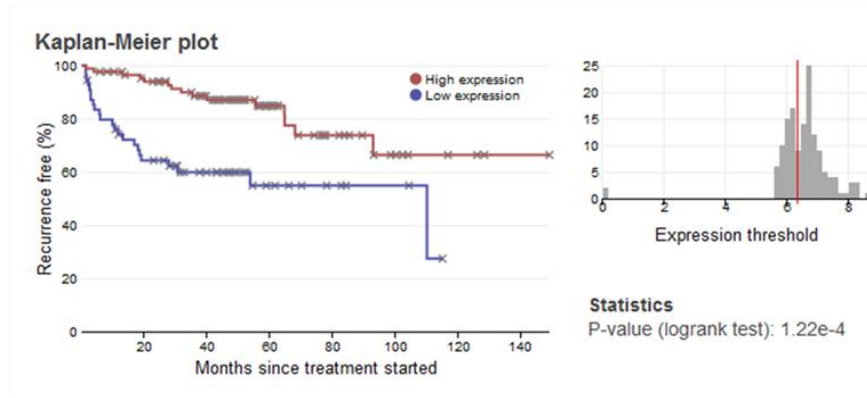
RARRES1
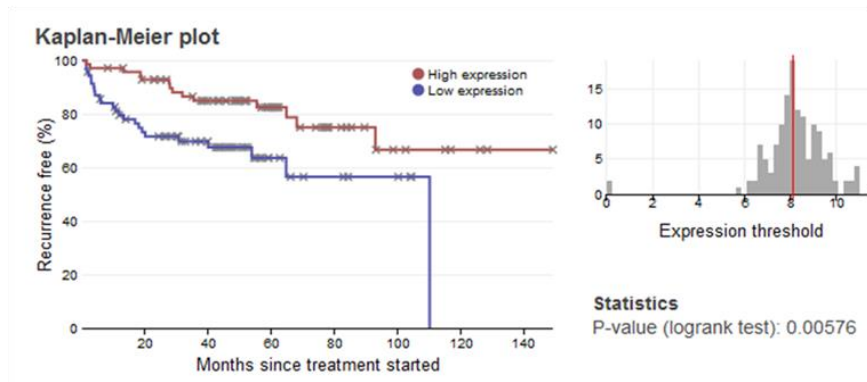
Fig. 32. High Expression of LXN or RARRES1 Correlates with Poor Prognosis in CaP.

Kaplan-Meier plots of LXN and RARRES1), generated from 218 prostate cancer samples (Taylor *et al*., 2010). In both cases the median expression was used as a threshold to categorise high and low expressers. Statistics were generated using a logrank test. Data was accessed through the Betastasis initiative.

From: (Taylor et al., 2010)

4.4. Co-expression of RARRES1 and LXN in Primary Prostate Cultures

Microarray expression profiling of primary prostate epithelial cultures of benign or malignant origin, either enriched for progenitor cells or more differentiated committed basal cells, was previously performed in our laboratory (Birnie et al., 2008). These cultured samples eliminate any non-epithelial contaminants that may artificially alter LXN and RARRES1 expression profiles. A caveat to this analysis is that due to the *in vitro* culture system employed the data may not be completely representative of the CaP *in vivo* i.e. culture conditions select for a proliferating phenotype and luminal cells do not survive in culture. This analysis, which was confirmed by RT-PCR, showed that LXN and RARRES1 are downregulated in SC fractions compared to CB cells (Oldridge, 2012, Oldridge et al., 2013). Moreover, there was a non-significant trend of malignant CB samples towards lower LXN and RARRES1 expression, compared to benign CB samples.

A re-analysis of these data showed a strong positive correlation exists between LXN and RARRES1 expression (R^2=0.92) (Fig. 33.) suggesting that these two genes could be co-regulated in both the benign and malignant prostate epithelium. This is likely, due to the close proximity of the two genes in the genome and the likelihood of regulation through common transcription factors and/or epigenetic control mechanisms.
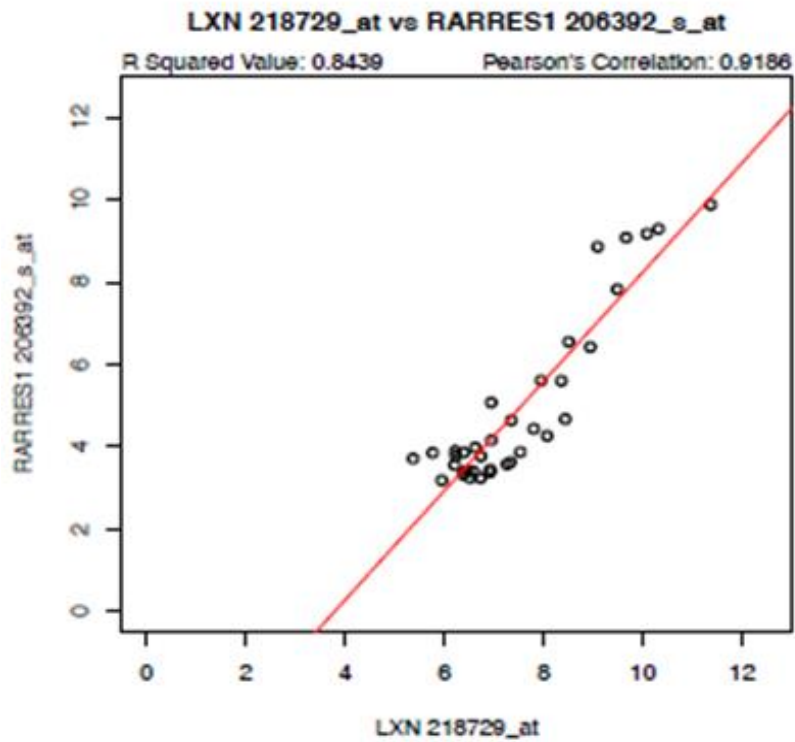
Fig. 33. Co-Expression of LXN and RARRES1 in Prostate Epithelial Cells of Benign and Malignant Origin.

Correlation analysis of Microarray gene expression data of a LXN probe vs a RARRES1 probe. Data was analysed using Pearson's correlation. R^2 values for correlation in prostate epithelial cells of benign and malignant origin

Re-analysis of data from: (Birnie et al., 2008) performed by Davide Pellacani

4.5. Regulation of LXN and RARRES1

Both RARRES1 and LXN have been shown to be targets of atRA mediated transcriptional control (Oldridge, 2012, Oldridge et al., 2013, Kamal et al., 2014). Studies of epigenetic regulation of LXN and RARRES1 have focused on CpG islands within the promoter regions of the two genes. Hypermethylation of CpG islands is an established mechanism of silencing tumour suppressor genes (Esteller, 2002, Liu et al., 2010b). Methylation of the LXN and RARRES1 promoters correlates with reduced LXN and RARRES1 expression (Liu et al., 2012, Peng et al., 2012, Youssef et al., 2004, Wu et al., 2011a). It has previously been shown that LXN and RARRES1 are regulated by promoter hypermethylation in CaP cell lines, but this is not observed in primary tissue or cultures (Oldridge et al., 2013). It is proposed, that in primary prostate epithelium, the major contributing factor in the epigenetic regulation of LXN and RARRES1 is through altered chromatin status by post-translational modification of histone proteins in the region of the LXN and RARRES1 genes. This form of epigenetic regulation is controlled by the post-translational modification of histone proteins.

The identification of structural homology (Liu et al., 2012, Aagaard et al., 2005) and co-regulation of LXN and RARRES1, coupled with their downregulation in undifferentiated cells and several cancers, resulting in enhanced invasion, colony formation and tumourigenic potential *in vivo,* highlights the importance of these genes (Oldridge et al., 2013, Liu et al., 2012, Bolger et al., 2012, Wu et al., 2006). The nearly ubiquitous silencing of RARRES1 in CaP, indicates that reactivation of RARRES1 and/or LXN or their downstream signalling targets represents a logical strategy to reduce tumour aggressiveness and dissemination, as well as induction of differentiation, thereby augmenting current treatment regimens (Jing et al., 2002, Oldridge et al., 2013).

4.6. Localisation of LXN in the Prostate Epithelium

Our laboratory has previously shown using confocal microscopy that LXN is localised to the nucleus in primary prostate epithelial cells and the prostate cell line LNCaP (Oldridge et al., 2013). Initial evidence for this came from immunofluorescence performed on fractionated primary epithelial cultures. In order to verify that this wasn't a result of non-specific binding of the anti-LXN antibody, LNCaP cells were transfected with a plasmid containing LXN fused to the HA epitope tag. This allowed the use of a second, well

characterised, antibody (anti-HA) to confirm the localisation of LXN. LNCaP cells were utilised for this purpose as they have very low expression of endogenous LXN. Using confocal microscopy it was shown that DAPI (nuclear stain), anti-LXN and anti-HA co-localised. The potential for controversy in this result is that LXN has no known nuclear localisation signal and as of 2016, this result remains the only study to show any localisation data for LXN. This nuclear localisation also opens the possibility for LXN to in-part exert its effects on colony formation, migration and invasion by directly affecting gene expression at the level of transcription.

4.7. Overview of Experimental Techniques Used in this Chapter

4.7.1. Chromatin Immunoprecipitation

Chromatin Immunoprecipitation (ChIP) is the 'gold standard' for precise localisation of the protein-DNA interactions which can control epigenetic regulation through histone modifications, and for confirmation of transcriptional regulation. Briefly, protein-DNA interactions are cross-linked *in situ* using formaldehyde. The cells are lysed and the chromatin is sheared by sonication to produce 200-500 bp fragments (Teytelman et al., 2013). The fragmented chromatin is then incubated with an antibody-bead complex specific for a particular protein bound to the DNA. The DNA-bound protein is known as a protein 'mark'. After the IP, the DNA is eluted from the antibody-bead complex and the cross-links are reversed. The resulting DNA (now free of protein interactions) is finally purified before analysis by qPCR using target specific primers.

The resulting data is often expressed as a percentage of the input chromatin (chromatin that has not been immunoprecipitated) e.g. a value of 10% of input indicates that 10% of the target loci exist in association with the protein mark to which the precipitating antibody was raised.

Recent advances in ChIP methodology have centred on reducing the amount of chromatin needed for successful immunoprecipitation (Schnerch et al., 2013, Collas, 2011). The result of this downscaling is micro- (μChIP) assays capable of measuring protein-DNA interactions from <1,000 cells which is equivalent to ~6 ng of DNA (Fig. 34.). In contrast, traditional ChIP protocols require 10^6-10^7 cells (6-60 μg of DNA) and are unsuitable for use in rare cell populations.

A functioning µChIP method was essential to study protein-DNA interactions in rare subpopulations of CaP cells, such as CSCs which account for <0.1% of tumour cells, and cannot be represented by established cell lines.
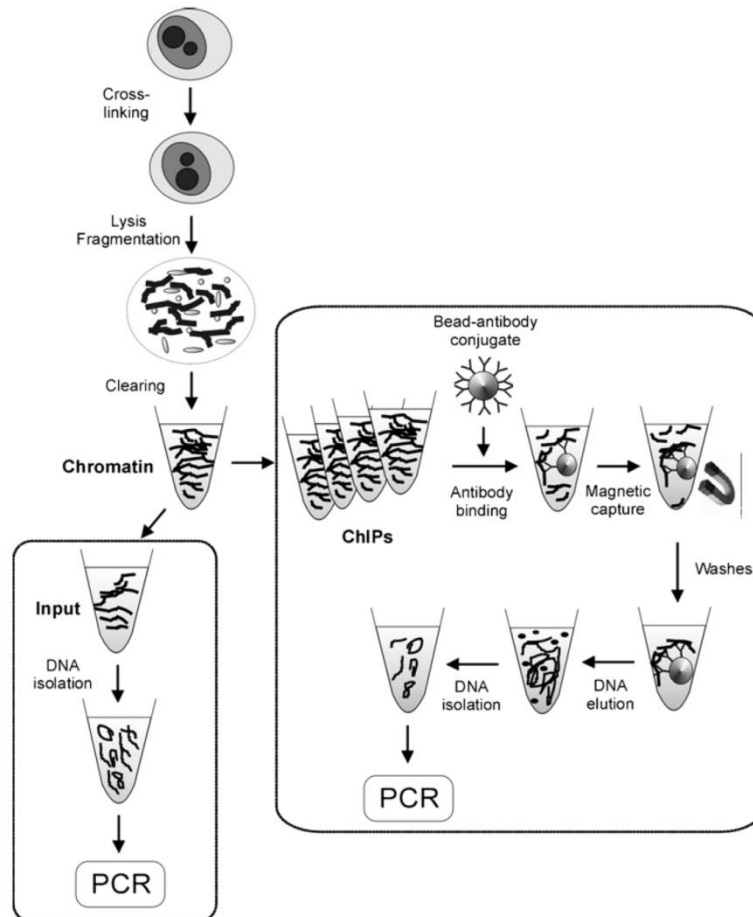
Fig. 34. Overview of µChIP Assay.

The main differences between this µChIP protocol and traditional large-scale ChIP, are the lower volumes used and magnetic capture beads (instead of sepharose capture beads) used in µChIP.

From: (Collas et al., 2011)

The chromatin status of the LXN and RARRES1 genes in primary epithelial cultures from benign and cancerous origin were investigated using ChIP. Capture molecules are antibodies that are specific for different histone modifications and markers of transcription. Downstream analysis, by PCR, assesses the enrichment of the target gene by each capture molecule. A list of targets for ChIP and control genes is provided in (Table. 5. and Table. 6.) respectively.

Target	Implication	Validated in Our Laboratory
H3K27me3	heterochromatin	✓
H3K4me3	euchromatin	✓
RNA pol II	transcription	✓
H3K9me2	heterochromatin	✓
H3K9ac	euchromatin	✓
H2AK119Ub	heterochromatin	✗
H4K20me3	heterochromatin (associated with tumour suppressor gene silencing)	✗
EZH2	heterochromatin (recruits polycombs, heterochromatin proteins and HDACs)	✗
PRC1	heterochromatin (binds H3K27me3 and adds Ub to H2AK119)	✗

Key
Primary Targets
Alternative/Future Targets

Table. 5. Primary and Alternative Targets for ChIP Capture Molecules.

Tabulated list of histone marks and associated proteins with information regarding the implication of theses marks to chromatin status. The table also contains the validation status of each mark capture molecule (antibody) within our laboratory.

Gene	Control	Information	Expected ChIP Analysis in Prostate Epithelium		
			H3K27me3	H3K4me3	RNA pol II
GAPDH Glyceraldehyde 3-phosphate dehydrogenase	Positive	Catalyzes the 6th step of glycolysis. Housekeeping gene - stably and constitutively expressed at high levels in most cells	-VE	+VE	+VE
PDYN Prodynorphin	Negative	Opioid polypeptide hormone gene for prodynorphin. Expressed in the endometrium and the striatum	+VE	-VE	-VE

Table. 6. ChIP Control Genes.

The identity, expression details and expected ChIP analysis in prostate epithelium of the positive control gene (*GAPDH*) and negative control gene (*PDYN*). Of note is that both control genes have been validated in our laboratory.

4.7.2. Lentiviral Vectors as Gene Delivery Systems

In order to determine the effect of LXN and RARRES1 on gene expression when overexpressed in a physiologically relevant model of primary prostate cancer (Collins et al., 2005). A lentiviral gene delivery system was established.

Lentivirus (LV) vectors, stably integrate into the genome of a transduced cell, forcing continued expression of the delivered gene. A major advantage of LV over γ-retroviral vectors is that they can transduce quiescent and senescent cells. The lentiviral vectors used in this project are based on human immunodeficiency virus (HIV), which has been modified to render the virus incapable of replication within the host. The modification in question (termed the self-inactivating (SIN) configuration) specifically targets the long terminal repeat (LTR) sequence through deletion of the U3 region of the 3' LTR, which is transferred to the 5' LTR during reverse transcription (Sanber et al., 2015). This deletion destroys the transcriptional activity of the LTR sequences, in turn abolishing the production of full-length vector RNA (Sanber et al., 2015). The use of the SIN configuration and heterologous envelopes has dramatically improved the overall safety of LV to the point that the later generation of LV vectors have the lowest hazard rating at the University of York.

Another safety feature of LV production is pseudotyping: the process of producing viral vectors in combination with foreign viral envelope proteins i.e. not encoded by the original virus (Mátrai et al., 2010). Pseudotyping of HIV vectors removes the safety concerns associated with native HIV envelope (gp120). The heterologous vesicular stomatitis Indiana virus protein G (VSV-G) envelope protein is the most commonly used viral envelope for LV pseudotyping (due to its broad spectrum of susceptible cells) although, choice of envelope used to pseudotype the LV is at least partly determined by the target cell or tissue that needs to be transduced.

The most widely employed method for the production of LV is by co-transfection of cell lines (packaging cells) with vector plasmid and the gag-pol, rev, and env packaging constructs resulting in LV production by the packaging cells, which are present in the supernatant (Fig. 35.) (Mátrai et al., 2010). The resulting supernatant is then filtered to remove any packaging cells that have sloughed off into the viral supernatant.

The normal human embryonic kidney cell line HEK-293 is commonly used for this purpose, and as such several modified HEK-293 lines have been produced to enhance LV

production. These include but are not limited to 293T cells and 293FT cells (Mátrai et al., 2010). These HEK-293 derivatives commonly contain the SV40 Large T-antigen, which mediates episomal replication of transfected plasmids containing the SV40 origin of replication (Durocher et al., 2002). Once the titre is known the multiplicity of infection (MOI) which indicates the number of vector particles per cell used in a transduction can be calculated and standardised across experiments e.g. a MOI of 1 means the addition 10^5 viral particles to 10^5 cells (Zhang et al., 2004).
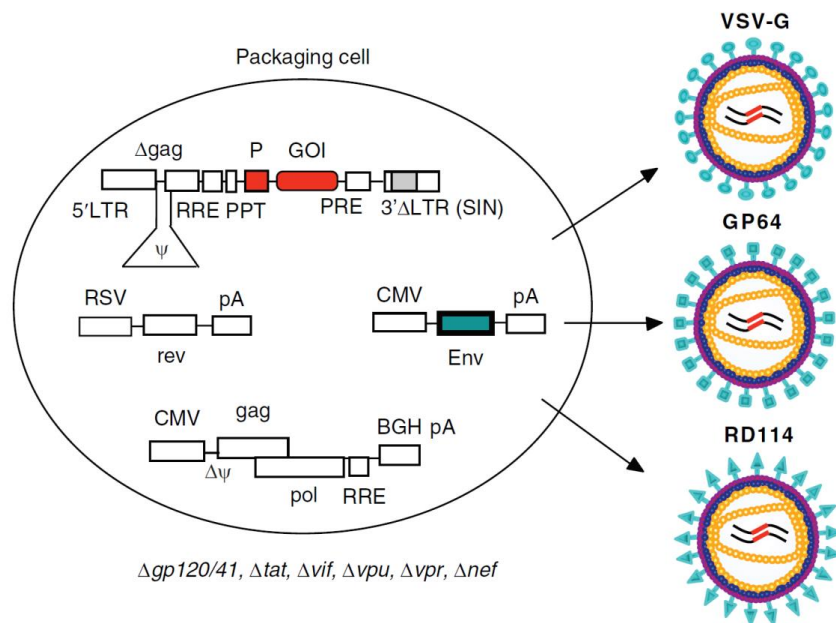
Fig. 35. Lentiviral Vector Production by Trans-Complementation.

Packaging cells are transfected with a combination of lentiviral vector plasmid and packaging plasmids which contain Gag, Pol, Rev, and VSV-G sequences. Only the vector contains the packaging sequence Ψ. The lentiviral sequence is flanked by 5' and 3' LTR sequences. The LTR sequences through their enhancer/promoter function are necessary for proper expression of the full-length vector transcript. Additionally, the LTR sequences also involved in reverse transcription and integration of the vector into the genome.

Viral particles are harvested from the medium the packaging cells are grown and used directly or further concentrated by purification methods. By changing the envelope genes encoded by the helper plasmids it is possible to pseudotype the lentivirus which directly effects the tropism of the resulting lentivirus.

Abbreviations: SIN = self-inactivating LTR sequences that contain Δ = LTR sequences that contain a partial deletion, WPRE = Woodchuck hepatitis virus post-transcriptional regulatory element, cPPT = central polypurine tract, RRE = Rev responsive element and LV = lentiviral vector.

From: (Mátrai et al., 2010)

4.7.3. Gateway™ Cloning

Invitrogen™ Gateway™ recombination cloning differs from traditional cloning techniques through the use of a reversible recombination reaction, as opposed to restriction enzymes and ligase reactions. This techniques offer several advantages:

- Certain restriction enzymes cannot be used in conventional cloning because they might cut within the gene of interest, truncating the insert and making the gene useless for downstream expression.
- Due to the removal of a death gene (ccb) from the vector upon recombination to insert the gene of interest, the amount of colony screening is reduced.

The basic protocol for cloning a gene of interest into a LV plasmid vector is as follows. Addition of flanking attB recombination sites to the gene of interest using primers that are specific for the gene of interest, but with overhangs which contain the attB sites. This typically involves two PCR steps as the attB sequences are quite long, using a high fidelity polymerase such as phusion. The first PCR reaction adds the first half of the attB sequence to the gene of interest. The PCR product is then separated on an agarose gel and from which extraction of the product is then performed.

The purified product from the gel extraction is then used as a substrate for a second PCR reaction which adds the 2nd half of the attB recombination site, before a second gel extraction is performed to yield the purified product which is the gene of interest flanked by the full attB sequence. This fully flanked sequence can now be added to an Entry vector through recombination using the Invitrogen BP clonase which, through recombination between the attB sites on the gene of interest and the attL sites which flank ccb, eliminates the ccb death gene from the Entry vector and replaces it with the gene of interest.

The Entry vector is a shuttle vector which can be used in subsequent steps to deliver the gene of interest into several commercially available LV vectors which have specific properties depending on experimental needs such as co-expression of eGFP to allow transduction efficiency to be visualised. Once the Entry vector has been quality controlled through PCR and/or restriction digestion to ensure the presence of the gene of interest it is typically sequenced to guarantee that no mutations have been introduced through the PCR and gel extraction steps.

Once the Entry vector containing the gene of interest has been validated it is used as to generate the LV destination vector containing the gene of interest. The gene of interest is now flanked by the attL sequences and through the use of LR clonase which performs recombination between attL sequences and attR sequences the gene of interest can be transferred to the LV destination at the expense of another copy of ccb present in the LV destination vector flanked by attR sequences. Colonies are then picked and screened for presence of the gene of interest. An overview of the main steps of vector generation and virus production used in this report are shown in (Fig. 36.).
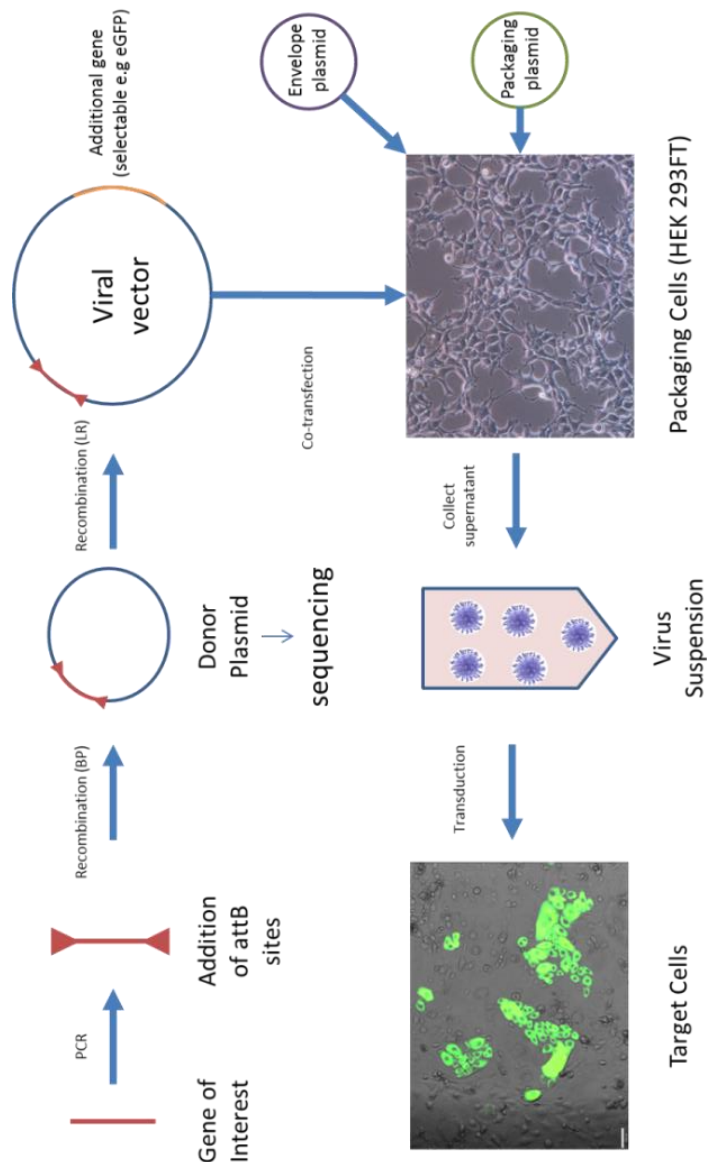
Fig. 36. Overview of Vector Production, Virus Production and Transduction Used in this Report.

The gene of interest is first flanked with attB recombination sequences, recombination with the BP clonase results in an Entry vector containing the gene of interest. A second recombination reaction with the LR clonase results in a destination vector that contains the gene of interest. Co-transfection of HEK 293FT packaging cells with the destination vector, envelope and packaging plasmids allows lentivirus production through trans-complementation. Supernatant (containing the lentiviral particles) is then harvested which can be directly used to transduce cells including primary prostate epithelial cells.

4.7.4. Microarray

DNA microarray technology is now a wide-spread method for analysing expression profiles of biological samples. The technology is based on DNA hybridisation of cDNA molecules to complementary probes which are attached in 'spots' on the surface of the microarray chip at known locations. Commonly a single gene is covered by several probes to increase accuracy of detection above background. The hybridisation reaction between the sample cDNA library and the microarray is performed under high-stringency conditions so that only highly specific interactions between cDNA molecules and their corresponding probes can occur (Wildsmith and Elcock, 2001). Microarrays use relative quantitation in which the intensity of a probe is compared to the intensity of the same probe under a different condition, and the identity of the probe is known by its position.

A typical protocol for expression profiling is as follows:

1. RNA is extracted from the biological sample and is quality controlled for quality and quantity. This is typically performed using an Agilent Bioanalyzer (utilises capillary electrophoresis) which as well as giving a yield also provides an RNA integrity (RIN) number which ranges from 1 (highly degraded) to 10 (not degraded).

2. The labelled cDNA library is generated via reverse transcription (an optional PCR amplification can be performed at this step if yield is too low). RNA is reverse transcribed with either polyT primers (which amplify only mRNA) or random primers (which amplify all RNA, most of which is ribosomal ribonucleic acid (rRNA)). The label (typically fluorescent) is added either during the reverse transcription step, or following amplification if it is performed.

3. The labelled samples are then mixed with a propriety hybridization solution which includes blocking agents to limit non-specific binding thereby reducing background and enhancing signal to noise.

4. The mixture is denatured and added to the pinholes of the microarray. The holes are sealed and the microarray hybridised.

5. After hybridisation washing steps are performed to remove nonspecific binding events.

6. The microarray is dried and scanned by using a laser to excite the fluorophore and emission levels which are proportional to the level of hybridisation and hence relative abundance of the cDNA species is measured by a detector.

7. As the location of each probe 'spot' is known the emission intensity can be mapped to specific genes.

8. The raw data is normalised through subtraction of background intensity.

9. Data is then analysed using bioinformatics software. The TAC console V3.0 was used in this report.

4.7.5. Mass Spectrometry

In addition to genomic approaches, the aim was also to characterise the function of LXN and RARRES1, using a proteomics based approach to investigate potential interacting partners. To this end affinity purification coupled to downstream mass spectrometry (MS) was used.

MS is regarded as the analytical technique of choice for identifying proteins within complex biological samples, particularly when coupled to high pressure liquid chromatography (HPLC) (Dunham et al., 2012). MS measures the mass to charge ratio of ionised molecules by measuring their time of flight with the mass spectrometer. This allows the determination of their molecular mass after charge state resolution. In order to apply this technique to proteins it is first necessary to digest the proteins within a sample to yield peptides fragments which are more amenable to MS than intact proteins.

Fragmentation of the intact (or parental peptide) results in 'diagnostic fragments' which can be used with the assistance of complex software tools and databases to elucidate the amino acid sequence of the parent peptide (Dunham et al., 2012, ten Have et al., 2011). The identified peptides are then used through the use of sophisticated software to assign a likely protein to the peptides.

Affinity purification up-stream of MS is commonly employed to reduce the complexity of biological samples, particularly when one is trying to identify binding partners. Typically, affinity purification is performed using antibodies specific to the protein of interest (commonly called the bait). The bait is immunoprecipitated in a buffer that maintains the baits interaction with interacting proteins. Unfortunately it is often difficult to obtain an antibody with the required affinity and specificity for the bait. If one can't be found, it is common for a tagged version of the protein to be constructed and introduced into the cell through transfection. This allows the use of highly validated anti-tag antibodies to

perform the IP. Typical epitope tags include but are not limited to: HA, GST, FLAG, HIS, c-Myc, and V5 (Dunham et al., 2012).

Once a suitable IP-grade antibody has been identified and validated, it is immobilised onto a matrix, usually a resin or micro-beads. Coupling is often performed through binding of the antibody to protein A or protein G which is pre-coupled to the matrix (Dunham et al., 2012, ten Have et al., 2011). Alternatively the antibody can be covalently linked to the matrix. The resulting antibody-linked matrix is exposed to the biological sample and incubated to allow capture of the bait in complex with its interactome. After several wash steps, the bait and its interacting partners are eluted from the matrix. An efficient but non-specific elution solution is Laemmli buffer with the addition of 2-Mercaptoethanol (Dunham et al., 2012).

Reduction of non-specific interactions is essential for enhancement of the signal to noise ratio and to allow the identification of low abundance interactions. Typically this is achieved through a pre-clear step in which 'naked' matrix (i.e. matrix without antibody) is incubated with the sample prior to affinity purification (Dunham et al., 2012). Alternatively or concomitantly stringent washing steps are included (ten Have et al., 2011). Stringent washing has a downside which is the increased potential for false negative results, whereby true weaker interactions are lost. Quantitative proteomics is used to identify true interactors as opposed to non-specific interactions post MS by comparison to a control sample. This post MS screening is made more efficient and robust through the use of proper controls which are as closely linked as possible to the biological samples they are associated with. The control should be harvested, affinity purified and analysed in parallel to the experimental sample.

4.8. Results

4.8.1. ChIP Primer Validation

qPCR was used to interrogate precipitated chromatin for the enrichment of target gene sequences by each mark (listed in Table. 6.). The primers pairs in (Appendix 2.) were used to determine the chromatin status of LXN and RARRES1 genes and promoter regions. The location of the genomic sequences covered by these primers is depicted in (Fig. 37.) As such the following parameters of the qPCR assays must be validated: efficiency, R^2 and presence of non-specific amplifications (multiple products). In order to expand the future applications of the assays two further parameters were investigated. Firstly, the cycle in which fluorescence rises above the threshold for detection, termed quantitation cycle (Cq) at 30 pg of genomic DNA (equivalent to 10 copies of template). This parameter was used to estimate the sensitivity of the primer pairs, with a view to measuring low chromatin yields obtained from low cell numbers i.e. μChIP. The second additional parameter is the species specificity of the primer pairs, which is important when downstream applications of the assays are considered e.g. analysis of samples derived from xenograft models. Xenograft samples contain a variable proportion of contaminating host (mouse) DNA, due to vascularisation and infiltration of engrafted tumours. Additionally, primary cultures of prostate epithelium are grown using a feeder layer of STO cells which are of mouse origin. If the primer pairs do not have a suitable human:mouse specificity ratio, the resulting data would be prone to artefacts and valid conclusions could not be able to be drawn.
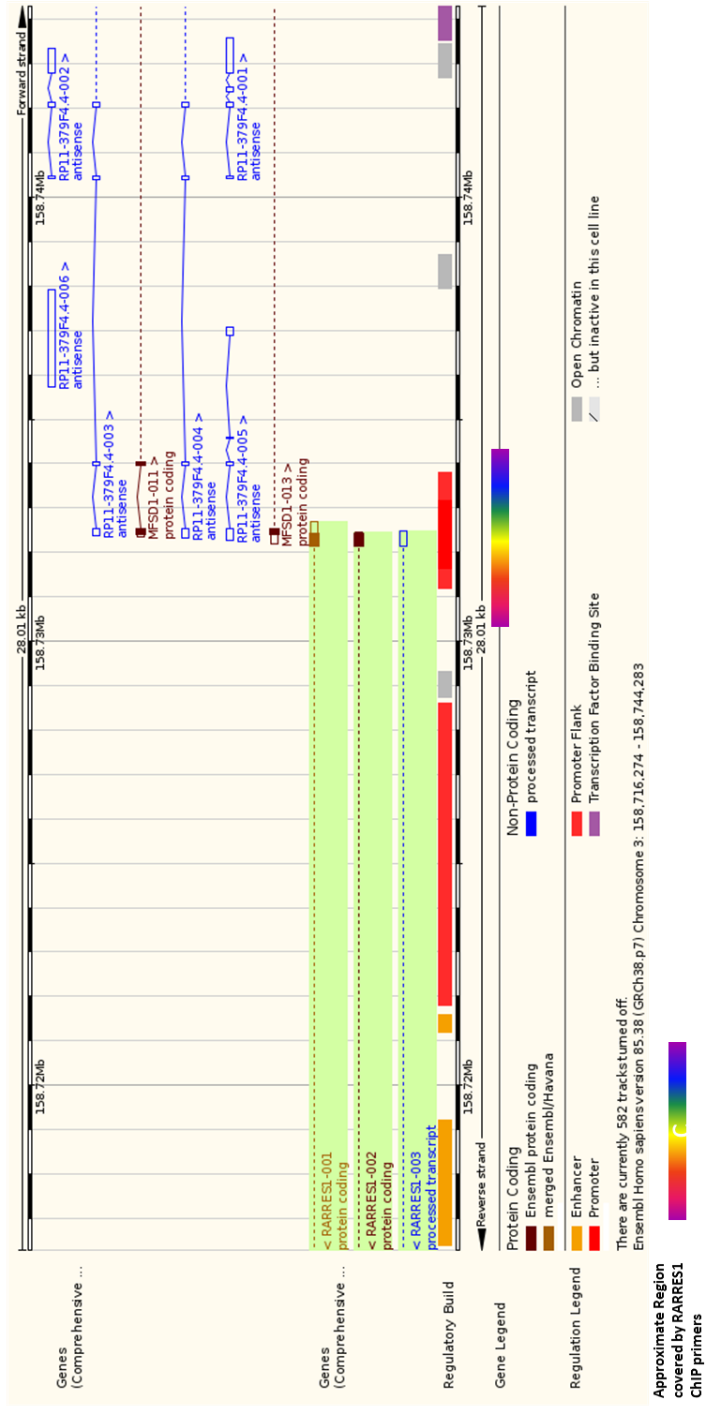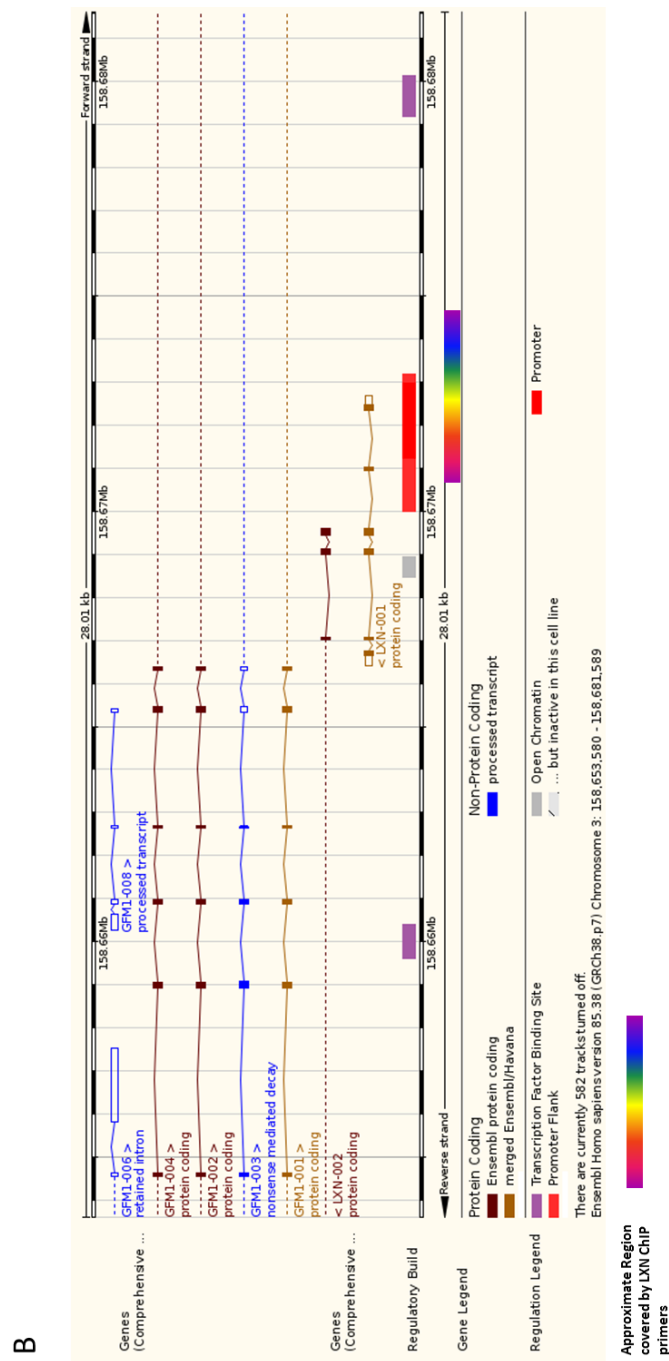
Fig. 37. Genomic Location of the Chromosome Region Covered by RARRES1 and LXN ChIP Primers.

The online annotated ensemble genome browser tool was used to construct a detailed diagram of the genomic regions around the transcription start site of RARRES1 **A.** and LXN **B.** The diagram shows the genes encoded in this region along with transcription factor binding sites, putative promoter regions and areas of open chromatin. The approximate region covered by the RARRES1 and LXN ChIP primers for each gene is depicted by the rainbow coloured box.

Table. 7. details the validation of all ChIP primer pairs analysed. The primers have been divided into two groups based on annealing temperature. The division allows streamlining of assays as multiple assays can be performed on a single plate and a single run.

All primer pairs have an efficiency (defined as the increase in amplicon per cycle) value which falls within well-established guide lines (90-110%). The R^2 value of all primers also meets the requirement of being greater than 0.98. qPCR reactions using all primers resulted in the amplification of a single product, as assessed using melt curve analysis. All assays are of high sensitivity, as the Cq values at 30 pg of genomic DNA are sufficiently low (<38), thus enabling quantitative analysis of small quantities of DNA. The human:mouse specificity ratio (determined by measuring the Cq observed in a reaction with 10 ng of human DNA template to the Cq observed in a reaction with 10 ng of mouse DNA) of all primer pairs is sufficiently large to avoid artefacts due to non-specific amplification of contaminating mouse DNA (Table. 7.).

Primer Pair	Temperature (°C)	Efficiency (%)	R^2	Single Product	Cq at 30pg (~10 copies)	Species Specificity (Human : Mouse)
LXN PP1	55	91.2	0.996	✓	35.20	Mouse not detected at 10ng (44 cycles)
LXN PP2	58.5	97.8	0.995	✓	34.95	310
LXN PP3	55	98.8	0.994	✓	35.76	1805
LXN PP4	55	97.8	0.996	✓	34.73	781
LXN PP5	58.5	100.8	0.987	✓	33.58	11123
GAPDH	58.5	95.6	0.991	✓	36.26	568
PDYN	55	104.2	0.995	✓	33.28	42.5
RARRES1 PP1	58.5	97.5	0.993	✓	33.87	62
RARRES1 PP2	58.5	101.2	0.996	✓	33.57	508
RARRES1 PP3	55	102.8	0.997	✓	33.16	478
RARRES1 PP4	58.5	103.1	0.996	✓	34.20	111
RARRES1 PP5	58.5	96.2	0.989	✓	34.85	43
Ideal	NA	90-110	>0.98	✓	<38	>10

Key

| Primer group 1 | Primer group 2 | Ideal example |

Table. 7. Performance and Parameters of ChIP Primer Pairs.

Tabulated list of assay parameters and details of the performance of each assay. Primer pairs have been divided into two groups based on annealing temperature. An extra row has been included to detail the characteristics of an ideal primer pair.

4.8.2. ChIP Validation

Before investigating the chromatin status of primary prostate epithelium, the ChIP assay, capture antibodies and reference genes were validated using chromatin derived from cell lines. Cell lines have several advantages as a validation tool. Their ease of culture and lack of feeder cells means that large quantities of target cell-derived chromatin can be prepared and repeat assayed. To cover the broad-spectrum of prostate epithelial cells, PNT2C2 (basal phenotype from normal origin) and LNCaP (luminal phenotype from cancer origin) were used to investigate reference gene and technique compatibility.

The data shown in (Fig. 38.) shows the expected pattern (Table. 6.) i.e. the active gene (*GAPDH*) being enriched by the euchromatin (H3K4me3) and transcription (RNA Pol II) marks but not the heterochromatin (H3K27me3) mark (Fig. 38A. and Fig. 38C. for PNT2C2 and LNCaP respectively). The silenced gene (*PDYN*) shows the converse pattern being enriched by H3K27me3 antibody but not anti- H3K4me3 or RNA Pol II (Fig. 38B. and Fig. 38D.) for PNT2C2 and LNCaP respectively).

Both cell lines showed the same pattern although the enrichment by all marks was higher in PNT2C2 cells when compared to LNCaP cells. It can be concluded that these antibodies and reference genes are compatible with cells representing the diversity of the human prostate epithelium.

Chapter 4. Results
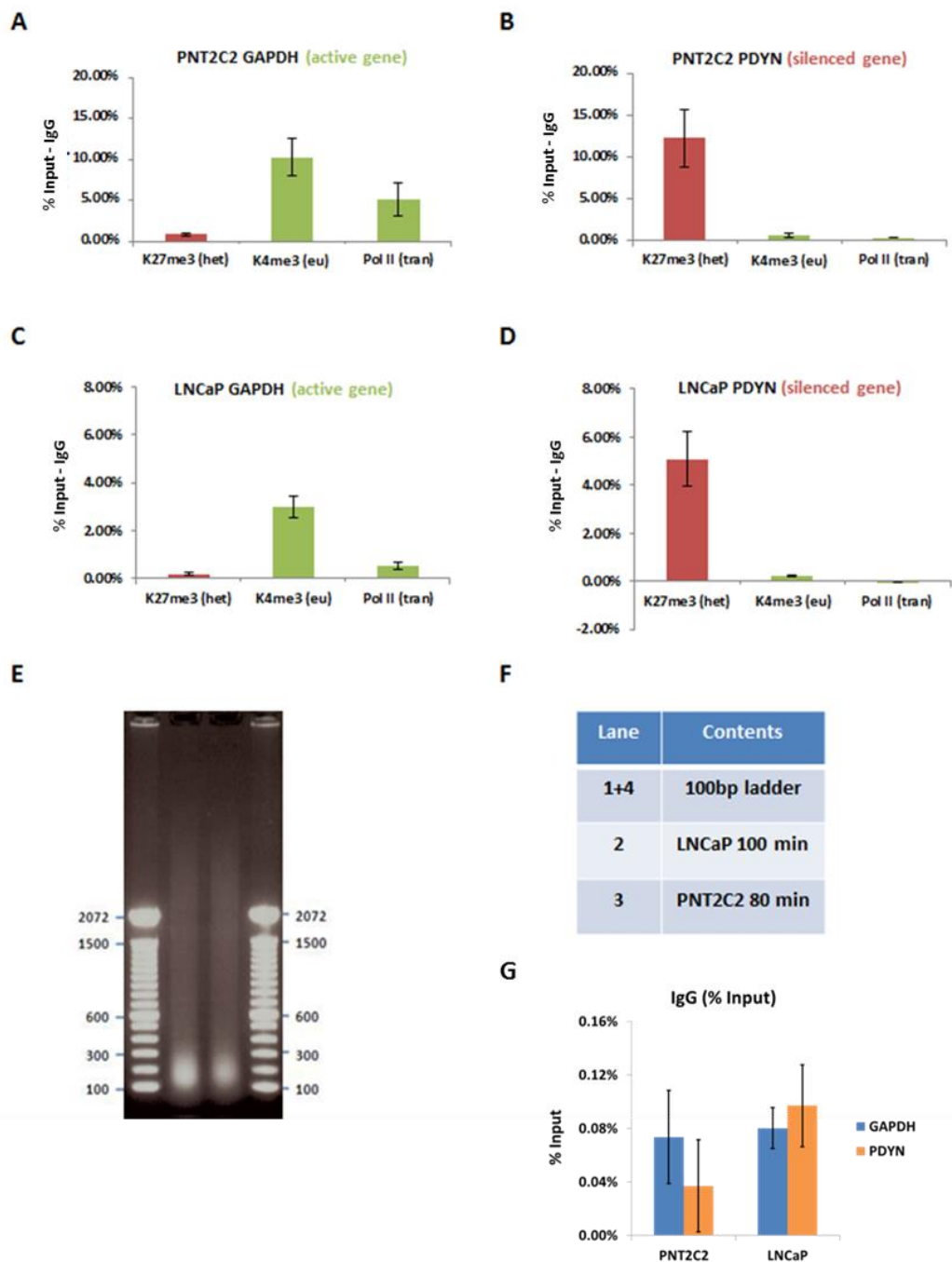
Fig. 38. Validation of H3K27me3, H3K4me3 and RNA Pol II Antibodies and +ve (GAPDH) and –ve (PDYN) Control Genes.

Graphical representation of enrichment of GAPDH and PDYN sequences by anti-H3K27me3 (K27me3), H3K4me3 (K4me3) and RNA Pol II antibodies in PNT2C2 **A.** and **B.** and LNCaP cells **C.** and **D.** Error bars = 1 standard error of the mean.

E. Agarose gel following gel electrophoresis loaded as described in the lane legend depicted in **F.** (minutes refer to length of sonication)**.**

G. Background binding levels of IgG control antibody.

Each sample represents 3 experimental replicates each comprising 4 technical replicates.

4.8.3. Chromatin Status of RARRES1 and LXN Promoter Sequences in PNT2C2 and LNCaP Cells

In PNT2C2 cells RARRES1 showed a substantial enrichment by anti- H3K4me3 especially near the transcription start site, compared to the enrichment by anti- H3K27me3 (Fig. 39A and 39C.). This indicates that the chromatin in this region exists as transcriptionally active euchromatin, in agreement With qPCR data which shows that PNT2C2 cells express a significant amount of RARRES1 mRNA. LNCaP cells showed a similar pattern to PNT2C2 cells at the RARRES1 promoter with these sequences showing a net-enrichment for the euchromatin mark, although with much lower values than PNT2C2 cells. The positive transcription mark (RNA pol II) was absent from the RARRES1 promoter sequence in LNCaP cells, in agreement With qPCR data from our lab which shows that RARRES1 mRNA is undetectable in LNCaP cells. Taken together these data suggest that histone modifications play a role in modulating RARRES1 expression in PNT2C2 to a much greater extent than in LNCaP cells.

The LXN promoter, in both cell lines, is not enriched for either histone mark, indicating that the chromatin in this region exists in an ambiguous intermediate state (Fig. 39B and 39D.). The transcription mark (RNA pol II) was positive at this region in both cell lines. In PNT2C2 cells, RNA pol ll is equally abundant at the RARRES1 and LXN promoters even though RARRES1 is expressed to a greater extent in these cells. The presence of a single marker of transcription (in this case RNA pol II) does not necessarily reflect the level of transcription as multiple cis and trans-regulatory elements contribute. Also the difference in mRNA levels between the two genes may be a result of differential mRNA stability. In LNCaP cells, enrichment of the LXN promoter sequence shows evidence of weak transcriptional activity compared to absence of the transcription mark at the RARRES1 promoter. This is again in agreement With qPCR quantification of mRNA expression, which shows that LXN is very weakly expressed in LNCaP cells compared with undetectable levels of RARRES1 mRNA.

It has previously been shown that these genes are regulated by DNA methylation at CpG islands in prostate cell lines. As such, histone modifications were not expected to play a dominant role in the regulation of these genes in cell lines. It was encouraging that the ChIP data presented here correlated with mRNA expression profiles and that there is evidence of a role for histone modifications in the regulation of RARRES1, particularly in PNT2C2 cells.
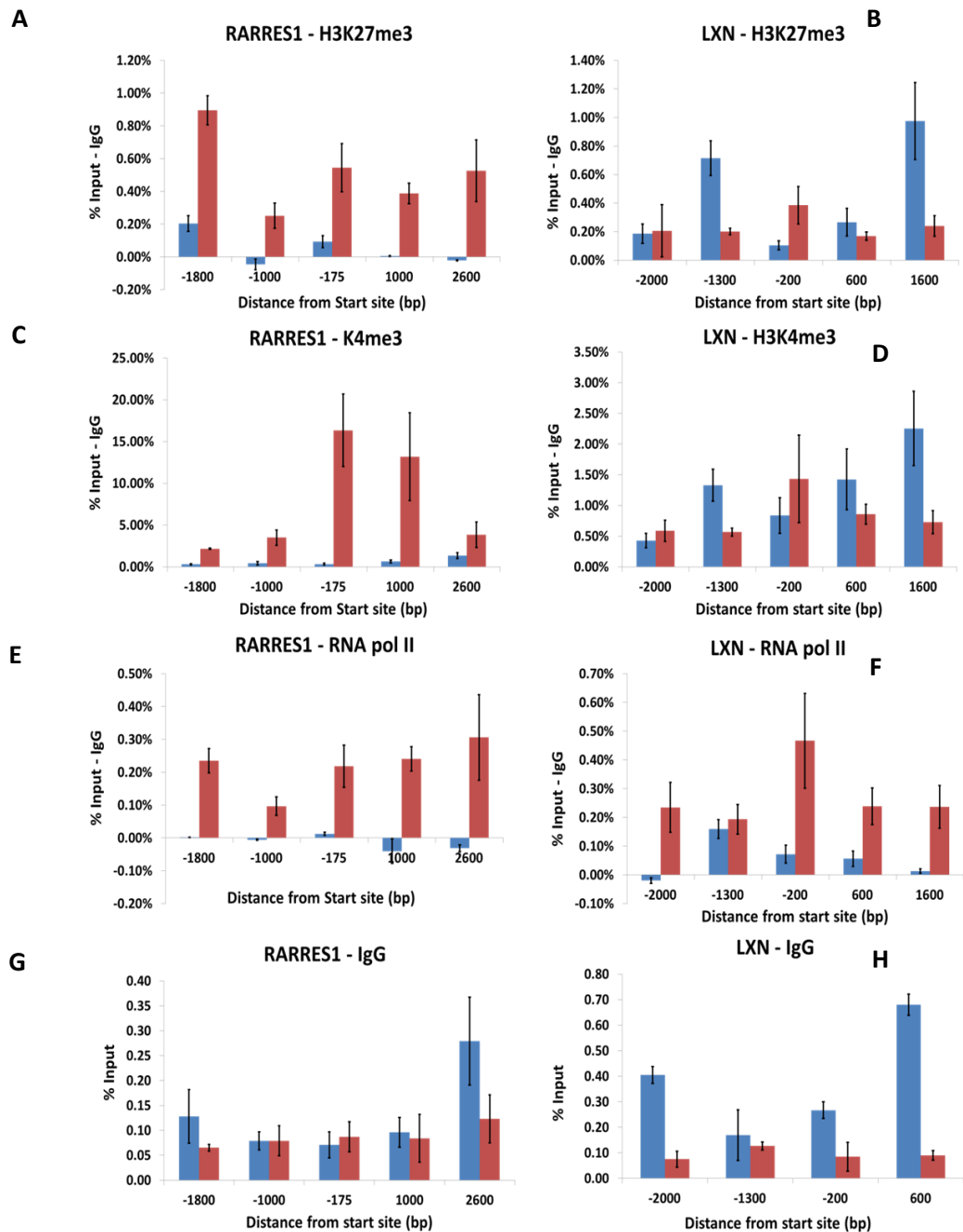
Fig. 39. ChIP of LXN and RARRES1 Promoters in PNT2C2 and LNCaP Cells.

A.-H. Graphical representation of enrichment of RARRES1 **A.**, **C., E.** and **G.**) and LXN (**B**, **D, F** and **H**) sequences by anti- H3K27me3 (**A** and **B**), H3K4me3 (**C** and **D**), RNA Pol II (**E.,** and **F.**), IgG (**G** and H) antibodies in PNT2C2 (red bars) and LNCaP (blue bars) cells. Error bars = 1 standard error of the mean.

Each sample represents 3 experimental replicates each comprising 4 technical replicates.

4.8.4. ChIP Scale Down

It became evident that the novelty and value of future experiments could be increased by expanding the application of ChIP to the analysis of very rare tumour sub-populations, such as CSCs which comprise <0.1% of tumour cells. For this aim to be achieved, a µChIP method, capable of interrogating low amounts of chromatin (~2 ng/IP, compared to 20 µg/IP in the standard ChIP) was established. To this end the µChIP method developed and published by (Collas, 2011) was adopted. The scale-down was performed using previously validated chromatin that was diluted in a stepwise manner from 20 µg to 2 ng with an intermediate step of 200 ng.

The Collas protocol advocated the use of magnetic capture particles as opposed to sepharose capture particles used thus far (Collas, 2011). Magnetic capture particles yielded a lower level of nonspecific binding to chromatin compared with sepharose (Fig. 40A.). It is important to note that 200 ng of chromatin had a greater background signal compared with 20 µg. This can be explained by the background binding following a non-linear binding curve, and the reduction in the input due to dilution following linear kinetics i.e. all nonspecific binding sites were saturated at 200 ng of chromatin/IP. For example if the 200 ng had an arbitrary background binding level of 1 and input was 10 then background would be one tenth of input. If the 20 µg sample also had an arbitrary background binding of 1 due to saturation of non-specific binding sites already being achieved at 200 ng and an input value of 1000 (due to 100-fold more chromatin) then background would be one thousandth of input.

The two histone marks (H3K27me3 and H3K4me3) exhibited a dramatic increase in signal when the starting chromatin was reduced (Fig. 40C. and 40D.). The signal for RNA pol II did not dramatically increase when chromatin levels were reduced, indicating that the capture antibody was not being saturated at 20 µg conditions (Fig. 40B.). However, an increase in signal was observed when changing from sepharose to magnetic capture particles.
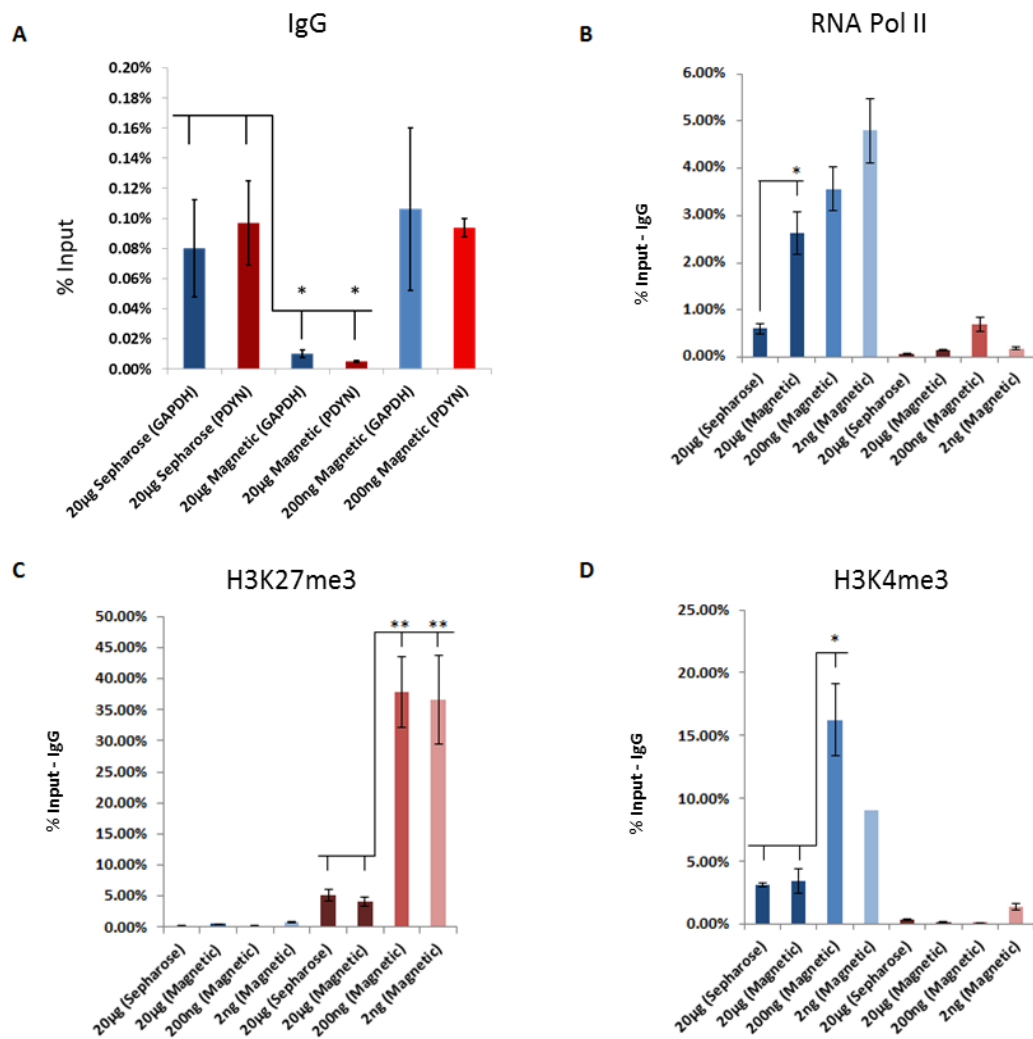
Fig. 40. ChIP Scale-Down Using Previously Validated LNCaP Chromatin.

A. Non-specific enrichment of GAPDH and PDYN sequences using either sepharose or magnetic capture-particles (labelled with anti-IgG)

B.-D. Enrichment of GAPDH and PDYN sequences using either sepharose or magnetic capture-particles (labelled with anti- RNA Pol II **B.**, H3K27me3 **C.** or, H3K4me3 **D.** antibodies in LNCaP cells.

In all graphs: BLUE bars equal GAPDH and RED equal PDYN. Shading is intended to represent initial chromatin levels with darker shades representing larger amounts of starting chromatin/IP.

Error bars = 1 standard error of the mean

Each sample represents 3 experimental replicates each comprising 4 technical replicates

 * = $P \leq 0.05$ ** = $P \leq 0.01$

4.8.5. Establishing a qPCR Protocol for the Estimation of Chromatin Fragmentation After Sonication of Small Quantities of DNA with a View to Micro-ChIP

In order for any ChIP to be successful, the optimal sonication time must be determined empirically for each sample. This is because over-sonication reduces sensitivity and under-sonication increases false positives; the optimum size of chromatin fragments is 200-500 bp.

In μChIP the amount of DNA is too low to yield a visible band on a gel. However, the size of the DNA fragments can be estimated using the ratio of a 100 bp to a 300 bp qPCR product and thus optimal sonication time can be determined (Dahl and Collas, 2008).

22Rv1 chromatin was sonicated and the resulting fragment size as a function of sonication cycles was assessed using both gel-based and qPCR-based methods (Fig. 41.). From these assays it can be seen that the chromatin fragments reduce in size as the number of sonication cycles increases. The qPCR ratio of the 100 bp to a 300 bp products increases as a function of sonication cycles, indicating that the mean chromatin fragment size is reducing with the number of cycles. The 300 bp template is broken at a greater rate than the 100 bp template, due to its size. The optimum sonication was 60 cycles. After this point there was an accumulation of chromatin fragments shorter than 200 bp (loss of sensitivity) and a consequent reduction in the 100 bp : 300 bp ratio (as for the first time in the time-course the 100 bp template is being broken).
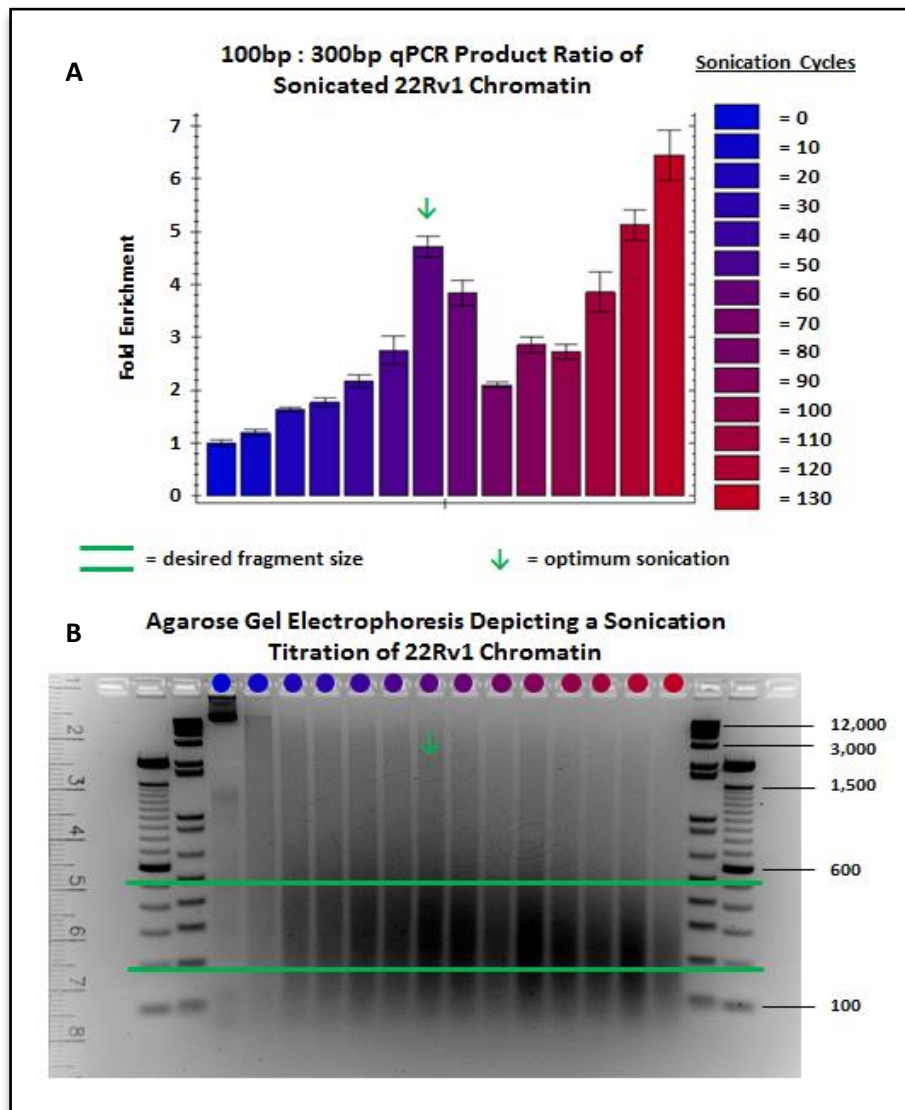
Fig. 41. Sonication Titration of 22RV1 Chromatin.

22Rv1 cells were cross-linked with formaldehyde prior to cell lysis. The resulting cross-linked chromatin was sonicated on ice. A chromatin sample was taken every 10 cycles. The chromatin was extracted and the degree of fragmentation was assessed by qPCR using two primer pairs, one generating 100bp product and the other a 300bp product. This was used to calculate the 100bp:300bp ratio at each sample point **A.**. In parallel 400ng of extracted chromatin was loaded on to a 2% agarose gel allowing the fragment size to be assessed by DNA staining following electrophoresis **B.**.

The desired fragment size of between 200 and 500bp and optimal sonication time is indicated by the green arrow.

Error bars = 1 standard error of the mean.

Data presented is a single representative experiment each data point was measured in quadruplicate.

4.8.6. µChIP of Fractionated Primary CaP Samples Interrogated for Relative Enrichment of RARRES1 and LXN Promoter Sequences Using anti- H3K27me3, H3K4me3 and RNApol II Antibodies.

In order to assess the contribution of histone modifications (and therefore chromatin status) to the epigenetic regulation of LXN and RARRES1, three primary epithelial cultures of malignant origin were fractionated in to CB, TA and SC populations (total nine cellular samples from three patients) and µChIP performed. The subfractionation of primary samples was chosen for this experiment as LXN and RARRES1 were previously shown to be upregulated upon differentiation from SC to TA and CB cells (Oldridge et al., 2013).

All samples analysed had enrichment (above the immunoglobulin G (IgG) control) of *RARRES1* and *LXN* promoter sequences when immuno-precipitated with the anti-H3K27me3 antibody (Fig. 42A. and B. respectively). This was significantly elevated (5.66% (*RARRES1*) and 8.89% (*LXN*) average for all samples across all primer pairs analysed) over the negative control gene for this mark (*GAPDH*) (2.16% average for all samples) but to a much lesser extent than the positive control gene for this mark (*PDYN*) (26.52% average for all samples). Control gene enrichment by anti-H3K27me3 is shown in (Fig. 42C.). Similarly, all samples analysed had enrichment of *RARRES1* and *LXN* promoter sequences when immuno-precipitated with the anti-H3K4me3 antibody (Fig. 42D. and E. respectively). Again the enrichment of these sequences was intermediate between that of the positive control *GAPDH* and the negative control *PDYN* (2.35% *RARRES1*, 2.71% *LXN*, 11.71% *GAPDH* and 0.81% for *PDYN*. Control gene enrichment by anti-H3K4me3 is shown in (Fig. 44F.) The enrichment of *RARRES1* promoter sequences by anti-RNApol II (0.63% (average across all primer pairs and samples Fig. 42G.) was not significantly different from that of the negative control gene *PDYN* (0.52%) (Fig. 42I.). Conversely, the enrichment of *LXN* promoter sequences by anti-RNApol II (2.19% (average across all primer pairs and samples; Fig. 42H.) was significantly different from that of the negative control gene *PDYN*, but was not enriched to the same level as that of the positive control gene *GAPDH* (4.07%) (Fig. 42I.)

For ease of analysis and interpretation, a single representative patient sample (H530) is shown in (Fig. 42M-R.). The pattern of results is the same as the entire cohort: enrichment of *RARRES* and *LXN* promoter sequences to an intermediate level between positive and negative controls by anti H3K27me3 (Fig. 42M. *RARRES1* and N. for *LXN*) and anti-H3K4me3 (Fig. 42O. *RARRES1* and P. for *LXN*). Finally, the differential enrichment of

RARRES1 and *LXN* promoter sequences by anti RNApol II is shown in (Fig. 42Q. and R.), respectively. Here, *RARRES1* was not enriched over the negative control *PDYN* and *LXN* was greatly enriched relative to *PDYN*, but to a lesser extent than that of the positive control gene *GAPDH* after subtraction of IgG-background binding.

Chapter 4. Results

Chapter 4. Results

Chapter 4. Results

M RARRES1

N LXN

O RARRES1

P LXN

RARRES1

LXN

Chapter 4. Results
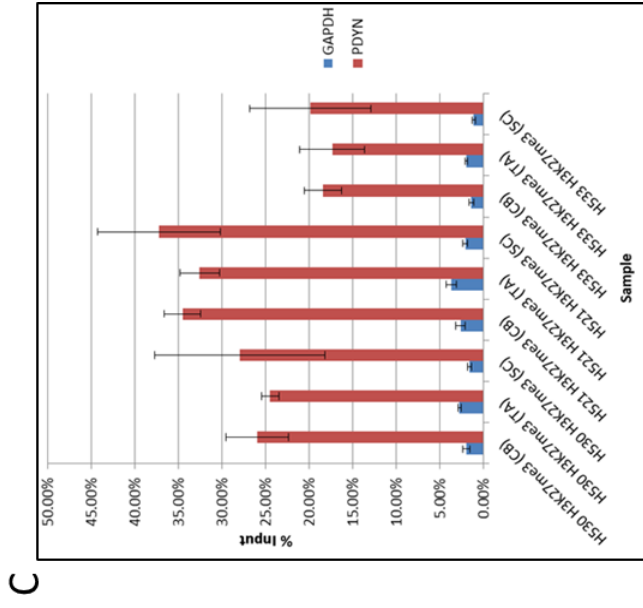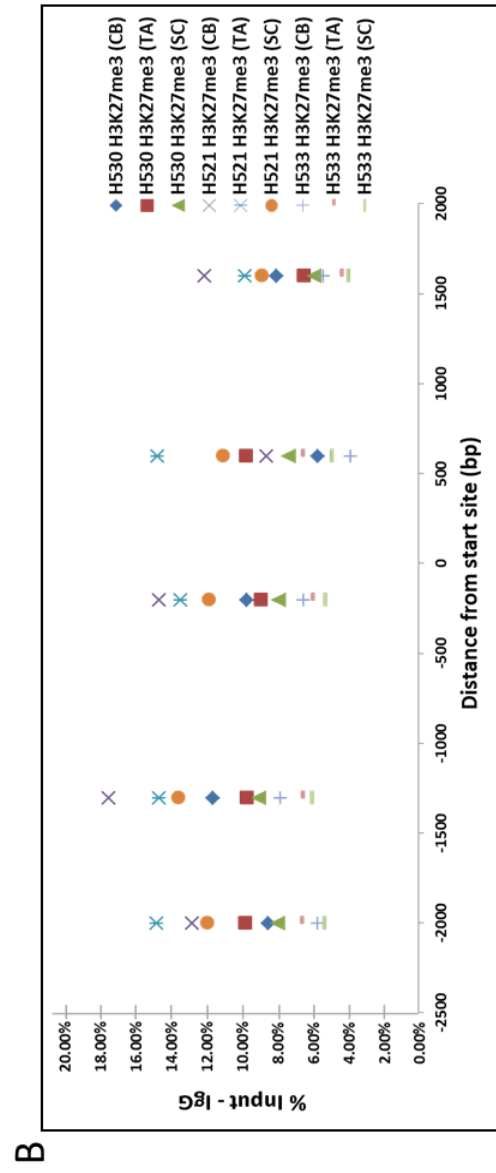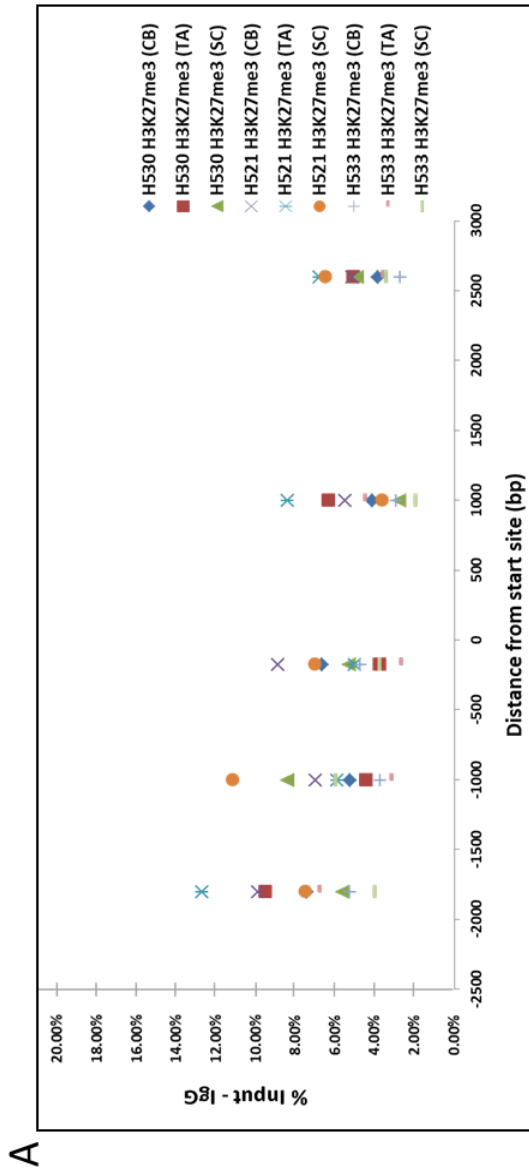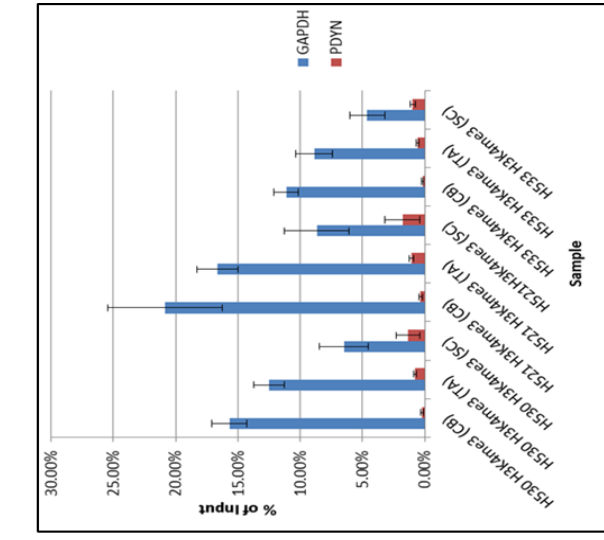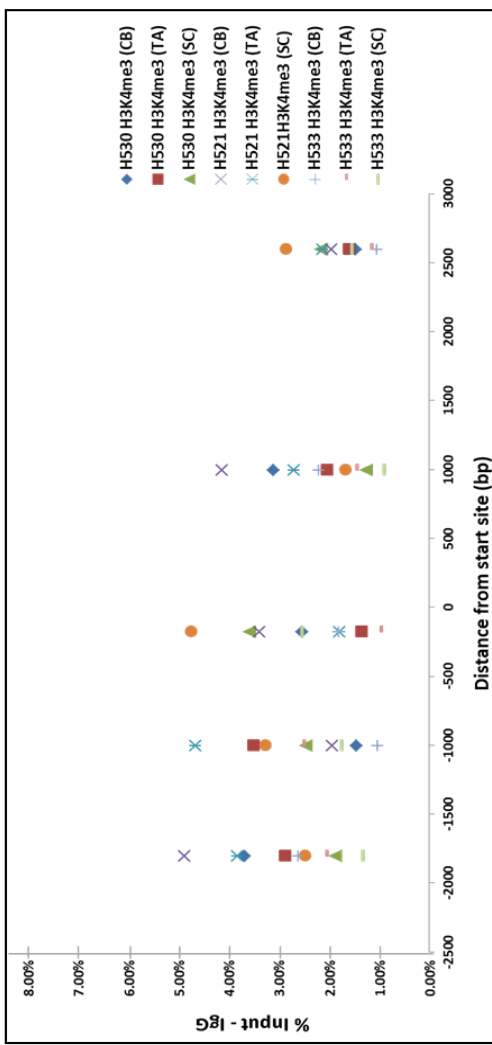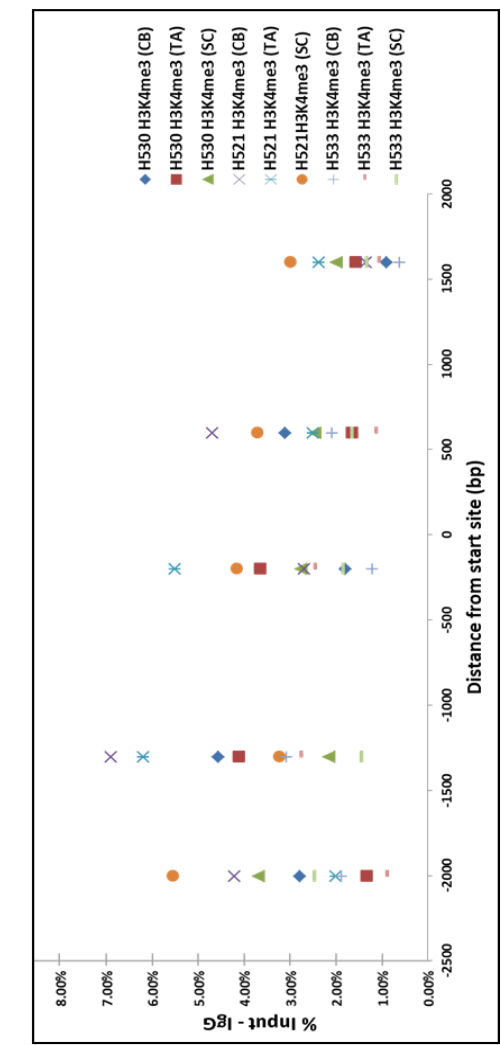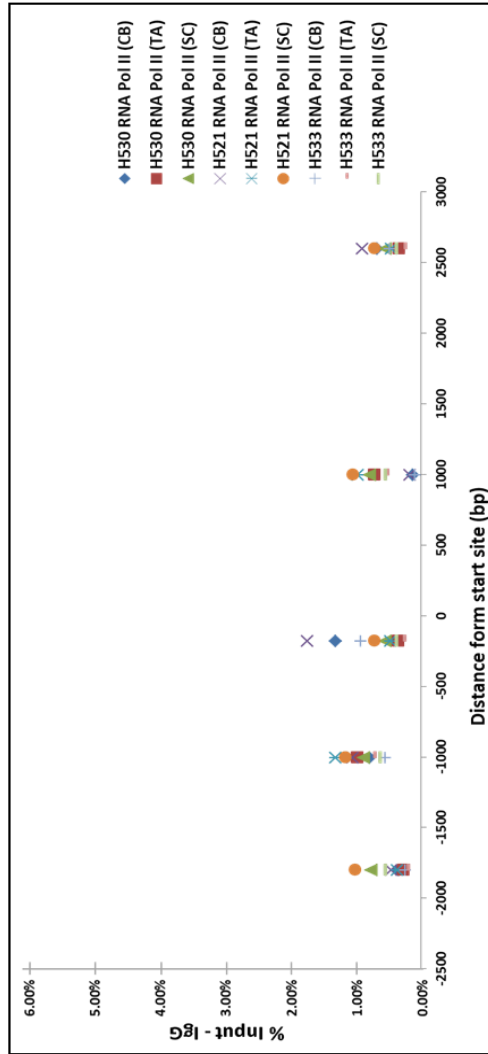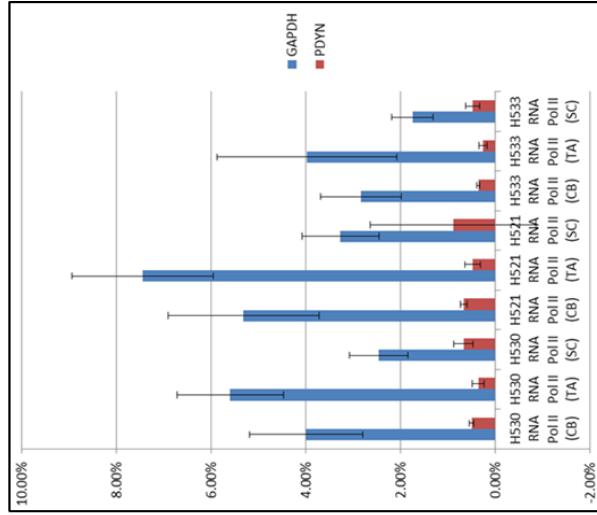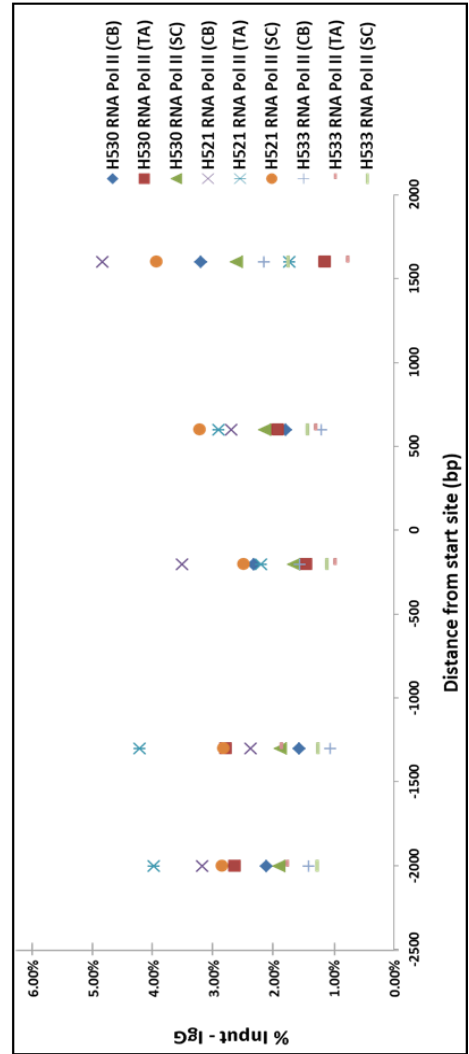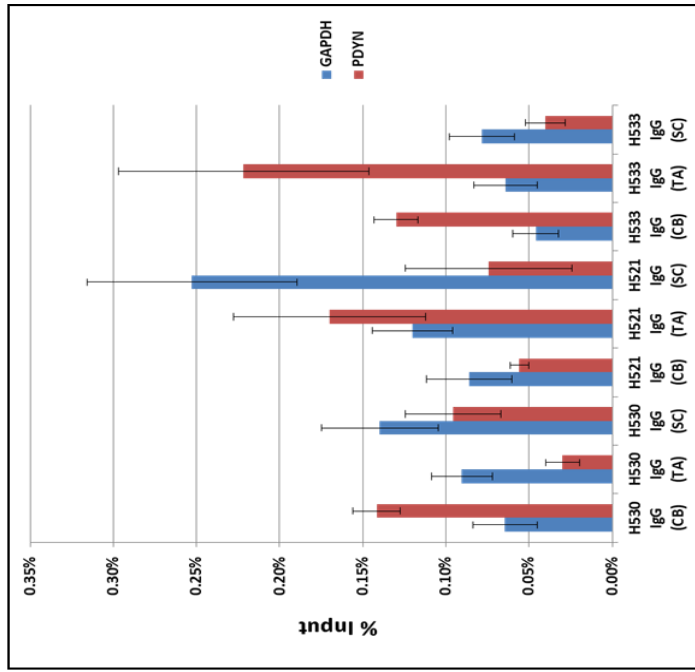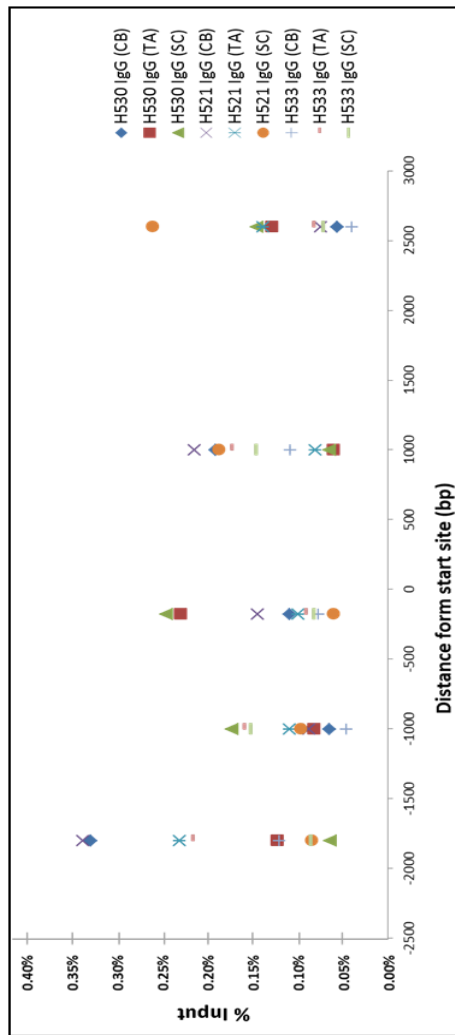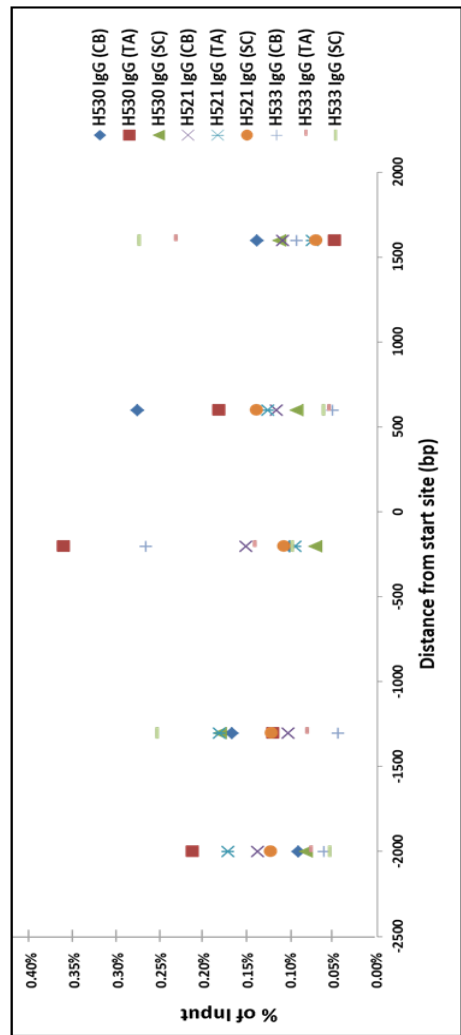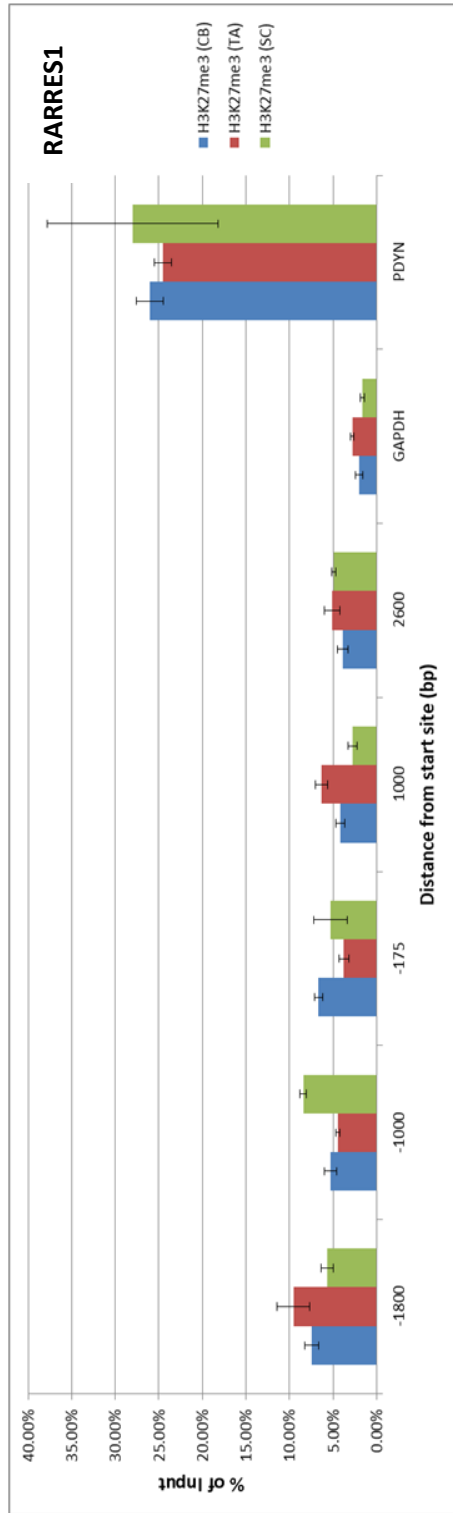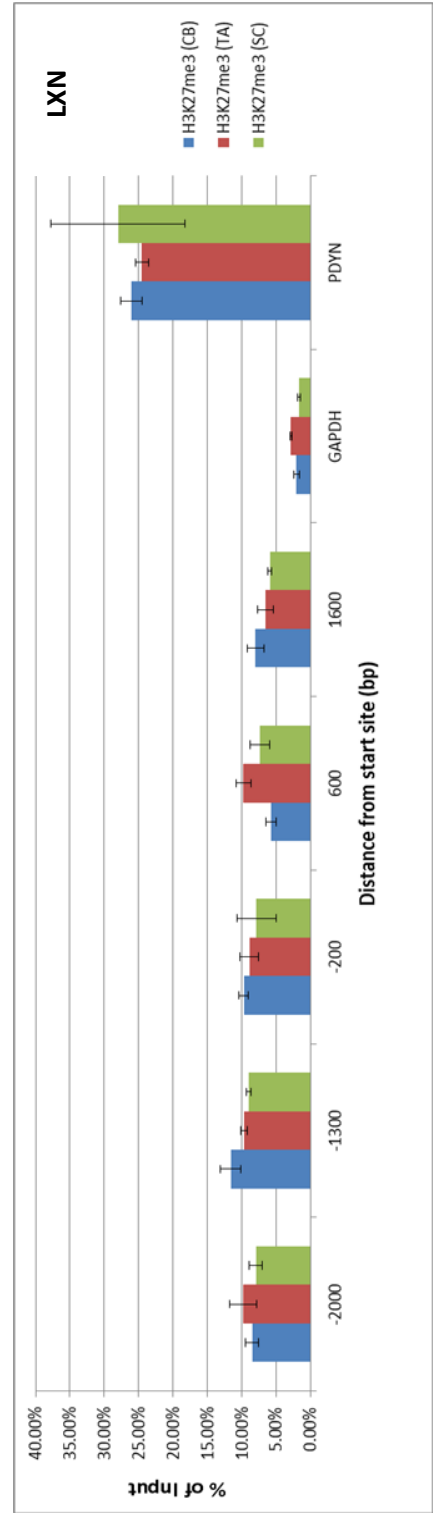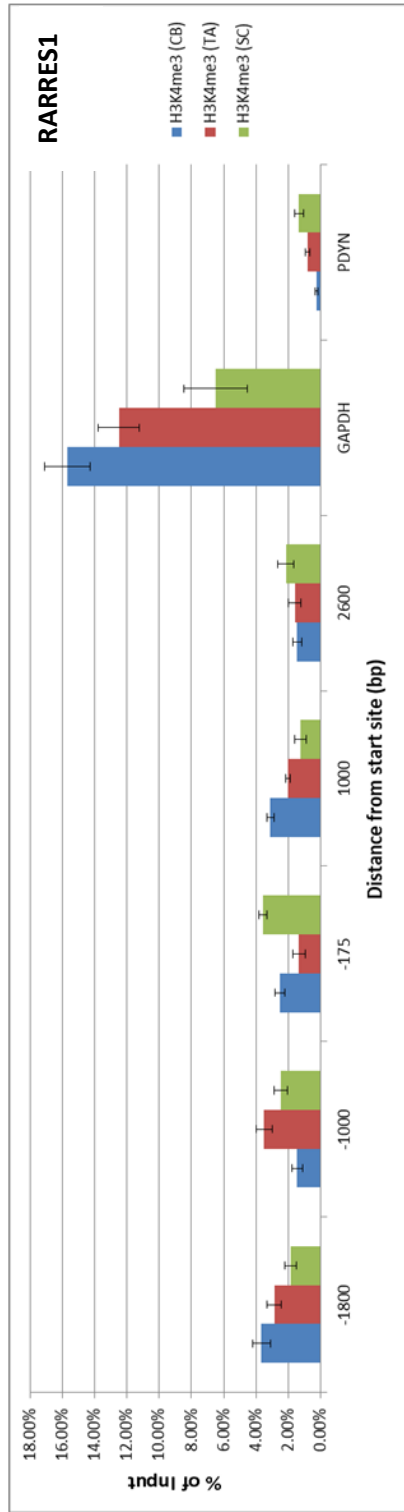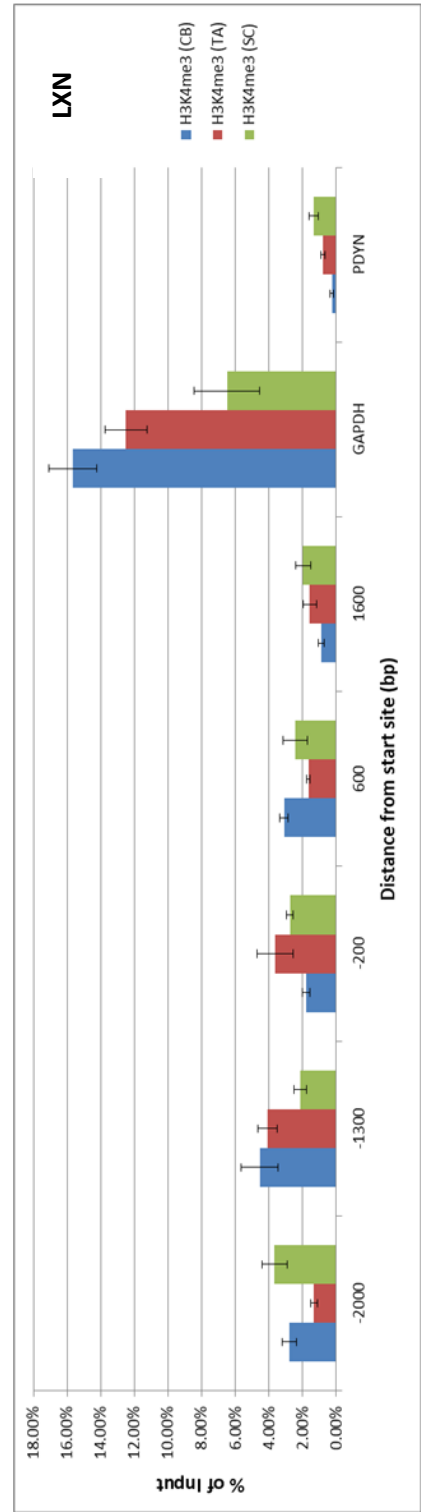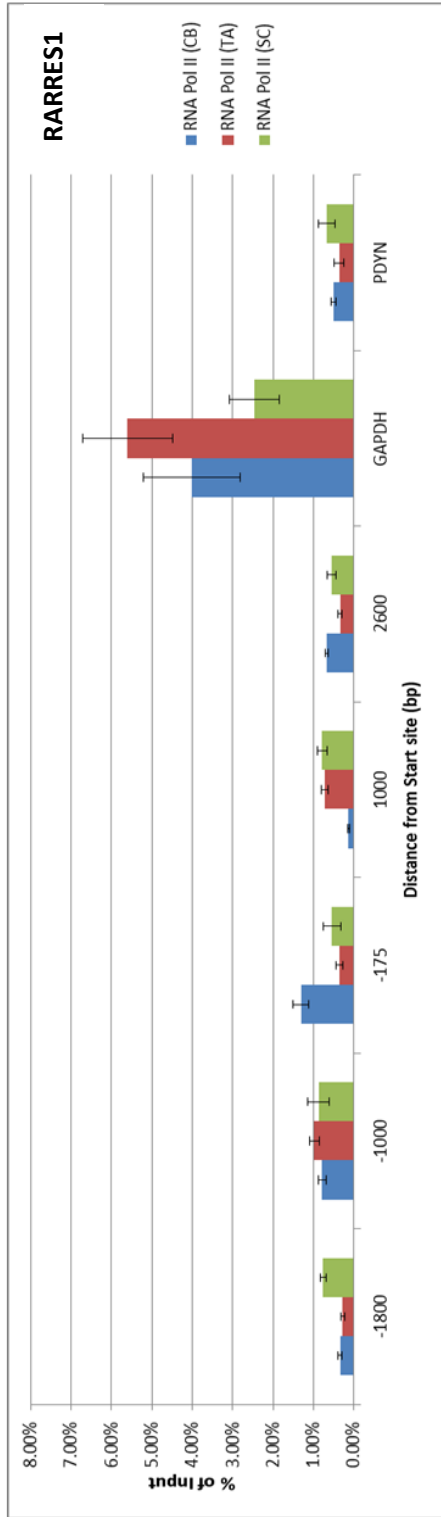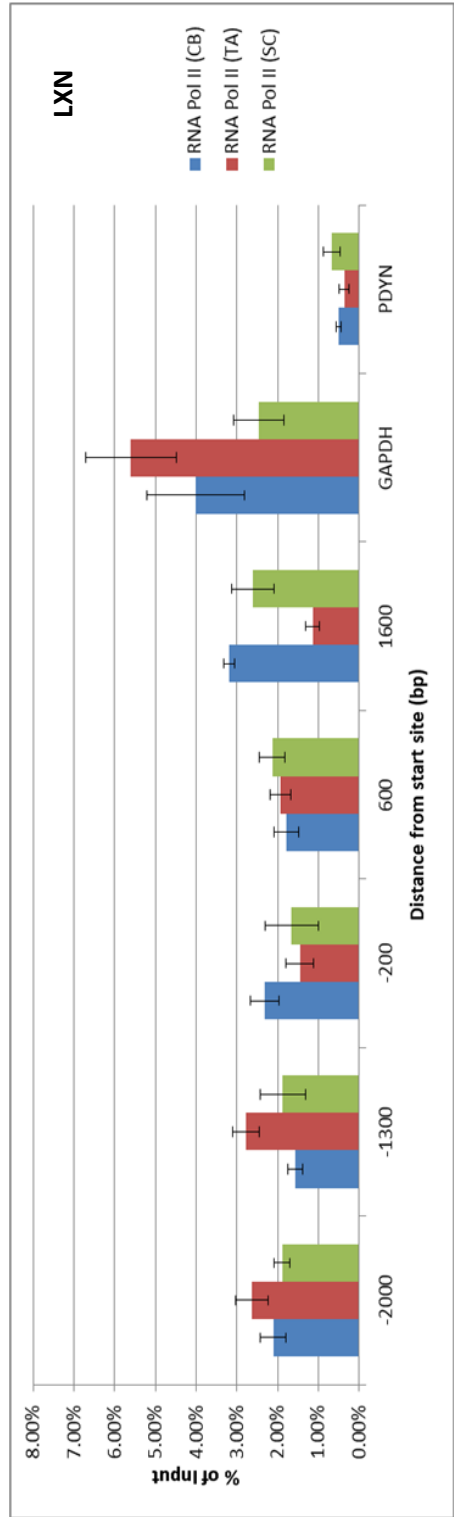
Fig. 42. μChIP of Fractionated Primary CaP Basal Cells.

Three primary CaP samples were grown to confluence in a 10cm dish in the presence of STO feeder cells. STO cells were removed with a 1 min trypsin-EDTA incubation at 37°C. Epithelial cells were then harvested and allowed to adhere to a collagen I coated 10cm dish for 20 mins. Non adherent cells are the CB fraction. Adherent cells were trypsinised once more before MACS selection using anti-CD133 for SC enrichment. Cells that were not selected as CD133$^+$ but rapidly adhered to collagen I are the TA fraction. After selection the cells were cross-linked with formaldehyde prior to cell lysis. The resulting cross-linked chromatin was sonicated on ice and the chromatin fragments were quality checked using qPCR before being immuno-precipitated with either anti- H3K27me3, H3K4me3, RNApol II or anti IgG (isotype control). After immunoprecipitation the captured DNA was eluted from the beads, extracted using phenol-chloroform and interrogated (in triplicate) using the *LXN* and *RARRES1* ChIP primers as well as control GAPDH and PDYN primers.

A. Enrichment of *RARESS1* promoter sequences by anti H3K27me3 antibody.
B. Enrichment of *LXN* promoter sequences by anti H3K27me3 antibody.
C. Enrichment of *GAPDH* and *PDYN* promoter sequences by anti H3K27me3 antibody.
D. Enrichment of *RARESS1* promoter sequences by anti H3K4me3 antibody.
E. Enrichment of *LXN* promoter sequences by anti H3K4me3 antibody.
F. Enrichment of *GAPDH* and *PDYN* promoter sequences by anti H3K4me3 antibody.
G. Enrichment of *RARESS1* promoter sequences by anti RNA pol II antibody.
H. Enrichment of *LXN* promoter sequences by anti RNA pol II antibody.
I. Enrichment of *GAPDH* and *PDYN* promoter sequences by anti RNA pol II antibody.
J. Background binding at *RARRES1* promoter sequences
K. Background binding at *LXN* promoter sequences
L. Background binding at *GAPDH* and *PDYN* promoter sequences
M. Enrichment of *RARESS1* promoter sequences by anti H3K27me3 antibody. Sample H530
N. Enrichment of *LXN* promoter sequences by anti H3K27me3 antibody. Sample H530
O. Enrichment of *RARESS1* promoter sequences by anti H3K4me3 antibody. Sample H530
P. Enrichment of *LXN* promoter sequences by anti H3K4me3 antibody Sample H530
Q. Enrichment of *RARESS1* promoter sequences by anti RNA pol II antibody Sample H530
R. Enrichment of *LXN* promoter sequences by anti RNA pol II antibody Sample H530

Error bars = 1 standard error of the mean.

The data presented is a 3 technical replicates of a single experiment.

4.8.7. Transient Transfection of Primary Prostate Epithelial Cells with Plasmid Vectors is Inefficient and Precludes Their Use

Transfection of primary samples with plasmid vectors proved inefficient (Fig. 43.) which has precluded analysis of the function of LXN and RARRES1 sequences in primary samples. Also due to the relatively quiescent phenotype of stem cells (SCs) and cancer stem cells (CSCs) plasmid vectors are not ideal for transfection of these cells, as they only transfect dividing cells. Furthermore transient transfection is not the ideal system for looking at long term effects such as a reduction in colony-forming efficiency as these assays (~2 weeks in duration) last longer than the transfection.

To overcome the deficits mentioned above LV vectors were considered the logical choice as they have previously been shown to infect prostate CSCs (Frame et al., 2010).
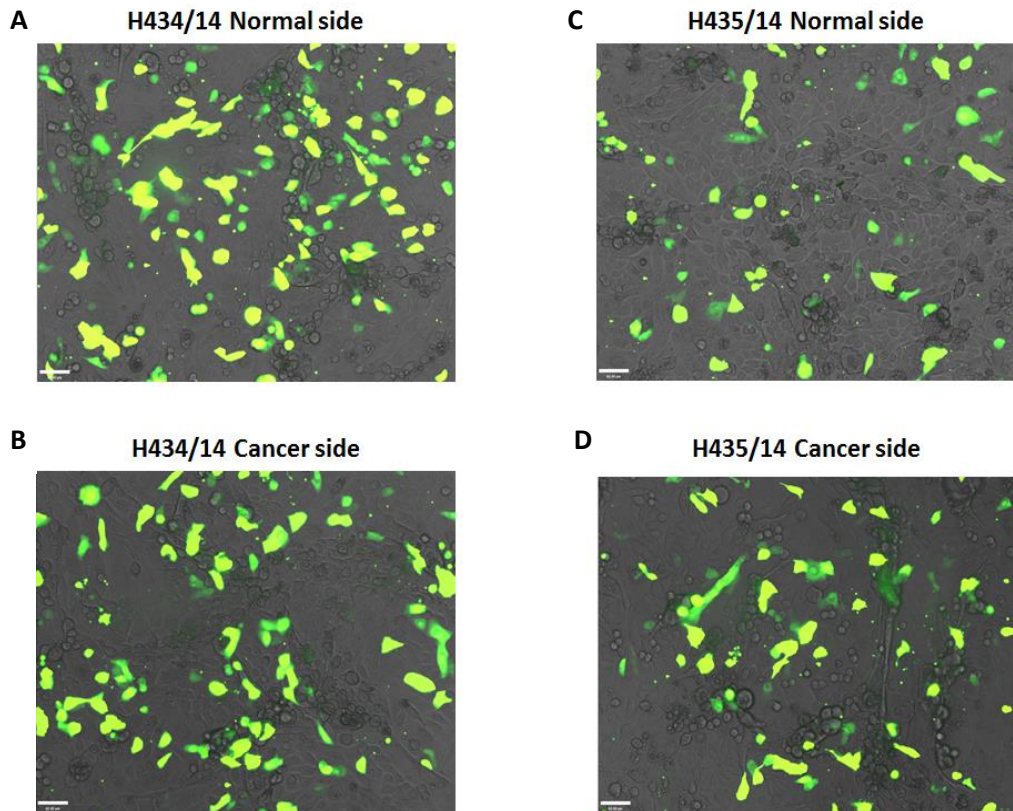
Fig. 43. Transfection of Primary Prostate Epithelial Cells.

Epithelial cultures derived from normal and malignant regions of two primary prostate biopsies were transfected with an eGFP plasmid using ViaFect transfection reagent at a ratio of 4 μl per μg of DNA. The optimal dose of ViaFect had been previously determined (data not shown). eGFP expression was determined using fluorescence microscopy 48 h post-transfection at this time all cultures were fully confluent. Representative images of forward transfection for the two samples (cells seeded overnight prior to transfection) are shown in **A.** and **B**. Representative images of reverse transfection for the two samples (seeding and transfection occur simultaneously) are shown in **C.** and **D.**.

Images were captured using a 10x objective lens.   Scale bars = 62μm

4.8.8. Lentiviral Cloning and Virus Production

A detailed example of the cloning strategy for the creation of all viral vectors is described in (Fig. 44.). Several lentiviral destination plasmids have been acquired by our group each with specific properties enabling different experiments to be performed:-

- pDest-236 (PuroR co-expression vector) – for the generation of stable cell line through puromycin selection. To this end stable cell lines derived from LNCaP, P4E6, PNT1A, DU145, BPH1 and PC3 parental lines for LXNwt, LXNcpa (corruption of CPA binding site), RARRES1wt, RARRES1cpa (corruption of CPA binding site) and RARRES1-TmDel (deletion of transmembrane domain) (total of 30 stable lines) were derived and validated (data not shown).
- pDeST-298 (eGFP co-expression vector) – for visualisation of transduction efficiency and potential Fluorescence-activated cell sorting of transduced primary cells.
- pDest-159 (mVenus (modified yellow fluorescent protein fusion generator) – for localisation experiments.
- FU-tetO-Gateway (Doxycycline inducible) could be used to investigate dose dependent and temporal effects of target proteins.

Alongside generation of lentiviral plasmid vectors, lentivirus particle generation and titre analysis was investigated using a control eGFP only lentiviral plasmid called p35. The investigation of plasmid generation also utilised cell line (LNCaP) and primary prostate epithelial cells to examine the variation of transduction efficiency in different cell types in our system, with a view to perform titrating experiments on LNCaP cells and then apply a correction factor to allow an accurate MOI in primary cells. The results of this analysis show that LNCaP cells (Fig. 45.) are more readily transduced than primary prostate epithelial cells (Fig. 46.) from the same p35 lentivirus batch (1.45×10^8 IU/ml in LNCaP cells vs 2.02×10^7 IU/ml in primary prostate epithelial cells). Also the importance of performing a titration to determine lentivirus titre was also confirmed i.e. a 1:1 ratio of viral supernatant and culture media yielded a titre of 4.9×10^5 IU/ml whilst a 1:10000 ratio of viral supernatant and culture media yielded a titre of 1.45×10^8 IU/ml in LNCaP cells. This discrepancy is due to multiple viral vectors entering a single cell in the less-dilute viral supernatant. When the viral supernatant is more diluted a single viral vector enters a single cell and an accurate titre can be determined.
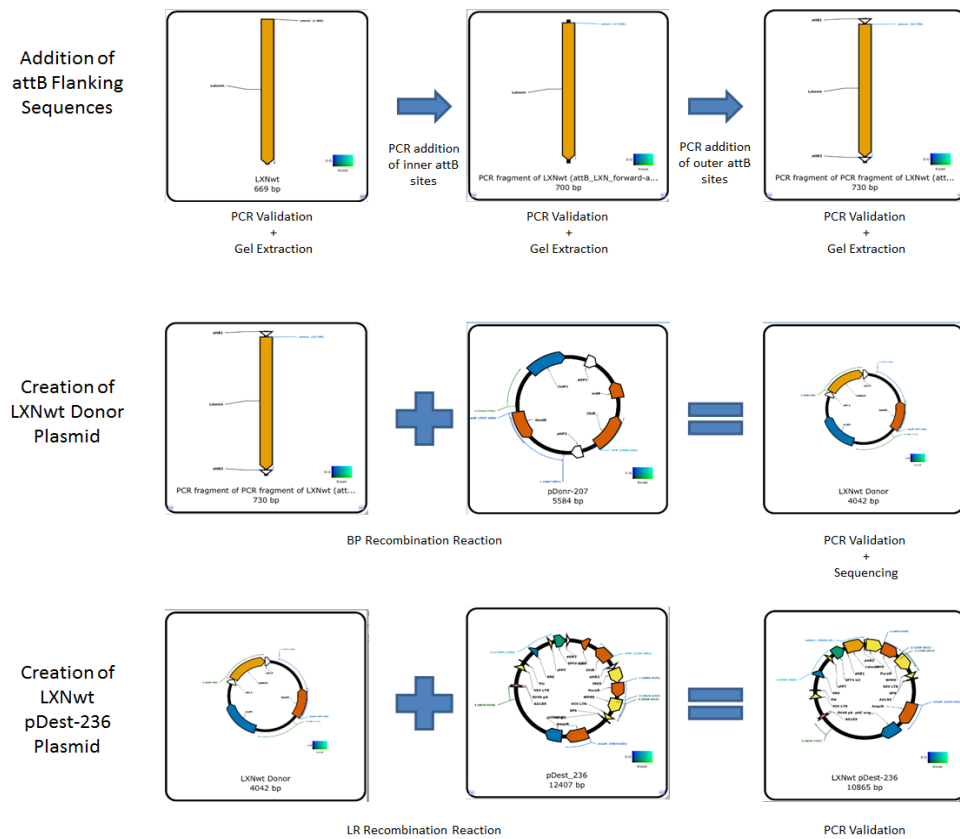
Fig. 44. Detailed Example of Cloning Strategy used to Generate LXNwt Destination Vectors.

Detailed steps of cloning strategy including generation of attb flanked target sequence (LXN), Gateway™ cloning to produce the Donor (shuttle) plasmid which is then sequenced and used to generate the lentiviral plasmids which are then validated for presence of the insert by PCR and expression of the target gene by RT-PCR and western blot analysis.

PlasmaDNA software was used to produce this cloning strategy.
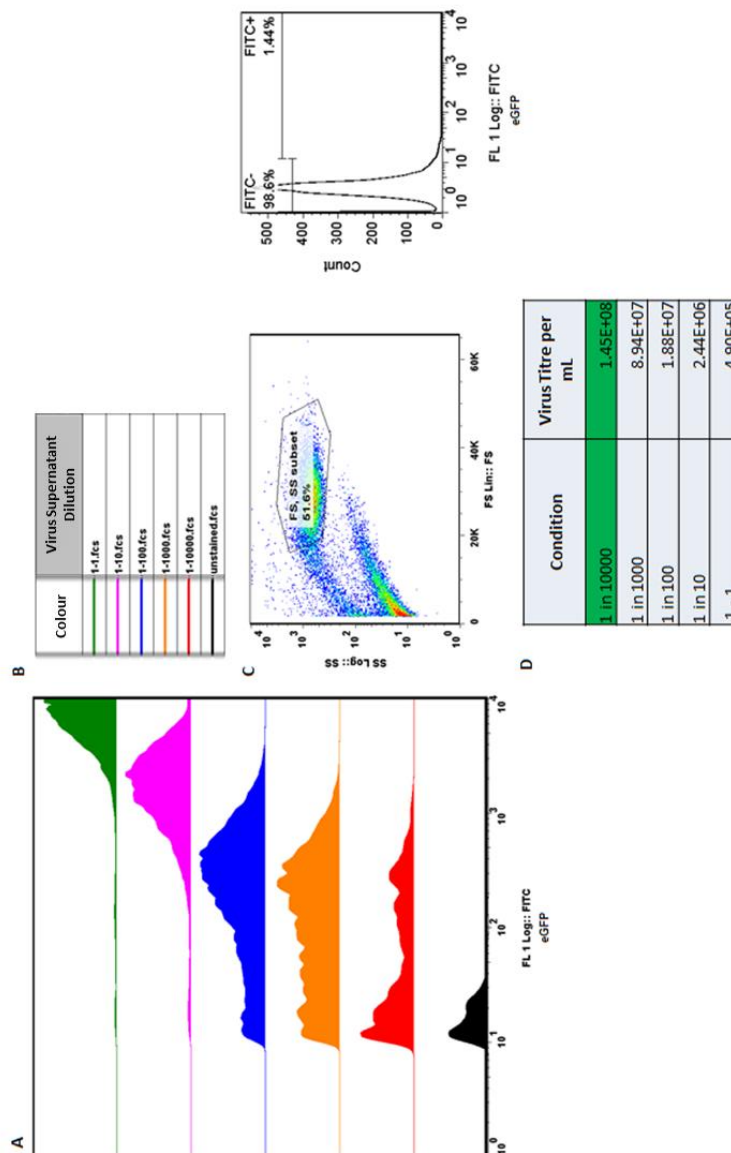
Fig. 45. Assessment of Lentiviral Titre.

HEK-293 cells were co-transfected with 3 μg of psPAX2, 1 μg of pVSV-G and 4μg of an eGFP-lentivirus plasmid. The ratio of 3:1:4 was previously identified as optimal for virus yield (data not shown). The viruses were harvested 48h post-transfection, filtered through a 0.45micron syringe filter and frozen at -80°C. $5x10^4$ LNCaP cells were seeded in 500 μl of media or media containing virus solution at various concentrations, in a 24 well plate. The cells were allowed to adhere overnight before the media was replaced. eGFP expression was determined by flow-cytometry 48 h post-transduction. **A.** sample colour key is shown in **B**. The gating strategy is show in **C.** and the calculated virus tire is shown in **D.**
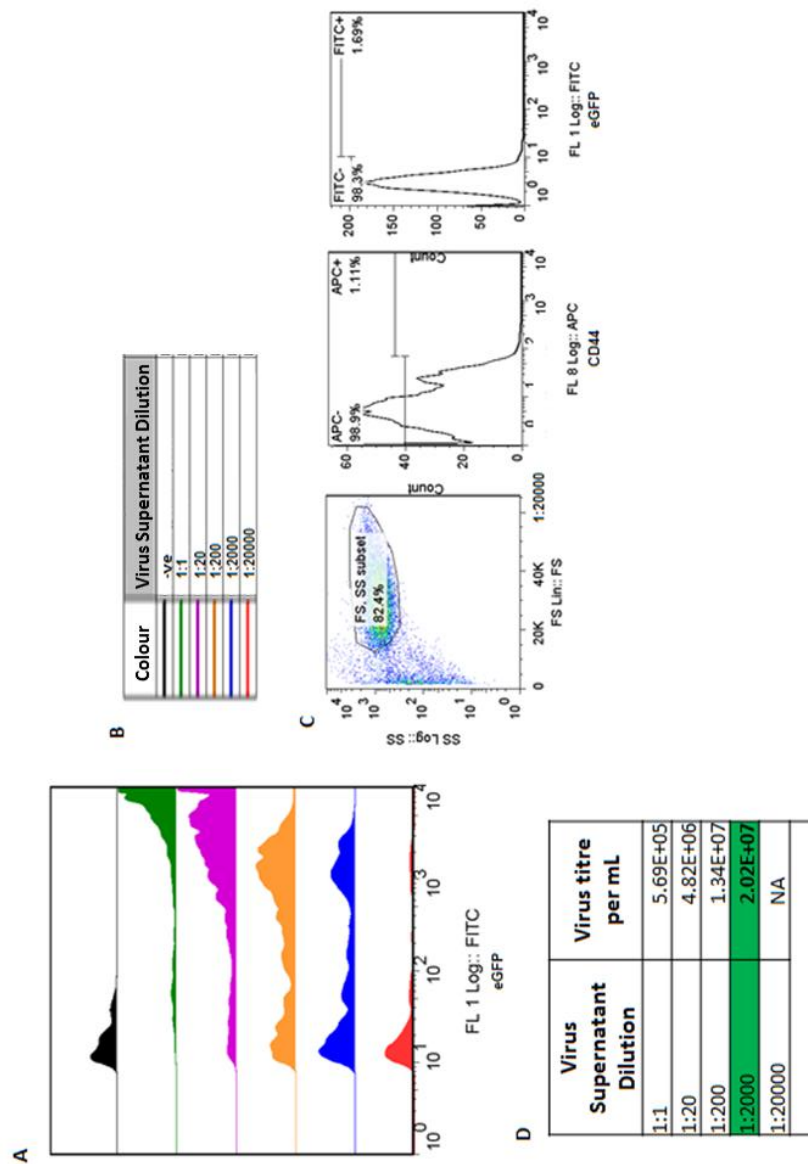
Fig. 46. Transduction of CD44+ Primary Prostate Epithelial Cells.

HEK-293 cells were co-transfected with 3µg of psPAX2, 1µg of pVSV-G and 4µg of an eGFP lentivirus plasmid. The ratio of 3:1:4 was previously identified as optimal for virus yield (data not shown). The viruses were harvested 48h post-transfection, filtered through a 0.45micron syringe filter and frozen at -80°C. 6x10⁴Primary Prostate Epithelial Cells were seeded in 500µl of media or media containing virus solution at various concentrations, in a 48 well plate. The cells were allowed to adhere overnight before the media was replaced. eGFP expression was determined by flow-cytometry 48h post-transduction prior to labelling (in the APC channel) the cells with anti-CD44+. **A.** sample colour key is shown in **B.** The gating strategy is shown in **C.** and the calculated virus tire for CD44+ cells is shown in **D.**

4.8.9. Optimisation of Lentivirus Titres

Unfortunately the pDEST-298 (eGFP co-expressing vector) produced much lower viral titres than the control p35 plasmid (rarely exceeding 1×10^6 IU/ml in LNCaP cells (data not shown). As such further optimisation of lentivirus production was needed. In order to optimise lentivirus production an investigation of several parameters was conducted. The parameters investigated were two types of transfection reagent: ViaFect and Xtremegene, pre-coating the culture surface with Poly-L-lysine and supplementing the virus production medium with 4 mM caffeine. The reasons for choosing these conditions are as follows:

- The transfection reagent was chosen because the efficiency of transfection directly impacts on virus production. ViaFect and Xtremegene have been shown to be the most potent transfection reagents on HEK 293 cells in our lab (data not shown).

- Coating the culture surfaces with Poly-L-lysine was investigated. It has previously been demonstrated in our lab that some cell lines have a greater transfection efficiency when cultured on Poly-L-lysine e.g. LNCaP cells (data not shown). Also disturbing the monolayer of HEK 293 cells during virus production, causing it to detach, has a negative impact on HEK 293 cell survival and consequently virus production. Coating the culture surfaces with Poly-L-lysine reduces this possibility.

An interesting publication demonstrated that lentiviral titres could be increased 4-fold with the addition of 4 mM caffeine to the virus production media (Ellis et al., 2011). The proposed mechanism by which caffeine increases viral titre is in part attributed to inhibition of DNA-dependent protein kinase catalytic subunit (DNA-PKcs). The results indicate (Fig. 47.) that the optimum lentivirus production protocol consists of; coating the culture surface with Poly-L-lysine, transfecting with ViaFect and omitting caffeine from the viral production media. Also, functional lentiviruses can be sequentially harvested for at least three days post transfection, but the virus titre decreases ~2 fold each day. Also the best time to harvest virus was 24 hours post-transfection of packaging cells although 48 hours post-transfection still yielded usable virus.

Caffine vs Transfection Reagent vs Poly-L-Lysine
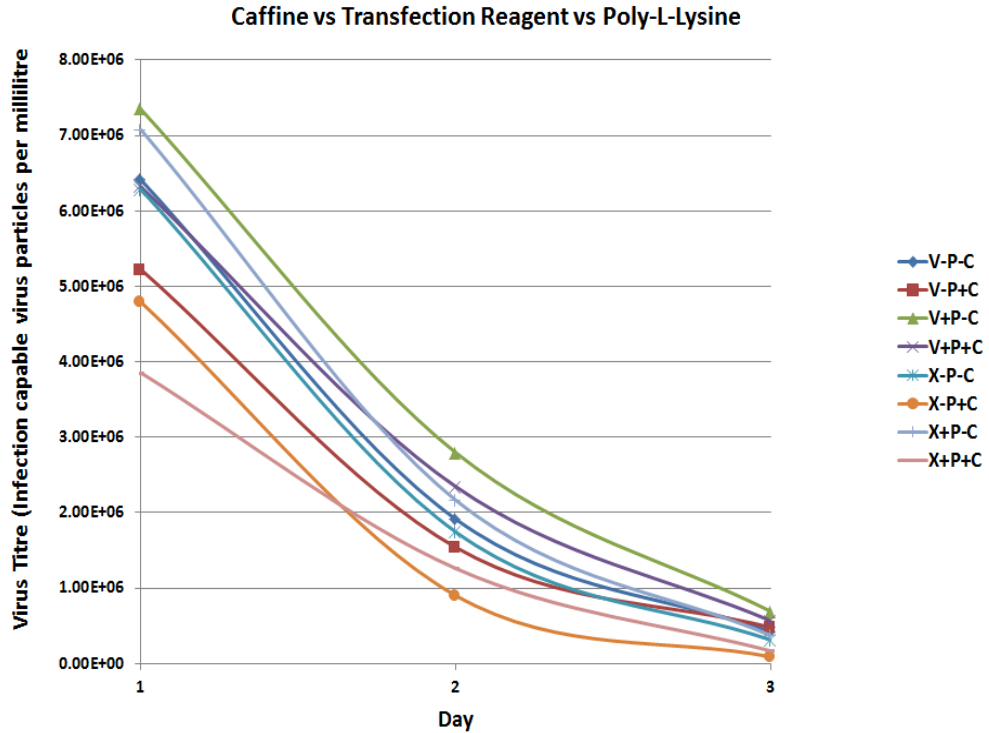
Fig. 47. Optimisation of Lentivirus Titres.

V = Viafect, X = Xtremegene, P = Poly-L-Lysine, C = Caffeine

e.g. V-P-C = Viafect reagent used to transfect cells in the absence of both Poly-L-Lysine and caffeine.

HEK 293 cells were seeded at a density of $2x10^5$ cells per well of a 24 well plate. Culture surfaces were either pre-coated with Poly-L-Lysine or not. The cells were allowed to adhere overnight. 2 hours before transfection the media was changed and either supplemented with 4 mM caffeine or not. Transfection was performed using either Viafect or Xtremegene at a ratio of 2:1 (µl of transection reagent: µg of plasmid DNA) and transfection was allowed to proceed for 8 hours before media was changed (+/- 4 mM caffeine). Lentiviruses were harvested 24, 48 and 72 hours after completion of transfection. Lentiviruses were harvested by aspirating the virus containing media from the HEK 293 cells, filtering and freezing. The media was replaced +/- 4 mM caffeine.

Viral titres were determined by performing serial dilutions ranging from neat to 1:1000 these dilutions were then used to transduce HEK 293 cells. 48 hours after transduction cells were harvested and were analysed by flow cytometry (incorporating live dead staining).

Titre/ml = (number of cells seeded at the time of transduction x % live cells positive x dilution factor) / transduction volume (ml).

4.8.10. Transduction with Lentivirus Results in Stable Transgene Expression in Primary Human Prostate Epithelial Cells.

A demonstration of stable transduction was needed to ensure that cells remained expressing the transgene of interest throughout long term experiments.

Early passage primary human epithelial cells were transduced with lentiviruses at a ratio of 2 virus particles per cell and maintained in culture for 3x 1:5 passages which lasted approximately 4 weeks. The images (Fig. 48.) demonstrate that the vast majority of colonies remained strongly positive for the presence of the transgene without any observable loss after 3 passages in culture.
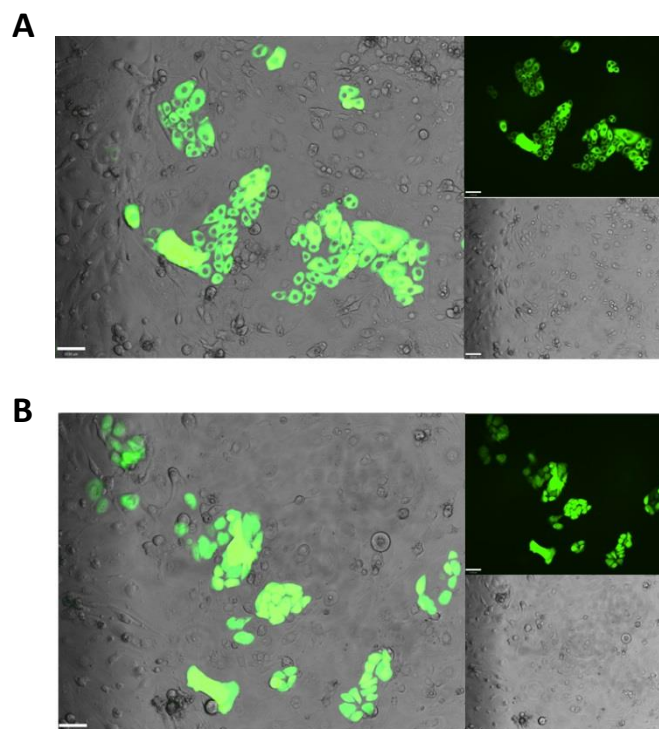
Fig. 48. Transduction with Lentivirus Results in Stable Transgene Expression in Primary Human Prostate Epithelial Cells.

Passage 1 primary human epithelial cells were transduced with lentiviruses at a ratio of 2 viral particles per cell and maintained in culture for three 1:5 passages in the presence of feeder cells (STO cells) which lasted approximately 4 weeks.

A. Transduction with β-glucuronidase (GUS)-159 (GUS-mVenus fusion)

B. Transduction with LXN-159 (LXN-mVenus fusion)

For both **A.** and **B.**, the main-panel is the composite of the upper-right (Fluorescent image) and lower-right panels (Bright-field image).

Images were captured using a 10x objective lens.   Scale bars = 62 μm

4.8.11. LXN is a Soluble Pan-cellular Protein

The subcellular localisation of LXN is a topic of some debate. Our laboratory has previously demonstrated for the first time that LXN has an almost exclusively nuclear localisation pattern in prostate cell lines (Oldridge et al., 2013).

In order to circumvent fixation artefacts, live cell confocal imaging utilising LXN-mVenus and β-glucuronidase (GUS)-mVenus (cytoplasmic control) protein-fusion lentiviral expression vectors was performed using primary human prostate epithelial cells (Fig. 49A.). Under these conditions LXN-mVenus fusion protein is present in both the nucleus and cytoplasm in these cells. This is in contrast to the GUS-mVenus fusion protein which is exclusively cytoplasmic. Similar results were obtained for several cell lines (data not shown).

The live cell imaging data using LXN-mVenus fusion agrees with that of endogenous LXN detected using two different antibodies (Fig. 49B.) in terms of LXN being able to access the nucleus. However, this data is in contrast to that produced when prostate epithelial cells are subcellular fractionated and analysed by western blot (Fig. 49C.). This discrepancy is explained by the solubility of nuclear LXN which leaches out of the nucleus during the first stage of subcellular fractionation which is disrupting the plasma membrane with hypotonic buffer (which causes cells to burst due to osmosis) (Fig. 50.). This rapid leaching from the nuclear compartment indicates that LXN is not tethered to either DNA or the nuclear matrix and is a reported issue in the literature for other soluble nuclear proteins (Stern and Mirsky, 1953).
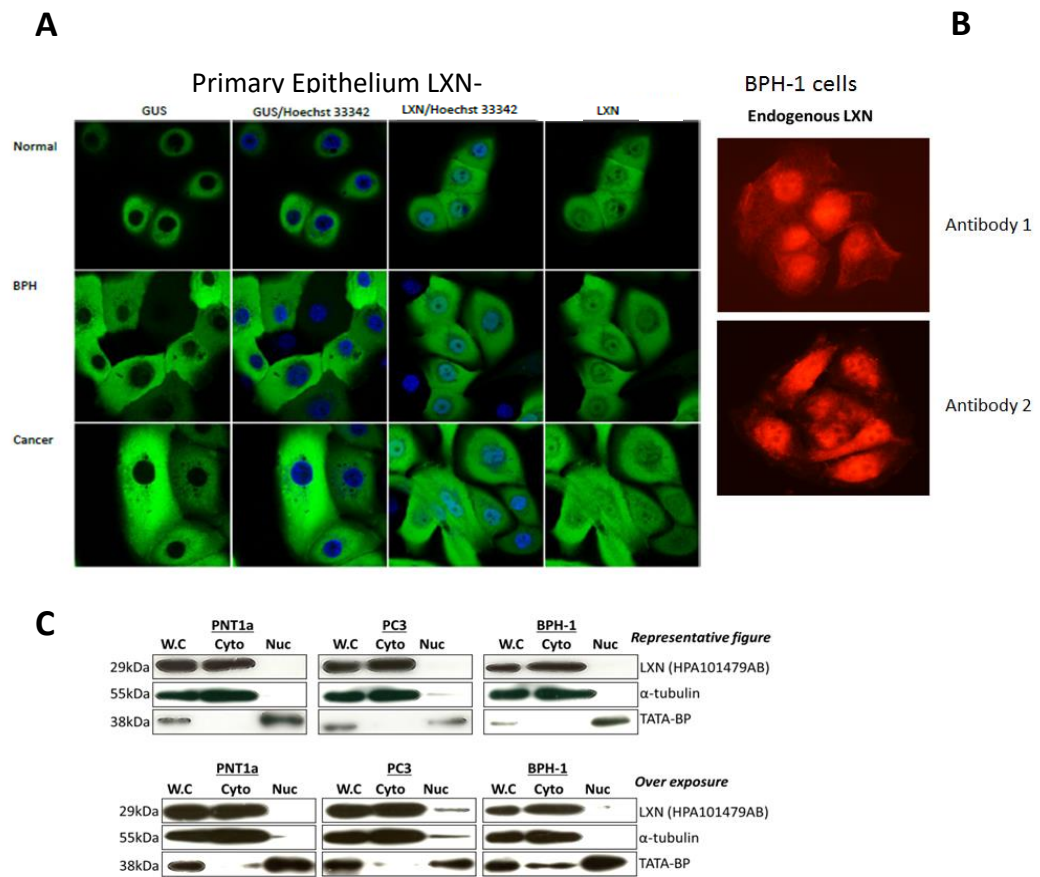
Fig. 49. LXN is a Soluble Pan-Cellular Protein.

A. Live cell confocal microscopy of primary human epithelial cells transduced with LXN-mVenus fusion lentiviral vector compared with that of the cytoplasmic GUS-mVenus fusion lentiviral vector. Cells were counter stained with Hoechst 33342. Images were taken using a 60x objective lens.

B. Immunofluorescence imaging of BPH-1 cell probed endogenous LXN using two separate antibodies. Images were taken using a 40x objective lens.

C. Western blot of whole cell, cytoplasmic and nuclear fractions of several cell lines. Blots were probed for endogenous LXN, and incorporate α tubulin as a cytoplasmic marker and TATA-binding protein (TATA-BP) as a nuclear marker. Over exposed images are also included.

Data generation was in part aided by Evangelia E. Kounatidou.
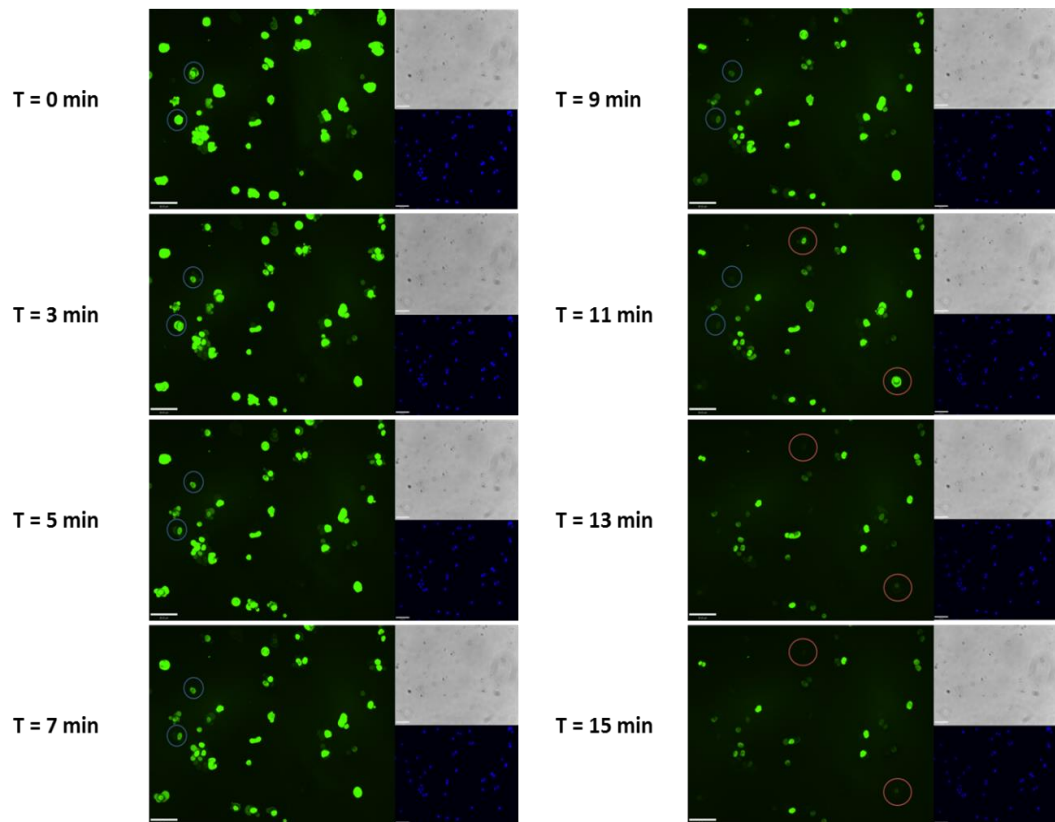
Fig. 50. LXN Leaches out of the Nuclear Compartment During Subcellular Fractionation.

Time lapse fluorescent imaging of primary human epithelial cells transduced with LXN-mVenus fusion lentiviral vector incubated hypertonic buffer on a microscope slide to mimic the first stage of subcellular fractionation cells were counter stained with Hoechst 33342.

Main sub-panel of each panel is fluorescent imaging of LXN-mVenus top right sub-panel of each panel is brightfield and bottom right sub-panel of each panel is fluorescent imaging of Hoechst 33342.

Coloured circles highlight leaching from nucleus.

Time is expressed in minutes and all images were taken using a 10x objective lens.

Scale bar = 90 µm

4.8.12. Generation of an Interactome for LXN-HA and RARRES1-HA in PC3 Cells

This section of the report represents collaboration between myself and Robert Seed, and it must be stated that Robert Seed was the experimental lead on this project and the majority of the work described was performed by him. It is included in this report to provide further rational for investigating potential transcriptome changes induced by forced overexpression of LXN and RARRES1 in primary prostate epithelial cells. A further reason for the inclusion of this data is that I was the sole performer of the attempt to validate the RARRES1 interactome by IP with downstream analysis by western blot.

The experimental approach for analysing potential binding partners of LXN and RARRES1 utilised the HA tag vectors described and validated in section 5.2.1. This approach was taken as the anti-HA antibody is well characterised for IP unlike the anti-LXN and anti-RARRES1 antibodies. Other important methodological features include:

- Pre-clearing of the cell-lysate with anti-keratin conjugated sepharose beads to reduce these common contaminating proteins as well as nonspecific interactions between proteins and the beads themselves.
- Directly conjugated anti-HA beads obtained and validated by the supplier (Sigma).
- The control IP reaction to which 'hits' were compared was decided experimentally to be mock transfected PC3 cells. This was chosen over eGFP-HA transfection as in these cells eGFP-HA was expressed many-fold greater than either LXN-HA or RARRES1-HA. As such eGFP-HA had many non-specific interactions which would lead to the inappropriate exclusion of true interactors of RARRES1 and LXN.
- Before liquid chromatography–mass spectrometry (LC-MS) the immunoprecipitated proteins were run on a full length polyacrylamide gel which was subsequently dissected into small fragments and digested with trypsin.
- A validation sodium dodecyl sulphate polyacrylamide gel electrophoresis (SDS-PAGE) gel for each IP was performed, which allowed visualisation of the bait by coomasie staining. 10% of immunoprecipitated fractions were used for this analysis. An example of this analysis is shown for LXN in (Fig. 51.).
- Analysis of the interactome for both proteins was augmented by eliminating common 'sticky' proteins by use of the contaminant repository for affinity

purification–mass spectrometry database (the CRAPome) (Mellacheruvu et al., 2013).

- At least three IP reactions with PC3 cells transfected with the target-HA vector and at least three mock transfected control IP reactions were generated and validated before being analysed by LC-MS. Hits were then analysed for the frequency of detection in mock and target IPs as well as spectral counts observed.

The results of these analyses for LXN and RARRES1 interactomes are shown in (Fig. 52A. and B.), respectively. An important finding of this series of experiments is that unique interactors of LXN are present within the nucleus (cyclin-dependent kinase 12, zinc finger and BTB domain-containing protein 4, Smith-Magenis syndrome chromosomal region candidate gene 8 protein, Transcription factor IIIB 90 kDa subunit and Zinc finger protein 583) which indicates that LXN may indirectly modulate transcription. The pan-cellular profile of LXN localisation is also corroborated by the aforementioned nuclear hits, cytoplasmic hits (calcium binding protein 39 and O60930-Ribonuclease H1) and Abnormal spindle like microcephaly-associated protein which has been shown to be located to the nucleus and cytoplasm. However, it must be noted that the spectral count of LXN is many-fold greater than that of the potential interactors.

The RARRES1 'hit-list' is enriched for proteins resident to the endoplasmic reticulum membrane (the published location of RARRES1 in prostate cells (Oldridge, 2012). These potential interactors include; Aspartyl/asparaginyl beta-hydroxylase, Dolichyl-diphosphooligosaccharide--protein glycosyltransferase 48 kDa subunits, Mannosyl-oligosaccharide glucosidase and Neuropathy target esterase. Perhaps surprisingly Importin-7 (IPO7), which is reported to be resident in the nucleus and cytoplasm, was the most abundant unique hit. This indicates that RARRES1, similarly to LXN, has the potential to indirectly affect transcription.
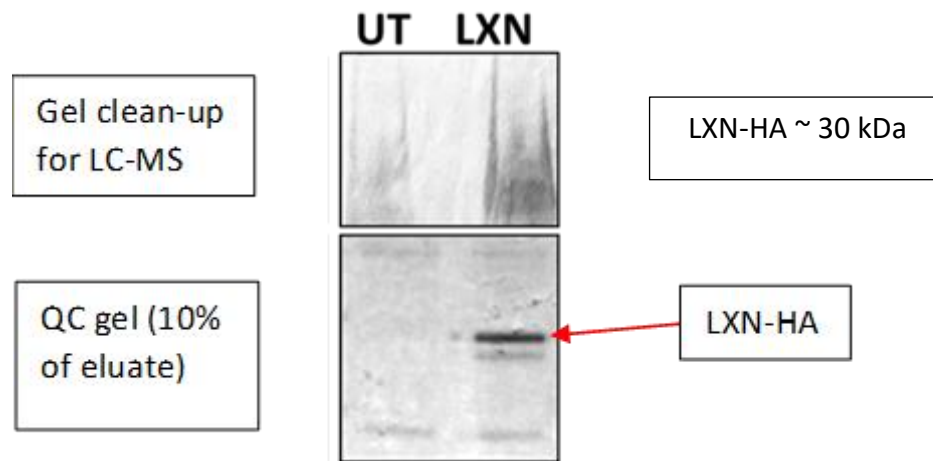
Fig. 51. Example of a Gel Clean-Up of Eluate Prior to LC-MS and Diagnostic Gel Validation Successful Bait IP.

Mock-transfected (UT) and LXN-HA transfected (LXN) PC3 cells were lysed with RIPA and precleared with anti-keratin conjugated sepharose beads were immunoprecipitated with anti-HA conjugated sepharose beads. The resulting precipitation was washed 5x with high salt RIPA (300 mM NaCl) to remove non-specific binding proteins. Interacting proteins were eluted with Laemmli sample buffer under reducing conditions. The resulting eluate was run on a polyacrylamide gel, which was subsequently dissected and trypsinised before being analysed by LC-MS. Before proceeding to LC-MS a quality control (QC) gel was made containing 10% of the eluate which was stained with coomasie to allow visualisation of the bait (LXN-HA) and hence validation of the IP.

A

Protein	UT count	RARRES1 count	LXN only (>2 vs n=0)	Average spectral count	GO: cellular localisation
Latexin	0	4	LXN only	133.0	
Cyclin dependent kinase 12	0	4	LXN only	2.0	Nucleus
Zinc finger and BTB domain containing protein 4	0	4	LXN only	6.0	Nucleus
Smith-Magenis syndrome chromosomal region candidate gene 8 protein	0	4	LXN only	3.0	Nucleus
Coiled-coil domain-cotaining protein 112	0	4	LXN only	8.5	-
Transcription factor IIIB 90 kDa subunit	0	4	LXN only	2.0	Nucleus
Abnormal spindle-like microcephaly-associated protein	0	3	LXN only	1.0	Cytoplasm & Nucleus
Zinc finger protein 583	0	3	LXN only	1.6	Nucleus
Calcium-binding protein 39	0	3	LXN only	1.8	Cytoplasm
O6O93O- Ribonuclease H1	0	3	LXN only	1.8	Cytoplasm

B

Protein	UT count	RARRES1 count	RARRES1 only (>2 vs n=0)	Average spectral count	GO: cellular localisation
Retinoic acid receptor responder protein 1- P49788	0	3	RARRES1 only	14	Membrane, extracellular exosome
Aspartyl/asparaginyl beta-hydroxylase - Q12797	0	3	RARRES1 only	2	Endoplasmic reticulum membrane
Calcium-binding mitochondrial carrier protein Aralar2 - Q9UJS0	0	3	RARRES1 only	6	Mitochondrion inner membrane
Dolichyl-diphosphooligosaccharide--protein glycosyltransferase 48 kDa subunit- P39656	0	3	RARRES1 only	2	Endoplasmic reticulum membrane
Exocyst complex component 8- Q8IYI6	0	3	RARRES1 only	1	Cytoplasm
Extracellular sulfatase Sulf-2 - Q8IWU5	0	3	RARRES1 only	7	Endoplasmic reticulum/Extracellular space
General transcription factor II-I - P78347	0	3	RARRES1 only	2	Cytoplasm & Nucleus
Importin-7 - O95373	0	3	RARRES1 only	10	Cytoplasm and nucleus
Mannosyl-oligosaccharide glucosidase - Q13724	0	3	RARRES1 only	2	Endoplasmic reticulum membrane
Neuropathy target esterase - Q8IY17	0	3	RARRES1 only	3	Endoplasmic reticulum membrane
Trifunctional enzyme subunit beta- P55084	0	3	RARRES1 only	5	Endoplasmic reticulum, mitochondrion inner membrane

Fig. 52. LXN (A) and RARESS1 (B) Potential Interactors.

$2x10^6$ PC3 cells transfected with either LXN-HA, RARRES1, or mock transfected were lysed with RIPA and precleared with anti-keratin conjugated sepharose beads were immunoprecipitated with anti-HA conjugated sepharose beads. The resulting precipitation was washed 5x with high salt RIPA (300 mM NaCl) to remove non-specific binding proteins. Interacting proteins were eluted with Laemmli sample buffer under reducing conditions. The resulting eluate was run on a polyacrylamide gel, which was subsequently dissected and trypsinised before being analysed by LC-MS. Common 'sticky' proteins were eliminated from the hit-list by comparison to the CRAPome database.

4.8.13. Unsuccessful Attempt to Validated RARRES1 Interactome Through Co-IP of Importin 7 in PC3 Cells Transfected with RARRES1-HA Plasmid and Subsequent Immunoprecipitation Using anti-HA Antibody.

In an attempt to validate the RARRES1 interactome generated in section 4.8.12, co-immunoprecipitation (Co-IP) experiments were performed with downstream analysis by western blot. $2x10^6$ PC3 cells transfected with, RARRES1, or mock transfected were lysed with RIPA and precleared with anti-keratin conjugated sepharose beads. The IP was performed using anti-HA conjugated sepharose beads.

From (Fig. 53.) it can be seen that the IP has been successful (large band corresponding to RARRES1-HA in the elution from the +ve but not the control. The IPO7 antibody successfully detects a band of approximate molecular weight of IPO7 (120 kDa) in the input and the flow through. However, there is no IPO7 detection in the eluate of the RARRES1-HA transfect sample. Therefore the interaction between RARRES1 and IPO7 has not been validated. It should be noted that the lack of RARRES1 detection in the input lane was due to the RARRES1 antibody having low affinity.

Further experimentation to validate the potential RARRES1-IPO7 interaction could be to perform a yeast two-hybrid assay (Brückner et al., 2009). This assay relies on the generation of two plasmid constructs: construct one would contain RARRES1 fused to the binding domain of the transcription factor. Construct two would contain IPO7 fused to the activation domain of the transcription factor. If RARRES1 and IPO7 interact then the binding domain and activation domain would be in close enough proximity to allow transcription of the reporter gene e.g. *LacZ*.

A further experiment that would allow investigation of a potential interaction in a prostate model would be to conduct a proximity ligation assay (Weibrecht et al., 2010). This assay utilises antibodies specific to each protein of the potential interaction in this case one antibody specific to RARRES1 and another that is specific to IPO7. The two antibodies are pre-conjugated to oligonucleotides that can participate in rolling circle DNA synthesis. If the two proteins interact or form part of a protein complex then the two oligonucleotides are positioned close enough for rolling circle DNA synthesis to occur (upon addition of polymerase). The resulting DNA synthesis can be visualised by utilising complimentary fluorescent oligonucleotide probes and downstream fluorescent microscopy.
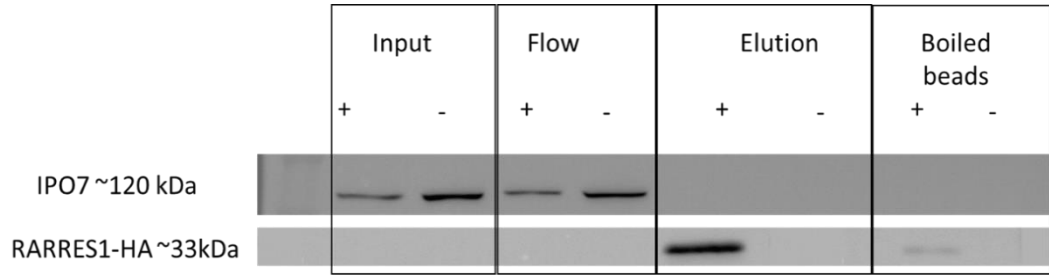
Fig. 53. IPO7 – RARRES1-HA Co-IP.

Representative image of 3 experiments.

$2x10^6$ PC3 cells transfected with, RARRES1, or mock transfected were lysed with RIPA and precleared with anti-keratin conjugated sepharose beads were immunoprecipitated with anti-HA conjugated sepharose beads. The resulting precipitation was washed 5x with high salt RIPA (300 mM NaCl) to remove non-specific binding proteins. Interacting proteins were eluted with Laemmli sample buffer under reducing conditions

Blots were probed with anti-IPO7 (sigma) and anti-RARRES1 (HPA) (sigma).

+ = transfected with RARRES1-HA.

- = mock transfected control.

4.8.14. Transcriptome Profiling of Primary Prostate Epithelial Cells – Transduced with LXN, RARRES1 or GUS (Control) Gene Lentiviral Vectors

Before analysis of the four primary samples presented in (Fig. 54. and 55.) a pilot experiment (data not shown) was performed using a single primary sample. This pilot study showed that GUS over-expression did not significantly alter the transcriptome relative to an un-transduced control, validating GUS as a control gene. Also 48 hours post-transcription showed the largest trend of transcriptome changes when LXN or RARRES1 were overexpressed relative to GUS overexpression.

Four passage-zero cultures derived from biopsies of normal areas of the prostate were used, each of the four patient samples was split into three populations each of which were transduced with LV vectors with a MOI of three (either pDest-298-GUS, pDest-298-LXNwt or pDest-298-RARRES1wt). Before progression to microarray analysis each of the 12 samples (four patient samples and three viruses) were quality controlled in the following ways:

- Confirmation of transgene overexpression at the mRNA level by RT-PCR.
- Confirmation of transgene overexpression at the protein level by western blot analysis.
- Viral integration was assessed using primers specific WPRE that is present in all our LV vectors.
- RIN and yield was measured by Agilent 2100 Bioanalyzer analysis.

The samples were then shipped on dry ice to Eurofins Laboratories Ltd (Broadoak Business Park, Ashburton Rd W, Manchester M17 1RW) who performed the generation of a labelled cDNA libraries and microarray hybridisation. The data was then exported back and analysed using TAC console V3.0.

All QC data (Fig. 54. and 55.) indicated that the experiment was performed correctly and to a high standard:

- Transduction efficiency ~90% as monitored by eGFP positive cells
- Overexpression confirmed at both mRNA and protein level
- RIN was 10 for all samples and yield was at least 3-fold excess than the minimum requirement.
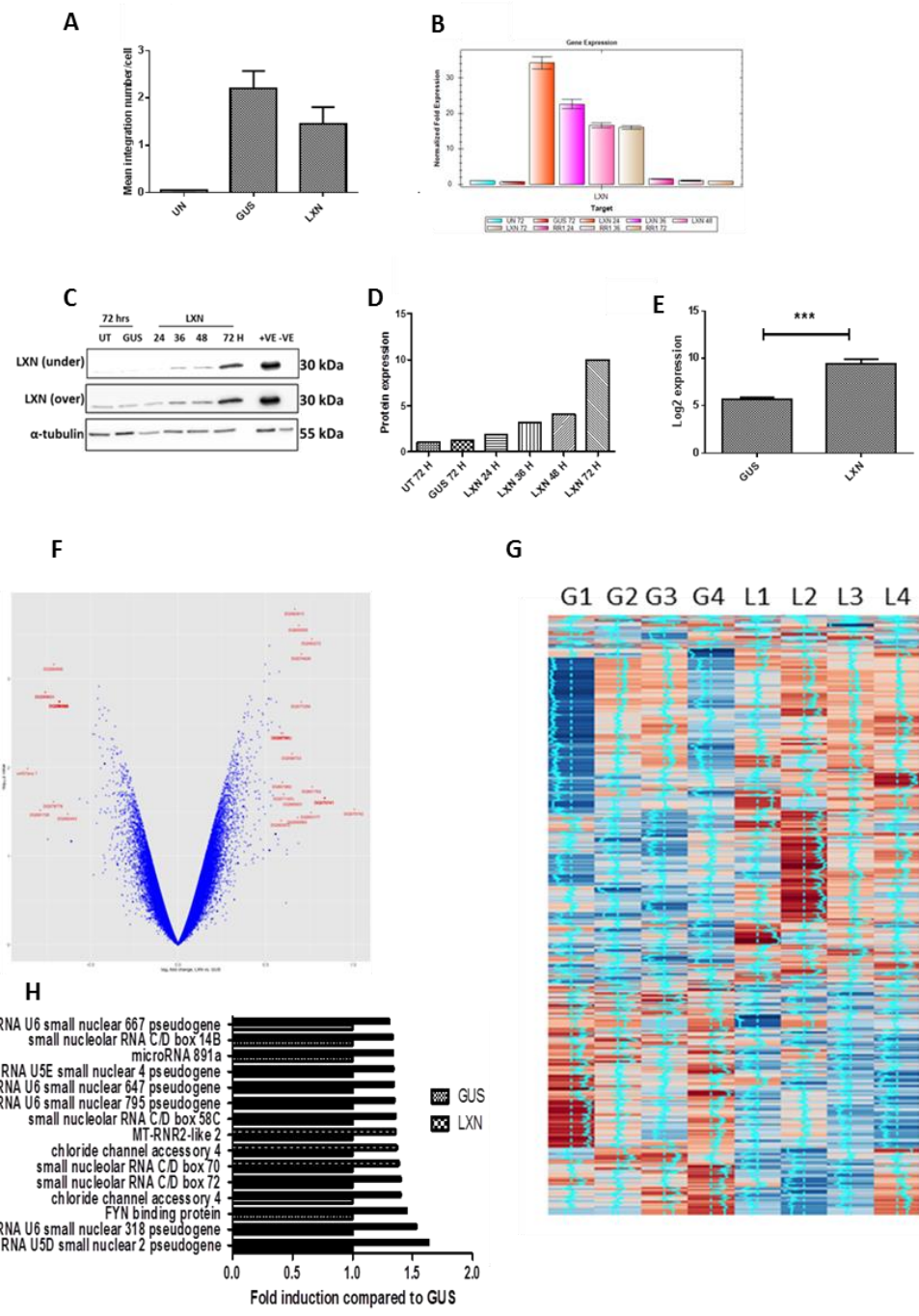
Fig. 54. Assessment of the Effects of LXN Overexpression on Gene Expression in Primary Prostate Epithelia.

A. QC data showing physiologically acceptable viral integration events
B. QC data showing successful overexpression of LXN mRNA across a time course
C. QC data showing successful overexpression of LXN protein across a time course with fold expression calculated using densitometry and normalised to GUS transduced control in **D.**
E. Data showing that LXN was significantly overexpressed in our transcriptome arrays
F., **G.**, **H.** a Volcano plot, Heat map and gene-chart respectively demonstrating the small number of genes that are non-significantly up or down-regulated in response to LXN overexpression.
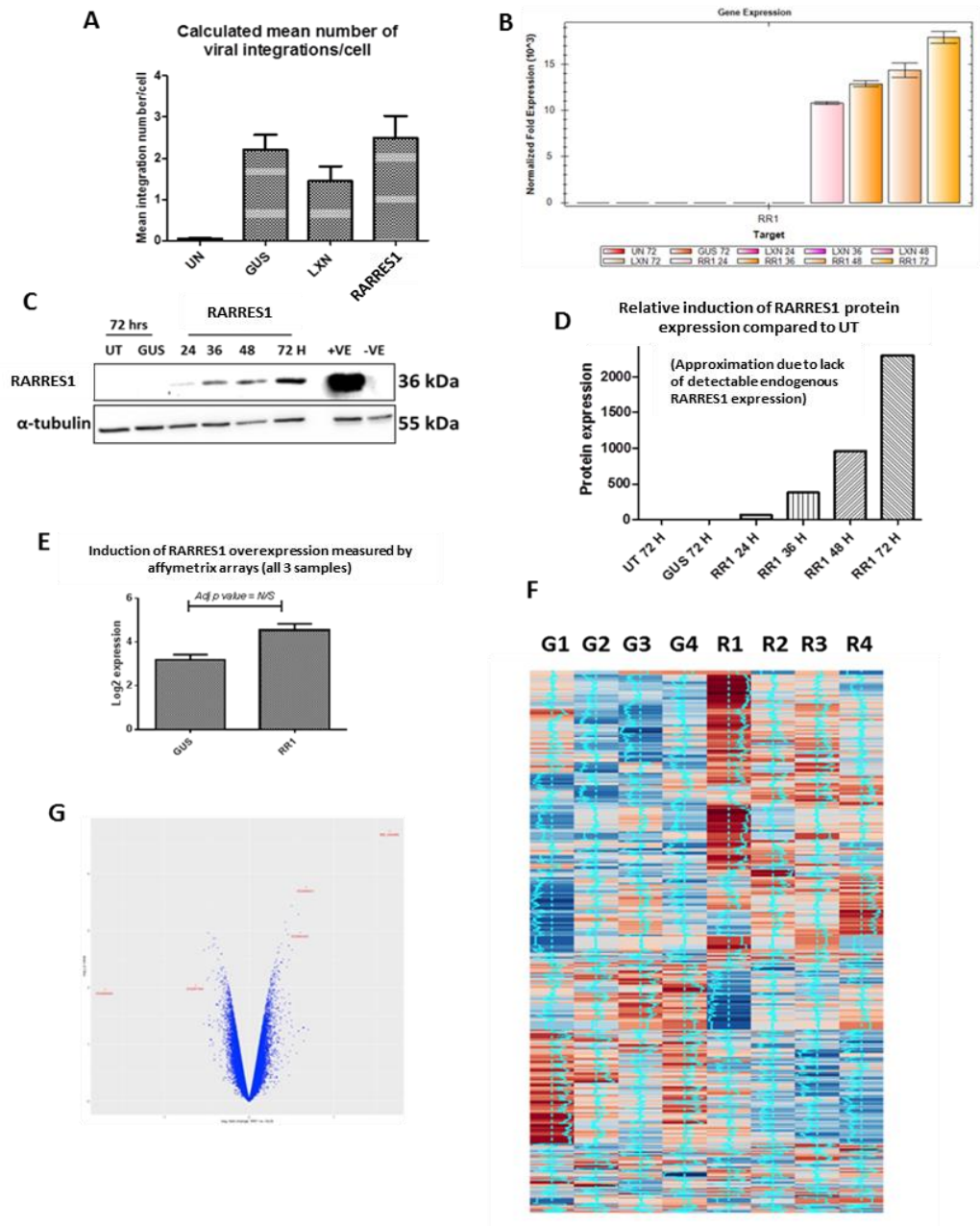
Fig. 55. Assessment of the Effects of RARRES1 Overexpression on Gene Expression in Primary Prostate Epithelia.

A. QC data showing physiologically acceptable viral integration events
B. QC data showing successful overexpression of RARRES1 mRNA across a time course.
C. QC data showing successful overexpression of RARRES1 protein across a time course with fold expression calculated using densitometry and normalised to GUS transduced control in **D.**
E. Data showing that RARRES1 was insignificantly overexpressed in our transcriptome arrays.
F., **G.** a Volcano plot and Heat map and gene-chart respectively, demonstrating the small number of genes that are insignificantly up or down-regulated in response to RARRES1 overexpression.

4.9. Discussion

Evidence from our lab has strongly indicated that LXN and RARRES1 are co-regulated in primary prostate epithelial cells of both benign and malignant origin (Birnie et al., 2008). A re-analysis of microarray data published by (Birnie et al., 2008) showed a correlation exists between both genes - Pearson's Correlation R^2=0.9186 (Fig. 33.). Subsequent data, generated by (Oldridge et al., 2013) showed two very important things: firstly, both genes are induced by the atRA (a known differentiation-inducing agent of prostate cultures (Peehl et al., 1993)) and secondly, epigenetic control of these genes is mediated by DNA methylation (at CpG islands located within the promoter regions) in several prostate cell lines (Oldridge et al., 2013). Interestingly, this epigenetic control mechanism was not observed in primary prostate epithelial cells, or near-patient xenografts (Oldridge, 2012). Given the precedence for epigenetic regulation of these genes and the differential expression of RARRES1 and LXN mRNA and protein through differentiation, it was hypothesised that an alternative epigenetic control mechanism may be active in primary prostate epithelial cells. As these genes are in close proximity to one another, epigenetic control in the form of histone modification, leading to changes in chromatin status (from heterochromatin to euchromatin as cells differentiate) seemed the most likely candidate. As such ChIP was employed in order to investigate this proposed regulatory mechanism.

4.9.1. Validation of a ChIP Protocol to Provide Proof of Principle for Epigenetic Control of RARRES1 and LXN by Histone Modification in Cell Lines

Before attempting to investigate a role for epigenetic regulation of RARRES1 and LXN in primary prostate epithelial cells (which like all primary *in vitro* models, are complicated by intra-patient variability and relative difficulty in working with) it was deemed prudent to start with well-established prostate cell lines. These laboratory 'work horses' are easy to handle, have low intra sample variability and can be cultured with ease to provide an abundance of material. Moreover, the expression profile with regard to RARRES1 and LXN was known (Oldridge, 2012). It was therefore possible to pick a high and low expresser of LXN and RARRES1 and compare the chromatin status at the *LXN* and *RARRES1* loci in these cells as a proof of principle pilot experiment. The caveat was that as DNA methylation had been discovered to regulate expression of these genes, it is possible that any further epigenetic regulation could be superfluous and therefore absent.

Our laboratory had validated several ChIP grade antibodies, which included anti-H3K27me3 (marker of inactive heterochromatin), anti-H3K4me3 (marker of active euchromatin) and anti-RNApol II (marker of transcription) as well as suitable active (*GAPDH*) and inactive (*PDYN*) control genes to which target gene enrichment by the aforementioned antibodies could be compared (Pellacani et al., 2011). A series of primer pairs, covering the putative promoter regions and downstream of the transcription start-sites were designed and validated for their suitability for qPCR downstream of ChIP.

As the end goal was to investigate the chromatin status of primary epithelial cells, which are grown in the presence of mouse feeder cells (STO), and the potential to analyse samples derived from near-patient xenografts, a further validation of the human:mouse specificity ratio was incorporated alongside traditional parameters, such as efficiency, R^2, sensitivity and specificity (single amplicon). Armed with these resources and the same ChIP protocol used in the study (Pellacani et al., 2011) a series of ChIP experiments were performed to interrogate and compare the chromatin status of *RARRES1* and *LXN* promoter regions in LNCaP and PNT2C2 cell lines.

The result of this analysis showed that the chromatin generated from both LNCaP and PNT2C2 cells was sonicated sufficiently (enriched for 200-500 bp fragments) after empirical optimisation of sonication time necessary for each sample. The control genes gave the expected enrichment profiles for each antibody used; *GAPDH* was enriched by anti-H3K4me3 and anti-RNApol II and was not enriched by anti-H3K27me3, on the other hand *PDYN* was enriched by anti-H3K27me3 but not by anti-H3K4me3 or anti-RNApol II. This result confirmed that the ChIP experiment was performed correctly. In the case of PNT2C2 cells it was found that all of the *RARRES1* promoter sequences analysed were enriched by anti-H3K4me3 antibody especially at -175 and 1000 bp from the transcription start site. Indicating that this region of DNA is in an active 'open' conformation. This is verified by a relatively modest enrichment of these sequences by the anti-RNApol II antibody which indicated this gene is actively transcribed in these cells. The data matches the RARRES1 expression profile generated by (Oldridge, 2012) which shows that RARRES1 is elevated in the PNT2C2 cell line. In contrast, LNCaP promoter regions, covering the RARRES1 promoter, was not enriched by any of the antibodies used, indicating that the chromatin is neither open nor closed (termed poised chromatin) and that the gene is not being actively transcribed, which is agreement with the (Oldridge, 2012) study which showed that this cell line does not express RARRES1 and transcriptional repression is

achieved through promoter hypermethylation (Oldridge et al., 2013, Oldridge, 2012). In the case of LXN in both cell lines the situation is rather more difficult to define. In PNT2C2 cells there is a modest enrichment of all three marks indicating that the gene is being actively transcribed (in agreement with previous data (Oldridge, 2012)) but that the chromatin is in an ambiguous state, again this can be due to epigenetic control through DNA methylation being the dominant mechanism. The results of LXN promoter enrichment by anti-H3K27me3 and anti-H3K4me3 in LNCaP are very similar to that of PNT2C2, however there is a noticeable reduction in enrichment by anti-RNApol II which is to be expected given that this cell line expresses LXN mRNA many fold less than PNT2C2.

4.9.2. Establishing and Validating a μChIP Method for the Interrogation of Chromatin Status in Rare Cell Populations such as the SC Fraction

There are several difficulties that exist when attempting to characterise any form of regulation in primary human prostate SC, not least of which are the complex culture systems used to maintain this undifferentiated population, but the most significant hurdle that needed to be overcome is that this population is exceedingly rare, accounting for less than 0.1% of total cells (Collins et al., 2001, Collins et al., 2005) . This means that in a fully confluent 10 cm dish containing approximately 2 million cells only 2000 will be selected as having a SC phenotype (through MACS selection for SC antigen CD133). Accordingly, one can only hope to obtain approximately 12 ng of chromatin from such a population. A traditional ChIP protocol, such as the one used to generate the data shown for the cell lines typically uses 20 μg per immunoprecipitation and is therefore not suitable for this application.

A μChIP method devised and validated by (Collas, 2011) is capable of performing a single ChIP reaction and subsequent downstream analysis by qPCR from as few as 100 cells. This method was adopted and a series of 'scale-down' experiments (from 20 μg to 2 ng per immunoprecipitation) were conducted to determine the sensitivity of this assay with ever diminishing amounts of input chromatin (as well as to gain experience with the new method), with the express aim of being able to perform μChIP from as little as 2 ng of chromatin. The approach of scaling-down the input of previously validated chromatin rather than preparing chromatin from different amounts of cells was chosen in order to reduce variables allowing a targeted investigation of the IP and qPCR analysis steps.

The first major difference between the ChIP and μChIP protocol was the use of magnetic capture beads (as opposed to sepharose beads) in the latter. The use of magnetic capture particles as opposed to sepharose led to a ~10 fold reduction in non-specific binding events when coupled to the same control anti-IgG. By reducing the background binding the 'signal to noise' ratio and therefore the sensitivity of the assay is improved. It was decided, that magnetic beads would be used for all subsequent ChIP experiments regardless of scale. Interestingly, it was found that 200 ng of chromatin had a greater background signal compared with 20 μg. This can be potentially explained by the background binding following a non-linear binding curve, and the reduction in the input due to dilution following linear kinetics i.e. all nonspecific binding sites were saturated at 200 ng of chromatin/IP. Experimentally this could be investigated by generating a background binding curve using many dilutions of chromatin allowing the identification of the chromatin concentration that is sufficient to saturate the non-specific binding sites present on bead and antibody (which are finite), indicated on the background binding curve as an upper-plateau.

An unexpected result was the observed increase in signal for the two histone marks (H3K27me3 and H3K4me3) when the starting chromatin was reduced to 200 ng and below. This indicates that with 20 μg of initial chromatin, the capture antibodies were beyond the point of saturation by these very abundant marks, and that the decrease in signal as a % of input, compared with 200 ng, is a function of increased input without further antibody capture (due to saturation). The human genome contains approximately 3 billion base pairs and is approximately 6 pg/cell, nucleosomes occur approximately every 200bp, and therefore 20 μg of chromatin contains approximately $5x10^{13}$ nucleosomes which equals $1x10^{14}$ H3 molecules. A caveat to this is that not all of the $1x10^{14}$ H3 molecules will be positive for H3K27me3 or H3K4me3. In contrast, the signal for RNA pol II did not dramatically increase when chromatin levels were reduced, indicating that the capture antibody was not being saturated by 20 μg chromatin. However, an increase in signal was observed when changing from sepharose to magnetic capture particles. This could be due to reduced background, enhanced antibody coupling and/or enhanced surface area of the smaller magnetic particles.

The results of these experiments show that a μChIP protocol has been successfully adapted and validated within our laboratory and is suitable for use with the current antibodies used in the 'traditional' high chromatin/IP ChIP experiments. However, there

was one more obstacle that needed to be overcome before the protocol was complete. This was to find the means to ensure that the chromatin obtained from ~2,000 cells was appropriately fragmented prior to IP.

As described previously, the sonication step while seemingly unimportant is critical to avoid both false positive and false negative results. Under-sonication results in large chromatin fragments with the potential for IP of target sequences through antibody interaction with a mark that is potentially kilobases or even megabases away. Conversely over-sonication results in chromatin fragments that are smaller than the amplicons used in the downstream detection of target sequences. Traditional ChIP methodology utilises a sonication control in which DNA from a sample of sonicated chromatin is extracted and its size is assessed by agarose gel electrophoresis. Obviously such small amounts of DNA ~2ng can't be readily visualised and the size determined. The µChIP method circumvents this problem through the use of qPCR using a 100 bp and a 300 bp amplicon (Dahl and Collas, 2008). Due to the sensitivity of qPCR such low levels of starting material pose no problem. Purely due to the function of size, the 300 bp template is broken at a greater rate than the 100 bp template. Accordingly, the qPCR ratio of the 100 bp to the 300 bp products increases as a function of sonication cycles (Dahl and Collas, 2008). While the genomic location of the 100 bp and 300 bp amplicons should be inconsequential it was decided that the 100 bp amplicon could be placed within the 300 bp amplicon (in this case both amplicons are resident in the coding region of the *β-actin* gene) to account for any sequence specific vulnerabilities to sonication (the 100 bp and 300 bp PCR reactions were performed as two separate reactions). By performing a side by side comparison of the qPCR and gel-based sizing methods it was found that the first incidence of a 4:1 ratio in 100 bp to 300 bp product ratio yielded chromatin that was optimally enriched for the desired level of fragmentation (200-500 bp). An interesting observation not documented by (Dahl and Collas, 2008) was that the 100 bp : 300 bp ratio falls after excessive sonication i.e. 4.63 at 60 cycles (determined to be optimal) to 2.04 at 80 cycles and then rises again to 6.64 at 130 cycles. This phenomenon may be in part explained by reaching the point in which there is accumulation of DNA fragments that are too small to be amplified by the 100 bp primers (this point was already reached much earlier for the 300 bp amplicon).

It can be concluded that a µChIP protocol suitable for use with the low abundance SC fraction has been validated.

4.9.3. Chromatin Status of the RARRES1 and LXN Promoter Sequences in Primary Prostate Epithelial Cells

This study is the first attempt to characterise the role that histone modifications play in the epigenetic regulation of *RARRES1* and *LXN* in primary human epithelial cells, specifically in the basal layer hierarchy (SC, TA and CB cells).

As with cell line experiments it was found that the control genes gave the expected enrichment profiles for each antibody used; *GAPDH* was enriched by anti-H3K4me3 and anti-RNApol II and was not enriched by anti-H3K27me3, on the other hand *PDYN* was enriched by anti-H3K27me3 but not by anti-H3K4me3 or anti-RNApol II. This analysis confirmed that the ChIP experiment was performed correctly and that subsequent analysis of the relative enrichment of the *RARRES1* and *LXN* promoter sequences is valid.

By comparing the relative enrichment by each mark it can be seen that there is no significant difference between the different basal cell fractions (SC, TA and CB cells) with regard to H3K27me3, H3K4me3 and RNApol II enrichment in the promoters of *RARRES1* and LXN. This result was unexpected, especially the RNApol II data, that one would expect to correlate with the differential expression of both RARRES1 and LXN mRNA published by (Oldridge et al., 2013). It is possible that the expression levels of these genes are fine-tuned by downstream epigenetic control mechanisms e.g. differential mRNA stability for these genes in the different cell fractions, or potentially mediated by either miRNA regulation or poly-A tail length, resulting in an accumulation of mRNA species in the more differentiated CB cells versus the SC fraction over time. Alternatively, the differing results between the two studies could be attributed to patient heterogeneity as different samples were used.

In the case of RARRES1 it was found that there was no significant enrichment of RNApol II when compared to the negative control gene for this mark – *PDYN* (0.63% vs 0.52% average across all samples). This result indicates that this gene is not expressed in these cells which is in contrast to data published by (Oldridge et al., 2013) In agreement with the data presented in here, recent data generated in our laboratory (Robert Seed-personal communication) using RT-PCR on the panel of patient samples published in (Rane et al., 2015)) showed that RARRES1 was only detected at significant levels in CD24+ luminal cells (sorted directly from patient biopsies and stromal cells (Fig. 56.).

There is evidence that these genomic regions exist in an intermediate state between 'open' euchromatin and 'closed' heterochromatin, as both genes in all samples tested were significantly enriched above the relevant negative control gene, albeit not to the same extent as a relevant positive control gene for both H3K27me3 and H3K4me3. This intermediate state is an observed phenomenon termed bivalent chromatin (Voigt et al., 2013). Bivalent chromatin is defined as a region of DNA with interacting histone complexes which are positive for both activating and repressing marks (Voigt et al., 2013). Usually these marks are mutually exclusive allowing the chromatin to exist in either an open or closed conformation allowing or preventing transcription, respectively. In the case of bivalent chromatin, both marks exist together (Voigt et al., 2013). This chromatin can be described as being 'poised' for either activation or repression of the gene by removal of one of the opposing histone modifications allowing the cell to rapidly alter the expression of a gene (Lesch and Page, 2014). As such, this bivalent chromatin regulates gene expression in embryonic stem cells (Harikumar and Meshorer, 2015). Another instance where bivalent chromatin is observed is in genomic imprinting (Kacem and Feil, 2009). Genomic imprinting is an epigenetic phenomenon in which cells express a single allele of a gene in a temporal or cell specific manner i.e. the allele inherited from the father is expressed while the allele expressed by the mother is silenced (Bartolomei and Tilghman, 1997). Of specific relevance to this study is that the most common opposing marks that are found in regions of bivalent chromatin are H3K27me3 and H3K4me3 which are the marks used in this investigation (Harikumar and Meshorer, 2015).
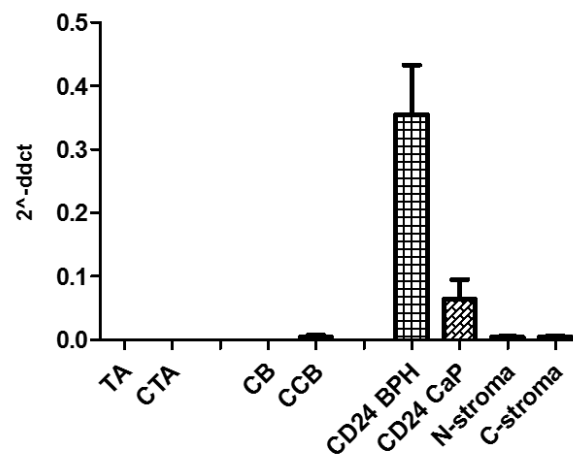
Fig. 56. RARRES1 Expression in a Cohort of Primary Samples.

RT-PCR for RARRES1 mRNA normalised to several 'housekeeping' genes, samples used in this analysis were from the date set presented in (Rane et al., 2015) Data provided by Robert Seed (personal communication).

4.9.4. Establishment of a Lentiviral Overexpression System to Study the Effects of LXN and RARRES1 Overexpression in Primary Prostate Epithelia

Previous attempts to generate and utilise LV transduction in our laboratory were plagued by several technical hurdles which precluded the routine use of this system (Frame et al., 2010). These limitations included: promoter silencing was observed in several cell lines (P4E6, BPH-1, PC3), low titres and perhaps the most importantly - low infection efficiency in primary cultures (Frame et al., 2010).

Here we present a functioning and highly optimised and validated protocol including a method for estimating integration number. Several LV plasmid backbones are now available in our laboratory which facilitated further experiments in this project and also other projects within the laboratory e.g. The E74 like ETS transcription factor 3 (ELF3)-mVenus fusion was used by Leanne Archer to identify its location after several immunofluorescence approaches on both native and un-tagged plasmid over expression systems gave variable and unsatisfactory data which were at odds with the literature (Do et al., 2006) (personal communication).

Future work aimed at further improvement of the LV production methodology developed as part of this report could be through investigation of viral titres achieved through the use of alternative packaging cells such as WinPac (Sanber et al., 2015). The major inherent advantage of the WinPac cell line is the continuous production of LV vectors as opposed to three days with HEK293FT cells which were used in this project. Also the use of LV-concentration should also be investigated. This approach would reduce unwanted secreted products (and serum) from the viral supernatant.

4.9.5. LXN is a Soluble Pan-Cellular Protein

Data published by (Oldridge et al., 2013) showed that LXN is exclusively nuclear in the LNCaP cell line and primary prostate epithelial cells. However, the experimental design used in this study had several short-comings, anti-LXN antibody used detection was not validated for use in immunofluorescence. This led to the utilisation of an anti-HA and LXN-HA transfection to define subcellular localisation of LXN. Plasmid transfection leads to un-physiological overexpression of LXN-HA protein (+ve control in Fig. 55C.). This overexpression is especially high when one considers efficiency in this sample is ~30%. It has been demonstrated that lentiviral transduction results in a less extreme level of LXN overexpression. The gross overexpression is likely due to many copies of the plasmid entering single cells within the transfected population.

A confounding set of results in the investigation of LXN localisation was that attempts to confirm immunofluorescence findings by cellular fractionation coupled to western blot found exclusive localisation to the cytoplasm (Fig. 49C.) i.e. the two methods give conflicting results. To circumvent these experimental limitations, the use of LXN-mVenus fusion LV vectors, coupled to confocal microscopy in a live-cell imaging approach, was used to settle this experimental quandary. The use of live-cell imaging was chosen to examine the localisation in an unbiased manner. Also the serendipitous discovery that GUS-mVenus fusion had an exclusively cytoplasmic distribution in all cell types used provided an excellent control for the identification of a nuclear localisation. The results of this analysis confirmed that LXN has the ability to access the nucleus however in contrast to previous studies – LXN was found not to be exclusively nuclear but rather pan-cellular. When subcellular fractionation coupled to downstream western blot analysis was performed on the same samples used for the live cell imaging experiments, it was found that the LXN-mVenus fusion protein was exclusively cytoplasmic (data not shown), mimicking previous data generated by LXN-HA transfection. Therefore I decided to investigate if the experimental approach of nuclear cytoplasmic fractionation was giving artefactual data. By analysing the first lysis step in preparing the separate cell fractions (only lyses the cell membrane but not the nuclear envelope) it was seen that LXN-mVenus and therefore, native LXN, is so soluble that it leaches out of the nucleus at this stage of the subcellular fractionation protocol. This result clearly demonstrates that nuclear cytoplasmic fractionation by this method is not suitable for determining the localisation of this protein in these cells. Therefore immunofluorescence and confocal imaging data should take precedence.

Whilst leaching of nuclear proteins into the cytoplasm is a well reported phenomenon, future work to confirm LXN localisation by a second method could utilise a recent method developed by (Nabbi and Riabowol, 2015). The protocol described in this report involves a rapid fractionation method using selective dissolution of the cytoplasmic membrane (but not the nuclear membrane) using a combination of low-concentration non-ionic detergent and rapid centrifugation to reduce the leaching events which occurs in a time-dependent manner. (Nabbi and Riabowol, 2015).

4.9.6. Identification of Potential LXN and RARRES1 Interacting Partners in Prostate Epithelial Cells

The first attempt to generate an interactome for RARRES1 and LXN in a prostate model (PC3 cells) is presented in this report. This analysis identified many unique 'hits' for both proteins. In the case of LXN several of the potential protein interactors have a reported nuclear distribution. This corroborates the LXN localisation profile described in this report and data previously published by our laboratory (Oldridge et al., 2013). The evidence for the pan-cellular localisation of LXN identified for the first time in this report is further strengthened by the identification of both nuclear and cytoplasmic potential interactors of LXN. A report by (You et al., 2014) in leukaemic cells, identified Ribosomal Protein S3 (RPS3), as an LXN-interacting protein. Initial identification of the LXN-RPS3 interaction was identified by mass spectrometry subsequently validated by reciprocal Co-IP. Interestingly, RPS3 is shown in the literature to be located mainly in the cytoplasm with small amounts in the nucleus but in cells undergoing apoptosis in response to hydrogen peroxide treatment RPS3 translocates to the nucleus. As such this report, while identifying that the LXN-RPS3 interaction serves to prevent RPS3 translocation to the nucleus in response to DNA damage it does leave the door open for LXN to shuttle RPS3 from the nucleus to the cytoplasm. Perhaps more importantly the exclusively cytoplasmic distribution of LXN reported in the (You et al., 2014) study demonstrates that LXN can access the cytoplasm.

Similarly to LXN, the 'hit-list' generated of potential RARRES1 interactors corroborates the observed localisation of RRARES1 in this report and the data published previously by our laboratory (Oldridge et al., 2013). RARRES1 interactors also reside in the endoplasmic reticulum including, Aspartyl/asparaginyl beta-hydroxylase, Dolichyl-diphosphooligosaccharide--protein glycosyltransferase 48 kDa subunits, Mannosyl-oligosaccharide glucosidase and Neuropathy target esterase.

Initial attempts to validate either data set by IP coupled to western blot has proved unsuccessful. In the case of RARRES1 the validation attempt has only focused on one hit IPO7 (albeit the most abundant in terms of spectral counts). It must be stated that other hits should be investigated before a definitive conclusion on this data set is to be made, especially those that show through gene ontology - localisation to the endoplasmic reticulum membrane.

Future work on the identification of LXN and RARRES1 interactors could utilise lentiviral vectors discussed extensively in this report, to generate a more physiological interactome through interrogation of primary prostate epithelial culture model. Furthermore this experimental approach could theoretically be used to analyse the interactome generated in CaP and normal cells derived from the same patient. This experimental approach may lead to novel binding events in either system which may shed light on how LXN and RARRES1 elicit their effects.

4.9.7. Understanding the Effects of LXN and RARRES1 Overexpression on Gene Expression in Primary Prostate Epithelia

This is the first attempt to look at transcriptional changes induced by LXN or RARRES1 overexpression in primary prostate epithelial cells. The rationale behind performing transcriptomic profiling in cells overexpressing either LXN or RARRES1 is multi-layered:

- These genes have been shown to effect fundamental processes in CaP progression namely, colony formation, cell migration and invasion.
- The confirmed localisation of LXN to the nucleus
- Mass-spectrometry data which shows that potential binding partners of LXN and to a lesser extent RARRES1 are in the nucleus.

It was decided that the most appropriate model for investigating transcriptional regulation by LXN and RARRES1 was the use of well validated lentiviral vectors. These vectors have been shown to transduce primary prostate epithelial cultures in a stable and highly efficient manner. This experimental approach was favoured over plasmid transfection as lentiviral vectors have been shown to transduce primary prostate epithelial culture with much greater efficiency than plasmid transfection. Additionally this approach allows MOI and therefore level of expression to be more tightly controlled. LV generated from pDEST-298 backbone (co-expression of eGFP) was used as this system allows visualisation of transduction efficiency and intensity across samples.

Downstream analysis of transcriptional changes was performed through Affymetrix microarray technology. This approach was chosen as it is a well validated system for measurement of transcriptome changes in our cell culture model (Birnie et al., 2008). Specifically the Affymetrix GeneChip® Human Transcriptome Array 2.0 was used. This microarray contains >6.0 million distinct probes covering coding and non-coding transcripts. 70% of the probes on this array cover exons for coding transcripts, and the

remaining 30% of probes on the array cover exon-exon splice junctions and non-coding transcripts.

No significant alterations that exceeded the traditional cut-off of 2-fold change compared to control were seen for either LXN or RARRES1 overexpression. In the case of RARRES1 analysis even RARRES1 itself was not significantly overexpressed vs control, even though RARRES1 as analysed by targeted RT-PCR and western blot with appropriate controls showed several thousand fold over expression of RARRES1 compared to GUS-transduced control (Fig. 55B. and D.). As a result, the validity of the whole dataset for both genes is cast into doubt and the ability (or lack of) of LXN or RARRES1 overexpression to elicit transcriptional changes in primary prostate epithelial cells remains unanswered.

An alternative to microarray profiling is RNA sequencing (RNA-seq) (Zhao et al., 2014). RNA-seq is a powerful technique for transcriptomic analysis which relies on massively parallel 'next generation' sequencing technologies such as ilumina's HiSeq 2500 Technology. The advantage of RNA-seq vs microarray technology include:

- Greater dynamic range.
- The ability to detect novel transcripts and mRNA variants such as those arising from: splicing events, alternative promoter usage and sequence variation within the sample compared to reference genome (Zhao et al., 2014).
- Enhanced signal to noise through lower background.

However, it is not without disadvantages:

- Increased sample requirements - especially important if rare cell populations such as the SC fraction are to be analysed.
- Complicated library preparation.
- Biases during sample preparation and sequencing that must be accounted for when analysing the data generated (Roberts et al., 2011).

It is widely accepted that RNA-seq will eventually overtake microarray approaches as the assay of choice (Zhao et al., 2014). As such future attempts to investigate transcriptomic changes induced by LXN and RARRES1, could be facilitated by utilisation of RNA-seq. This approach would preclude any issues regarding the ability of microarray probes to reflect RT-PCR (RARRES1 probe is capable of detecting endogenous RARRES1 mRNA but this was below the level of detection in un-transduced and GUS-transduced samples) and western

blot QC data which showed massive (thousand-fold) expression of RARRES1 in cells transduced with RARRES1 LV compared to those transduced with the control (GUS LV). It must be noted that both LXN and RARRES1 are only covered by a single probe set each (on the microarray used). Also as GUS is not a human sequence it is not covered by any Affymetrix probes thus precluding expression analysis of this control by this approach.

5. Overall Discussion: Integration of the Research into Emerging Paradigms of Cancer Treatment and Future Directions of the Research

5.1. Differentiation Therapy as a Strategy to Treat Cancer

Traditional cancer therapies are cytotoxic in nature- aiming to kill cancer cells directly. Unfortunately, these treatments often fail and the cancer recurs. Reasons for treatment failure include; toxicity and drug resistance often attributed to the properties of CSCs (discussed in section 1.4.1.). In contrast, 'differentiation therapy' describes a form of therapeutic strategy for the treatment of malignancies, through hyper-activation of endogenous differentiation pathways (Cruz and Matushansky, 2012). Differentiation leads to maturation of the cancer cells and subsequent loss of several key properties of cancer such as self-renewal potential and resistance to apoptosis (Xu et al., 2014). This strategy is by no means new, having been initially proposed in 1961 (Pierce and Verney, 1961). However, due to a relatively recent wave of evidence supporting the CSC hypothesis of cancer, it has now been investigated in many cancers including: several forms of leukaemia, and solid tumours such as breast, colon and CaP (Walczak et al., 2001, Munster et al., 2001, Castaigne et al., 1990, Xu et al., 2014).

There are many different differentiation inducing agents. The main strategies include: interference of signal transduction and transcription, CSC targeting and modulation of the epigenome and miRNA expression.

Targeting signal transduction: It has been shown that mesenchymal stem cells (MSCs) are the progenitors of malignant fibrous histiocytoma (MFH) (Matushansky et al., 2007). Furthermore, elevated Dickkopf-related protein 1 (DKK1) (a Wnt inhibitor), mediates the transformation of MSC to the MFH phenotype (Matushansky et al., 2007). Importantly, restoration of Wnt signalling caused reversion to the MSC phenotype and loss of tumour cell properties through differentiation into connective tissue lineages (Matushansky et al., 2007).

Peroxisome proliferator-activated receptor (PPAR)-γ agonists: PPAR-γ is member of the PPAR transcription factor superfamily. PPARs are nuclear receptors that elicit their effects on transcription by interaction with RXRs in a heterodimeric conformation (Tontonoz et al., 1997). PPAR-γ is involved in the regulation of key cellular functions such as cell proliferation, differentiation and apoptosis (Grommes et al., 2004). Agonists of PPARγ are

well established inducers of differentiation. They have been shown to induce differentiation in several types of cancer cell lines, including: monocytic leukaemia, breast, colorectal, non-small-cell lung cancer, and CaP (Zaytseva et al., 2011, Cruz and Matushansky, 2012). In the latter, treatment of the PC-3 cells (high expression of PPARγ), with troglitazone (synthetic PPARγ agonist of the thiazolidinediones class) resulted in a potent reduction of proliferation (Kubota et al., 1998).

Modulation of posttranscriptional modification of histone proteins: Modification of the 'histone code' and subsequent accessibility of the chromatin to transcription machinery is known to play a crucial role in development, cellular differentiation and programed cell death. Importantly, aberration of this control mechanism is implicated in oncogenesis. Histone deacetylation, performed by HDACs, results in transcriptional silencing of tumour-suppressor genes in several cancers. Concordantly, HDACI, have been shown to induce differentiation in several cell lines (Gallinari et al., 2007, Marks et al., 2001). A breakthrough for differentiation therapy through modulation of the histone code is Vorinostat for treatment of cutaneous T cell lymphoma which has been approved by the Food and Drug Administration (FDA).

Modulation of the miRNA expression profile of cancer cells is another strategy for forcing differentiation of cancers cells. One of the key advantages of this approach is that a single miRNA targets multiple mRNA species. Supporting the potential of miRNA modulation comes from the reintroduction of miR-1 and miR-124 resulted in inhibition of growth through induction of differentiation (Lim et al., 2005). Additionally the CSC fraction can be directly targeted e.g. upregulation of miR-145 leads to differentiation through the mechanism of repressing octamer-binding transcription factor 4 (OCT4) in human endometrial adenocarcinoma cells (Wu et al., 2011b). Alternatively, elimination of miRNAs required for the maintenance of CSC 'stemness' is another strategy e.g. miR-21 (Yu et al., 2013).

Hypermethylation of CpG islands present in the promoters of tumour-suppressor genes is a well-described mechanism of gene silencing in cancer. CpG island methylation is performed by DNA methyltransferases. Two of the first epigenetic drugs used in AML were the nucleoside analogues 5-azacytidine and 5-aza-20deoxycytidine (Schenk et al., 2014). Which are examples of DNA methyltransferase inhibitors (DNMTi). The mechanism of DNMTi action is through DNMTi incorporation into the DNA, where they complex with the DNA methyltransferases (Schenk et al., 2014). Covalent coupling of DNMTi to DNA

methyltransferases results in the degradation of the enzyme and subsequent loss of CpG island hypermethylation in cancer and re-expression of tumour suppressor genes.

Retinoids have been shown to control differentiation, proliferation and apoptosis through interaction with nuclear retinoic acid receptors (RAR and RXR). The best example of a retinoid as a differentiation promoting agent is atRA. As well as the effects of atRA on transcription discussed previously, there are also extra-nuclear effects of this agent. Non-classical functions of atRA include activation of extracellular signal-regulated kinases (Erks) via PI3K and Proto-oncogene tyrosine-protein kinase Src (Src) kinases in neuronal cells leading to repression of Oct4 (Al Tanoury et al., 2013). Although the non-genomic effects of atRA are not fully understood, it is clear that these effects have to be taken into consideration when evaluating the response to retinoids (Schenk et al., 2014).

The first successful clinical application of differentiation therapy was provided when atRA was used to treat acute promyelocytic leukaemia (APL) (Castaigne et al., 1990, Schenk et al., 2014, Stone et al., 1988). This breakthrough resulted in APL being a curable disease rather than a fatal one. atRA treatment resulted in the terminal differentiation and loss of long-term proliferative capacity and eventually induction of apoptosis (Schenk et al., 2014). Incorporation of chemotherapy and up-front use of atRA in combination with arsenic trioxide led to complete remission rates in excess of 93% with patients achieving 5-year overall survival rates approaching 100% (Schenk et al., 2014). Mechanistically, most APL patients, have the chromosomal translocation t(15;17) producing a fusion of RARα and promyelocytic leukaemia gene (PML) (Cruz and Matushansky, 2012). atRA treatment induces dissociation of PML-RARα/HDAC interaction and subsequent degradation of PML-RARα (Cruz and Matushansky, 2012). Ultimately this leads to the reactivation of myeloid differentiation processes in APL cells (Schenk et al., 2014, Stone et al., 1988). The very successful use of atRA in the treatment of APL validates the concept of differentiation therapy. It also provides the rationale for differentiation therapy in the treatment of other cancers.

Unfortunately, there are currently no other differentiation-inducing agents that mirror the effectiveness of atRA treatment of APL. The major reason for this is that APL represents a simple karyotype disease, characterised by the presence of the PML-RARα gene. Thus, the reversal of one pathway is sufficient to reverse the tumourigenicity of APL and induce normal differentiation. Solid tumours on the other hand, are heterogeneous with respect to cell proliferation, differentiation and most importantly – epigenetic and

genetic abnormalities. For solid tumours, the application of differentiation therapy has been further compounded by the absence of developmental models of cancer progression that correlate cancer subtypes to stages of normal development.

Most solid tumours are now viewed as aberrantly-differentiated heterogeneous tissues containing a hierarchy of cells that originate from CSCs. Due to this intra-tumour heterogeneity it is perhaps naïve to believe that a single agent can elicit a cure. Accordingly, combined regimens with different targets are likely to have greater efficacy. Such combinations can take the form of two or more differentiation promoting agents or the combination of differentiation therapy with conventional radiation or chemotherapy (Sung and Waxman, 2007, Vainstein et al., 2012).

Mechanistically, 'combined regimens' can exert additive or even synergistic effects in many ways. One example is retinoid resistance of many solid tumours which limits the effectiveness of atRA treatment. HDACI can increase the expression of retinoid receptors and therefore the combination of HDACI with atRA is logical (Ferrara et al., 2001, David et al., 2010, Xu et al., 2014). CSCs are resistant to traditional cytotoxic cancer therapies. By inducing differentiation of CSCs one could hope to sensitise these cells to the traditional therapy and thus achieved greater efficacy (Cruz and Matushansky, 2012, Xu et al., 2014).

Both LXN and RARRES1 have been shown to be regulated by atRA, hypermethylation of CpG islands and modulation of the histone code. These proteins have also been shown to have tumour suppressive roles in several malignancies. The upregulation of LXN and RARRES1 through differentiation promoting agent(s) has the potential to improve patient outcomes in CaP and other cancers particularly when administered in combination with a traditional cytotoxic therapy to destroy the bulk tumour. This bivalent assault of the main population of tumour cells and the CSC fraction has the potential benefit of reducing tumour burden, reducing metastatic potential, resistance to therapy and relapse rates (all of which are attributed to CSCs).

5.2. Targeted Medicine as a Means to Improve Outcomes in Cancer

Every patient is unique and accordingly every patient's cancer is unique. This well-established paradigm is the root cause of the inter-patient variability seen with regards to: prognosis, tumour response, clinical presentation, treatment tolerance and risk of metastasis. Recent advances in molecular profiling technologies, biomarkers and drugs which exploit 'molecular weaknesses' of cancer have precipitated a trend towards a targeted medicine approach for the treatment of cancer. Targeted medicine is a term used in this report to encompass several distinct but overlapping terms which include:

- Precision medicine - Genomic profiling to inform and guide treatment decisions.
- Stratified medicine - The use of diagnostic tests for grouping of patients based risk, prognosis and/or response to therapy.
- Personalised medicine - Profiling of an individual at the level of the genome, transcriptome and/or proteome - used to direct healthcare on a patient by patient basis.

The ultimate goal of targeted medicine strategies is to provide patients with the most suitable therapeutic intervention at the correct time. Traditional 'one-dose-fits-all' approach to clinical intervention has proven unsatisfactory in many diseases with response rates in oncological disorders the most disappointing (Spear et al., 2001).

The inter- and intra-heterogeneity of cancer is a fundamental problem that has resulted in poor response rates to therapeutic intervention. Cancer is characterised by mutations, and mutation is a random process (although specific mutations can be preferentially selected and therefore enriched in certain disease types). This randomness combined with a unique starting point i.e. an individual's genome and epigenome is unique, increases the spectrum of driver mutations that are present even within a single subtype of cancer. This situation is further complicated by the observed multi-focal nature of many cancers i.e. a patient may present with CaP but in fact the cancer is composed of several distinct clones, each exploiting a different genomic lesion. Current 'omics' technology allows the molecular interrogation of the cancer genome in direct comparison to the genome of normal cells. This approach enables the detection of aberrant genes and pathways, and the patient to be treated accordingly.

Targeted medicine offers several advantages to both the patient and healthcare system. These include:

- Accurately defining prognosis - reducing 'over-treatment' and waiting time for patients with aggressive disease (Jackson and Chester, 2015).
- Reduced administration of drugs which are unlikely to be of benefit - reduced exposure to side-effects for patients and reduced expenditure for the health care system (Bell, 2013).

Targeted medicine is currently employed in many disease settings (Bell, 2013). One of the most well-known examples of targeted medicine is the identification of heredity genetic factors which increase the life time risk of breast cancer- breast cancer 1 (BRCA1) and breast cancer 2 (BRCA2) (Jackson and Chester, 2015, Struewing et al., 1997, Cho et al., 2012). By predicting that a disease is likely to occur within an individual or within a sub-group of the population, clinicians are able to monitor the patient (by regular mammography) allowing early diagnosis. Also, if risk management dictates, prophylactic surgery or other intervention can be administered.

Sub-classification of cancer types based on molecular profiling of somatic mutations has already begun in several cancer fields leading to targeted therapeutic strategies being employed.

Molecular profiling of breast cancer has resulted in the identification of a subtype of the disease defined by overexpression of the human epidermal growth factor receptor 2 (HER2) oncogene. Commonly this is a result of genomic amplification of HER2 which can be identified by FISH. This driver mutation, which is present in approximately 20-30% of breast cancer patients, can be targeted by treatment with trastuzumab (Rodríguez-Antona and Taron, 2015, Vogel et al., 2002). The use of targeted medicine in this setting has been shown to reduce disease recurrence in HER2 positive breast cancer by 40% (Pinto et al., 2013).

In colorectal cancer patients with WT Kirsten rat sarcoma viral oncogene homolog (KRAS) (approximately 60% of colorectal cancer patients) which is a downstream signalling molecule of epidermal growth factor receptor (EGFR) have been shown to respond to treatment with cetuximab (Jackson and Chester, 2015). Cetuximab is a monoclonal antibody directed against EGFR. Importantly patients with mutant KRAS do not respond to cetuximab treatment and therefore can be triaged in an appropriate manner (Jackson and Chester, 2015, Karapetis et al., 2008).

In malignant melanoma, the presence of oncogenic murine sarcoma viral oncogene homolog B (BRAF) mutation which is present in approximately 66% of malignant melanoma patients has been shown to predict increased aggressiveness and resistance to traditional chemotherapy (Tsai et al., 2008). Additionally and most significantly, the presence of BRAF mutations has been shown to predict disease sensitivity to the Raf inhibitor vemurafenib (Tursz et al., 2011, Jackson and Chester, 2015). Accordingly, treatment of this disease subtype with vemurafenib led to a reduction of disease progression in 74% of a patients and a reduction of overall mortality of 63% (Chapman et al., 2011).

Application of a targeted medicine approach to the treatment of CaP is currently hampered by the high level of molecular heterogeneity of the disease. However, several common molecular abnormalities have been identified which include: TMPRSS2/ERG fusions, loss of PTEN, mutations affecting the PI3K pathway and perturbations of AR signalling.

As part of the COU-AA-302 CaP trial (Abiraterone acetate in metastatic CRPC in chemotherapy naïve patients) it was found that patients who have fusion of *TMPRSS2* to *ERG* sequences together with interstitial deletion of sequences 5' to *ERG* (2+EDel) variant of TMPRSS2/ERG translocation had an increased benefit from Abiraterone treatment (Ryan et al., 2015).

Perturbations of the AR signalling pathways and the increased efficacy of 2nd generation ADT in patients with *AR* amplification has already been discussed. However, it has also been shown that the expression of AR-V7 splice variant predicts resistant to enzalutamide but also susceptibility to galeterone, (an androgen receptor therapy) (Maughan and Antonarakis, 2015).

It has been shown that 19% of CRPC patients have a DNA repair pathway alterations, including 12.7% of patients with a hereditary BRCA2 mutation (Mullane and Van Allen, 2016, Agalliu et al., 2007). It was subsequently shown that the use of the poly ADP ribose polymerase inhibitor (olaparib) in patients with DNA repair gene mutations resulted in a response rate of 87.5% (14 out of 16 patients) (Mateo et al., 2015, Mullane and Van Allen, 2016).

It can be seen that the revolution of targeted medicine is currently gathering momentum - buoyed by success seen in several disease types and oncological disorders. This trend is

set to continue as high-throughput sequencing technologies are expected to become more accessible to healthcare providers, as technological progress is driving a fall in cost (Fig. 57.) (Cho et al., 2012). This information explosion must be accompanied by a concomitant increase in bioinformatics and data processing capability for maximum benefit to be realised.

Currently we are in an era of targeted medicine which relies on targeted tests to identify a particular molecular lesion within a patient and matching this incomplete 'molecular signature' with the most appropriate therapy available. It is at this juncture that the qPCR assay described in this report would be most applicable to determining prognosis and response to therapy. As deep sequencing improves particularly in the resolution of minor-populations present within a tumour biopsy, it is expected that our understanding, and detection, of deregulated pathways will increase (Cho et al., 2012, Bell, 2013). This information as well as being used to triage patients, will also feed forward to the pharmaceutical industry, allowing the generation of therapeutic agents that exploit these abnormalities. Additionally, reducing costs and increasing the through-put of diagnostic methodologies will enable target medicine to be utilised in more patients. Further progress in targeted medicine, in the longer-term, will likely benefit from the integration of many 'omics' data e.g. genomic, epigenomic, transcriptomic and proteomic approaches to further-refine molecular diagnosis and disease phenotypes.
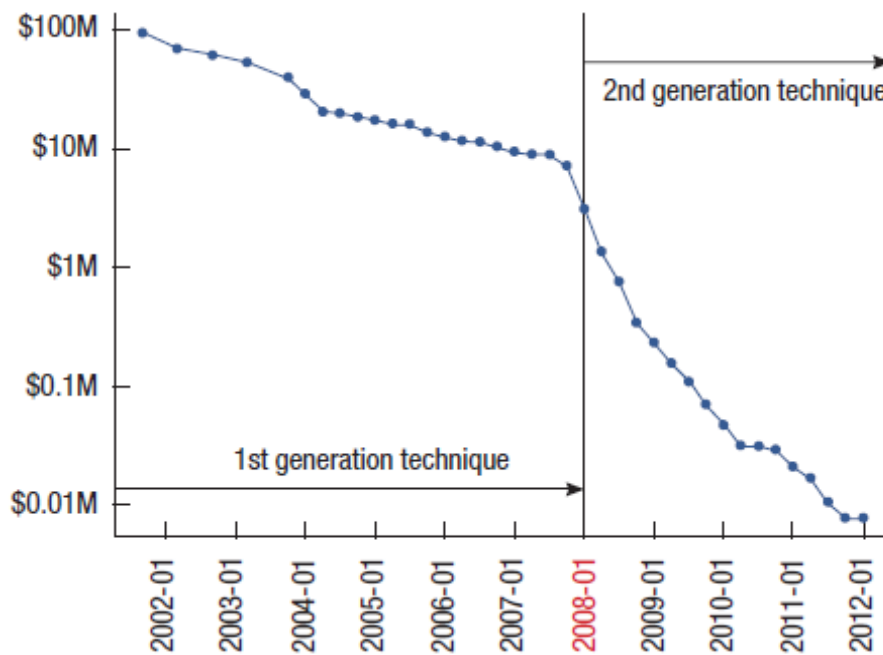
Fig. 57. Cost of Sequencing a Human-Sized Genome.

The cost of sequencing decreased from 2001 to 2007. This was followed by dramatic fall in cost upon technique evolution from 1st generation to 2nd generation technology in January 2008. The cost of sequencing continued to decrease following 2008.

From: (Cho et al., 2012)

Chapter 5. Overall Discussion

5.3. Future Directions of the Research

5.3.1. Future Directions: Utilising the GAAR Assay in a Clinical Setting

The field of biomarker research has often focused on the utilisation of liquid biopsies due to less invasive sampling methodologies when compared to a tissue biopsy approach. In this regard a collaboration was initiated with the Medical University of Innsbruck to explore the possibility of analysing XCA and GAAR status of circulating tumour cells (CTC). Unfortunately with current methodology of CTC enrichment from liquid biopsies in CaP and the vanishingly small numbers of CTCs recorded in the literature the project was quickly abandoned. However should the technology for CTC purification from liquid biopsy be improved, then such a study had the potential to allow urologists to quickly and easily monitor the patient's suitability and responsiveness to ADT. A proposed study design devised in collaboration with Frédéric Santer is shown in (Fig. 58.). The proposed study design advocates the use of whole-genome sequencing in parallel to utilisation of the GAAR qPCR assay. While this would provide an enormous amount of additional information a more AR-targeted approach would be to use targeted sequencing of the *AR* alleles and/or investigation of AR mRNA species such as AR-V7.

With current methodology of CTC isolation which is plagued by high levels of cellular contamination particularly by white blood cells, as such analysis by FISH would be the preferred methodology.

A more achievable way of establishing usefulness of this assay in a clinical setting would be through performing a retrospective trial. As the assay is compatible with FFPE tissue then historical archived samples of repeated patient biopsies could be used and compared against known outcomes. The goal of this trial would be to predict:

1. Which patients are likely to be at risk of developing a clinically relevant CaP?

2. Out of the patients that failed first line ADT, which ones responded to subsequent total androgen blockade through second line ADT therapeutics, such as Enzalutamide.

This approach is dependent on the availability of multiple biopsies from different stages of treatment, for each patient in the trial which has serious logistic problems, but would

provide genuine insights into the development of castration resistance, and its relationship to GAAR and XCA.

Detection of AR amplification in CTCs of patients undergoing anti-androgen therapy (Enza)
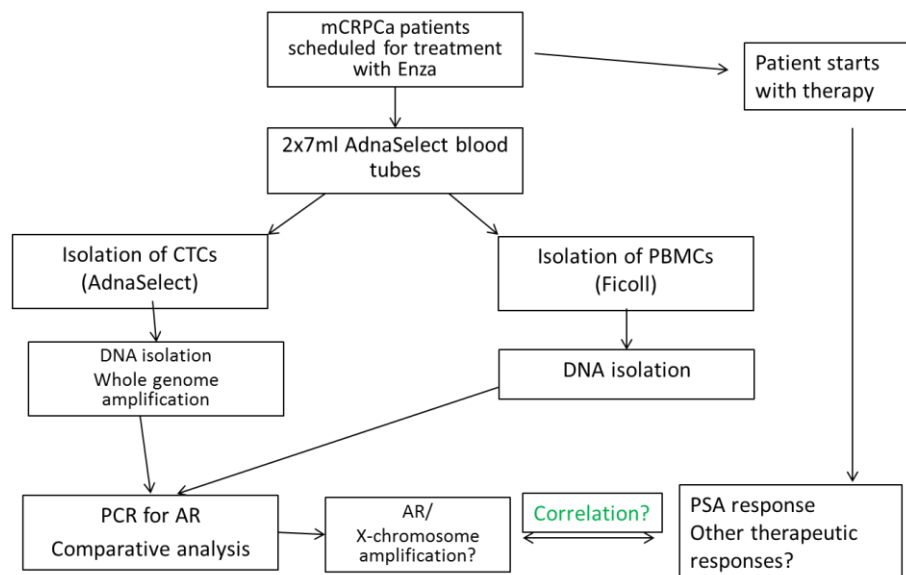
Fig. 58. Proposed Trial Design for Monitoring ADT Resistance Through the use of the AR Assay Described in this Report by Analysing CTCs Isolated from Liquid Biopsies.

Enza = Enzalutamide

5.3.2. Future Directions: Potential qPCR Assay Modifications

The assay described in this chapter has several advantages over FISH in terms of being amenable to high-throughput screening compared to competitor technologies such as FISH and whole genome sequencing. However, there are several modifications that could result in significant streamlining, specificity and sensitivity gains as well as increasing usefulness of the assay in the case of CaP patient stratification.

Use of TaqMan® to allow multiplexing - TaqMan® assays utilise a 3rd probe in the PCR reaction which binds to the target sequence in-between the forward and reverse primers. This 3rd probe is chemically labelled at the 5' end with a fluorescent reporter dye and a quencher is present at the 3' end. When the 3rd probe is bound to its complementary sequence and included into the PCR product the reporter and quencher are cleaved by the 5' to 3' activity of the DNA polymerase. This cleavage releases the reporter dye from the quencher and hence fluorescence is observed which is proportional to product amplification. By utilising different reporter dyes it is possible for multiple PCR reactions to be performed simultaneously e.g. *AR* reported by FAM, *DMD* reported by Texas Red and *GAPDH* reported by NED reporter dye. By converting the assay to a 'triplex' would theoretically lead to a reduction in assay preparation and sample usage (template DNA) by a factor of three. Additionally, through the use of a 3rd probe, specificity of the assay would also increase.

Use of Digital PCR - Digital PCR is a relatively new version of quantitative PCR and is depicted in (Fig. 59.) (Thermofisher, 2016). The defining feature of digital PCR vs traditional methodology is the partitioning of the sample into many parallel reactions (all in the same well). Upon partitioning some reactions will contain the template molecule and others will not, during the reaction each partition is measured for fluorescence accumulation akin to traditional qPCR (partitions which do not contain the target template will not be positive for fluorescence accumulation). Following PCR analysis, the number of positive and negative partitions is used to calculate, in absolute terms, the number of target molecules in the starting sample. The key advantages of digital PCR vs traditional qPCR are increased precision by using more PCR replicates without extra assay preparation and the elimination of the need for a 'reference' reaction and standards.

Incorporation of a sister assay such as 'primer walking' or an additional set of PCR probes specific for the ligand binding domain of *AR* (frequently truncated in CaP) to detect *AR*

mutations resulting in androgen independent AR activity and/or relaxed ligand specificity. This would allow patients with AR mutations to be stratified and treated accordingly.
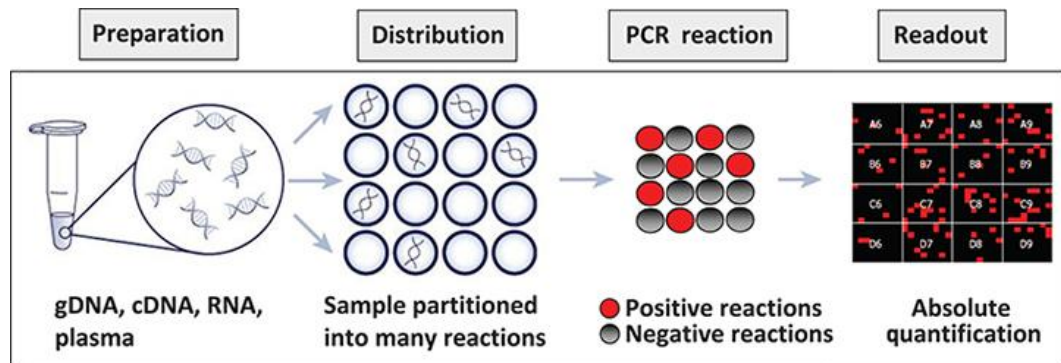
Fig. 59. Overview of Digital PCR.

From: (Thermofisher, 2016)

5.3.3. Future Directions: Increasing the Likelihood of Detecting Changes in Chromatin Status in the RARRES1 and LXN Genes through Experimental Modifications

It is possible that changes in chromatin status at the *RARRES1* and *LXN* genes in the prostate epithelium could be more thoroughly characterised through direct selection of cellular phenotypes from primary prostate tissue (without culture). This experimental design would preclude any artefactual changes in chromatin structure that may occur in *in vitro* cell culture. Another advantage of this experimental approach is that it would allow the interrogation of the most differentiated luminal cell population. Currently our laboratory are unable to maintain the terminally differentiated quiescent luminal fraction in culture.

Another possibility to enhance the potential identification of regulation through histone modifications would be to expose cells, differentially, to the known inducer of RARRES1 and LXN - atRA. This form of cellular manipulation has the potential to enhance the differences between tested samples to a greater extent than that achieved through 'enforced' differentiation in our culture system. A potential caveat to this approach is that atRA is known to induce differentiation which would deplete the SC population in the +atRA condition and may preclude analysis of this fraction. Even so, this approach should be considered for future studies on the epigenetic regulation of RARRES1 and LXN.

5.3.4. Future Directions: Increasing the Likelihood of Detecting Changes in Chromatin Status in the RARRES1 and LXN Genes through an Enhancement of the μChIP Protocol

The μChIP protocol used in this study has proven effective, allowing interrogation of epigenetic regulation from as little as 2 ng of chromatin/IP. This is incredible sensitivity, when one considers that 2 ng of chromatin can theoretically be derived from as few as 330 cells. However, no method can ever be considered perfect and incremental gains can still be made.

One possibility to enhance the current protocol is through use of 'hard' plastic sonication tubes. Harder plastics have been shown to transfer ultra-sonic waves more efficiently than softer plastic tubes, allowing the chromatin to be sheared more evenly and by fewer sonication cycles. Although hard plastic sonication tubes (such as those made from polystyrene) were advocated by the Collas protocol (Collas, 2011, Dahl and Collas, 2008), it was deemed a low-priority optimisation step given that many things had to be validated and that soft polypropylene tubes had proven to be adequate in previous publications

from our laboratory. The plastic tubes that I would advocate the use of in any further µChIP optimisation would be TPX® Polymethylpentene (PMP) tubes from Diagenode to improve sonication and shearing efficiency. As these tubes have been validated for use on the Bioruptor® Standard sonicator which is currently use for fragmenting chromatin in our laboratory.

Another possibility is to completely avoid sonication altogether through use of enzymatic digestion of chromatin to yield the desired chromatin fragment lengths (Duband-Goulet, 2016). The advantage of enzymatic digestion versus sonication is that enzymatic digestion is less 'harsh' than sonication. This property has the potential to preserve the integrity of the chromatin and antibody epitopes leading to enhanced efficiency, which may be even more apparent when trying to detect transcription factor-DNA interactions which are weaker than that of histone-DNA interactions.

One of the main limiting factors in antibody-based biological assays is the affinity and specificity of the capture antibody itself. The assays presented here used validated and well published antibodies against canonical marks. However, as no direct comparison was made to other capture antibodies it is possible that more effective antibodies are available which through increased affinity have the potential to increase IP efficiency.

5.3.5. Future Directions: Bivalent Chromatin or Mono-allelic Expression?

A very recent publication by (Shema et al., 2016) attempted to address the issue of bivalent chromatin, specifically the question to address was 'do opposing marks exist on the same histone molecule or is one allele enriched for one histone mark and the other allele enriched for the antagonistic histone mark?'

ChIP is incapable of answering this question. Although, the sequence that is enriched for the mark of interest can be obtained, it cannot provide information on the allele from which that sequence was derived (Rane et al., 2015). Moreover, ChIP is incapable of deciding whether a nucleosome is modified by two (or more) marks simultaneously, as the immunoprecipitations for each mark are performed in separate reactions and hence interrogate different nucleosomes populations. On the other hand, MS can detect the presence of two antagonistic marks on the same histone tail but it does not provide information on the sequence in which these modifications are associated with (Sidoli and Garcia, 2015). Through the use of sequential ChIP and MS it is possible to identify

coexistence of the opposing marks. However, it is not possible to definitely identify an individual bivalent-nucleosome which would be the best evidence of bivalent chromatin.

The method that was established and validated by this group uses a single molecule approach and involves the isolation of mono-nucleosomes and labelling them with fluorescent biotinylated oligonucleotides (Shema et al., 2016). The labelled nucleosomes are captured on polyethylene glycol (PEG) and streptavidin coated slides. After capturing, the nucleosomes are then incubated with fluorescently labelled antibodies to histone modifications of interest. Total internal reflection microscopy is then used to record the position of each nucleosome along with the presence of histone modifications - indicated by antibody binding (Shema et al., 2016).

5.3.6. Future Directions: Potential Transcription Factor and miRNA Regulators of LXN and RARRES1 Loci

Transcription factors that have the potential to co-regulate LXN and RARRES1 have been identified *in silico* using the Genomatix bioinformatics suite, including PromoterInspector MatInspector and ModelInspector (Table. 8.). This list was refined based on expression profiles of prostate epithelial cells of benign and malignant origin conducted by (Birnie et al., 2008) (Fig. 60.). Through this analysis, four lead candidates: hepatoma-derived growth factor (HDGF), DNA damage-inducible transcript 3 (DDIT3), nuclear factor erythroid 2-related factor 1 (NFE2L1) and activating transcription factor 4 (ATF4) have been discovered which merit experimental analysis through either knockdown or ChIP experiments.

Similarly, miRNAs with predicted binding sites on both LXN and RARRES1 mRNA 3' untranslated region (UTR)s have been identified (Table. 9). This *in silico* analysis was performed using microrna.org and mirwalk online tools bioinformatics tools. Alongside this analysis, the expression levels of the identified potential miRNA regulators in SC, TA, CB and PrEC cell populations and BPH, CaP and CRPC disease types. The miRNA data base published by (Rane et al., 2015) was used for expression analysis. Experimental validation of regulation by these miRNAs can be conducted through a 3' UTR luciferase reporter assay (Jin et al., 2013). This assay involves the generation of a DNA construct consisting a strong promoter, 3'UTR of RARRES1 or LXN, and luciferase DNA sequence (construct 1). A separate DNA construct containing potential miRNA identified by software screen (construct 2). Cells can then be transfected with either (construct 1) or (construct 2) alone

or the combination of (construct 1) and (construct 2). Interference by the miRNA will lead to a reduction in luminescence and hence confirmation of regulation.

Transcription Factor	p-value
Hepatoma-derived growth factor-**HDGF**	0.000222
Germ cell nuclear factor GCNR - **NR6A1**	0.003169
C/EBP homologous protein CHOP-**DDIT3**	0.007845
Zinc Finger Protein 628 - **ZNF628**	0.008663
Nuclear Factor, Erythroid 2-Like 1- **NFE2L1**	0.008831
Activating Transcription Factor 4-**ATF4**	0.009516
Paired Box 1-**PAX1**	0.009516

Table. 8. Potential Transcriptional Co-regulators of LXN and RARRES1.

Transcriptional co-regulators of LXN and RARRES1 were predicted using several tools of the online bioinformatics suite: Genomatix, including PromoterInspector MatInspector and ModelInspector. This data was combined and the most significant 'hits' are tabularised with the corresponding p-value.

miRNA name	Expression						
	SC	TA	CB	PrEC	BPH	PCa	CRPC
hsa-miR-148a*	3.40E-01	1.35E-04	1.87E-05	9.23E-05	4.53E-05	8.46E-05	5.28E-01
hsa-miR-148b*	2.47E-01	7.05E-02	1.10E-01	1.27E-01	6.44E-02	2.64E-01	7.53E-02
hsa-miR-452	4.26E-01	7.03E+00	6.98E+00	4.66E+00	3.47E+00	6.41E+00	4.45E+00
hsa-miR-450b-3p	6.40E-01	3.07E-01	5.83E-02	6.85E-01	2.86E-01	9.12E-02	7.04E-01
hsa-miR-450b-5p	3.54E-03	1.23E-04	1.04E-03	5.16E-03	3.16E-03	1.88E-04	2.17E-05
hsa-miR-1284	1.16E-01	7.33E-05	2.60E-05	2.51E-04	5.22E-05	1.06E-04	1.80E-01
hsa-miR-548k	1.64E+00	3.15E-01	1.88E-01	1.18E+00	5.66E-01	9.04E-01	4.96E-01
hsa-miR-20b*	1.07E-04	1.39E-04	7.28E-02	1.58E-05	3.18E-05	6.80E-02	1.99E-04
hsa-miR-20b	3.24E+01	2.58E+02	1.60E+02	1.60E+02	1.46E+02	1.57E+02	1.41E+02
hsa-miR-1208	2.72E+00	2.05E+00	3.35E+00	1.57E+00	4.72E+00	1.95E+00	1.00E+00
hsa-miR-1284	1.16E-01	7.33E-05	2.60E-05	2.51E-04	5.22E-05	1.06E-04	1.80E-01
hsa-miR-200c	2.17E+02	7.81E+02	2.70E+02	2.96E+02	4.65E+02	4.07E+02	4.19E+02
hsa-miR-200c*	1.55E+00	1.82E+00	8.35E-01	1.04E+00	1.57E+00	1.68E+00	7.82E-01
hsa-miR-429	5.49E+00	6.04E+01	2.63E+01	2.02E+01	2.34E+01	4.01E+01	3.07E+01
hsa-miR-374a	2.75E+00	5.51E+01	1.89E+01	1.68E+01	2.09E+01	3.27E+01	2.45E+01
hsa-miR-374a*	3.64E-03	7.67E-04	2.34E-05	1.60E-02	8.44E-04	6.53E-05	3.33E-05
hsa-miR-374b	2.69E+00	3.02E+01	3.70E+01	2.62E+01	1.99E+01	2.52E+01	2.47E+01
hsa-miR-374b*	4.78E-01	4.05E-01	4.43E-01	1.77E+00	2.92E-01	4.28E-01	2.74E-01
hsa-miR-17*	1.36E+00	3.90E+01	1.41E+01	1.35E+01	1.54E+01	2.00E+01	2.12E+01

Table. 9. Potential Post-Translational Co-regulators of LXN and RARRES1.

Post-translational co-regulators of LXN and RARRES1 were predicted using microrna.org and mirwalk. miRNA expression in the prostate epithelia of potentially important miRNAs was investigated using an 'in-house' miRNA expression database Rane et al (2015). This data was combined and shown in the table.

SC. Stem Cell, **TA.** Transit Amplifying Cell, **CB.** Committed Basal Cell, **PrEC.** Normal Human Prostate Epithelial Cells, **BPH.** Benign Prostatic Hyperplasia, **PCa.** Prostate Cancer and **CRPC.** Castration-resistant Prostate Cancer
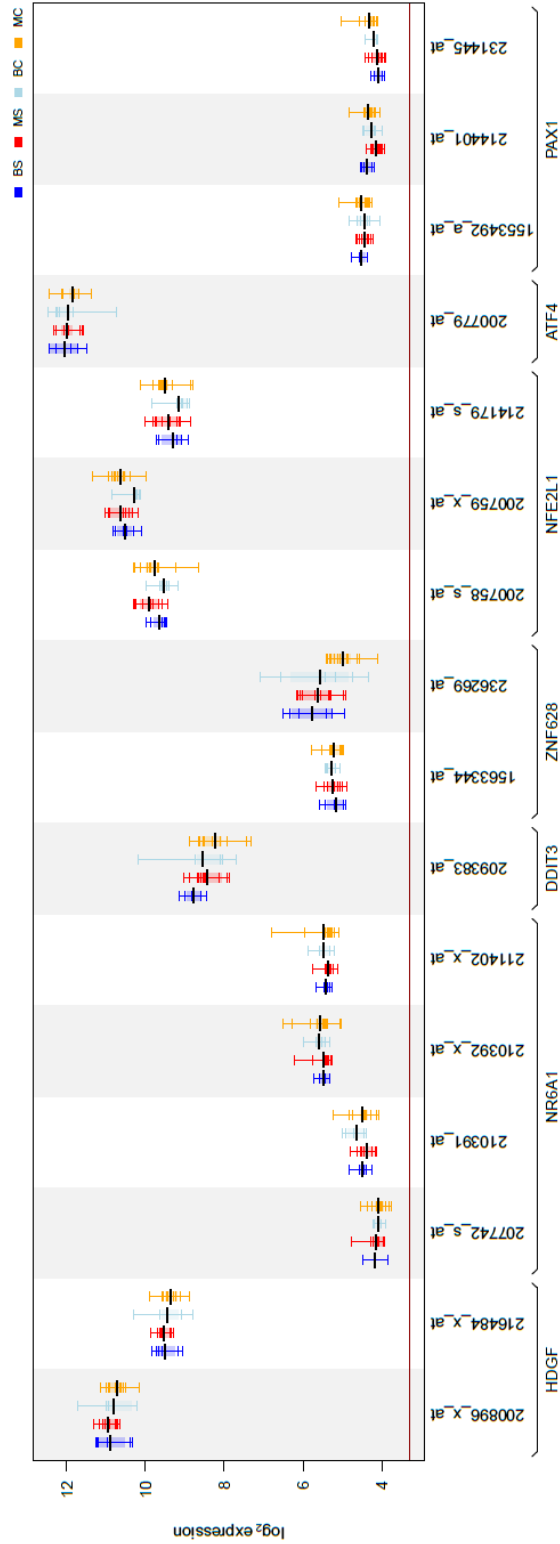
Fig. 60. mRNA Expression of Potential Transcriptional Co-regulators of LXN and RARRES1 in Basal Prostate Cells.

The mRNA Expression of Potential Transcriptional Co-regulators of LXN and RARRES1 previously identified by bioinformatics analysis was determined using an 'in-house' mRNA database. Expression was compared between Benign Stem Cells (**BS**), Malignant Stem Cells (**MS**), Benign Committed Basal Cells (**BC**) and Malignant Committed Basal Cells (**MC**). Labels on the X-axis are the probe numbers used in the micro-array.

HDGF = Hepatoma-derived growth factor, NR6A1 = Germ cell nuclear factor GCNR, DDIT3 = C/EBP homologous protein CHOP, ZNF628 = Zinc Finger Protein 628 NFE2L1 = Nuclear Factor, Erythroid 2-Like 1, ATF4 = Activating Transcription Factor 4, PAX1 =Paired Box 1.

6. Conclusions

The aim of developing a qPCR based method for the identification and quantification of *AR* gene amplification has been comprehensively met. The assay described in this report can distinguish between male (one copy of *AR*) and female (two copies) DNA and is sensitive enough to detect the presence of a duplication of the *AR* gene even if only 20% of the sample harbours the duplication. It is therefore suitable for the interrogation of heterogeneous biopsy samples. The inclusion of *DMD* as an X-encoded control gene has expanded the applicability of this assay by allowing simultaneous detection of XCA which is common in hormone naïve CaP (~25%) and is a poor prognostic indicator. Assay validation was performed using ten blinded samples (five positive and five negative) in which the GAAR status was independently verified by FISH. All GAAR positive samples were identified and none of the GAAR negative samples were misidentified. GAAR and XCA were detected in at least two near-patient xenografts derived from CRPC tissue. One such passage zero xenograft (H455X) exhibited an inferred XCA of four and a GAAR of seven relative to patient-derived lymphocyte DNA. The assay was subsequently shown to be compatible with DNA derived from FFPE tissue. Detection of GAAR and XCA in near-patient xenografts derived from CRPC tissue is strong evidence that these genetic abnormalities are present in cells capable of tumour reconstitution *in vivo*. This new method has several advantages over FISH including a shorter 'turnaround time' and it is more amenable to high throughput scaling. The technique has the potential to triage patients according to their GAAR and XCA status, allowing an improved personalised-medicine approach for the treatment of CRPC.

In order to facilitate further study of RARRES1 and LXN overexpression, particularly in primary prostate epithelial cells, lentiviral vector production using Gateway™ cloning and viral particle generation was established, validated and optimised. This allowed the production of viral titres in excess of $1x10^7$ IU/ml. These vectors stably transduced primary prostate epithelial cells with high efficiency and transgene silencing was not observed. This is in contrast to a published, previous attempt to utilise lentiviral vectors by our lab, which were limited by low titres, low transduction efficiency and promoter silencing. Lentiviral vectors permitted the analysis of changes in gene expression induced by RARRES1 and LXN overexpression and analysis of the intracellular localisation of LXN.

I have investigated the intracellular localisation of LXN utilising confocal microscopy of live cell imaging of mVenus tagged LXN and subcellular fractionation. The results of this

analysis show that in primary prostate epithelial cells that LXN is a pan-cellular protein capable of accessing both the cytoplasm and the nucleus.

ChIP was used to investigate the role that posttranslational modification of histone proteins plays in the epigenetic regulation of RARRES1 and LXN. It was discovered that RARRES1 is epigenetically regulated through histone protein modifications in PNT2C2 cells. In order to investigate this regulatory mechanism in primary prostate SCs, a µChIP method was established and validated. This allowed the first targeted study of *LXN* and *RARRES1* promoter regions. The results of this analysis provided evidence for 'poised chromatin' (a characteristic of embryonic stem cells) in both the *LXN* and *RARRES1* promoters which were both enriched above the IgG control by anti-H3K27me3 (inactive mark) and anti-H3K4me3 (active mark) relative to negative control genes (*GAPDH* for H3K27me3 and *PDYN* for H3K4me3).

Progress has been made on the identification of LXN and RARRES1 interactors, to this end MS was used to generate a 'hit list' for both proteins. Whilst both data sets remain un-validated, the LXN hits agree with the newly discovered pan-cellular distribution and the RARRES1 hits agree with the published localisation of RARRES1 to the endoplasmic reticulum membrane.

Appendices

Appendix 1. Patient samples

Sample ID	Pathology
H024	CaP 4+3=7
H027	CaP 5+4=9
H042	CaP 3+4=7
H110	CaP 3+4=7
H135	CaP 5+4=9
H217	CaP 3+4=7
H220	CaP 3+4=7
H224	CaP 4+5=9
H226	BPH
H227	BPH
H229	CaP 4+4=8
H427	CaP 4+5=9
H455	CRPC
H460	CaP 4+5=9
H493	CaP 4+5=9
H521	CaP 3+4=7
H530	CaP 4+4=8
H533	BPH
HaCaP	CRPC
Y018	CRPC
Y019	CRPC

Appendix 2. Primers

Name	Sequence		Annealing Temperature °C
	Forward	**Reverse**	
AR	TCATTATCAGGTCTATCAACTCTT	GTCATCCCTGCTTCATAACATTTC	58
DMD	TTGGTTGCCAGTTATGGGCT	CCAGCTGTCATGCAAAACCC	58
GAPDH	ATGCTGCATTCGCCCTCTTA	GCGCCCAATACGACCAAATC	58
LXN PP1	TCCAGTATGCAAGCGAAGCA	CGCTGGGATTGCATCTTTCG	55
LXN PP2	GACAGTGTCTGCAAAGCAAA	TACCATCTGTCTGCTTGCCC	58.5
LXN PP3	TCCTGGACTGCACATATAATGACA	AAACTGGCTGTAGCTCACCT	55
LXN PP4	CCCGGGACTGTTTTCACCTT	GAAAGTGCTGCCCCTTACCT	55
LXN PP5	AGCCCCTCCAACCAAATGAG	GGTGATACTTATGTCCTCTTCCTGG	58.5
RARRES1 PP1	GCTGCGGCCTGCCCCTTTCTC	ACTTGGCGTTTCCCCTGCGGTTTC	58.5
RARRES1 PP2	ACCACCCACTGGCAAAAAGA	TGCTAGGCACTCCCAACATC	58.5
RARRES1 PP3	ATGACTGGGTTCTGGGAGGT	GATCAGCGGATCCTGGAGTT	55
RARRES1 PP4	TAATTGCAGTCCACCACGCT	ATCAGACGCCAGCATTAGCA	58.5
RARRES1 PP5	CCTAGTCCAACAGAGCAGTGA	CCCTTCTTTAGGCTCTGGGC	58.5
GAPDH(ChIP)	CCTAGGTGGGGGACGTTTCTTTC	AACGGCTGCCCATTCATTTCCTTC	58.5
PDYN	AGGGCTTTGGTGGTGTTC	AGTGCCCCCCTCTGGATGTTAC	55

Appendix 3. Antibodies

Antibody	Source	Dilution Factor	
		WB	IF
anti-HA	Sigma	1 : 10,000	1 : 1,000
anti-Latexin	Sigma	1 : 3,000	N/A
anti-RARRES1	Sigma	1 : 1,000	N/A
anti-IPO7	Sigma	1 : 10,000	N/A
anti-alpha-tubulin	Abcam	1 : 10,000	N/A
anti-TBP	Abcam	1 : 10,000	N/A
ant-GAPDH	Proteintech	1 : 10,000	N/A
anti-RNApol II	Abcam	N/A	N/A
anti-H3K4me3	Millipore	N/A	N/A
anti-H3K27me27	Millipore	N/A	N/A
IgG control	Millipore	N/A	N/A

Appendix 4. Plasmids

Plasmid	Backbone	Resistance
GFP-HA	pReciever-M06	Ampicillin
LXN-HA	pReciever-M06	Ampicillin
LXNcpa-HA	pReciever-M06	Ampicillin
RARRES1-HA	pReciever-M45	Ampicillin
RARRES1cpa-HA	pReciever-M45	Ampicillin
RARRS1tmdel-HA	pReciever-M45	Ampicillin
LXN-pDonor-221	pDonor-221	Kanamycin
LXNcpa-pDonor-221	pDonor-221	Kanamycin
RARRES1-pDonor-221	pDonor-222	Kanamycin
RARRES1cpa-pDonor-221	pDonor-223	Kanamycin
RARRES1tmdel-pDonor-221	pDonor-224	Kanamycin
GUS-pDonor-221	pDonor-225	Kanamycin
LXN-pDest-298	pDest-298	Ampicillin
LXNcpa-pDest-298	pDest-298	Ampicillin
RARRES1-pDest-298	pDest-298	Ampicillin
RARRES1cpa-pDest-298	pDest-298	Ampicillin
RARRES1tmdel-pDest-298	pDest-298	Ampicillin
GUS-pDest-298	pDest-298	Ampicillin
LXN-pDest-159	pDest-159	Ampicillin
LXNcpa-pDest-159	pDest-159	Ampicillin
RARRES1-pDest-159	pDest-159	Ampicillin
RARRES1cpa-pDest-159	pDest-159	Ampicillin
RARRES1tmdel-pDest-159	pDest-159	Ampicillin
GUS-pDest-159	pDest-159	Ampicillin
LXN-pDest-236	pDest-236	Ampicillin
LXNcpa-pDest-236	pDest-236	Ampicillin
RARRES1-pDest-236	pDest-236	Ampicillin
RARRES1cpa-pDest-236	pDest-236	Ampicillin
RARRES1tmdel-pDest-236	pDest-236	Ampicillin
GUS-pDest-236	pDest-236	Ampicillin
LXN-FU-tetO	FU-tetO-Gateway	Ampicillin
LXNcpa-FU-tetO	FU-tetO-Gateway	Ampicillin
RARRES1-FU-tetO	FU-tetO-Gateway	Ampicillin
RARRES1cpa-FU-tetO	FU-tetO-Gateway	Ampicillin
RARRES1tmdel-FU-tetO	FU-tetO-Gateway	Ampicillin
GUS-pDest-FU-tetO	FU-tetO-Gateway	Ampicillin

Appendix 5. IgH and EBV Testing of Xenogratft Models
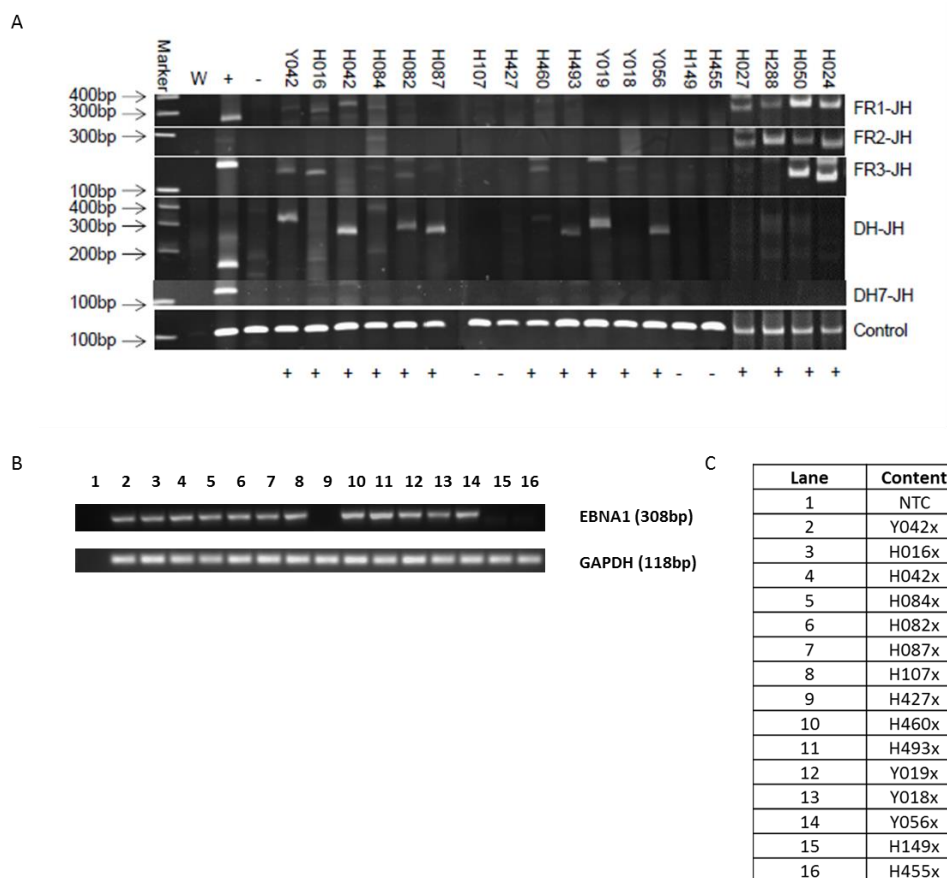
A = *IGH* rearrangements in a PDX panel. PCR amplification of VJD regions using a multiplex PCR. W = water control. + = positive control (B cell lymphoma clonal control). - = negative control (prostate epithelial primary culture). 暨Rearrangements in Y042, H016, H042, H084, H027, H288, H050, H024 are within the valid size range (310-360bp). FR2-JH: H084, H027, H288, H050, H024 are within the valid size range (250-295bp). FR3-JH: Y042, H016, H084, H082, H087, H460, Y018, H050, H024 are within the valid size range (100-170bp). DH-JH: H084, H087, H493, Y056 are within the valid size range (110-290 and 390-420bp). DH7-JH: valid size range is 100-130bp.

Clonality was evaluated by PCR for V-J gene rearrangements of the *IgH* locus using the IdentiClone™ diagnostic kit from Invivoscribe. The assay employs multiple consensus DNA primers that target conserved genetic regions within the *IgH* locus. The test includes 6 master mixes targeting the conserved framework (FR) of the variable (V) regions and the conserved joining (J) regions, as well as the diversity (D) and joining regions. PCR products were loaded onto a non-denaturing 6% polyacrylamide TBE gel and visualised under UV light using GeneSnap ID software (Syngene).

B = EBV testing of xenograft samples. Xenograft samples were interrogated for presence of EBV by PCR using primers specific for Epstein–Barr nuclear antigen 1 (*EBNA1*).psPCR products were loaded on to a 1.5% Agarose TBE gel and visualised under UV light using GeneSnap ID software (Syngene). Lane guide is shown in C.

Abbreviations

Abbreviation	Description
°C	Degree(s) Celsius
18S	18S ribosomal RNA
2+Edel	Fusion of *TMPRSS2* to the *ERG* sequence together with interstitial deletion of sequences 5' to *ERG*
ADP	Adenosine diphosphate
ADT	Androgen deprivation therapy
AF	Activation function
Akt	Serine/threonine Kinase 1
ALL	Acute lymphoblastic leukaemia
AML	Acute myeloid leukaemia
APL	Acute promyelocytic leukaemia
AR	Androgen Receptor
ARE	Androgen response element
AR-V7	Androgen-receptor splice variant 7
ATF4	Activating transcription factor 4
ATP	Adenosine triphosphate
atRA	All-trans retinoic acid
attB	Site of site-specific recombination B
attP	Site of site-specific recombination P
attR	Site of site-specific recombination R
B cell	B lymphocyte
BALB/c	Albino, laboratory-bred strain of the house mouse
BCA	Bicinchoninic acid
bcl-2	B-cell lymphoma 2
BCR/ABL	Fusion gene juxta positioning the Abl1 gene on chromosome 9 (region q34) to a part of the BCR ("breakpoint cluster region") gene on chromosome 22 (region q11)
BM	Basement membrane
BMP	Bone morphogenetic protein
bp	Base pairs
BPH	Benign prostatic hyperplasia
BRAF	Murine sarcoma viral oncogene homolog B
BRCA1	Breast cancer 1
BRCA2	Breast cancer 2
BRDU	5-bromo-2'-deoxyuridine
BSA	Bovine serum albumin
CAIS	Complete androgen insensitivity syndrome
Camp	Cyclic adenosine monophosphate
CaP	Prostate cancer
CARN	Castration-resistant Nkx3.1-expressing cells
CB	Committed basal cell
ccb	Bacterial death gene
CD	Cluster of differentiation

cDNA	Complementary DNA
ChIP	Chromatin immunoprecipitation
CI	Confidence interval
CIN	Chromosomal instability
CK	Cytokeratin
c-met	Tyrosine-protein kinase Met
c-Myc	Avian myelocytomatosis viral oncogene homolog
CNL	Chronic neutrophilic leukaemia
CO_2	Carbon dioxide
Co-IP	Co-immunoprecipitation
CPA	Carboxypeptidase A
CpG	A cytosine base followed immediately by a guanine base
CPI	Carboxypeptidase inhibitor
cPPT	Central polypurine tract
cPSA	Complexed PSA
Cq	Quantification cycle
CRAPome	The contaminant repository for affinity purification
CREB	Camp response element-binding protein
CRE-LOX	Site-specific recombinase technology utilising Cre recombinase and Lox sequence both derived from bacteriophage P1
CRPC	Castration-resistant prostate cancer
CSC	Cancer stem cell
Ct	Threshold cycle
CTC	Circulating tumour cells
CYP17	Cytochrome P450 17alpha hydroxylase/17,20 lyase
D10	DMEM + 10% FCS
DAPI	4',6-diamidino-2-phenylindole
DBD	DNA-binding domain
ddH20	Double distilled water
DDIT3	DNA damage-inducible transcript 3
DEPC	Diethylpyrocarbonate
DHFR	Dihydrofolate reductase
DHT	5α-dihydrotestosterone
DKK1	Dickkopf-related protein 1
DMD	Dystrophin
DMEM	Dulbecco's modified eagle medium
DMSO	Dimethyl sulfoxide
DNA	Deoxyribonucleic acid
DNMTi	DNA methyltransferase inhibitors
dNTP	Deoxynucleotide
dsDNA	Double-stranded DNA
DTT	Dithiothreitol
EB1	End-binding protein-1
EBV	Epstein–Barr virus
E.Coli	Escherichia coli
EDTA	Ethylenediaminetetraacetic acid

EGF	Epidermal growth factor
eGFP	Enhanced GFP
EGFR	Epidermal growth factor receptor
EGTA	ethylene glycol-bis(β-aminoethyl ether)-N,N,N',N'-tetraacetic acid
ELF-3	E74 like ETS transcription factor 3
EMA	European medicines agency
EMT	Epithelial–mesenchymal transition
env	HIV virulence gene – env
ER	Oestrogen receptor
ERG	ETS-related gene
Erks	Extracellular signal–regulated kinases
ESR1	Oestrogen receptor alpha
EZH2	Enhancer of zeste homolog 2
FAM	Fluorescein
FCS	Foetal calf serum
FDA	Food and drug administration
FFPE	Formalin fixed paraffin embedded
FGF	Fibroblast growth factor
FISH	Fluorescent in situ hybridization
FLAG	FLAG epitope tag, sequence motif = DYKDDDDK
fmol	Femtomole
Foxa1	Forkhead box protein A1
fPSA	Free PSA
g/L	Gram per litre
GAAR	Genomic amplification of the AR gene
gag-pol	Polyprotein – reverse transcriptase derived from HIV
GAPDH	Glyceraldehyde 3-phosphate dehydrogenase
GC:AT	Guanine and cytosine to adenine and thymine ratio
gDNA	Genomic DNA
GFP	Green fluorescent protein
GIN	Genomic instability
GnRH	Gonadotropin-releasing hormone
gp120	Envelope glycoprotein GP120
GPCRs	G-protein-coupled receptors
GRK5	G-protein-coupled receptor kinase 5
GST	Glutathione S-transferases
GUS	β-glucuronidase
Gy	Gray
h	Hours
H&E	Haematoxylin and eosin stain
H1	Histone 1
H2A	Histone 2A
H2AK119Ub	Monoubiquitination of lysine-119 of Histone 2A
H2B	Histone 2B
H3	Histone H3
H3K27	Lysine 27 on histone 3

H3K27me3	Trimethylation of lysine 27 on histone 3
H3K36	Lysine 36 on histone 3
H3K4	Lysine 27 on histone 3
H3K4me3	Trimethylation of lysine 4 on histone 3
H3K79	Lysine 79 on histone 3
H3K9	Lysine 9 on histone 3
H3K9ac	Acetylation of lysine 9 on histone 3
H3K9me2	Dimethylation of lysine 9 on histone 3
H4	Histone 4
H4K20	Lysine 20 on histone 4
H4K20me3	Trimethylation of lysine 20 on histone 4
HA	Hemagglutinin
HAT	Histone acetyltransferase
HCl	Hydrochloric acid
HDAC	Histone deacetylases
HDACI	Histone deacetylase inhibitor
HDGF	Hepatoma-derived growth factor
HER2	Human epidermal growth factor receptor 2
HGPIN	High-grade PIN
HIS	Polyhistidine-tag
HIV	Human immunodeficiency virus
HPLC	High performance liquid chromatography
HR	Hormone responsive
HRP	Horseradish peroxidase
HSC	Hematopoietic stem cell
HSP	Heat shock protein
IF	Immunofluorescence
IgG	Immunoglobulin G
IGH	Immunoglobulin heavy chain locus
IL	Interleukin
IP	Immunoprecipitation
IPO7	Importin-7
IU/ml	Infectious units per millilitre
kb	Kilobase
KCl	Potassium chloride
kDa	Kilo Dalton
Ki67	Antigen KI-67
KRAS	Kirsten rat sarcoma viral oncogene homolog
KSFM	Keratinocyte serum-free medium
LB	Lysogeny broth
LBD	Ligand-binding domain
LC-MS	Liquid chromatography–mass spectrometry
LiCl	Lithium chloride
Lin	Lineage markers
lncRNA	Long non-coding RNA
LTR	Long terminal repeat
LV	Lentivirus

LXN	Latexin
M	Molar
MACS	Magnetic-activated cell sorting
Mek	Mitogen-activated kinase
MFH	Malignant fibrous histiocytoma
mg	Milligrams
min	Minutes
miR	Mature form of the miRNA
miRNA	microRNA
ml	Millilitre
mm	Millimetre
Mm	Millimolar
MOI	Multiplicity of infection
MOPS	3-(N-morpholino)propanesulfonic acid
mRNA	Messenger RNA
MS	Mass spectrometry
MSCs	Mesenchymal stem cells
mTOR	Mechanistic target of rapamycin
MTX	Methotrexate
mVenus	Modified version of yellow fluorescent protein
MW	Molecular weight
NaAc	Sodium acetate
NaCl	Sodium chloride
NaOH	Sodium hydroxide
NCBI	National center for biotechnology information
NED	Reporter dye used in TaqMan assays
NF κβ	Nuclear factor kappa-light-chain-enhancer of activated B cells
NFE2L1	Nuclear factor erythroid 2-related factor 1
ng	Nanogram
ng/ml	Nanogram per millilitre
NHS	National health service
NICE	The national institute for health and care excellence
Nkx3.1	Homeobox protein Nkx-3.1
nM	Nanomolar
nm	Nanometre
NOD/SCID	Nonobese diabetic/severe combined immunodeficiency
NP-40	Tergitol-type NP-40
ns	Non-significant
NTD	Amino-terminal domain
OCT4	Octamer-binding transcription factor 4
OG	Oncogenes
p53	Tumour protein p53
p63	Tumour protein p63
PAP	Prostatic acid phosphatase
psPAX2	Lentiviral packaging plasmid containing Gag, Pol, Rev sequences
PBS	Phosphate-buffered saline

PCA3	Prostate cancer gene 3
PCNA	Proliferating cell nuclear antigen
PCR	Polymerase chain reaction
pDEST	Destination plasmid
PDGFRB	Platelet derived growth factor receptor beta
PDK1	Phosphoinositide-dependent kinase-1
Pdonr-221	Gateway™ cloning plasmid containing Puc origin for high plasmid yields and universal M13 sequencing sites
PDX	Patient-derived xenograft
PDYN	Neoendorphin-dynorphin-enkephalin prepropeptide gene
PEG	Polyethylene glycol
PGE2	Prostaglandin E2
pH	Potential of hydrogen
PI3K	Phosphatidylinositol-4,5-bisphosphate 3-kinase
PIN	Prostatic intraepithelial neoplasia
PIP2	Phosphatidylinositol 4,5-bisphosphate
PIP3	Phosphatidylinositol (3,4,5)-trisphosphate
PIPES	piperazine-N,N'-bis(2-ethanesulfonic acid)
PML	Promyelocytic leukaemia
PMP	Polymethylpentene
PP2A	Serine/threonine-protein phosphatase 2A
PPAR	Peroxisome proliferator-activated receptor
PPP2CB	Serine/threonine-protein phosphatase 2A catalytic subunit beta isoform
Pre-miRNA	Precursor microRNA
Pri-miRNA	Primary miRNA
PSA	Prostate-specific antigen
PSMA	Prostate-specific membrane antigen
PTEN	Phosphatase and tensin homolog
PURO-R	Puromycin-resistance gene
QC	Quality Control
qPCR	Quantitative polymerase chain reaction
R10	RPMI + 10% FCS
R^2	Statistical measure of closeness of fit to a regression line
RA	Retinoic acid
Raf	Proto-oncogene serine/threonine-protein kinase
RAG2	Recombination activating gene 2
RAR	Retinoic acid receptor
RARE	Retinoic acid response element
RARRES1	Retinoic acid receptor responder 1
Rb	Retinoblastoma protein
rev	Regulatory protein Rev, essential for post-transcriptional transport of the un-spliced and incompletely spliced viral mRNAs from nuclei to cytoplasm
RIN	RNA integrity number
RIPA	Radioimmunoprecipitation assay
RISC	RNA-induced silencing complex

RNA	**Ribonucleic acid**
RNA pol II	**RNA polymerase II**
RNase	**Ribonuclease**
RNA-seq	**RNA sequencing**
RPLPO	**60S acidic ribosomal protein P0**
RPM	**Revolutions per minute**
RPMI	**Roswell park memorial institute-1640 medium**
RPS3	**Ribosomal protein S3**
RRE	**Rev responsive element**
rRNA	**Ribosomal RNA**
RT	**Room temperature**
RT-PCR	**Reverse transcription polymerase chain reaction**
RXR	**Retinoid X receptor**
S100P	**S100 calcium-binding protein P**
SC	**Stem cell**
Sca-1	**Stem cells antigen-1**
SDS	**Sodium dodecyl sulphate**
SDS-PAGE	**Sodium dodecyl sulphate polyacrylamide gel electrophoresis**
secs	**Seconds**
SHH	**Sonic hedgehog**
SIN	**Self-inactivating configuration**
SLPI	**Secretory leukocyte protease inhibitor**
SOC	**Super optimal broth with catabolite repression**
SP	**Side population**
SQ	**Starting quantity**
Src	**Proto-oncogene tyrosine-protein kinase Src**
ssDNA	**Single-stranded DNA**
SV40	**Simian vacuolating virus 40**
T cell	**T lymphocyte**
TA	**Transit amplifying cells**
TAE	**Tris-acetate-EDTA**
TAF	**TBP-associated factor**
TAQ	**Thermus aquaticus**
TBP	**TATA-binding protein**
TBST	**Tris-buffered saline with 0.1% Tween 20**
TCF	**T cell factor**
TE	**Tris-EDTA**
TIC	**Tumour initiating cells**
TMPRSS2	**Transmembrane protease, serine 2**
TMPRSS2-ERG	**Fusion of *TMPRSS2* gene to the *ERG* gene**
TRAIL	**Tumour necrosis factor-related apoptosis-inducing ligand**
TRAMP	**Transgenic adenocarcinoma of the mouse prostate**
Tris	**(HOCH2)3CNH2**
tRNA	**Transfer ribonucleic acid**
Trop2	**Tumour-associated calcium signal transducer 2**
TSG	**Tumour suppressor genes**

TURP	Transurethral resection of the prostate
U/ml	Unit per millilitre
UGE	Urogenital sinus epithelium
UK	United Kingdom
USM	Urogenital sinus mesenchyme
UTR	Untranslated region
UV	Ultraviolet
V	Volt
v/v	Volume per volume
V5	Epitope tag derived from the RNA polymerase α subunit of simian parainfluenza virus type 5
VSV-G	Vesicular stomatitis Indiana virus – protein G
w/v	Weight per volume
WFDC1	WAP four-disulphide core domain 1
Wnt	Wingless-related integration site protein
WPRE	Woodchuck hepatitis virus post-transcriptional regulatory element
WT	Wild type
x g	Times gravity – units of relative centrifugal force
XCA	X chromosome aneuploidy
α2β1	Collagen receptor
γC	Common gamma chain
γH2AX	Phosphorylation on serine 139 of histone H2A variant X
µChIP	Micro chromatin immunoprecipitation
µg	Microgram
µg/ml	Microgram per millilitre
µl	Microlitre
mM	Micromolar
µm	Micrometre

References

Aagaard, A., Listwan, P., Cowieson, N., Huber, T., Ravasi, T., Wells, C. A., Flanagan, J. U., Kellie, S., Hume, D. A., Kobe, B. and Martin, J. L. (2005) 'An inflammatory role for the mammalian carboxypeptidase inhibitor latexin: relationship to cystatins and the tumor suppressor TIG1', *Structure,* 13(2), pp. 309-17.

Adhikari, A. S., Agarwal, N. and Iwakuma, T. (2011) 'Metastatic potential of tumor-initiating cells in solid tumors', *Front Biosci (Landmark Ed),* 16, pp. 1927-38.

Agalliu, I., Kwon, E. M., Zadory, D., McIntosh, L., Thompson, J., Stanford, J. L. and Ostrander, E. A. (2007) 'Germline mutations in the BRCA2 gene and susceptibility to hereditary prostate cancer', *Clin Cancer Res,* 13(3), pp. 839-43.

Ahuja, D., Sáenz-Robles, M. T. and Pipas, J. M. (2005) 'SV40 large T antigen targets multiple cellular pathways to elicit cellular transformation', *Oncogene,* 24(52), pp. 7729-45.

Al Tanoury, Z., Piskunov, A. and Rochette-Egly, C. (2013) 'Vitamin A and retinoid signaling: genomic and nongenomic effects', *J Lipid Res,* 54(7), pp. 1761-75.

Al-Hajj, M., Becker, M. W., Wicha, M., Weissman, I. and Clarke, M. F. (2004) 'Therapeutic implications of cancer stem cells', *Curr Opin Genet Dev,* 14(1), pp. 43-7.

Al-Hajj, M., Wicha, M. S., Benito-Hernandez, A., Morrison, S. J. and Clarke, M. F. (2003) 'Prospective identification of tumorigenic breast cancer cells', *Proc Natl Acad Sci U S A,* 100(7), pp. 3983-8.

Al-Mehdi, A. B., Tozawa, K., Fisher, A. B., Shientag, L., Lee, A. and Muschel, R. J. (2000) 'Intravascular origin of metastasis from the proliferation of endothelium-attached tumor cells: a new model for metastasis', *Nat Med,* 6(1), pp. 100-2.

Albertson, D. G. (2012) 'ESR1 amplification in breast cancer: controversy resolved?', *J Pathol,* 227(1), pp. 1-3.

Altieri, D. C. (2013) 'Targeting survivin in cancer', *Cancer Lett,* 332(2), pp. 225-8.

An, J., Chervin, A. S., Nie, A., Ducoff, H. S. and Huang, Z. (2007) 'Overcoming the radioresistance of prostate cancer cells with a novel Bcl-2 inhibitor', *Oncogene,* 26(5), pp. 652-61.

Asamoto, M., Hokaiwado, N., Cho, Y. M., Takahashi, S., Ikeda, Y., Imaida, K. and Shirai, T. (2001) 'Prostate carcinomas developing in transgenic rats with SV40 T antigen expression under probasin promoter control are strictly androgen dependent', *Cancer Res,* 61(12), pp. 4693-700.

Attard, G., Rizzo, S., Ledaki, I., Clark, J., Reid, A. H., Thompson, A., Khoo, V., de Bono, J. S., Cooper, C. S. and Hudson, D. L. (2009) 'A novel, spontaneously immortalized, human prostate cancer cell line, Bob, offers a unique model for pre-clinical prostate cancer studies', *Prostate,* 69(14), pp. 1507-20.

Azzouni, F. and Mohler, J. (2012) 'Biology of castration-recurrent prostate cancer', *Urol Clin North Am,* 39(4), pp. 435-52.

Bannister, A. J. and Kouzarides, T. (2011) 'Regulation of chromatin by histone modifications', *Cell Res,* 21(3), pp. 381-95.

Bao, S., Wu, Q., McLendon, R. E., Hao, Y., Shi, Q., Hjelmeland, A. B., Dewhirst, M. W., Bigner, D. D. and Rich, J. N. (2006) 'Glioma stem cells promote radioresistance by preferential activation of the DNA damage response', *Nature,* 444(7120), pp. 756-60.

Barros, S. P. and Offenbacher, S. (2009) 'Epigenetics: connecting environment and genotype to phenotype and disease', *J Dent Res,* 88(5), pp. 400-8.

Bartolomei, M. S. and Tilghman, S. M. (1997) 'Genomic imprinting in mammals', *Annu Rev Genet,* 31, pp. 493-525.

Bastien, J. and Rochette-Egly, C. (2004) 'Nuclear retinoid receptors and the transcription of retinoid-target genes', *Gene,* 328, pp. 1-16.

Bell, J. (2013) *Realising the potential of stratified medicine*, Journal of Academy of Medical Sciences: The Academy of Medical Sciences.

Berry, P. A., Maitland, N. J. and Collins, A. T. (2008) 'Androgen receptor signalling in prostate: effects of stromal factors on normal and cancer stem cells', *Mol Cell Endocrinol,* 288(1-2), pp. 30-7.

Berry, S. J., Coffey, D. S., Walsh, P. C. and Ewing, L. L. (1984) 'The development of human benign prostatic hyperplasia with age', *J Urol,* 132(3), pp. 474-9.

Berthon, P., Cussenot, O., Hopwood, L., Leduc, A. and Maitland, N. (1995) 'Functional expression of sv40 in normal human prostatic epithelial and fibroblastic cells - differentiation pattern of nontumorigenic cell-lines', *Int J Oncol,* 6(2), pp. 333-43.

Bhatia-Gaur, R., Donjacour, A. A., Sciavolino, P. J., Kim, M., Desai, N., Young, P., Norton, C. R., Gridley, T., Cardiff, R. D., Cunha, G. R., Abate-Shen, C. and Shen, M. M. (1999) 'Roles for Nkx3.1 in prostate development and cancer', *Genes Dev,* 13(8), pp. 966-77.

Bhavsar, A. and Verma, S. (2014) 'Anatomic imaging of the prostate', *Biomed Res Int,* 2014, pp. 728539.

Biermann, J., Boyle, J., Pielen, A. and Lagrèze, W. A. (2011) 'Histone deacetylase inhibitors sodium butyrate and valproic acid delay spontaneous cell death in purified rat retinal ganglion cells', *Mol Vis,* 17, pp. 395-403.

Bill-Axelson, A., Holmberg, L., Ruutu, M., Häggman, M., Andersson, S. O., Bratell, S., Spångberg, A., Busch, C., Nordling, S., Garmo, H., Palmgren, J., Adami, H. O., Norlén, B. J., Johansson, J. E. and 4, S. P. C. G. S. N. (2005) 'Radical prostatectomy versus watchful waiting in early prostate cancer', *N Engl J Med,* 352(19), pp. 1977-84.

Birnie, R., Bryce, S. D., Roome, C., Dussupt, V., Droop, A., Lang, S. H., Berry, P. A., Hyde, C. F., Lewis, J. L., Stower, M. J., Maitland, N. J. and Collins, A. T. (2008) 'Gene expression profiling of human prostate cancer stem cells reveals a pro-inflammatory phenotype and the importance of extracellular matrix interactions', *Genome Biol,* 9(5), pp. R83.

Blackwood, J. K., Williamson, S. C., Greaves, L. C., Wilson, L., Rigas, A. C., Sandher, R., Pickard, R. S., Robson, C. N., Turnbull, D. M., Taylor, R. W. and Heer, R. (2011) 'In situ lineage tracking of human prostatic epithelial stem cell fate reveals a common clonal origin for basal and luminal cells', *J Pathol,* 225(2), pp. 181-8.

Bogdanović, O. and Veenstra, G. J. (2009) 'DNA methylation and methyl-CpG binding proteins: developmental requirements and function', *Chromosoma,* 118(5), pp. 549-65.

Bolger, J., Walsh, C., McCartan, D., Byrne, C., McIlroy, M., Hill, A. D. K. and Young, L. (2012) 'A Novel Mechanism for SRC-1 in Suppressing the Luminal a Phenotype in Endocrine Resistant Breast Cancer', *Irish Journal of Medical Science,* 181, pp. S177-S178.

Bonkhoff, H. and Remberger, K. (1996) 'Differentiation pathways and histogenetic aspects of normal and abnormal prostatic growth: a stem cell model', *Prostate,* 28(2), pp. 98-106.

Bonkhoff, H., Stein, U. and Remberger, K. (1994) 'The proliferative function of basal cells in the normal and hyperplastic human prostate', *Prostate,* 24(3), pp. 114-8.

Bonnet, D. and Dick, J. E. (1997) 'Human acute myeloid leukemia is organized as a hierarchy that originates from a primitive hematopoietic cell', *Nat Med,* 3(7), pp. 730-7.

Bostwick, D. G., Liu, L., Brawer, M. K. and Qian, J. (2004) 'High-grade prostatic intraepithelial neoplasia', *Rev Urol,* 6(4), pp. 171-9.

Bowman, G. D. and Poirier, M. G. (2015) 'Post-translational modifications of histones that influence nucleosome dynamics', *Chem Rev,* 115(6), pp. 2274-95.

Bozdar, H. R., Memon, S. R. and Paryani, J. P. (2010) 'Outcome of transurethral resection of prostate in clinical benign prostatic hyperplasia', *J Ayub Med Coll Abbottabad,* 22(4), pp. 194-6.

Brawer, M. K. (1999) 'Prostate-specific antigen: current status', *CA Cancer J Clin,* 49(5), pp. 264-81.

Brothman, A. R., Watson, M. J., Zhu, X. L., Williams, B. J. and Rohr, L. R. (1994) 'Evaluation of 20 archival prostate tumor specimens by fluorescence in situ hybridization (FISH)', *Cancer Genet Cytogenet,* 75(1), pp. 40-4.

Brown, M. D., Gilmore, P. E., Hart, C. A., Samuel, J. D., Ramani, V. A., George, N. J. and Clarke, N. W. (2007) 'Characterization of benign and malignant prostate epithelial Hoechst 33342 side populations', *Prostate,* 67(13), pp. 1384-96.

Brückner, A., Polge, C., Lentze, N., Auerbach, D. and Schlattner, U. (2009) 'Yeast two-hybrid, a powerful tool for systems biology', *Int J Mol Sci,* 10(6), pp. 2763-88.

Bubendorf, L., Kononen, J., Koivisto, P., Schraml, P., Moch, H., Gasser, T. C., Willi, N., Mihatsch, M. J., Sauter, G. and Kallioniemi, O. P. (1999) 'Survey of gene amplifications during prostate cancer progression by high-throughout fluorescence in situ hybridization on tissue microarrays', *Cancer Res,* 59(4), pp. 803-6.

Bubendorf, L., Schöpfer, A., Wagner, U., Sauter, G., Moch, H., Willi, N., Gasser, T. C. and Mihatsch, M. J. (2000) 'Metastatic patterns of prostate cancer: an autopsy study of 1,589 patients', *Hum Pathol,* 31(5), pp. 578-83.

Bártová, E., Krejcí, J., Harnicarová, A., Galiová, G. and Kozubek, S. (2008) 'Histone modifications and nuclear architecture: a review', *J Histochem Cytochem,* 56(8), pp. 711-21.

Campos, B., Wan, F., Farhadi, M., Ernst, A., Zeppernick, F., Tagscherer, K. E., Ahmadi, R., Lohr, J., Dictus, C., Gdynia, G., Combs, S. E., Goidts, V., Helmke, B. M., Eckstein, V., Roth, W., Beckhove, P., Lichter, P., Unterberg, A., Radlwimmer, B. and Herold-Mende, C. (2010) 'Differentiation therapy exerts antitumor effects on stem-like glioma cells', *Clin Cancer Res,* 16(10), pp. 2715-28.

Cancer Research UK (2016) *Prostate cancer statistics* Prostate cancer statistics for the United Kindom. http://www.cancerresearchuk.org/health-professional/cancer-statistics/statistics-by-cancer-type/prostate-cancer: Cancer Research UK (Accessed: September 25th 2016).

Carpino, A., Sisci, D., Aquila, S., Salerno, M., Siciliano, L., Sessa, M. and Andò, S. (1994) 'Adnexal gland secretion markers in unexplained asthenozoospermia', *Arch Androl,* 32(1), pp. 37-43.

Carter, A. J. and Nguyen, C. N. (2012) 'A comparison of cancer burden and research spending reveals discrepancies in the distribution of research funding', *BMC Public Health,* 12, pp. 526.

Castaigne, S., Chomienne, C., Daniel, M. T., Ballerini, P., Berger, R., Fenaux, P. and Degos, L. (1990) 'All-trans retinoic acid as a differentiation therapy for acute promyelocytic leukemia. I. Clinical results', *Blood,* 76(9), pp. 1704-9.

Catalona, W. J., Carvalhal, G. F., Mager, D. E. and Smith, D. S. (1999) 'Potency, continence and complication rates in 1,870 consecutive radical retropubic prostatectomies', *J Urol,* 162(2), pp. 433-8.

Catalona, W. J., Partin, A. W., Slawin, K. M., Brawer, M. K., Flanigan, R. C., Patel, A., Richie, J. P., deKernion, J. B., Walsh, P. C., Scardino, P. T., Lange, P. H., Subong, E.

N., Parson, R. E., Gasior, G. H., Loveland, K. G. and Southwick, P. C. (1998) 'Use of the percentage of free prostate-specific antigen to enhance differentiation of prostate cancer from benign prostatic disease: a prospective multicenter clinical trial', *JAMA,* 279(19), pp. 1542-7.

Cerri, K. H., Knapp, M. and Fernandez, J. L. (2013) 'Decision making by NICE: examining the influences of evidence, process and context', *Health Econ Policy Law*, pp. 1-23.

Chandler, J. M. and Lagasse, E. (2010) 'Cancerous stem cells: deviant stem cells with cancer-causing misbehavior', *Stem Cell Res Ther,* 1(2), pp. 13.

Chapman, P. B., Hauschild, A., Robert, C., Haanen, J. B., Ascierto, P., Larkin, J., Dummer, R., Garbe, C., Testori, A., Maio, M., Hogg, D., Lorigan, P., Lebbe, C., Jouary, T., Schadendorf, D., Ribas, A., O'Day, S. J., Sosman, J. A., Kirkwood, J. M., Eggermont, A. M., Dreno, B., Nolop, K., Li, J., Nelson, B., Hou, J., Lee, R. J., Flaherty, K. T., McArthur, G. A. and Group, B.-S. (2011) 'Improved survival with vemurafenib in melanoma with BRAF V600E mutation', *N Engl J Med,* 364(26), pp. 2507-16.

Chen, S., Principessa, L. and Isaacs, J. T. (2012) 'Human prostate cancer initiating cells isolated directly from localized cancer do not form prostaspheres in primary culture', *Prostate,* 72(13), pp. 1478-89.

Chen, X., Zhu, H., Yuan, M., Fu, J., Zhou, Y. and Ma, L. (2010) 'G-protein-coupled receptor kinase 5 phosphorylates p53 and inhibits DNA damage-induced apoptosis', *Journal of Biological Chemistry,* 285(17), pp. 12823-30.

Cho, S. H., Jeon, J. and Kim, S. I. (2012) 'Personalized medicine in breast cancer: a systematic review', *J Breast Cancer,* 15(3), pp. 265-72.

Choi, N., Zhang, B., Zhang, L., Ittmann, M. and Xin, L. (2012) 'Adult murine prostate basal and luminal cells are self-sustained lineages that can both serve as targets for prostate cancer initiation', *Cancer Cell,* 21(2), pp. 253-65.

Chute, J. P., Muramoto, G. G., Whitesides, J., Colvin, M., Safi, R., Chao, N. J. and McDonnell, D. P. (2006) 'Inhibition of aldehyde dehydrogenase and retinoid signaling induces the expansion of human hematopoietic stem cells', *Proc Natl Acad Sci U S A,* 103(31), pp. 11707-12.

Collas, P. (2011) 'A chromatin immunoprecipitation protocol for small cell numbers', *Methods Mol Biol,* 791, pp. 179-93.

Collins, A. T., Berry, P. A., Hyde, C., Stower, M. J. and Maitland, N. J. (2005) 'Prospective identification of tumorigenic prostate cancer stem cells', *Cancer Res,* 65(23), pp. 10946-51.

Collins, A. T., Habib, F. K., Maitland, N. J. and Neal, D. E. (2001) 'Identification and isolation of human prostate epithelial stem cells based on alpha(2)beta(1)-integrin expression', *J Cell Sci,* 114(Pt 21), pp. 3865-72.

Collins, A. T. and Maitland, N. J. (2006) 'Prostate cancer stem cells', *Eur J Cancer,* 42(9), pp. 1213-8.

Costello, R. T., Mallet, F., Gaugler, B., Sainty, D., Arnoulet, C., Gastaut, J. A. and Olive, D. (2000) 'Human acute myeloid leukemia CD34+/CD38- progenitor cells have decreased sensitivity to chemotherapy and Fas-induced apoptosis, reduced immunogenicity, and impaired dendritic cell transformation capacities', *Cancer Res,* 60(16), pp. 4403-11.

Crawford, E. D., Eisenberger, M. A., McLeod, D. G., Spaulding, J. T., Benson, R., Dorr, F. A., Blumenstein, B. A., Davis, M. A. and Goodman, P. J. (1989) 'A controlled trial of leuprolide with and without flutamide in prostatic carcinoma', *N Engl J Med,* 321(7), pp. 419-24.

Cruz, F. D. and Matushansky, I. (2012) 'Solid tumor differentiation therapy - is it possible?', *Oncotarget,* 3(5), pp. 559-67.

Cunha, G. R. and Donjacour, A. (1987) 'Stromal-epithelial interactions in normal and abnormal prostatic development', *Prog Clin Biol Res,* 239, pp. 251-72.

Cunha, G. R., Donjacour, A. A., Cooke, P. S., Mee, S., Bigsby, R. M., Higgins, S. J. and Sugimura, Y. (1987) 'The endocrinology and developmental biology of the prostate', *Endocr Rev,* 8(3), pp. 338-62.

Curradi, M., Izzo, A., Badaracco, G. and Landsberger, N. (2002) 'Molecular mechanisms of gene silencing mediated by DNA methylation', *Mol Cell Biol,* 22(9), pp. 3157-73.

Céraline, J., Cruchant, M. D., Erdmann, E., Erbs, P., Kurtz, J. E., Duclos, B., Jacqmin, D., Chopin, D. and Bergerat, J. P. (2004) 'Constitutive activation of the androgen receptor by a point mutation in the hinge region: a new mechanism for androgen-independent growth in prostate cancer', *Int J Cancer,* 108(1), pp. 152-7.

Dahl, J. A. and Collas, P. (2008) 'A rapid micro chromatin immunoprecipitation assay (microChIP)', *Nat Protoc,* 3(6), pp. 1032-45.

Danila, D. C., Fleisher, M. and Scher, H. I. (2011) 'Circulating tumor cells as biomarkers in prostate cancer', *Clin Cancer Res,* 17(12), pp. 3903-12.

David, K. A., Mongan, N. P., Smith, C., Gudas, L. J. and Nanus, D. M. (2010) 'Phase I trial of ATRA-IV and Depakote in patients with advanced solid tumor malignancies', *Cancer Biol Ther,* 9(9), pp. 678-84.

de Bono, J. S., Logothetis, C. J., Molina, A., Fizazi, K., North, S., Chu, L., Chi, K. N., Jones, R. J., Goodman, O. B., Jr., Saad, F., Staffurth, J. N., Mainwaring, P., Harland, S., Flaig, T. W., Hutson, T. E., Cheng, T., Patterson, H., Hainsworth, J. D., Ryan, C. J., Sternberg, C. N., Ellard, S. L., Flechon, A., Saleh, M., Scholz, M., Efstathiou, E., Zivi, A., Bianchini, D., Loriot, Y., Chieffo, N., Kheoh, T., Haqq, C. M., Scher, H. I. and Investigators, C.-A.-. (2011) 'Abiraterone and increased survival in metastatic prostate cancer', *N Engl J Med,* 364(21), pp. 1995-2005.

Dean, M. (2009) 'ABC transporters, drug resistance, and cancer stem cells', *J Mammary Gland Biol Neoplasia,* 14(1), pp. 3-9.

DeRose, Y. S., Wang, G., Lin, Y. C., Bernard, P. S., Buys, S. S., Ebbert, M. T., Factor, R., Matsen, C., Milash, B. A., Nelson, E., Neumayer, L., Randall, R. L., Stijleman, I. J., Welm, B. E. and Welm, A. L. (2011) 'Tumor grafts derived from women with breast cancer authentically reflect tumor pathology, growth, metastasis and disease outcomes', *Nat Med,* 17(11), pp. 1514-20.

Di Oto, E., Monti, V., Cucchi, M. C., Masetti, R., Varga, Z. and Foschini, M. P. (2015) 'X chromosome gain in male breast cancer', *Hum Pathol,* 46(12), pp. 1908-12.

Do, H. J., Song, H., Yang, H. M., Kim, D. K., Kim, N. H., Kim, J. H., Cha, K. Y. and Chung, H. M. (2006) 'Identification of multiple nuclear localization signals in murine Elf3, an ETS transcription factor', *FEBS Lett,* 580(7), pp. 1865-71.

Donato, L. J. and Noy, N. (2005) 'Suppression of mammary carcinoma growth by retinoic acid: proapoptotic genes are targets for retinoic acid receptor and cellular retinoic acid-binding protein II signaling', *Cancer Res,* 65(18), pp. 8193-9.

Dragu, D. L., Necula, L. G., Bleotu, C., Diaconu, C. C. and Chivu-Economescu, M. (2015) 'Therapies targeting cancer stem cells: Current trends and future challenges', *World J Stem Cells,* 7(9), pp. 1185-201.

Duband-Goulet, I. (2016) 'Lamin ChIP from Chromatin Prepared by Micrococcal Nuclease Digestion', *Methods Mol Biol,* 1411, pp. 325-39.

Dubrovska, A., Elliott, J., Salamone, R. J., Telegeev, G. D., Stakhovsky, A. E., Schepotin, I. B., Yan, F., Wang, Y., Bouchez, L. C., Kularatne, S. A., Watson, J., Trussell, C.,

Reddy, V. A., Cho, C. Y. and Schultz, P. G. (2012) 'CXCR4 expression in prostate cancer progenitor cells', *PLoS One,* 7(2), pp. e31226.

Ducasse, M. and Brown, M. A. (2006) 'Epigenetic aberrations and cancer', *Mol Cancer,* 5, pp. 60.

Duchesne, G. (2011) 'Localised prostate cancer - current treatment options', *Aust Fam Physician,* 40(10), pp. 768-71.

Dunham, W. H., Mullin, M. and Gingras, A. C. (2012) 'Affinity-purification coupled to mass spectrometry: basic principles and strategies', *Proteomics,* 12(10), pp. 1576-90.

Durocher, Y., Perret, S. and Kamen, A. (2002) 'High-level and high-throughput recombinant protein production by transient transfection of suspension-growing human 293-EBNA1 cells', *Nucleic Acids Res,* 30(2), pp. E9.

Elliott, A., Elliot, A., Adams, J. and Al-Hajj, M. (2010) 'The ABCs of cancer stem cell drug resistance', *IDrugs,* 13(9), pp. 632-5.

Elliott, M. A., Dewald, G. W., Tefferi, A. and Hanson, C. A. (2001) 'Chronic neutrophilic leukemia (CNL): a clinical, pathologic and cytogenetic study', *Leukemia,* 15(1), pp. 35-40.

Ellis, B. L., Potts, P. R. and Porteus, M. H. (2011) 'Creating higher titer lentivirus with caffeine', *Hum Gene Ther,* 22(1), pp. 93-100.

English, H. F., Kyprianou, N. and Isaacs, J. T. (1989) 'Relationship between DNA fragmentation and apoptosis in the programmed cell death in the rat prostate following castration', *Prostate,* 15(3), pp. 233-50.

English, H. F., Santen, R. J. and Isaacs, J. T. (1987) 'Response of glandular versus basal rat ventral prostatic epithelial cells to androgen withdrawal and replacement', *Prostate,* 11(3), pp. 229-42.

Epstein, J. I. (2010) 'An update of the Gleason grading system', *J Urol,* 183(2), pp. 433-40.

Eramo, A., Lotti, F., Sette, G., Pilozzi, E., Biffoni, M., Di Virgilio, A., Conticello, C., Ruco, L., Peschle, C. and De Maria, R. (2008) 'Identification and expansion of the tumorigenic lung cancer stem cell population', *Cell Death Differ,* 15(3), pp. 504-14.

Esplin, E. D., Ramos, P., Martinez, B., Tomlinson, G. E., Mumby, M. C. and Evans, G. A. (2006) 'The glycine 90 to aspartate alteration in the Abeta subunit of PP2A (PPP2R1B) associates with breast cancer and causes a deficit in protein function', *Genes Chromosomes Cancer,* 45(2), pp. 182-90.

Esteller, M. (2002) 'CpG island hypermethylation and tumor suppressor genes: a booming present, a brighter future', *Oncogene,* 21(35), pp. 5427-40.

Evans, G. S. and Chandler, J. A. (1987) 'Cell proliferation studies in the rat prostate: II. The effects of castration and androgen-induced regeneration upon basal and secretory cell proliferation', *Prostate,* 11(4), pp. 339-51.

Ferrara, F. F., Fazi, F., Bianchini, A., Padula, F., Gelmetti, V., Minucci, S., Mancini, M., Pelicci, P. G., Lo Coco, F. and Nervi, C. (2001) 'Histone deacetylase-targeted treatment restores retinoic acid signaling and differentiation in acute myeloid leukemia', *Cancer Res,* 61(1), pp. 2-7.

Frame, F. M., Hager, S., Pellacani, D., Stower, M. J., Walker, H. F., Burns, J. E., Collins, A. T. and Maitland, N. J. (2010) 'Development and limitations of lentivirus vectors as tools for tracking differentiation in prostate epithelial cells', *Exp Cell Res,* 316(19), pp. 3161-71.

Frame, F. M., Pellacani, D., Collins, A. T. and Maitland, N. J. (2016) 'Harvesting Human Prostate Tissue Material and Culturing Primary Prostate Epithelial Cells', *Methods Mol Biol,* 1443, pp. 181-201.

Gallinari, P., Di Marco, S., Jones, P., Pallaoro, M. and Steinkühler, C. (2007) 'HDACs, histone deacetylation and gene transcription: from molecular biology to cancer therapeutics', *Cell Res,* 17(3), pp. 195-211.

Gao, N., Ishii, K., Mirosevich, J., Kuwajima, S., Oppenheimer, S. R., Roberts, R. L., Jiang, M., Yu, X., Shappell, S. B., Caprioli, R. M., Stoffel, M., Hayward, S. W. and Matusik, R. J. (2005) 'Forkhead box A1 regulates prostate ductal morphogenesis and promotes epithelial cell maturation', *Development,* 132(15), pp. 3431-43.

Garraway, I. P., Sun, W., Tran, C. P., Perner, S., Zhang, B., Goldstein, A. S., Hahm, S. A., Haider, M., Head, C. S., Reiter, R. E., Rubin, M. A. and Witte, O. N. (2010) 'Human prostate sphere-forming cells represent a subset of basal epithelial cells capable of glandular regeneration in vivo', *Prostate,* 70(5), pp. 491-501.

Gatti, L., Beretta, G. L., Cossa, G., Zunino, F. and Perego, P. (2009) 'ABC transporters as potential targets for modulation of drug resistance', *Mini Rev Med Chem,* 9(9), pp. 1102-12.

Ghosh, S. and Jacobson, A. (2010) 'RNA decay modulates gene expression and controls its fidelity', *Wiley Interdiscip Rev RNA,* 1(3), pp. 351-61.

Giam, M. and Rancati, G. (2015) 'Aneuploidy and chromosomal instability in cancer: a jackpot to chaos', *Cell Div,* 10, pp. 3.

Ginestier, C., Wicinski, J., Cervera, N., Monville, F., Finetti, P., Bertucci, F., Wicha, M. S., Birnbaum, D. and Charafe-Jauffret, E. (2009) 'Retinoid signaling regulates breast cancer stem cell differentiation', *Cell Cycle,* 8(20), pp. 3297-302.

Gingrich, J. R., Barrios, R. J., Morton, R. A., Boyce, B. F., DeMayo, F. J., Finegold, M. J., Angelopoulou, R., Rosen, J. M. and Greenberg, N. M. (1996) 'Metastatic prostate cancer in a transgenic mouse', *Cancer Res,* 56(18), pp. 4096-102.

Giri, D., Ropiquet, F. and Ittmann, M. (1999) 'FGF9 is an autocrine and paracrine prostatic growth factor expressed by prostatic stromal cells', *J Cell Physiol,* 180(1), pp. 53-60.

Giuliano, M., Giordano, A., Jackson, S., De Giorgi, U., Mego, M., Cohen, E. N., Gao, H., Anfossi, S., Handy, B. C., Ueno, N. T., Alvarez, R. H., De Placido, S., Valero, V., Hortobagyi, G. N., Reuben, J. M. and Cristofanilli, M. (2014) 'Circulating tumor cells as early predictors of metastatic spread in breast cancer patients with limited metastatic dissemination', *Breast Cancer Res,* 16(5), pp. 440.

Gleason, D. F. (1966) 'Classification of prostatic carcinomas', *Cancer Chemother Rep,* 50(3), pp. 125-8.

Gleason, D. F. (1992) 'Histologic grading of prostate cancer: a perspective', *Hum Pathol,* 23(3), pp. 273-9.

Goldstein, A. S., Huang, J., Guo, C., Garraway, I. P. and Witte, O. N. (2010) 'Identification of a cell of origin for human prostate cancer', *Science,* 329(5991), pp. 568-71.

Gonçalves, B. F., Campos, S. G., Costa, C. F., Scarano, W. R., Góes, R. M. and Taboga, S. R. (2015) 'Key participants of the tumor microenvironment of the prostate: an approach of the structural dynamic of cellular elements and extracellular matrix components during epithelial-stromal transition', *Acta Histochem,* 117(1), pp. 4-13.

Goodpaster, T., Legesse-Miller, A., Hameed, M. R., Aisner, S. C., Randolph-Habecker, J. and Coller, H. A. (2008) 'An immunohistochemical method for identifying fibroblasts in formalin-fixed, paraffin-embedded tissue', *J Histochem Cytochem,* 56(4), pp. 347-58.

Grabowska, M. M., DeGraff, D. J., Yu, X., Jin, R. J., Chen, Z., Borowsky, A. D. and Matusik, R. J. (2014) 'Mouse models of prostate cancer: picking the best model for the question', *Cancer Metastasis Rev,* 33(2-3), pp. 377-97.

Green, R. A., Wollman, R. and Kaplan, K. B. (2005) 'APC and EB1 function together in mitosis to regulate spindle dynamics and chromosome alignment', *Molecular Biology of the Cell,* 16(10), pp. 4609-22.

Greenberg, N. M., DeMayo, F., Finegold, M. J., Medina, D., Tilley, W. D., Aspinall, J. O., Cunha, G. R., Donjacour, A. A., Matusik, R. J. and Rosen, J. M. (1995) 'Prostate cancer in a transgenic mouse', *Proc Natl Acad Sci U S A,* 92(8), pp. 3439-43.

Grisanzio, C. and Signoretti, S. (2008) 'p63 in prostate biology and pathology', *J Cell Biochem,* 103(5), pp. 1354-68.

Grishina, I. B., Kim, S. Y., Ferrara, C., Makarenkova, H. P. and Walden, P. D. (2005) 'BMP7 inhibits branching morphogenesis in the prostate gland and interferes with Notch signaling', *Dev Biol,* 288(2), pp. 334-47.

Grommes, C., Landreth, G. E. and Heneka, M. T. (2004) 'Antineoplastic effects of peroxisome proliferator-activated receptor gamma agonists', *Lancet Oncol,* 5(7), pp. 419-29.

Gupta, P. B., Onder, T. T., Jiang, G., Tao, K., Kuperwasser, C., Weinberg, R. A. and Lander, E. S. (2009) 'Identification of selective inhibitors of cancer stem cells by high-throughput screening', *Cell,* 138(4), pp. 645-59.

Göker, E., Waltham, M., Kheradpour, A., Trippett, T., Mazumdar, M., Elisseyeff, Y., Schnieders, B., Steinherz, P., Tan, C. and Berman, E. (1995) 'Amplification of the dihydrofolate reductase gene is a mechanism of acquired resistance to methotrexate in patients with acute lymphoblastic leukemia and is correlated with p53 gene mutations', *Blood,* 86(2), pp. 677-84.

Hambardzumyan, D., Becher, O. J., Rosenblum, M. K., Pandolfi, P. P., Manova-Todorova, K. and Holland, E. C. (2008) 'PI3K pathway regulates survival of cancer stem cells residing in the perivascular niche following radiation in medulloblastoma in vivo', *Genes Dev,* 22(4), pp. 436-48.

Hammerich, K. H., Ayala, G. E., and Wheeler, T. M. (2009) *Anatomy of the prostate gland and surgical pathology of prostate cancer* Cambridge University Press.

Harikumar, A. and Meshorer, E. (2015) 'Chromatin remodeling and bivalent histone modifications in embryonic stem cells', *EMBO Rep,* 16(12), pp. 1609-19.

Harris, D. M., Cohn, H. I., Pesant, S. and Eckhart, A. D. (2008) 'GPCR signalling in hypertension: role of GRKs', *Clin Sci (Lond),* 115(3), pp. 79-89.

Hayward, S. W., Dahiya, R., Cunha, G. R., Bartek, J., Deshpande, N. and Narayan, P. (1995) 'Establishment and characterization of an immortalized but non-transformed human prostate epithelial cell line: BPH-1', *In Vitro Cell Dev Biol Anim,* 31(1), pp. 14-24.

Hayward, S. W., Del Buono, R., Deshpande, N. and Hall, P. A. (1992) 'A functional model of adult human prostate epithelium. The role of androgens and stroma in architectural organisation and the maintenance of differentiated secretory function', *J Cell Sci,* 102 (Pt 2), pp. 361-72.

Hayward, S. W., Rosen, M. A. and Cunha, G. R. (1997) 'Stromal-epithelial interactions in the normal and neoplastic prostate', *Br J Urol,* 79 Suppl 2, pp. 18-26.

He, X., Marchionni, L., Hansel, D. E., Yu, W., Sood, A., Yang, J., Parmigiani, G., Matsui, W. and Berman, D. M. (2009) 'Differentiation of a highly tumorigenic basal cell compartment in urothelial carcinoma', *Stem Cells,* 27(7), pp. 1487-95.

Heidenreich, A., Pfister, D., Merseburger, A. and Bartsch, G. (2013) 'Castration-resistant prostate cancer: where we stand in 2013 and what urologists should know', *Eur Urol,* 64(2), pp. 260-5.

Hermann, P. C., Huber, S. L., Herrler, T., Aicher, A., Ellwart, J. W., Guba, M., Bruns, C. J. and Heeschen, C. (2007) 'Distinct populations of cancer stem cells determine

tumor growth and metastatic activity in human pancreatic cancer', *Cell Stem Cell,* 1(3), pp. 313-23.

Holcomb, I. N., Young, J. M., Coleman, I. M., Salari, K., Grove, D. I., Hsu, L., True, L. D., Roudier, M. P., Morrissey, C. M., Higano, C. S., Nelson, P. S., Vessella, R. L. and Trask, B. J. (2009) 'Comparative analyses of chromosome alterations in soft-tissue metastases within and across patients with castration-resistant prostate cancer', *Cancer Res,* 69(19), pp. 7793-802.

Holzbeierlein, J., Lal, P., LaTulippe, E., Smith, A., Satagopan, J., Zhang, L., Ryan, C., Smith, S., Scher, H., Scardino, P., Reuter, V. and Gerald, W. L. (2004) 'Gene expression analysis of human prostate carcinoma during hormonal therapy identifies androgen-responsive genes and mechanisms of therapy resistance', *Am J Pathol,* 164(1), pp. 217-27.

Horoszewicz, J. S., Leong, S. S., Chu, T. M., Wajsman, Z. L., Friedman, M., Papsidero, L., Kim, U., Chai, L. S., Kakati, S., Arya, S. K. and Sandberg, A. A. (1980) 'The LNCaP cell line--a new model for studies on human prostatic carcinoma', *Prog Clin Biol Res,* 37, pp. 115-32.

Hu, R., Isaacs, W. B. and Luo, J. (2011) 'A snapshot of the expression signature of androgen receptor splicing variants and their distinctive transcriptional activities', *Prostate,* 71(15), pp. 1656-67.

Hu, R., Lu, C., Mostaghel, E. A., Yegnasubramanian, S., Gurel, M., Tannahill, C., Edwards, J., Isaacs, W. B., Nelson, P. S., Bluemn, E., Plymate, S. R. and Luo, J. (2012) 'Distinct transcriptional programs mediated by the ligand-dependent full-length androgen receptor and its splice variants in castration-resistant prostate cancer', *Cancer Res,* 72(14), pp. 3457-62.

Huang, H. J., Reed, C. P., Zhang, J. S., Shridhar, V., Wang, L. and Smith, D. I. (1999) 'Carboxypeptidase A3 (CPA3): A novel gene highly induced by histone deacetylase inhibitors during differentiation of prostate epithelial cancer cells', *Cancer Res,* 59(12), pp. 2981-2988.

Huang, J., Bi, Y., Zhu, G. H., He, Y., Su, Y., He, B. C., Wang, Y., Kang, Q., Chen, L., Zuo, G. W., Luo, Q., Shi, Q., Zhang, B. Q., Huang, A., Zhou, L., Feng, T., Luu, H. H., Haydon, R. C., He, T. C. and Tang, N. (2009) 'Retinoic acid signalling induces the differentiation of mouse fetal liver-derived hepatic progenitor cells', *Liver Int,* 29(10), pp. 1569-81.

Huggins, C., Scott, W. W. and Heinen, J. H. (1942) 'Chemical composition of human semen and of the secretions of the prostate and seminal vehicles', *American Journal of Physiology,* 136, pp. 467-473.

Huggins, C., Stevens, R. E. and Hodges, C. V. (1941) 'Studies On Prostatic Cancer. II. The Effects Of Castration On Advanced Carcinoma Of The Prostate Gland', *Archives of Surgery,* 43, pp. 209-223.

Humphrey, P. A. (2004) 'Gleason grading and prognostic factors in carcinoma of the prostate', *Mod Pathol,* 17(3), pp. 292-306.

Huntzinger, E. and Izaurralde, E. (2011) 'Gene silencing by microRNAs: contributions of translational repression and mRNA decay', *Nat Rev Genet,* 12(2), pp. 99-110.

Huss, W. J., Gray, D. R., Werdin, E. S., Funkhouser, W. K. and Smith, G. J. (2004) 'Evidence of pluripotent human prostate stem cells in a human prostate primary xenograft model', *Prostate,* 60(2), pp. 77-90.

Hörnberg, E., Ylitalo, E. B., Crnalic, S., Antti, H., Stattin, P., Widmark, A., Bergh, A. and Wikström, P. (2011) 'Expression of androgen receptor splice variants in prostate cancer bone metastases is associated with castration-resistance and short survival', *PLoS One,* 6(4), pp. e19059.

Isaacs, J. T., Schulze, H. and Coffey, D. S. (1987) 'Development of androgen resistance in prostatic cancer', *Prog Clin Biol Res,* 243A, pp. 21-31.

Ishii, H., Iwatsuki, M., Ieta, K., Ohta, D., Haraguchi, N., Mimori, K. and Mori, M. (2008) 'Cancer stem cells and chemoradiation resistance', *Cancer Sci,* 99(10), pp. 1871-7.

Ito, T., Williams-Nate, Y., Iwai, M., Tsuboi, Y., Hagiyama, M., Ito, A., Sakurai-Yageta, M. and Murakami, Y. (2011) 'Transcriptional regulation of the CADM1 gene by retinoic acid during the neural differentiation of murine embryonal carcinoma P19 cells', *Genes Cells,* 16(7), pp. 791-802.

Iyer, K. S. and Saksena, V. N. (1970) 'A stochastic model for the growth of cells in cancer', *Biometrics,* 26(3), pp. 401-10.

Jackson, S. E. and Chester, J. D. (2015) 'Personalised cancer medicine', *Int J Cancer,* 137(2), pp. 262-6.

Jin, B., Li, Y. and Robertson, K. D. (2011) 'DNA methylation: superior or subordinate in the epigenetic hierarchy?', *Genes Cancer,* 2(6), pp. 607-17.

Jin, Y., Chen, Z., Liu, X. and Zhou, X. (2013) 'Evaluating the microRNA targeting sites by luciferase reporter gene assay', *Methods Mol Biol,* 936, pp. 117-27.

Jing, C., El-Ghany, M. A., Beesley, C., Foster, C. S., Rudland, P. S., Smith, P. and Ke, Y. (2002) 'Tazarotene-induced gene 1 (TIG1) expression in prostate carcinomas and its relationship to tumorigenicity', *J Natl Cancer Inst,* 94(7), pp. 482-90.

Jones, P. A. and Laird, P. W. (1999) 'Cancer epigenetics comes of age', *Nat Genet,* 21(2), pp. 163-7.

Jones, P. H. and Watt, F. M. (1993) 'Separation of human epidermal stem cells from transit amplifying cells on the basis of differences in integrin function and expression', *Cell,* 73(4), pp. 713-24.

Kacem, S. and Feil, R. (2009) 'Chromatin mechanisms in genomic imprinting', *Mamm Genome,* 20(9-10), pp. 544-56.

Kaighn, M. E., Narayan, K. S., Ohnuki, Y., Lechner, J. F. and Jones, L. W. (1979) 'Establishment and characterization of a human prostatic carcinoma cell line (PC-3)', *Invest Urol,* 17(1), pp. 16-23.

Kamal, A. H., Han, B. S., Choi, J. S., Cho, K., Kim, S. Y., Kim, W. K., Lee, S. C. and Bae, K. H. (2014) 'Proteomic analysis of the effect of retinoic acids on the human breast cancer cell line MCF-7', *Mol Biol Rep*.

Kang, J., Lee, H. J., Kim, J., Lee, J. J. and Maeng, L. S. (2015) 'Dysregulation of X chromosome inactivation in high grade ovarian serous adenocarcinoma', *PLoS One,* 10(3), pp. e0118927.

Karapetis, C. S., Khambata-Ford, S., Jonker, D. J., O'Callaghan, C. J., Tu, D., Tebbutt, N. C., Simes, R. J., Chalchal, H., Shapiro, J. D., Robitaille, S., Price, T. J., Shepherd, L., Au, H. J., Langer, C., Moore, M. J. and Zalcberg, J. R. (2008) 'K-ras mutations and benefit from cetuximab in advanced colorectal cancer', *N Engl J Med,* 359(17), pp. 1757-65.

Kastner, P., Mark, M., Ghyselinck, N., Krezel, W., Dupé, V., Grondona, J. M. and Chambon, P. (1997) 'Genetic evidence that the retinoid signal is transduced by heterodimeric RXR/RAR functional units during mouse development', *Development,* 124(2), pp. 313-26.

Kayashima, T., Yamasaki, K., Yamada, T., Sakai, H., Miwa, N., Ohta, T., Yoshiura, K., Matsumoto, N., Nakane, Y., Kanetake, H., Ishino, F., Niikawa, N. and Kishino, T. (2003) 'The novel imprinted carboxypeptidase A4 gene (CPA4) in the 7q32 imprinting domain', *Human Genetics,* 112(3), pp. 220-226.

Ke Y, X. G., Hagiwara K, Zhang JM, Ning T, Wang B, Su XL, Feng LY, Lu GR, Lu YY, Harris CC. (1996) 'Isolation and sequencing of the target genes induced by chemical carcinogen.', *Science in China (Series C),* 26(1), pp. 85–91.

Kellokumpu-Lehtinen, P., Santti, R. S. and Pelliniemi, L. J. (1981) 'Development of human fetal prostate in culture', *Urol Res,* 9(2), pp. 89-98.

Kim, Y., Joo, K. M., Jin, J. and Nam, D. H. (2009) 'Cancer stem cells and their mechanism of chemo-radiation resistance', *Int J Stem Cells,* 2(2), pp. 109-14.

Kim, Y. Z. (2014) 'Altered histone modifications in gliomas', *Brain Tumor Res Treat,* 2(1), pp. 7-21.

Klokk, T. I., Kurys, P., Elbi, C., Nagaich, A. K., Hendarwanto, A., Slagsvold, T., Chang, C. Y., Hager, G. L. and Saatcioglu, F. (2007) 'Ligand-specific dynamics of the androgen receptor at its response element in living cells', *Mol Cell Biol,* 27(5), pp. 1823-43.

Kooistra, A., Elissen, N. M., König, J. J., Vermey, M., van der Kwast, T. H., Romijn, J. C. and Schröder, F. H. (1995) 'Immunocytochemical characterization of explant cultures of human prostatic stromal cells', *Prostate,* 27(1), pp. 42-9.

Korenchuk, S., Lehr, J. E., MClean, L., Lee, Y. G., Whitney, S., Vessella, R., Lin, D. L. and Pienta, K. J. (2001) 'VCaP, a cell-based model system of human prostate cancer', *In Vivo,* 15(2), pp. 163-8.

Korsten, H., Ziel-van der Made, A., Ma, X., van der Kwast, T. and Trapman, J. (2009) 'Accumulating progenitor cells in the luminal epithelial cell layer are candidate tumor initiating cells in a Pten knockout mouse prostate cancer model', *PLoS One,* 4(5), pp. e5662.

Krieger, J. N., Lee, S. W., Jeon, J., Cheah, P. Y., Liong, M. L. and Riley, D. E. (2008) 'Epidemiology of prostatitis', *Int J Antimicrob Agents,* 31 Suppl 1, pp. S85-90.

Kubota, T., Koshizuka, K., Williamson, E. A., Asou, H., Said, J. W., Holden, S., Miyoshi, I. and Koeffler, H. P. (1998) 'Ligand for peroxisome proliferator-activated receptor gamma (troglitazone) has potent antitumor effect against human prostate cancer both in vitro and in vivo', *Cancer Res,* 58(15), pp. 3344-52.

Kubota, Y., Shuin, T., Uemura, H., Fujinami, K., Miyamoto, H., Torigoe, S., Dobashi, Y., Kitamura, H., Iwasaki, Y. and Danenberg, K. (1995) 'Tumor suppressor gene p53 mutations in human prostate cancer', *Prostate,* 27(1), pp. 18-24.

Kung, J. T., Colognori, D. and Lee, J. T. (2013) 'Long noncoding RNAs: past, present, and future', *Genetics,* 193(3), pp. 651-69.

Kwak, M. K., Johnson, D. T., Zhu, C., Lee, S. H., Ye, D. W., Luong, R. and Sun, Z. (2013) 'Conditional deletion of the Pten gene in the mouse prostate induces prostatic intraepithelial neoplasms at early ages but a slow progression to prostate tumors', *PLoS One,* 8(1), pp. e53476.

Kwok, W. K., Pang, J. C., Lo, K. W. and Ng, H. K. (2009) 'Role of the RARRES1 gene in nasopharyngeal carcinoma', *Cancer Genet Cytogenet,* 194(1), pp. 58-64.

Kyprianou, N. and Isaacs, J. T. (1988) 'Activation of programmed cell death in the rat ventral prostate after castration', *Endocrinology,* 122(2), pp. 552-62.

Lang, S. H., Frame, F. M. and Collins, A. T. (2009) 'Prostate cancer stem cells', *J Pathol,* 217(2), pp. 299-306.

Langley, R. R. and Fidler, I. J. (2011) 'The seed and soil hypothesis revisited--the role of tumor-stroma interactions in metastasis to different organs', *Int J Cancer,* 128(11), pp. 2527-35.

Lapidot, T., Sirard, C., Vormoor, J., Murdoch, B., Hoang, T., Caceres-Cortes, J., Minden, M., Paterson, B., Caligiuri, M. A. and Dick, J. E. (1994) 'A cell initiating human acute myeloid leukaemia after transplantation into SCID mice', *Nature,* 367(6464), pp. 645-8.

Lapouge, G., Erdmann, E., Marcias, G., Jagla, M., Monge, A., Kessler, P., Serra, S., Lang, H., Jacqmin, D., Bergerat, J. P. and Céraline, J. (2007) 'Unexpected paracrine action of prostate cancer cells harboring a new class of androgen receptor mutation--a new paradigm for cooperation among prostate tumor cells', *Int J Cancer,* 121(6), pp. 1238-44.

Lawrence, M. G., Taylor, R. A., Toivanen, R., Pedersen, J., Norden, S., Pook, D. W., Frydenberg, M., Papargiris, M. M., Niranjan, B., Richards, M. G., Wang, H., Collins, A. T., Maitland, N. J., Risbridger, G. P. and BioResource, A. P. C. (2013) 'A preclinical xenograft model of prostate cancer using human tumors', *Nat Protoc,* 8(5), pp. 836-48.

Lawson, D. A., Zong, Y., Memarzadeh, S., Xin, L., Huang, J. and Witte, O. N. (2010) 'Basal epithelial stem cells are efficient targets for prostate cancer initiation', *Proc Natl Acad Sci U S A,* 107(6), pp. 2610-5.

Lee, J., Kotliarova, S., Kotliarov, Y., Li, A., Su, Q., Donin, N. M., Pastorino, S., Purow, B. W., Christopher, N., Zhang, W., Park, J. K. and Fine, H. A. (2006) 'Tumor stem cells derived from glioblastomas cultured in bFGF and EGF more closely mirror the phenotype and genotype of primary tumors than do serum-cultured cell lines', *Cancer Cell,* 9(5), pp. 391-403.

Leid, M., Kastner, P. and Chambon, P. (1992) 'Multiplicity generates diversity in the retinoic acid signalling pathways', *Trends Biochem Sci,* 17(10), pp. 427-33.

Leong, K. G., Wang, B. E., Johnson, L. and Gao, W. Q. (2008) 'Generation of a prostate from a single adult stem cell', *Nature,* 456(7223), pp. 804-8.

Lesch, B. J. and Page, D. C. (2014) 'Poised chromatin in the mammalian germ line', *Development,* 141(19), pp. 3619-26.

Li, J. and Al-Azzawi, F. (2009) 'Mechanism of androgen receptor action', *Maturitas,* 63(2), pp. 142-8.

Li, Y., Basang, Z. M., Ding, H. R., Lu, Z. M., Ning, T., Wei, H. R., Cai, H. and Ke, Y. (2011) 'Latexin expression is downregulated in human gastric carcinomas and exhibits tumor suppressor potential', *BMC Cancer,* 11.

Li, Y., Hwang, T. H., Oseth, L. A., Hauge, A., Vessella, R. L., Schmechel, S. C., Hirsch, B., Beckman, K. B., Silverstein, K. A. and Dehm, S. M. (2012) 'AR intragenic deletions linked to androgen receptor splice variant expression and activity in models of prostate cancer progression', *Oncogene,* 31(45), pp. 4759-67.

Liang, G. and Zhang, Y. (2013) 'Genetic and epigenetic variations in iPSCs: potential causes and implications for application', *Cell Stem Cell,* 13(2), pp. 149-59.

Liang, Y. and Van Zant, G. (2008) 'Aging stem cells, latexin, and longevity', *Exp Cell Res,* 314(9), pp. 1962-72.

Lim, L. P., Lau, N. C., Garrett-Engele, P., Grimson, A., Schelter, J. M., Castle, J., Bartel, D. P., Linsley, P. S. and Johnson, J. M. (2005) 'Microarray analysis shows that some microRNAs downregulate large numbers of target mRNAs', *Nature,* 433(7027), pp. 769-73.

Liu, A., Wei, L., Gardner, W. A., Deng, C. X. and Man, Y. G. (2009) 'Correlated alterations in prostate basal cell layer and basement membrane', *Int J Biol Sci,* 5(3), pp. 276-85.

Liu, A. Y. and True, L. D. (2002) 'Characterization of prostate cell types by CD cell surface molecules', *Am J Pathol,* 160(1), pp. 37-43.

Liu, P., Wang, X., Gao, N., Zhu, H., Dai, X., Xu, Y., Ma, C., Huang, L., Liu, Y. and Qin, C. (2010a) 'G protein-coupled receptor kinase 5, overexpressed in the alpha-synuclein up-regulation model of Parkinson's disease, regulates bcl-2 expression', *Brain Res,* 1307, pp. 134-41.

Liu, W. B., Ao, L., Zhou, Z. Y., Cui, Z. H., Zhou, Y. H., Yuan, X. Y., Xiang, Y. L., Cao, J. and Liu, J. Y. (2010b) 'CpG island hypermethylation of multiple tumor suppressor genes associated with loss of their protein expression during rat lung carcinogenesis induced by 3-methylcholanthrene and diethylnitrosamine', *Biochem Biophys Res Commun,* 402(3), pp. 507-14.

Liu, Y., Howard, D., Rector, K., Swiderski, C., Brandon, J., Schook, L., Mehta, J., Bryson, J. S., Bondada, S. and Liang, Y. (2012) 'Latexin is down-regulated in hematopoietic malignances and restoration of expression inhibits lymphoma growth', *PLoS One,* 7(9), pp. e44979.

Lohnes, D., Mark, M., Mendelsohn, C., Dollé, P., Decimo, D., LeMeur, M., Dierich, A., Gorry, P. and Chambon, P. (1995) 'Developmental roles of the retinoic acid receptors', *J Steroid Biochem Mol Biol,* 53(1-6), pp. 475-86.

Lorente, D., Mateo, J., Zafeiriou, Z., Smith, A. D., Sandhu, S., Ferraldeschi, R. and de Bono, J. S. (2015) 'Switching and withdrawing hormonal agents for castration-resistant prostate cancer', *Nat Rev Urol,* 12(1), pp. 37-47.

Luo, P., Wang, A., Payne, K. J., Peng, H., Wang, J. G., Parrish, Y. K., Rogerio, J. W., Triche, T. J., He, Q. and Wu, L. (2007) 'Intrinsic retinoic acid receptor alpha-cyclin-dependent kinase-activating kinase signaling involves coordination of the restricted proliferation and granulocytic differentiation of human hematopoietic stem cells', *Stem Cells,* 25(10), pp. 2628-37.

Macfarlane, L. A. and Murphy, P. R. (2010) 'MicroRNA: Biogenesis, Function and Role in Cancer', *Curr Genomics,* 11(7), pp. 537-61.

Maitland, N. J. (2013) 'Stem Cells in the Normal and Malignant Prostate', in D.J., T. (ed.) *Prostate Cancer Biochemistry, Molecular Biology and Genetics.* 1 ed: Springer, pp. 3-41.

Maitland, N. J., Bryce, S. D., Stower, M. J. and Collins, A. T. (2006) 'Prostate cancer stem cells: a target for new therapies', *Ernst Schering Found Symp Proc,* (5), pp. 155-79.

Maitland, N. J., Frame, F. M., Polson, E. S., Lewis, J. L. and Collins, A. T. (2011) 'Prostate cancer stem cells: do they have a basal or luminal phenotype?', *Horm Cancer,* 2(1), pp. 47-61.

Maitland, N. J., Macintosh, C. A., Hall, J., Sharrard, M., Quinn, G. and Lang, S. (2001) 'In vitro models to study cellular differentiation and function in human prostate cancers', *Radiat Res,* 155(1 Pt 2), pp. 133-142.

Majumder, P. K. and Sellers, W. R. (2005) 'Akt-regulated pathways in prostate cancer', *Oncogene,* 24(50), pp. 7465-74.

Malkin, D. (2011) 'Li-fraumeni syndrome', *Genes Cancer,* 2(4), pp. 475-84.

Marcias, G., Erdmann, E., Lapouge, G., Siebert, C., Barthélémy, P., Duclos, B., Bergerat, J. P., Céraline, J. and Kurtz, J. E. (2010) 'Identification of novel truncated androgen receptor (AR) mutants including unreported pre-mRNA splicing variants in the 22Rv1 hormone-refractory prostate cancer (PCa) cell line', *Hum Mutat,* 31(1), pp. 74-80.

Mariño-Ramírez, L., Kann, M. G., Shoemaker, B. A. and Landsman, D. (2005) 'Histone structure and nucleosome stability', *Expert Rev Proteomics,* 2(5), pp. 719-29.

Marker, P. C., Donjacour, A. A., Dahiya, R. and Cunha, G. R. (2003) 'Hormonal, cellular, and molecular control of prostatic development', *Dev Biol,* 253(2), pp. 165-74.

Marks, P., Rifkind, R. A., Richon, V. M., Breslow, R., Miller, T. and Kelly, W. K. (2001) 'Histone deacetylases and cancer: causes and therapies', *Nat Rev Cancer,* 1(3), pp. 194-202.

Marques, R. B., van Weerden, W. M., Erkens-Schulze, S., de Ridder, C. M., Bangma, C. H., Trapman, J. and Jenster, G. (2006) 'The human PC346 xenograft and cell line

panel: a model system for prostate cancer progression', *Eur Urol,* 49(2), pp. 245-57.

Mateo, J., Carreira, S., Sandhu, S., Miranda, S., Mossop, H., Perez-Lopez, R., Nava Rodrigues, D., Robinson, D., Omlin, A., Tunariu, N., Boysen, G., Porta, N., Flohr, P., Gillman, A., Figueiredo, I., Paulding, C., Seed, G., Jain, S., Ralph, C., Protheroe, A., Hussain, S., Jones, R., Elliott, T., McGovern, U., Bianchini, D., Goodall, J., Zafeiriou, Z., Williamson, C. T., Ferraldeschi, R., Riisnaes, R., Ebbs, B., Fowler, G., Roda, D., Yuan, W., Wu, Y. M., Cao, X., Brough, R., Pemberton, H., A'Hern, R., Swain, A., Kunju, L. P., Eeles, R., Attard, G., Lord, C. J., Ashworth, A., Rubin, M. A., Knudsen, K. E., Feng, F. Y., Chinnaiyan, A. M., Hall, E. and de Bono, J. S. (2015) 'DNA-Repair Defects and Olaparib in Metastatic Prostate Cancer', *N Engl J Med,* 373(18), pp. 1697-708.

Matsugi, S., Hamada, T., Shioi, N., Tanaka, T., Kumada, T. and Satomura, S. (2007) 'Serum carboxypeptidase A activity as a biomarker for early-stage pancreatic carcinoma', *Clinica Chimica Acta,* 378(1-2), pp. 147-153.

Matushansky, I., Hernando, E., Socci, N. D., Mills, J. E., Matos, T. A., Edgar, M. A., Singer, S., Maki, R. G. and Cordon-Cardo, C. (2007) 'Derivation of sarcomas from mesenchymal stem cells via inactivation of the Wnt pathway', *J Clin Invest,* 117(11), pp. 3248-57.

Maughan, B. L. and Antonarakis, E. S. (2015) 'Clinical Relevance of Androgen Receptor Splice Variants in Castration-Resistant Prostate Cancer', *Curr Treat Options Oncol,* 16(12), pp. 57.

McNeal, J. E. (1978) 'Origin and evolution of benign prostatic enlargement', *Invest Urol,* 15(4), pp. 340-5.

McNeal, J. E. (1981) 'The zonal anatomy of the prostate', *Prostate,* 2(1), pp. 35-49.

McNeal, J. E., Redwine, E. A., Freiha, F. S. and Stamey, T. A. (1988) 'Zonal distribution of prostatic adenocarcinoma. Correlation with histologic pattern and direction of spread', *Am J Surg Pathol,* 12(12), pp. 897-906.

Meissner, A., Mikkelsen, T. S., Gu, H., Wernig, M., Hanna, J., Sivachenko, A., Zhang, X., Bernstein, B. E., Nusbaum, C., Jaffe, D. B., Gnirke, A., Jaenisch, R. and Lander, E. S. (2008) 'Genome-scale DNA methylation maps of pluripotent and differentiated cells', *Nature,* 454(7205), pp. 766-70.

Mellacheruvu, D., Wright, Z., Couzens, A. L., Lambert, J. P., St-Denis, N. A., Li, T., Miteva, Y. V., Hauri, S., Sardiu, M. E., Low, T. Y., Halim, V. A., Bagshaw, R. D., Hubner, N. C., Al-Hakim, A., Bouchard, A., Faubert, D., Fermin, D., Dunham, W. H., Goudreault, M., Lin, Z. Y., Badillo, B. G., Pawson, T., Durocher, D., Coulombe, B., Aebersold, R., Superti-Furga, G., Colinge, J., Heck, A. J., Choi, H., Gstaiger, M., Mohammed, S., Cristea, I. M., Bennett, K. L., Washburn, M. P., Raught, B., Ewing, R. M., Gingras, A. C. and Nesvizhskii, A. I. (2013) 'The CRAPome: a contaminant repository for affinity purification-mass spectrometry data', *Nat Methods,* 10(8), pp. 730-6.

Merson, S., Yang, Z. H., Brewer, D., Olmos, D., Eichholz, A., McCarthy, F., Fisher, G., Kovacs, G., Berney, D. M., Foster, C. S., Møller, H., Scardino, P., Cuzick, J., Cooper, C. S., Clark, J. P. and Group, T. P. (2014) 'Focal amplification of the androgen receptor gene in hormone-naive human prostate cancer', *Br J Cancer,* 110(6), pp. 1655-62.

Miki, J., Furusato, B., Li, H., Gu, Y., Takahashi, H., Egawa, S., Sesterhenn, I. A., McLeod, D. G., Srivastava, S. and Rhim, J. S. (2007) 'Identification of putative stem cell markers, CD133 and CXCR4, in hTERT-immortalized primary nonmalignant and malignant tumor-derived human prostate epithelial cell lines and in prostate cancer specimens', *Cancer Res,* 67(7), pp. 3153-61.

Morais, C. L., Guedes, L. B., Hicks, J., Baras, A. S., De Marzo, A. M. and Lotan, T. L. (2016) 'ERG and PTEN status of isolated high-grade PIN occurring in cystoprostatectomy specimens without invasive prostatic adenocarcinoma', *Hum Pathol,* 55, pp. 117-25.

Mulholland, D. J., Tran, L. M., Li, Y., Cai, H., Morim, A., Wang, S., Plaisier, S., Garraway, I. P., Huang, J., Graeber, T. G. and Wu, H. (2011) 'Cell autonomous role of PTEN in regulating castration-resistant prostate cancer growth', *Cancer Cell,* 19(6), pp. 792-804.

Mullane, S. A. and Van Allen, E. M. (2016) 'Precision medicine for advanced prostate cancer', *Curr Opin Urol,* 26(3), pp. 231-9.

Munster, P. N., Troso-Sandoval, T., Rosen, N., Rifkind, R., Marks, P. A. and Richon, V. M. (2001) 'The histone deacetylase inhibitor suberoylanilide hydroxamic acid induces differentiation of human breast cancer cells', *Cancer Res,* 61(23), pp. 8492-7.

Murray, S., Briasoulis, E., Linardou, H., Bafaloukos, D. and Papadimitriou, C. (2012) 'Taxane resistance in breast cancer: mechanisms, predictive biomarkers and circumvention strategies', *Cancer Treat Rev,* 38(7), pp. 890-903.

Muruganandham, K., Dubey, D. and Kapoor, R. (2007) 'Acute urinary retention in benign prostatic hyperplasia: Risk factors and current management', *Indian J Urol,* 23(4), pp. 347-53.

Mátrai, J., Chuah, M. K. and VandenDriessche, T. (2010) 'Recent advances in lentiviral vector development and applications', *Mol Ther,* 18(3), pp. 477-90.

Nabbi, A. and Riabowol, K. (2015) 'Rapid Isolation of Nuclei from Cells In Vitro', *Cold Spring Harbor Protocols,* 8, pp. 769-772.

Nadiminty, N. and Gao, A. C. (2012) 'Mechanisms of persistent activation of the androgen receptor in CRPC: recent advances and future perspectives', *World J Urol,* 30(3), pp. 287-95.

Nagle, R. B., Ahmann, F. R., McDaniel, K. M., Paquin, M. L., Clark, V. A. and Celniker, A. (1987) 'Cytokeratin characterization of human prostatic carcinoma and its derived cell lines', *Cancer Res,* 47(1), pp. 281-6.

Nagpal, S., Patel, S., Asano, A. T., Johnson, A. T., Duvic, M. and Chandraratna, R. A. (1996) 'Tazarotene-induced gene 1 (TIG1), a novel retinoic acid receptor-responsive gene in skin', *J Invest Dermatol,* 106(2), pp. 269-74.

Nagrath, S., Sequist, L. V., Maheswaran, S., Bell, D. W., Irimia, D., Ulkus, L., Smith, M. R., Kwak, E. L., Digumarthy, S., Muzikansky, A., Ryan, P., Balis, U. J., Tompkins, R. G., Haber, D. A. and Toner, M. (2007) 'Isolation of rare circulating tumour cells in cancer patients by microchip technology', *Nature,* 450(7173), pp. 1235-9.

Navdaev, A. and Eble, J. A. (2011) 'Components of cell-matrix linkage as potential new markers for prostate cancer', *Cancers (Basel),* 3(1), pp. 883-96.

Nemeth, J. A., Harb, J. F., Barroso, U., He, Z., Grignon, D. J. and Cher, M. L. (1999) 'Severe combined immunodeficient-hu model of human prostate cancer metastasis to human bone', *Cancer Res,* 59(8), pp. 1987-93.

Nickel, J. C. (2008) 'Inflammation and benign prostatic hyperplasia', *Urol Clin North Am,* 35(1), pp. 109-15; vii.

Niranjan, B., Lawrence, M. G., Papargiris, M. M., Richards, M. G., Hussain, S., Frydenberg, M., Pedersen, J., Taylor, R. A. and Risbridger, G. P. (2013) 'Primary culture and propagation of human prostate epithelial cells', *Methods Mol Biol,* 945, pp. 365-82.

Oldridge, E. E., Walker, H. F., Stower, M. J., Simms, M. S., Mann, V. M., Collins, A. T., Pellacani, D. and Maitland, N. J. (2013) 'Retinoic acid represses invasion and

stem cell phenotype by induction of the metastasis suppressors RARRES1 and LXN', *Oncogenesis,* 2, pp. e45.

Oldridge. E, E. (2012) 'Gene Expression Patterns in Human Prostate Stem Cell Differentiation' PhD Biology. University of York. United Kingdom.

Ory, S., Zhou, M., Conrads, T. P., Veenstra, T. D. and Morrison, D. K. (2003) 'Protein phosphatase 2A positively regulates Ras signaling by dephosphorylating KSR1 and Raf-1 on critical 14-3-3 binding sites', *Curr Biol,* 13(16), pp. 1356-64.

Pallarès, I., Bonet, R., García-Castellanos, R., Ventura, S., Avilés, F. X., Vendrell, J. and Gomis-Rüth, F. X. (2005) 'Structure of human carboxypeptidase A4 with its endogenous protein inhibitor, latexin', *Proc Natl Acad Sci U S A,* 102(11), pp. 3978-83.

Palmberg, C., Koivisto, P., Hyytinen, E., Isola, J., Visakorpi, T., Kallioniemi, O. P. and Tammela, T. (1997) 'Androgen receptor gene amplification in a recurrent prostate cancer after monotherapy with the nonsteroidal potent antiandrogen Casodex (bicalutamide) with a subsequent favorable response to maximal androgen blockade', *Eur Urol,* 31(2), pp. 216-9.

Parisotto, M. and Metzger, D. (2013) 'Genetically engineered mouse models of prostate cancer', *Mol Oncol,* 7(2), pp. 190-205.

Peehl, D. M. (2005) 'Primary cell cultures as models of prostate cancer development', *Endocr Relat Cancer,* 12(1), pp. 19-47.

Peehl, D. M., Leung, G. K. and Wong, S. T. (1994) 'Keratin expression: a measure of phenotypic modulation of human prostatic epithelial cells by growth inhibitory factors', *Cell Tissue Res,* 277(1), pp. 11-8.

Peehl, D. M., Wong, S. T. and Stamey, T. A. (1993) 'Vitamin A regulates proliferation and differentiation of human prostatic epithelial cells', *Prostate,* 23(1), pp. 69-78.

Peeling, W. B. (1989) 'Phase III studies to compare goserelin (Zoladex) with orchiectomy and with diethylstilbestrol in treatment of prostatic carcinoma', *Urology,* 33(5 Suppl), pp. 45-52.

Pellacani, D., Packer, R. J., Frame, F. M., Oldridge, E. E., Berry, P. A., Labarthe, M. C., Stower, M. J., Simms, M. S., Collins, A. T. and Maitland, N. J. (2011) 'Regulation of the stem cell marker CD133 is independent of promoter hypermethylation in human epithelial differentiation and cancer', *Mol Cancer,* 10, pp. 94.

Peng, Z., Shen, R., Li, Y. W., Teng, K. Y., Shapiro, C. L. and Lin, H. J. (2012) 'Epigenetic repression of RARRES1 is mediated by methylation of a proximal promoter and a loss of CTCF binding', *PLoS One,* 7(5), pp. e36891.

Pierce, G. B. and Verney, E. L. (1961) 'An in vitro and in vivo study of differentiation in teratocarcinomas', *Cancer,* 14, pp. 1017-29.

Pinto, A. C., Ades, F., de Azambuja, E. and Piccart-Gebhart, M. (2013) 'Trastuzumab for patients with HER2 positive breast cancer: delivery, duration and combination therapies', *Breast,* 22 Suppl 2, pp. S152-5.

Placer, J. and Morote, J. (2011) '[Usefulness of prostatic specific antigen (PSA) for diagnosis and staging of patients with prostate cancer]', *Arch Esp Urol,* 64(8), pp. 659-80.

Prins, G. S. and Putz, O. (2008) 'Molecular signaling pathways that regulate prostate gland development', *Differentiation,* 76(6), pp. 641-59.

Psaila, B. and Lyden, D. (2009) 'The metastatic niche: adapting the foreign soil', *Nat Rev Cancer,* 9(4), pp. 285-93.

Pu, Y., Huang, L. and Prins, G. S. (2004) 'Sonic hedgehog-patched Gli signaling in the developing rat prostate gland: lobe-specific suppression by neonatal estrogens reduces ductal growth and branching', *Dev Biol,* 273(2), pp. 257-75.

Quigley, C. A., De Bellis, A., Marschke, K. B., el-Awady, M. K., Wilson, E. M. and French, F. S. (1995) 'Androgen receptor defects: historical, clinical, and molecular perspectives', *Endocr Rev,* 16(3), pp. 271-321.

Rajasekhar, V. K., Studer, L., Gerald, W., Socci, N. D. and Scher, H. I. (2011) 'Tumour-initiating stem-like cells in human prostate cancer exhibit increased NF-κB signalling', *Nat Commun,* 2, pp. 162.

Rane, J. K., Scaravilli, M., Ylipää, A., Pellacani, D., Mann, V. M., Simms, M. S., Nykter, M., Collins, A. T., Visakorpi, T. and Maitland, N. J. (2015) 'MicroRNA expression profile of primary prostate cancer stem cells as a source of biomarkers and therapeutic targets', *Eur Urol,* 67(1), pp. 7-10.

Rea, D., Del Vecchio, V., Palma, G., Barbieri, A., Falco, M., Luciano, A., De Biase, D., Perdonà, S., Facchini, G. and Arra, C. (2016) 'Mouse Models in Prostate Cancer Translational Research: From Xenograft to PDX', *Biomed Res Int,* 2016, pp. 9750795.

Reverter, D., Fernandez-Catalan, C., Baumgartner, R., Pfander, R., Huber, R., Bode, W., Vendrell, J., Holak, T. A. and Aviles, F. X. (2000) 'Structure of a novel leech carboxypeptidase inhibitor determined free in solution and in complex with human carboxypeptidase A2', *Nat Struct Biol,* 7(4), pp. 322-8.

Rhinn, M. and Dollé, P. (2012) 'Retinoic acid signalling during development', *Development,* 139(5), pp. 843-58.

Ricci-Vitiani, L., Lombardi, D. G., Pilozzi, E., Biffoni, M., Todaro, M., Peschle, C. and De Maria, R. (2007) 'Identification and expansion of human colon-cancer-initiating cells', *Nature,* 445(7123), pp. 111-5.

Rich, J. N. (2007) 'Cancer stem cells in radiation resistance', *Cancer Res,* 67(19), pp. 8980-4.

Richardson, G. D., Robson, C. N., Lang, S. H., Neal, D. E., Maitland, N. J. and Collins, A. T. (2004) 'CD133, a novel marker for human prostatic epithelial stem cells', *J Cell Sci,* 117(Pt 16), pp. 3539-45.

Roberts, A., Trapnell, C., Donaghey, J., Rinn, J. L. and Pachter, L. (2011) 'Improving RNA-Seq expression estimates by correcting for fragment bias', *Genome Biol,* 12(3), pp. R22.

Robertson, K. D. (2005) 'DNA methylation and human disease', *Nat Rev Genet,* 6(8), pp. 597-610.

Rodríguez-Antona, C. and Taron, M. (2015) 'Pharmacogenomic biomarkers for personalized cancer treatment', *J Intern Med,* 277(2), pp. 201-17.

Rossetto, D., Avvakumov, N. and Côté, J. (2012) 'Histone phosphorylation: a chromatin modification involved in diverse nuclear events', *Epigenetics,* 7(10), pp. 1098-108.

Rumpold, H., Heinrich, E., Untergasser, G., Hermann, M., Pfister, G., Plas, E. and Berger, P. (2002) 'Neuroendocrine differentiation of human prostatic primary epithelial cells in vitro', *Prostate,* 53(2), pp. 101-8.

Ryan, C. J., Smith, M. R., Fizazi, K., Saad, F., Mulders, P. F., Sternberg, C. N., Miller, K., Logothetis, C. J., Shore, N. D., Small, E. J., Carles, J., Flaig, T. W., Taplin, M. E., Higano, C. S., de Souza, P., de Bono, J. S., Griffin, T. W., De Porre, P., Yu, M. K., Park, Y. C., Li, J., Kheoh, T., Naini, V., Molina, A., Rathkopf, D. E. and Investigators, C.-A.-. (2015) 'Abiraterone acetate plus prednisone versus placebo plus prednisone in chemotherapy-naive men with metastatic castration-resistant prostate cancer (COU-AA-302): final overall survival analysis of a randomised, double-blind, placebo-controlled phase 3 study', *Lancet Oncol,* 16(2), pp. 152-60.

Röpke, A., Erbersdobler, A., Hammerer, P., Palisaar, J., John, K., Stumm, M. and Wieacker, P. (2004) 'Gain of androgen receptor gene copies in primary prostate cancer due to X chromosome polysomy', *Prostate,* 59(1), pp. 59-68.

Sahab, Z. J., Hall, M. D., Me Sung, Y., Dakshanamurthy, S., Ji, Y., Kumar, D. and Byers, S. W. (2011) 'Tumor suppressor RARRES1 interacts with cytoplasmic carboxypeptidase AGBL2 to regulate the α-tubulin tyrosination cycle', *Cancer Res,* 71(4), pp. 1219-28.

Sahab, Z. J., Hall, M. D., Zhang, L., Cheema, A. K. and Byers, S. W. (2010) 'Tumor Suppressor RARRES1 Regulates DLG2, PP2A, VCP, EB1, and Ankrd26', *J Cancer,* 1, pp. 14-22.

Sanber, K. S., Knight, S. B., Stephen, S. L., Bailey, R., Escors, D., Minshull, J., Santilli, G., Thrasher, A. J., Collins, M. K. and Takeuchi, Y. (2015) 'Construction of stable packaging cell lines for clinical lentiviral vector production', *Sci Rep,* 5, pp. 9021.

Sanchez, P., Hernández, A. M., Stecca, B., Kahler, A. J., DeGueme, A. M., Barrett, A., Beyna, M., Datta, M. W., Datta, S. and Ruiz i Altaba, A. (2004) 'Inhibition of prostate cancer proliferation by interference with SONIC HEDGEHOG-GLI1 signaling', *Proc Natl Acad Sci U S A,* 101(34), pp. 12561-6.

Saraon, P., Jarvi, K. and Diamandis, E. P. (2011) 'Molecular alterations during progression of prostate cancer to androgen independence', *Clin Chem,* 57(10), pp. 1366-75.

Sarker, D., Reid, A. H., Yap, T. A. and de Bono, J. S. (2009) 'Targeting the PI3K/AKT pathway for the treatment of prostate cancer', *Clin Cancer Res,* 15(15), pp. 4799-805.

Sassen, S., Miska, E. A. and Caldas, C. (2008) 'MicroRNA: implications for cancer', *Virchows Arch,* 452(1), pp. 1-10.

Schenk, T., Stengel, S. and Zelent, A. (2014) 'Unlocking the potential of retinoic acid in anticancer therapy', *Br J Cancer,* 111(11), pp. 2039-45.

Scher, H. I., Halabi, S., Tannock, I., Morris, M., Sternberg, C. N., Carducci, M. A., Eisenberger, M. A., Higano, C., Bubley, G. J., Dreicer, R., Petrylak, D., Kantoff, P., Basch, E., Kelly, W. K., Figg, W. D., Small, E. J., Beer, T. M., Wilding, G., Martin, A., Hussain, M. and Group, P. C. C. T. W. (2008) 'Design and end points of clinical trials for patients with progressive prostate cancer and castrate levels of testosterone: recommendations of the Prostate Cancer Clinical Trials Working Group', *J Clin Oncol,* 26(7), pp. 1148-59.

Schlomm, T., Iwers, L., Kirstein, P., Jessen, B., Köllermann, J., Minner, S., Passow-Drolet, A., Mirlacher, M., Milde-Langosch, K., Graefen, M., Haese, A., Steuber, T., Simon, R., Huland, H., Sauter, G. and Erbersdobler, A. (2008) 'Clinical significance of p53 alterations in surgically treated prostate cancers', *Mod Pathol,* 21(11), pp. 1371-8.

Schmittgen, T. D. and Livak, K. J. (2008) 'Analyzing real-time PCR data by the comparative C(T) method', *Nat Protoc,* 3, pp. 1101-1108.

Schnerch, A., Rampalii, S. and Bhatia, M. (2013) 'Histone modification profiling in normal and transformed human embryonic stem cells using micro chromatin immunoprecipitation, scalable to genome-wide microarray analyses', *Methods Mol Biol,* 1029, pp. 149-61.

Schroder, F. H. (2012) 'Landmarks in prostate cancer screening', *BJU Int,* 110 Suppl 1, pp. 3-7.

Senoo, M., Pinto, F., Crum, C. P. and McKeon, F. (2007) 'p63 Is essential for the proliferative potential of stem cells in stratified epithelia', *Cell,* 129(3), pp. 523-36.

Seo, R., McGuire, M., Chung, M. and Bushman, W. (1997) 'Inhibition of prostate ductal morphogenesis by retinoic acid', *J Urol,* 158(3 Pt 1), pp. 931-5.

Shema, E., Jones, D., Shoresh, N., Donohue, L., Ram, O. and Bernstein, B. E. (2016) 'Single-molecule decoding of combinatorially modified nucleosomes', *Science,* 352(6286), pp. 717-21.

Shen, M. M. and Abate-Shen, C. (2010) 'Molecular genetics of prostate cancer: new prospects for old challenges', *Genes Dev,* 24(18), pp. 1967-2000.

Sidoli, S. and Garcia, B. A. (2015) 'Properly reading the histone code by MS-based proteomics', *Proteomics,* 15(17), pp. 2901-2.

Simandi, Z., Balint, B. L., Poliska, S., Ruhl, R. and Nagy, L. (2010) 'Activation of retinoic acid receptor signaling coordinates lineage commitment of spontaneously differentiating mouse embryonic stem cells in embryoid bodies', *FEBS Lett,* 584(14), pp. 3123-30.

Singh, S. K., Hawkins, C., Clarke, I. D., Squire, J. A., Bayani, J., Hide, T., Henkelman, R. M., Cusimano, M. D. and Dirks, P. B. (2004) 'Identification of human brain tumour initiating cells', *Nature,* 432(7015), pp. 396-401.

Siolas, D. and Hannon, G. J. (2013) 'Patient-derived tumor xenografts: transforming clinical samples into mouse models', *Cancer Res,* 73(17), pp. 5315-9.

Smith, D. C. and Pienta, K. J. (1999) 'Paclitaxel in the treatment of hormone-refractory prostate cancer', *Semin Oncol,* 26(1 Suppl 2), pp. 109-11.

Smith, M. R., Biggar, S. and Hussain, M. (1995) 'Prostate-specific antigen messenger RNA is expressed in non-prostate cells: implications for detection of micrometastases', *Cancer Res,* 55(12), pp. 2640-4.

Spear, B. B., Heath-Chiozzi, M. and Huff, J. (2001) 'Clinical application of pharmacogenetics', *Trends Mol Med,* 7(5), pp. 201-4.

Srimatkandada, S., Medina, W. D., Cashmore, A. R., Whyte, W., Engel, D., Moroson, B. A., Franco, C. T., Dube, S. K. and Bertino, J. R. (1983) 'Amplification and organization of dihydrofolate reductase genes in a human leukemic cell line, K-562, resistant to methotrexate', *Biochemistry,* 22(25), pp. 5774-81.

Stanevsky, Y., Tsivian, A. and Tsivian, M. (2013) 'Castration-resistant prostate cancer: a strategy to enhance response to androgen deprivation', *Asian J Androl,* 15(6), pp. 709-10.

Stern, H. and Mirsky, A. E. (1953) 'Soluble enzymes of nuclei isolated in sucrose and nonaqueous media; a comparative study', *J Gen Physiol,* 37(2), pp. 177-87.

Stoletov, K., Kato, H., Zardouzian, E., Kelber, J., Yang, J., Shattil, S. and Klemke, R. (2010) 'Visualizing extravasation dynamics of metastatic tumor cells', *J Cell Sci,* 123(Pt 13), pp. 2332-41.

Stone, K. R., Mickey, D. D., Wunderli, H., Mickey, G. H. and Paulson, D. F. (1978) 'Isolation of a human prostate carcinoma cell line (DU 145)', *Int J Cancer,* 21(3), pp. 274-81.

Stone, R. M., Maguire, M., Goldberg, M. A., Antin, J. H., Rosenthal, D. S. and Mayer, R. J. (1988) 'Complete remission in acute promyelocytic leukemia despite persistence of abnormal bone marrow promyelocytes during induction therapy: experience in 34 patients', *Blood,* 71(3), pp. 690-6.

Struewing, J. P., Hartge, P., Wacholder, S., Baker, S. M., Berlin, M., McAdams, M., Timmerman, M. M., Brody, L. C. and Tucker, M. A. (1997) 'The risk of cancer associated with specific mutations of BRCA1 and BRCA2 among Ashkenazi Jews', *N Engl J Med,* 336(20), pp. 1401-8.

Sung, M. W. and Waxman, S. (2007) 'Combination of cytotoxic-differentiation therapy with 5-fluorouracil and phenylbutyrate in patients with advanced colorectal cancer', *Anticancer Res,* 27(2), pp. 995-1001.

Swanson, G. P. and Basler, J. W. (2010) 'Prognostic factors for failure after prostatectomy', *J Cancer,* 2, pp. 1-19.

Tabarestani, S. and Ghafouri-Fard, S. (2012) 'Cancer stem cells and response to therapy', *Asian Pac J Cancer Prev,* 13(12), pp. 5951-8.

Taylor, B. S., Schultz, N., Hieronymus, H., Gopalan, A., Xiao, Y., Carver, B. S., Arora, V. K., Kaushik, P., Cerami, E., Reva, B., Antipin, Y., Mitsiades, N., Landers, T., Dolgalev, I., Major, J. E., Wilson, M., Socci, N. D., Lash, A. E., Heguy, A., Eastham, J. A., Scher, H. I., Reuter, V. E., Scardino, P. T., Sander, C., Sawyers, C. L. and Gerald, W. L. (2010) 'Integrative genomic profiling of human prostate cancer', *Cancer Cell,* 18(1), pp. 11-22.

ten Have, S., Boulon, S., Ahmad, Y. and Lamond, A. I. (2011) 'Mass spectrometry-based immuno-precipitation proteomics - the user's guide', *Proteomics,* 11(6), pp. 1153-9.

Tentler, J. J., Tan, A. C., Weekes, C. D., Jimeno, A., Leong, S., Pitts, T. M., Arcaroli, J. J., Messersmith, W. A. and Eckhardt, S. G. (2012) 'Patient-derived tumour xenografts as models for oncology drug development', *Nat Rev Clin Oncol,* 9(6), pp. 338-50.

Teytelman, L., Thurtle, D. M., Rine, J. and van Oudenaarden, A. (2013) 'Highly expressed loci are vulnerable to misleading ChIP localization of multiple unrelated proteins', *Proc Natl Acad Sci U S A,* 110(46), pp. 18602-7.

Thermofisher (2016) *Digital PCR for higher accuracy, sensitivity and absolute quantification*. https://www.thermofisher.com/uk/en/home/life-science/pcr/digital-pcr.html: Thermo Fisher Scientific (Accessed: September 25th 2016.

Thompson, I. M., Pauler, D. K., Goodman, P. J., Tangen, C. M., Lucia, M. S., Parnes, H. L., Minasian, L. M., Ford, L. G., Lippman, S. M., Crawford, E. D., Crowley, J. J. and Coltman, C. A. (2004) 'Prevalence of prostate cancer among men with a prostate-specific antigen level < or =4.0 ng per milliliter', *N Engl J Med,* 350(22), pp. 2239-46.

Tontonoz, P., Singer, S., Forman, B. M., Sarraf, P., Fletcher, J. A., Fletcher, C. D., Brun, R. P., Mueller, E., Altiok, S., Oppenheim, H., Evans, R. M. and Spiegelman, B. M. (1997) 'Terminal differentiation of human liposarcoma cells induced by ligands for peroxisome proliferator-activated receptor gamma and the retinoid X receptor', *Proc Natl Acad Sci U S A,* 94(1), pp. 237-41.

Tsai, F. M., Wu, C. C., Shyu, R. Y., Wang, C. H. and Jiang, S. Y. (2011) 'Tazarotene-induced gene 1 inhibits prostaglandin E2-stimulated HCT116 colon cancer cell growth', *J Biomed Sci,* 18, pp. 88.

Tsai, J., Lee, J. T., Wang, W., Zhang, J., Cho, H., Mamo, S., Bremer, R., Gillette, S., Kong, J., Haass, N. K., Sproesser, K., Li, L., Smalley, K. S., Fong, D., Zhu, Y. L., Marimuthu, A., Nguyen, H., Lam, B., Liu, J., Cheung, I., Rice, J., Suzuki, Y., Luu, C., Settachatgul, C., Shellooe, R., Cantwell, J., Kim, S. H., Schlessinger, J., Zhang, K. Y., West, B. L., Powell, B., Habets, G., Zhang, C., Ibrahim, P. N., Hirth, P., Artis, D. R., Herlyn, M. and Bollag, G. (2008) 'Discovery of a selective inhibitor of oncogenic B-Raf kinase with potent antimelanoma activity', *Proc Natl Acad Sci U S A,* 105(8), pp. 3041-6.

Tsujimura, A., Koikawa, Y., Salm, S., Takao, T., Coetzee, S., Moscatelli, D., Shapiro, E., Lepor, H., Sun, T. T. and Wilson, E. L. (2002) 'Proximal location of mouse prostate epithelial stem cells: a model of prostatic homeostasis', *J Cell Biol,* 157(7), pp. 1257-65.

Tursz, T., Andre, F., Lazar, V., Lacroix, L. and Soria, J. C. (2011) 'Implications of personalized medicine--perspective from a cancer center', *Nat Rev Clin Oncol,* 8(3), pp. 177-83.

Uratani, Y., Takiguchi-Hayashi, K., Miyasaka, N., Sato, M., Jin, M. H. and Arimatsu, Y. (2000) 'Latexin, a carboxypeptidase A inhibitor, is expressed in rat peritoneal mast cells and is associated with granular structures distinct from secretory granules and lysosomes', *Biochemical Journal,* 346, pp. 817-826.

Vainstein, V., Kirnasovsky, O. U., Kogan, Y. and Agur, Z. (2012) 'Strategies for cancer stem cell elimination: insights from mathematical modeling', *J Theor Biol,* 298, pp. 32-41.

Vakoc, C. R., Sachdeva, M. M., Wang, H. and Blobel, G. A. (2006) 'Profile of histone lysine methylation across transcribed mammalian chromatin', *Mol Cell Biol,* 26(24), pp. 9185-95.

Valastyan, S. and Weinberg, R. A. (2011) 'Tumor metastasis: molecular insights and evolving paradigms', *Cell,* 147(2), pp. 275-92.

Valkenburg, K. C. and Williams, B. O. (2011) 'Mouse models of prostate cancer', *Prostate Cancer,* 2011, pp. 895238.

Vermeulen, L., Sprick, M. R., Kemper, K., Stassi, G. and Medema, J. P. (2008) 'Cancer stem cells--old concepts, new insights', *Cell Death Differ,* 15(6), pp. 947-58.

Vezina, C. M., Allgeier, S. H., Fritz, W. A., Moore, R. W., Strerath, M., Bushman, W. and Peterson, R. E. (2008) 'Retinoic acid induces prostatic bud formation', *Dev Dyn,* 237(5), pp. 1321-33.

Vinogradova, T. V., Chernov, I. P., Monastyrskaya, G. S., Kondratyeva, L. G. and Sverdlov, E. D. (2015) 'Cancer Stem Cells: Plasticity Works against Therapy', *Acta Naturae,* 7(4), pp. 46-55.

Visakorpi, T., Hyytinen, E., Koivisto, P., Tanner, M., Keinänen, R., Palmberg, C., Palotie, A., Tammela, T., Isola, J. and Kallioniemi, O. P. (1995) 'In vivo amplification of the androgen receptor gene and progression of human prostate cancer', *Nat Genet,* 9(4), pp. 401-6.

Vogel, C. L., Cobleigh, M. A., Tripathy, D., Gutheil, J. C., Harris, L. N., Fehrenbacher, L., Slamon, D. J., Murphy, M., Novotny, W. F., Burchmore, M., Shak, S., Stewart, S. J. and Press, M. (2002) 'Efficacy and safety of trastuzumab as a single agent in first-line treatment of HER2-overexpressing metastatic breast cancer', *J Clin Oncol,* 20(3), pp. 719-26.

Voigt, P., Tee, W. W. and Reinberg, D. (2013) 'A double take on bivalent promoters', *Genes Dev,* 27(12), pp. 1318-38.

Walczak, J., Wood, H., Wilding, G., Williams, T., Bishop, C. W. and Carducci, M. (2001) 'Prostate cancer prevention strategies using antiproliferative or differentiating agents', *Urology,* 57(4 Suppl 1), pp. 81-5.

Walsh, P. C. (2005) 'Radical prostatectomy versus watchful waiting in early prostate cancer', *J Urol,* 174(4 Pt 1), pp. 1291-2.

Waltering, K. K., Urbanucci, A. and Visakorpi, T. (2012) 'Androgen receptor (AR) aberrations in castration-resistant prostate cancer', *Mol Cell Endocrinol,* 360(1-2), pp. 38-43.

Wang, B. E., Wang, X., Long, J. E., Eastham-Anderson, J., Firestein, R. and Junttila, M. R. (2015) 'Castration-resistant Lgr5(+) cells are long-lived stem cells required for prostatic regeneration', *Stem Cell Reports,* 4(5), pp. 768-79.

Wang, G., Wang, Z., Sarkar, F. H. and Wei, W. (2012) 'Targeting prostate cancer stem cells for cancer therapy', *Discov Med,* 13(69), pp. 135-42.

Wang, S., Gao, J., Lei, Q., Rozengurt, N., Pritchard, C., Jiao, J., Thomas, G. V., Li, G., Roy-Burman, P., Nelson, P. S., Liu, X. and Wu, H. (2003) 'Prostate-specific deletion of the murine Pten tumor suppressor gene leads to metastatic prostate cancer', *Cancer Cell,* 4(3), pp. 209-21.

Wang, S. S., Virmani, A., Gazdar, A. F., Minna, J. D. and Evans, G. A. (1999) 'Refined mapping of two regions of loss of heterozygosity on chromosome band 11q23 in lung cancer', *Genes Chromosomes Cancer,* 25(2), pp. 154-9.

Wang, W. C., Mihlbachler, K. A., Bleecker, E. R., Weiss, S. T. and Liggett, S. B. (2008) 'A polymorphism of G-protein coupled receptor kinase5 alters agonist-promoted desensitization of beta2-adrenergic receptors', *Pharmacogenet Genomics,* 18(8), pp. 729-32.

Wang, X., Kruithof-de Julio, M., Economides, K. D., Walker, D., Yu, H., Halili, M. V., Hu, Y. P., Price, S. M., Abate-Shen, C. and Shen, M. M. (2009) 'A luminal epithelial stem cell that is a cell of origin for prostate cancer', *Nature,* 461(7263), pp. 495-500.

Wang, Y., Revelo, M. P., Sudilovsky, D., Cao, M., Chen, W. G., Goetz, L., Xue, H., Sadar, M., Shappell, S. B., Cunha, G. R. and Hayward, S. W. (2005) 'Development and characterization of efficient xenograft models for benign and malignant human prostate tissue', *Prostate,* 64(2), pp. 149-59.

Weibrecht, I., Leuchowius, K. J., Clausson, C. M., Conze, T., Jarvius, M., Howell, W. M., Kamali-Moghaddam, M. and Söderberg, O. (2010) 'Proximity ligation assays: a recent addition to the proteomics toolbox', *Expert Rev Proteomics,* 7(3), pp. 401-9.

Weinstein, G. D., Koo, J. Y., Krueger, G. G., Lebwohl, M. G., Lowe, N. J., Menter, M. A., Lew-Kaya, D. A., Sefton, J., Gibson, J. R., Walker, P. S. and Group, T. C. C. S. (2003) 'Tazarotene cream in the treatment of psoriasis: Two multicenter, double-blind, randomized, vehicle-controlled studies of the safety and efficacy of tazarotene creams 0.05% and 0.1% applied once daily for 12 weeks', *J Am Acad Dermatol,* 48(5), pp. 760-7.

Wildsmith, S. E. and Elcock, F. J. (2001) 'Microarrays under the microscope', *Mol Pathol,* 54(1), pp. 8-16.

Wu, C. C., Shyu, R. Y., Chou, J. M., Jao, S. W., Chao, P. C., Kang, J. C., Wu, S. T., Huang, S. L. and Jiang, S. Y. (2006) 'RARRES1 expression is significantly related to tumour differentiation and staging in colorectal adenocarcinoma', *Eur J Cancer,* 42(4), pp. 557-65.

Wu, C. C., Tsai, F. M., Shyu, R. Y., Tsai, Y. M., Wang, C. H. and Jiang, S. Y. (2011a) 'G protein-coupled receptor kinase 5 mediates Tazarotene-induced gene 1-induced growth suppression of human colon cancer cells', *BMC Cancer,* 11, pp. 175.

Wu, Y., Liu, S., Xin, H., Jiang, J., Younglai, E., Sun, S. and Wang, H. (2011b) 'Up-regulation of microRNA-145 promotes differentiation by repressing OCT4 in human endometrial adenocarcinoma cells', *Cancer,* 117(17), pp. 3989-98.

Xu, W. P., Zhang, X. and Xie, W. F. (2014) 'Differentiation therapy for solid tumors', *J Dig Dis,* 15(4), pp. 159-65.

Yamamoto, K., Nagata, K., Kida, A. and Hamaguchi, H. (2002) 'Acquired gain of an X chromosome as the sole abnormality in the blast crisis of chronic neutrophilic leukemia', *Cancer Genet Cytogenet,* 134(1), pp. 84-7.

Yang, T., Rycaj, K., Liu, Z. M. and Tang, D. G. (2014) 'Cancer stem cells: constantly evolving and functionally heterogeneous therapeutic targets', *Cancer Res,* 74(11), pp. 2922-7.

Yoder, J. A., Walsh, C. P. and Bestor, T. H. (1997) 'Cytosine methylation and the ecology of intragenomic parasites', *Trends Genet,* 13(8), pp. 335-40.

Yoshimoto, M., Cutz, J. C., Nuin, P. A., Joshua, A. M., Bayani, J., Evans, A. J., Zielenska, M. and Squire, J. A. (2006) 'Interphase FISH analysis of PTEN in histologic sections shows genomic deletions in 68% of primary prostate cancer and 23% of high-grade prostatic intra-epithelial neoplasias', *Cancer Genet Cytogenet,* 169(2), pp. 128-37.

You, Y., Wen, R., Pathak, R., Li, A., Li, W., St Clair, D., Hauer-Jensen, M., Zhou, D. and Liang, Y. (2014) 'Latexin sensitizes leukemogenic cells to gamma-irradiation-induced cell-cycle arrest and cell death through Rps3 pathway', *Cell Death Dis,* 5, pp. e1493.

Youssef, E. M., Chen, X. Q., Higuchi, E., Kondo, Y., Garcia-Manero, G., Lotan, R. and Issa, J. P. (2004) 'Hypermethylation and silencing of the putative tumor suppressor Tazarotene-induced gene 1 in human cancers', *Cancer Res,* 64(7), pp. 2411-7.

Yu, C., Yao, Z., Jiang, Y. and Keller, E. T. (2012) 'Prostate cancer stem cell biology', *Minerva Urol Nefrol,* 64(1), pp. 19-33.

Yu, Y., Sarkar, F. H. and Majumdar, A. P. (2013) 'Down-regulation of miR-21 Induces Differentiation of Chemoresistant Colon Cancer Cells and Enhances Susceptibility to Therapeutic Regimens', *Transl Oncol,* 6(2), pp. 180-6.

Yurchenco, P. D. and O'Rear, J. J. (1994) 'Basal lamina assembly', *Curr Opin Cell Biol,* 6(5), pp. 674-81.

Zaytseva, Y. Y., Wallis, N. K., Southard, R. C. and Kilgore, M. W. (2011) 'The PPARgamma antagonist T0070907 suppresses breast cancer cell proliferation and motility via both PPARgamma-dependent and -independent mechanisms', *Anticancer Res,* 31(3), pp. 813-23.

Zhang, B., Metharom, P., Jullie, H., Ellem, K. A., Cleghorn, G., West, M. J. and Wei, M. Q. (2004) 'The significance of controlled conditions in lentiviral vector titration and in the use of multiplicity of infection (MOI) for predicting gene transfer events', *Genet Vaccines Ther,* 2(1), pp. 6.

Zhao, S., Fung-Leung, W. P., Bittner, A., Ngo, K. and Liu, X. (2014) 'Comparison of RNA-Seq and microarray in transcriptome profiling of activated T cells', *PLoS One,* 9(1), pp. e78644.